



National Library
of Canada

Bibliothèque nationale
du Canada

Canadian Theses Service

Services des thèses canadiennes

Ottawa, Canada
K1A 0N4

CANADIAN THESES

THÈSES CANADIENNES

NOTICE

The quality of this microfiche is heavily dependent upon the quality of the original thesis submitted for microfilming. Every effort has been made to ensure the highest quality of reproduction possible.

If pages are missing, contact the university which granted the degree.

Some pages may have indistinct print especially if the original pages were typed with a poor typewriter ribbon or if the university sent us an inferior photocopy.

Previously copyrighted materials (journal articles, published tests, etc.) are not filmed.

Reproduction in full or in part of this film is governed by the Canadian Copyright Act, R.S.C. 1970, c. C-30. Please read the authorization forms which accompany this thesis.

**THIS DISSERTATION
HAS BEEN MICROFILMED
EXACTLY AS RECEIVED**

AVIS

La qualité de cette microfiche dépend grandement de la qualité de la thèse soumise au microfilmage. Nous avons tout fait pour assurer une qualité supérieure de reproduction.

S'il manque des pages, veuillez communiquer avec l'université qui a conféré le grade.

La qualité d'impression de certaines pages peut laisser à désirer, surtout si les pages originales ont été dactylographiées à l'aide d'un ruban usé ou si l'université nous a fait parvenir une photocopie de qualité inférieure.

Les documents qui font déjà l'objet d'un droit d'auteur (articles de revue, examens publiés, etc.) ne sont pas microfilmés.

La reproduction, même partielle, de ce microfilm est soumise à la Loi canadienne sur le droit d'auteur, SRC 1970, c. C-30. Veuillez prendre connaissance des formules d'autorisation qui accompagnent cette thèse.

**LA THÈSE A ÉTÉ
MICROFILMÉE TELLE QUE
NOUS L'AVONS REÇUE**



National Library
of Canada

Bibliothèque nationale
du Canada

0-315-26851-4

Canadian Theses Division / Division des thèses canadiennes

Ottawa: Canada
K1A 0N4

PERMISSION TO MICROFILM — AUTORISATION DE MICROFILMER

• Please print or type — Ecrire en lettres mouillées ou dactylographier

Full Name of Author — Nom complet de l'auteur

CARL JAMES WARREN

Date of Birth — Date de naissance

JULY 12 1957

Country of Birth — Lieu de naissance

CANADA

Permanent Address — Residence fixe

3301-1194 HOOKE ROAD

EDMONTON, ALBERTA T5A 4A4

Title of Thesis — Titre de la thèse

THE CHEMISTRY AND MINERALOGY OF ARTIFICIALLY
WEATHERED FLY ASH

University — Université

UNIVERSITY OF ALBERTA

Degree for which thesis was presented — Grade pour lequel cette thèse fut présentée

MASTER OF SCIENCE

Year this degree conferred — Année d'obtention de ce grade

1983

Name of Supervisor — Nom du directeur de thèse

M. J. DUDAS

Permission is hereby granted to the NATIONAL LIBRARY OF CANADA to microfilm this thesis and to lend or sell copies of the film.

The author reserves other publication rights, and neither the thesis nor extensive extracts from it may be printed or otherwise reproduced without the author's written permission.

L'autorisation est, par la présente, accordée à la BIBLIOTHÈQUE NATIONALE DU CANADA de microfilmer cette thèse et de prêter ou de vendre des exemplaires du film.

L'auteur se réserve les autres droits de publication, ni la thèse ni de longs extraits de celle-ci ne doivent être imprimés ou autrement reproduits sans l'autorisation écrite de l'auteur.

Date

OCTOBER 14 1983

Signature

C. J. Warren

THE UNIVERSITY OF ALBERTA

THE CHEMISTRY AND MINERALOGY OF ARTIFICIALLY WEATHERED
FLY ASH

by

CARL JAMES WARREN

A THESIS

SUBMITTED TO THE FACULTY OF GRADUATE STUDIES AND RESEARCH
IN PARTIAL FULFILMENT OF THE REQUIREMENTS FOR THE DEGREE
OF MASTER OF SCIENCE

DEPARTMENT OF SOIL SCIENCE

EDMONTON, ALBERTA

FALL 1983

THE UNIVERSITY OF ALBERTA
FACULTY OF GRADUATE STUDIES AND RESEARCH

The undersigned certify that they have read, and recommend to the Faculty of Graduate Studies and Research, for acceptance, a thesis entitled THE CHEMISTRY AND MINERALOGY OF ARTIFICIALLY WEATHERED FLY ASH submitted by CARL JAMES WARREN in partial fulfilment of the requirements for the degree of MASTER OF SCIENCE in SOIL SCIENCE.

.....
.....

Supervisor

.....
.....
.....
.....

Date... OCTOBER... 7... 1983.....

In memory of my grandfathe

U

ABSTRACT

Fly ash is produced in vast quantities by power plants as a by-product of pulverized-coal burning. In North America fly ash is usually considered a waste material and is commonly deposited in disposal sites located on or near the land's surface. Our knowledge of the solid phase reaction products resulting from fly ash weathering is deficient. This study was initiated to determine the chemical processes and mineralogical transformations which accompany the accelerated weathering of fly ash.

Two Alberta fly ashes of alkaline reactivity were artificially weathered in a series of five leaching columns using two types of acid weathering regimes (0.005 M H_2SO_4 and a mixture of 0.01 M acetic acid and 0.002 M salicylic acid). Leachates were transferred sequentially through the five column series and monitored for pH and concentration of Si, Al, Ca, Fe, Mg, K, Na, and Mn. On termination of leaching the ash residues were characterized by chemical and mineralogical methods.

Analyses indicated unreacted fly ashes consist of spherical micron-sized particles composed of mullite enclosed in a two phase glassy matrix. The ashes also contained a highly reactive inorganic phase composed of CaO seen as sub-micron sized fragments (dust-like flecks) on the surface of ash particles. Dissolution characteristics were largely dictated by the reactions of the dust-like flecks

and the glassy matrix.

Initial weathering characteristics included dissolution of soluble Na and K salts and hydrolysis of CaO flecks. Soluble forms of Na and K were either incorporated into the exterior glass matrix of the particles or occurred as discrete fragments indistinguishable from CaO flecks. A greater percentage of total Na than total K was associated with soluble salts. Hydrolysis of CaO and subsequent dissolution of Ca(OH)_2 was responsible for the extreme alkalinity of the initial leachates.

After acidification of the ashes, weathering was characterized by release of high levels of Si and Al from the external glassy matrix. The interior glass matrix was comprised primarily of Si with some Na, K, and Pb. Solid state migration and removal of Na from the glassy interior was active under acidic leaching conditions.

Three groups of minerals formed in response to weathering: those containing Ca, those containing Fe, and clays of short-range order. Calcium oxide was converted to transient Ca(OH)_2 in one of the ashes. Some Ca^{++} was precipitated through reaction with dissolved CO_2 as CaCO_3 on translocation into alkaline regions. Translocated Fe precipitated as amorphous coatings on fly ash particles. Aluminum and Si dissolved under acidic conditions precipitated in alkaline ash as an aluminosilicate of short-range order similar to proto-imogolite and allophane. In essence, fly ash weathers similar to volcanic ash.

ACKNOWLEDGEMENTS

The author would like to thank all those directly involved in the preparation of this manuscript. I would like to express sincere thanks to my supervisor, Dr. M.J. Dudas, for his guidance, encouragement, constructive comments, and endless patience throughout the entire course of this study. I have benefitted immeasurably from the experience of working with him. I would also like to thank Dr. S. Pawluk and Dr. F.J. Longstaffe for reviewing the manuscript and serving on the examining committee.

Much thanks are also extended to those university personnel who aided with the many specialized facets of this study. Mr. George Braybrook of the Department of Entomology was of great assistance with the SEM work. Mr. Jim Hoyle of the Department of Chemistry graciously generated the IR patterns. Mr. Steve Ross of the Department of Zoology aided with the TEM work. Mr. Park Yee of the Department of Soil Science was also tremendously helpful with his suggestions and assistance throughout much of the tedium in the laboratory. The author would also like to thank all those staff and students too numerous to mention whose many comments and suggestions made life in the lab and library just a little bit easier.

I would especially like to express deepest appreciation of my loving wife, Victoria, for her many sacrifices and the innumerable hours she spent alone. For her patience and

understanding I am eternally grateful.

Finally, I would like to thank the Department of Soil Science and the Natural Science and Engineering Research Council (NSERC) for their generous financial support.

Table of Contents

Chapter	Page
I. INTRODUCTION	1
II. LITERATURE REVIEW	6
A. Inorganic Components of Coal	6
Mineral Phase Impurities	7
Elemental Impurities	9
B. Particle Formation and Morphologies	10
Fly Ash Formation	12
Particle Morphologies	14
C. Collection and Particle Size Distribution	16
D. The Mineralogy of Fly Ash	18
Quartz	18
Mullite	19
Magnetic Spinels	20
Other Crystalline Species	21
Coal Fragments	22
E. The Chemistry of Fly Ash	22
Bulk Chemistry	22
Elemental Distribution	24
Dissolution Characteristics	28
Residue Characteristics	30
III. METHODS AND MATERIALS	34
A. Sample Selection	34
B. Artificial Leaching	35
Leaching Column Construction	35
Column Packing	36

Leaching	37
Leachate Analysis	39
C. Sectioning of the Core Residues	40
D. Analysis of the Core Sections	41
Total Chemical Analysis	41
X-Ray Diffraction	43
Differential Thermal Analysis	43
Electron Microscopy	44
Infrared Analysis	44
Extractions	45
Total Inorganic Carbon	45
E. Ferromagnetic Particle Analysis	45
Ferromagnetic Separation	45
Chemical Analysis	46
IV. RESULTS AND DISCUSSION	48
A. Leachate Chemistry	49
B. Residue Chemistry	70
Bulk Chemistry	70
Calcium and Magnesium	78
Sodium and Potassium	87
Silicon and Aluminum	90
Iron	92
Trace Elements	97
C. Residue Mineralogy	103
Unweathered Ash	103
Leached Residues	110
Precipitation Products	128

V. SUMMARY AND CONCLUSIONS 154
REFERENCES 162
APPENDIX 181

List of Tables

		Page
Table 1.	Quantity and core thickness of fly ash, volume of leaching solution, and corresponding number of pore volumes generated per incremental addition for each leaching column.....	39
Table 2.	Designated names and descriptions of the core sections of the weathered ash residues....	42
Table 3.	Mean concentrations of Na and K in leachate increments 16 to 30 for the first columns of the Forestburg and Sundance fly ash leaching series.....	62
Table 4.	Chemical composition of the unweathered fly ash samples.....	71
Table 5.	Percentage change in the chemical composition of weathered Forestburg fly ash relative to unweathered ash, for the 0.005 M sulfuric acid leaching regime.....	73
Table 6.	Percentage change in the chemical composition of weathered Forestburg fly ash relative to unweathered ash, for the AASA leaching regime.....	74
Table 7.	Percentage change in the chemical composition of weathered Sundance fly ash relative to unweathered ash, for the 0.005 M sulfuric acid leaching regime.....	75
Table 8.	Percentage change in the chemical composition of weathered Sundance fly ash relative to unweathered ash, for the AASA leaching regime.....	76 ³
Table 9.	Calcium carbonate equivalent of leached and unleached fly ash samples.....	84

Table 10.	Chemical characteristics of the ferromagnetic fractions separated from the unleached fly ash samples.....	96
Table 11.	Elements with concentrations in the weathered ash residues exhibiting significant correlations.....	98
Table 12.	Acid ammonium oxalate extractable Fe, Al, Si, and Mn in the leached Forestburg fly ash samples expressed as percent of the total content of each core section.....	122
Table 13.	Acid ammonium oxalate extractable Fe, Al, Si, and Mn in the leached Sundance fly ash samples expressed as percent of the total content of each core section.....	123
Table 14.	Percent loss on ignition for all leached and unleached fly ash samples.....	126

List of Appendix Tables

Page

Table 1.	Leachate pH values of the Forestburg fly ash leached with 0.005 <u>M</u> sulfuric acid.....	182
Table 2.	Concentration of Ca in the leachates of the Forestburg fly ash leached with 0.005 <u>M</u> sulfuric acid.....	183
Table 3.	Concentration of Na in the leachates of the Forestburg fly ash leached with 0.005 <u>M</u> sulfuric acid.....	184
Table 4.	Concentration of K in the leachates of the Forestburg fly ash leached with 0.005 <u>M</u> sulfuric acid.....	185
Table 5.	Concentration of Mg in the leachates of the Forestburg fly ash leached with 0.005 <u>M</u> sulfuric acid.....	186
Table 6.	Concentration of Fe in the leachates of the Forestburg fly ash leached with 0.005 <u>M</u> sulfuric acid.....	187
Table 7.	Concentration of Mn in the leachates of the Forestburg fly ash leached with 0.005 <u>M</u> sulfuric acid.....	188
Table 8.	Concentration of Al in the leachates of the Forestburg fly ash leached with 0.005 <u>M</u> sulfuric acid.....	189
Table 9.	Concentration of Si in the leachates of the Forestburg fly ash leached with 0.005 <u>M</u> sulfuric acid.....	189
Table 10.	Leachate pH values of the Sundance fly ash leached with 0.005 <u>M</u> sulfuric acid.....	190

Table 11.	Concentration of Ca in the leachates of the Sundance fly ash leached with 0.005 <u>M</u> sulfuric acid.....	191
Table 12.	Concentration of Na in the leachates of the Sundance fly ash leached with 0.005 <u>M</u> sulfuric acid.....	192
Table 13.	Concentration of K in the leachates of the Sundance fly ash leached with 0.005 <u>M</u> sulfuric acid.....	193
Table 14.	Concentration of Mg in the leachates of the Sundance fly ash leached with 0.005 <u>M</u> sulfuric acid.....	194
Table 15.	Concentration of Fe in the leachates of the Sundance fly ash leached with 0.005 <u>M</u> sulfuric acid.....	195
Table 16.	Concentration of Mn in the leachates of the Sundance fly ash leached with 0.005 <u>M</u> sulfuric acid.....	196
Table 17.	Concentration of Al in the leachates of the Sundance fly ash leached with 0.005 <u>M</u> sulfuric acid.....	197
Table 18.	Concentration of Si in the leachates of the Sundance fly ash leached with 0.005 <u>M</u> sulfuric acid.....	197
Table 19.	Leachate pH values of the Forestburg fly ash leached with AASA solution.....	198
Table 20.	Concentration of Ca in the leachates of the Forestburg fly ash leached with AASA solution.	199
Table 21.	Concentration of Na in the leachates of the Forestburg fly ash leached with AASA solution.	200
Table 22.	Concentration of K in the leachates of the Forestburg fly ash leached with AASA solution.	201

Table 23.	Concentration of Mg in the leachates of the Forestburg fly ash leached with AASA solution.	202
Table 24.	Concentration of Fe in the leachates of the Forestburg fly ash leached with AASA solution.	203
Table 25.	Concentration of Mn in the leachates of the Forestburg fly ash leached with AASA solution.	204
Table 26.	Concentration of Al in the leachates of the Forestburg fly ash leached with AASA solution.	205
Table 27.	Concentration of Si in the leachates of the Forestburg fly ash leached with AASA solution.	205
Table 28.	Leachate pH values of the Sundance fly ash leached with AASA solution.	206
Table 29.	Concentration of Ca in the leachates of the Sundance fly ash leached with AASA solution.	207
Table 30.	Concentration of Na in the leachates of the Sundance fly ash leached with AASA solution.	208
Table 31.	Concentration of K in the leachates of the Sundance fly ash leached with AASA solution.	209
Table 32.	Concentration of Mg in the leachates of the Sundance fly ash leached with AASA solution.	210
Table 33.	Concentration of Fe in the leachates of the Sundance fly ash leached with AASA solution.	211
Table 34.	Concentration of Mn in the leachates of the Sundance fly ash leached with AASA solution.	212
Table 35.	Concentration of Al in the leachates of the Sundance fly ash leached with AASA solution.	213
Table 36.	Concentration of Si in the leachates of the Sundance fly ash leached with AASA solution.	213

Table 37.	Chemical composition of the Forestburg fly ash after leaching with 0.005 M H ₂ SO ₄	214
Table 38.	Chemical composition of the Forestburg fly ash after leaching with AASA solution.....	215
Table 39.	Chemical composition of the Sundance fly ash after leaching with 0.005 M H ₂ SO ₄	216
Table 40.	Chemical composition of the Sundance fly ash after leaching with AASA solution.....	217
Table 41.	Correlation matrix of the chemical components in the weathered Forestburg ash samples.....	218
Table 42.	Correlation matrix of the chemical components in the weathered Sundance ash samples.....	219
Table 43.	Percent acid ammonium oxalate and citrate-bicarbonate-dithionite extractable Fe, Al, Si, and Mn in the 0.005 M H ₂ SO ₄ leached Forestburg fly ash.....	220
Table 44.	Percent acid ammonium oxalate and citrate-bicarbonate-dithionite extractable Fe, Al, Si, and Mn in the 0.005 M H ₂ SO ₄ leached Sundance fly ash.....	221
Table 45.	Percent acid ammonium oxalate and citrate-bicarbonate-dithionite extractable Fe, Al, Si, and Mn in the AASA leached Forestburg fly ash.....	222
Table 46.	Percent acid ammonium oxalate and citrate-bicarbonate-dithionite extractable Fe, Al, Si, and Mn in the AASA leached Sundance fly ash.....	223

List of Figures

Page

Figure 1.	Leachate pH values of the Forestburg and Sundance fly ashes leached with 0.005 M H_2SO_4 .	51
Figure 2.	Leachate pH values of the Forestburg and Sundance fly ashes leached with AASA solution.	52
Figure 3.	Concentration of Ca in the leachates of the Forestburg and Sundance fly ashes leached with 0.005 M H_2SO_4 .	55
Figure 4.	Concentration of Ca in the leachates of the Forestburg and Sundance fly ashes leached with AASA solution.	56
Figure 5.	Concentration of Mg in the leachates of the Forestburg and Sundance fly ashes leached with AASA solution.	58
Figure 6.	Concentration of Na and K in the leachates of the Forestburg fly ash leached with AASA solution.	60
Figure 7.	Concentration of Na and K in the leachates of the Forestburg fly ash leached with 0.005 M H_2SO_4 .	61
Figure 8.	Concentration of Si and Al in the leachates of the Forestburg fly ash leached with 0.005 M H_2SO_4 .	64
Figure 9.	Concentration of Si and Al in the leachates of the Sundance fly ash leached with 0.005 M H_2SO_4 .	65
Figure 10.	Concentration of Fe and Mn in the leachates of the Sundance fly ash leached with AASA solution.	69

Figure 11.	X-ray diffractograms of the unweathered Forestburg and Sundance fly ash samples and their respective ferromagnetic fractions.....	104
Figure 12.	Infrared spectra of the unweathered Forestburg ash and surface core sections from the first columns of the AASA leached Sundance ash and the 0.005 M H ₂ SO ₄ leached Forestburg ash.....	109
Figure 13.	X-ray diffractograms of the three ash core sections from column one of the Sundance ash leached with 0.005 M H ₂ SO ₄	117
Figure 14.	DTA patterns for selected weathered and unweathered fly ash samples.....	125
Figure 15.	X-ray diffractograms of the surface precipitates from columns two, three, and four of the 0.005 M H ₂ SO ₄ leached Forestburg ash.....	130
Figure 16.	X-ray diffractograms of the surface precipitates from columns two, three, and four of the AASA leached Sundance ash.....	131
Figure 17.	Infrared spectra of the surface precipitates from the second column of the Forestburg ash and the fifth column of the Sundance ash for the H ₂ SO ₄ weathering regime.....	135
Figure 18.	Infrared spectra of the surface precipitates from the third columns of the H ₂ SO ₄ leached, and AASA leached Forestburg ash.....	137

List of Photographic Plates

Page

- Plate 1. Scanning electron micrographs and energy dispersive spectra of particles of the unweathered fly ash samples.....107
- Plate 2. Scanning electron micrographs and energy dispersive spectra of particles of some 1% HF etched fly ash particles and some weathered fly ash particles.....114
- Plate 3. Scanning electron micrographs of some calcium-rich precipitates from selected weathered ash samples.....133
- Plate 4. Scanning electron micrographs of precipitation products from selected weathered ash core sections.....141
- Plate 5. Transmission electron micrographs of material in the surface precipitate sample from the third column of the 0.005 M H_2SO_4 leached Forestburg ash series.....152

I. INTRODUCTION

The amount of coal used to produce thermal electric power has increased substantially over the last few decades. In the United States where coal is the major source of energy used for electrical power generation, consumption has approximately doubled every decade since the mid 1930's to levels of over 600 million tonnes annually since 1978 (White 1977a; Torrey 1978). Similiar increases have occurred in most areas of the world. Consumption in Alberta has tripled in the last decade from 4.0 million tonnes in 1972 to an estimated 12.0 million tonnes in 1982 (ERCB 1982a).

Coal usage is projected to increase further over the next twenty years. Coal is expected to supply one-half to two-thirds of the world's additional energy requirements between 1980 and 2000 (Greene and Gallagher 1980). United States utilities are expected to consume approximately 1.8 billion tonnes annually by the turn of the century (Gordon 1978; Greene and Gallagher 1980). Projections for Alberta indicate annual consumption will reach 21.0 million tonnes by the year 2000 (ERCB 1982b). These predictions are conservative and based on moderate energy growth assumptions.

Coal combustion generates a variety of by-products, many of environmental concern. Gaseous by-products include SO_x and NO_x compounds and a large assortment of other organic and inorganic vapours suspected of being

environmentally hazardous. Solid residues of coal combustion include coal ash, which is derived mainly from the noncombustible residues in coal, and flue gas desulfurization sludges (Bern 1976). Coal ash is generated in the largest quantities and is ranked ninth in abundance among solid minerals produced in the United States (Meikle 1975).

Most coal-fired electrical utilities employ a pulverized coal burning process which generates two fractions of coal ash. The process involves the injection of finely ground coal into a boiler-furnace combustion chamber. Fragments of noncombustible inorganic material are included with the finely divided coal and during combustion fuse to form coal ash. Some of the ash fuses into large aggregates which fall to the furnace bottom while the remainder, usually comprising the bulk, is carried out of the furnace entrained as finely divided particles in the flue gases. The ash falling to the furnace bottom is termed bottom ash, if retrieved as a solid residue, or boiler slag if removed in the molten state. The finely divided ash fraction suspended in the flue gases is referred to as fly ash and generally accounts for between 10% to 20% of coal by weight. On average, fly ash comprises about 70% of all coal ash residues produced by most large (>480MW) boiler-furnace units (Bern 1976; Torrey 1978).

Fly ash presents a number of environmental problems related to its inherent chemistry. Fly ash is comprised of

micron-sized spherical particles largely composed of Si and Al. During combustion various inorganic components dispersed within the coal are volatilized and subsequently condense on fused silicate material to form the ash. Most trace elements, particularly those of higher volatility, become concentrated in and on the fly ash. Concentrations are commonly many times greater than the levels in the parent coals. Some of these elements are potentially noxious if mobilized from ash and released into the environment.

Power plants are required by government regulation to control fly ash emissions. Without collection devices fly ash would be discharged as an aerosol into the atmosphere with the flue gases. A variety of particulate control systems have been developed to collect fly ash particles entrained in flue gas streams. Most systems currently in use are extremely efficient; retaining in most cases close to 100% of the fly ash generated by power plants.

Fly ash is utilized in the production of concrete and road asphalt, and as an ameliorant for some soils and acid mine spoils. Other uses have also been suggested such as a source of industrial iron and aluminum and as a source of mullite for the ceramic industry. At present all uses account for only 10 to 20% of the total amount of fly ash annually produced in North America (Rohrman 1971). Most of the fly ash produced by electrical utilities is therefore regarded as a waste material requiring disposal.

Present methods of fly ash disposal include dry surface dumping, burial, and slurry-lagoon disposal. These methods have been used extensively in the past and appear to be the primary method of disposal for the future. All methods of disposal are similar. The ash is deposited on or within close proximity to the land's surface. Questions have been raised as to the possible hazards presented through the mobilization of some fly ash components from disposal sites. Contamination of ground or surface waters may result from the release of elements such as boron, arsenic, or heavy metals. Problems may also arise because of dissolution of large quantities of soluble salts or generation of extreme alkalinity. Problems such as nutrient imbalances and availability may also occur when fly ash is used as a soil amendment.

Current research on the environmental impact of fly ash centres on the dissolution of fly ash components and the chemical and physical characterization of unreacted fly ash particles. These studies have focused on aqueous leachate characteristics and the association of major constituent elements with soluble and insoluble ash fractions.

Studies have yet to be conducted on solid phase transformations, reactions, and the formation of secondary minerals which accompany the weathering of fly ash. Such studies would provide new information regarding the association of potentially noxious constituents with major phases of fly ash and provide a clear insight as to the

potential release and mobility of these constituents during weathering.

Knowledge of the solid phase reaction products of weathering is extremely limited yet crucial to our understanding of the behaviour of fly ash in the terrestrial environment. Accordingly, the present study was approached with the following objective in mind:

To determine the major chemical processes and mineralogical transformations that accompany the artificial weathering of fly ash.

II. LITERATURE REVIEW

The physical and chemical characteristics of fly ash are dictated mainly by the chemical content of the parent coal and the mechanics of formation during combustion. The weathering behaviour of fly ash is consequently also dependent on these parameters. Accordingly, the objective of this review is to outline the factors contributing to the composition, fundamental characteristics, and related chemical weathering behaviour of fly ash.

A. Inorganic Components of Coal

Coal varies in its characteristics and chemical content according to its geologic history. Coal fields formed from ancient peat swamps that were buried and subjected to intense heat and pressure over geologic time. The inherent properties of coal are continually developed from the time of burial. The composition and quantity of inorganic impurities in coal are therefore also largely determined by the conditions of deposition and diagenesis.

All coals contain inorganic impurities intimately mixed with the combustible organic material. These impurities are responsible for the production of coal ash. Ash residues produced from thermal coals generally range from 3 to 30% of coal by weight (Torrey 1978). Inorganic impurities encompass all noncoal materials including mineral phases and elements considered to be inorganic (Gluskoter 1975). Coal

impurities can be classified into three categories: finely disseminated inclusions observed as tiny pockets within the coal matrix, discrete mineral grains, and inorganic elements bound in organic combination (Shibaoke and Ramsden 1978; Smith 1980). Rock and mineral inclusions constitute the majority of the residues contributing to fly ash. Organically bound elements play an important role in the ash chemistry.

Mineral Phase Impurities

Rock and mineral fragments become incorporated into coal during both sedimentation and diagenesis. Some of the material is derived from inorganic constituents contained in the original coal-forming plants. Included matter is mostly derived from clay-sized detrital particles deposited by sedimentation with the decaying organic matter. Other included minerals such as sulfides and carbonates are authigenic, forming in the coal through precipitation of dissolved groundwater constituents (Shibaoke and Ramsden 1978). Larger mineral grains and rock fragments are strictly detritus, incorporated as individually sedimented grains or as thin discontinuous layers of strata within the coal seam. The practice of including thin layers of mineral strata as well as other overburden materials with the coal during mining substantially increases the ash content of many coals (Torrey 1978).

The vast majority of minerals found in coal fall into one of the following groups (Watt and Thorne 1965; Gluskoter 1978):

1. Aluminosilicates
2. Sulfides
3. Carbonates
4. Silica (Quartz)
5. Accessory minerals

Of these five groups aluminosilicate clays are the most abundant, constituting up to 50% of the mineral matter found in coal. The most frequently reported clay minerals are kaolinites, smectites, and micas (Gluskoter 1975, 1978). The ingredients of clays therefore make up a large portion of coal ash.

Pyrite (FeS_2) is the dominant sulfide mineral found in coal. Marcasite, a dimorph of pyrite, has also been reported as well as a multitude of other metal sulfides (Gluskoter 1978). Isomorphous substitution of many chalcophylic elements for Fe in pyrite is also common.

Sulfides form authigenically in coal under strongly reducing conditions. Sulfur is released from the organic matrix to precipitate with iron (Fe^{2+}) or other dissolved metals. The presence of sulfides in coal is usually responsible for most SO_x emissions and high concentrations of toxic elements (e.g. As, Cd, and Pb) in the ash (Gluskoter 1975)

Carbonates found in coal exhibit wide ranges in composition. Solid solutions of Ca, Mg, Fe, and Mn are possible. The end members calcite (CaCO_3) and siderite (FeCO_3) are frequently reported; however, dolomite ($\text{Ca,Mg}(\text{CO}_3)_2$) and ankerite ($\text{Ca,(Mg,Fe}^{2+},\text{Mn)}(\text{CO}_3)_2$) constitute the majority of carbonates found in coals (Gluskoter 1978). Carbonates are primarily responsible for the Ca and Mg contents in fly ash (Fisher et al. 1978).

Quartz is ubiquitous in coals and appears to be the only form of silica found in coals. Approximately 15% of the mineral matter in coal is usually quartz, although reported contents range from 1% to 20% (Gluskoter 1978). Quartz is usually observed as discrete mineral grains in coal.

Accessory minerals are those minerals found in very minute quantities. These include feldspars, amphiboles, and an assortment of highly resistant minerals. Contributions to the composition of the ash from these minerals are in most cases negligible (Watt and Thorne 1965).

Elemental Impurities

Coal contains high concentrations of many trace elements compared to crustal abundances (Kronberg et al. 1981). Organically bound inorganic elements are incorporated into coal through two main processes. Inorganic elements are initially taken up by the coal-forming plants and retained during coalification or

they are incorporated later, during diagenesis, through complexation and retention by the coal organics. Metals, dissolved in groundwater passing through the coal seam, are particularly susceptible to organic complexation. Depletion or enrichment of specific elements may occur over time depending on the groundwater composition, the chemistry of the element, and the oxidation-reduction conditions in the coal seam (Smith 1980).

Some elements exhibit a high affinity for either the organic or inorganic fractions of the coal while others do not. The elements B, Be, Ge and Sb have been shown to be highly associated with coal organic fractions. Ba, Co, Cr, Hf, Pb, Rb, Sc, Sr, and Tl are elements strongly associated with mineral phases. Most other elements (e.g. As, Cd, Cu, Ga, Hg, Mn, Mo, Ni, Ti, Se, V, and Zn) show varying degrees of intermediate affinity (Gluskoter 1975; Block and Dams 1976).

The main contribution of the parent coal to the make up of fly ash is its constituent inorganic elements. The assemblage of these constituents into fly ash particles is controlled through combustion processes.

B. Particle Formation and Morphologies

The highly complex process of coal combustion controls many variables influencing the formation of fly ash particles. On a localized basis both oxygen availability and temperature are very diverse in a boiler-furnace. Wide

ranges in mineral melting points, phase transitions, and decomposition temperatures further complicate ash formation (Shibaoke and Ramsden 1978). The fate of a noncombustible fragment traveling through a pulverized coal furnace is therefore dependent on a large number of poorly definable variables.

Many coal combustion processes are available to the electrical industry. Pulverized coal combustion is the most popular process mainly because it presently provides the most efficient method of releasing the chemical energy bound within coal. In preparation for pulverized combustion coal is crushed or pulverized to an extremely small particle size (35 to 75 μ m) to obtain a large surface area per unit mass (Smith 1980). The fine coal particles are then blown into suspension with preheated air and injected into the furnace. Secondary and tertiary additions of air are usually made to aid in combustion (White 1977b; Torrey 1978). The coal is ignited in suspension consuming the oxygen provided to produce a diffuse flame. Continuous furnace injection sustains continuous combustion (Smith 1980).

On injection into the furnace pulverized coal particles act in diverse ways. Particles of a variety of sizes, ash contents and chemical compositions are consumed at different rates and for different durations. The resultant temperature pattern in the furnace generally takes the form of two overlapping combustion zones. The first zone, located adjacent to the injection port, is of relatively

high temperature. This zone forms as a result of very rapid combustion of highly volatile organics on immediate entry into the furnace. The second zone is a more diffuse lower temperature zone where less volatile organics are consumed at a much slower rate. The temperatures encountered in the furnace usually range from above 1600°C in the high temperature zone to as low as 1000°C in the outer reaches of the low temperature zone (Shibaoke and Ramsden 1978).

Fly Ash Formation

Most fly ash particles are derived from included mineral matter. As the coal particles combust and are consumed, fusion of the included mineral matter takes place just behind the combustion fronts. As the melting points of the included minerals are exceeded, they transform into small spherical droplets of molten ash. The spherical shape develops as a result of surface tension (Raask 1969). The transformation is extremely rapid, usually occurring in less than a second. Quenching occurs while the particles are in suspension exiting from the low temperature combustion zone. Most fly ash particles are therefore vitreous spheres composed primarily of amorphous aluminosilicate glass.

The size of fly ash particles depends on both the amount of inorganic material available and the temperature zone into which the material is released. Larger particles form as a result of coalescence of smaller droplets (Ramsden 1969). In the high temperature zone small droplets of

molten ash are freed quickly from the coal matrix. Release of the molten ash into an environment where the temperature is much higher than the ash fusion temperature allows time for the small droplets to coalesce into larger droplets before quenching occurs. In the low temperature combustion zone, droplet release takes place at a much slower rate. Droplets are released into a thermal environment closer to the fusion temperature of the ash and therefore they do not have time to coalesce extensively before solidification. As a result, particles formed in the low temperature zone are usually smaller than those formed in the high temperature zone of the furnace (Ramsden 1969; Shibaoka and Ramsden 1978).

Some smaller discrete mineral fragments also form spherical fly ash particles. Discrete mineral particles not in immediate contact with carbonaceous material tend to be subjected to lower temperatures compared to included mineral material. Many discrete mineral grains therefore undergo only partial fusion. The degree of fusion depends on the size and composition of the mineral grain and the temperatures in its immediate vicinity. Due to the short residence time in the furnace only small fragments with low heat capacities undergo total fusion. Exceptionally large particles are most susceptible to partial fusion; however, these tend to fall out as bottom ash or slag and do not become part of the fly ash fraction (Shibaoka and Ramsden 1978).

Particle Morphologies

More than 90% of the particles in most fly ashes have spherical morphologies (Fisher et al. 1978). However, a number of distinct fly ash particle morphologies, including glassy spheres, have been identified. Classification systems of particle morphologies are based not only on shape but also degree of transparency, colour, and associated mineralogies. Most classification schemes usually identify only four or five morphological classes (e.g. Natusch et al. 1975). Fisher et al. (1978) described eleven morphological particle types and quantified them in relation to four size fractions. Morphological classes included opaque, nonopaque, vesicular, rounded, and hollow particle types. All morphological types tended to increase in occurrence with increasing particle size except for the most common morphological type (nonopaque solid spheres) which showed the opposite trend. Larger particles tended to exhibit much more irregularity in morphologies mostly because of partial fusion and coalescence of the larger materials they are derived from.

One of the oddities in the mechanics of fly ash particle formation is the production of hollow spheres commonly known as cenospheres (Gr. hollow-sphere) (Raask 1968). These thin-walled, bubble-like, low bulk density ($0.4 - 0.6 \text{ g cm}^{-3}$) particles average between one to two percent by volume of most fly ashes and are commonly observed floating on the surface of ash slurry ponds. The

formation mechanism for these particles is not well understood although production seems to be highly correlated with furnace temperature and iron content of the ash. A dramatic increase in cenosphere production, up to 20% by volume, generally occurs when the Fe_2O_3 content of the ash exceeds 8%. Optimum cenosphere formation temperatures reported range from 1200°C to 1400°C (Raask 1968; Sarofim et al. 1977)

Some cenosphere-type particles have been found to encapsulate a number (5 to 100) of smaller spherical particles, usually $<1\mu\text{m}$ in diameter. The term plerosphere (Gr. full-sphere) has been used to describe this morphology (Fisher et al. 1976). The mechanism of formation is similar to that of cenospheres except, instead of being entirely hollow, the encapsulated spheres form within the host particle through budding off of molten material from the inside walls (Natusch et al. 1975). Recent observations indicate plerospheres are relatively rare compared to the amount of cenospheres present in most ashes (Carpenter et al. 1980).

On leaving the furnace, fly ash contains a variety of particle sizes and morphologies. The vast majority of the particles are solid spheres formed from rapid melting, coalescence and fusion of the small fragments of mineral matter included in the coal matrix. A small percentage of particles may form as cenospheres or plerospheres. Fragments of unburnt coal and partially fused mineral

matter also form part of the ash. The size distribution of particles is mainly predetermined by the distribution and characteristics of the intrinsic impurities in the source coal; however, the mode of collection also has some influence on the particle size distribution.

C. Collection and Particle Size Distribution

All modern coal-fired electrical generating units are equipped with particulate control equipment designed to comply with government emission regulations. The major types of devices in use are cyclone collectors, electrostatic precipitators, wet scrubbers and bag houses. All have varying abilities to collect fly ash. The choice and design of a collection device or combination of devices is plant specific and usually based on a balance between collection and cost efficiencies (Levy et al. 1980).

Electrostatic precipitators (ESPs) are the most common and efficient particulate control device used in large pulverized-coal-fired installations (Levy et al. 1980). Maximum collection efficiencies for most modern ESPs are about 99.8% (White 1977a). A typical particle size distribution for ESP fly ash is about 4% clay-size (<2 μ m), 70% silt-size (2-50 μ m), 20% very fine sand-size (50-100 μ m), and 6% medium and fine sand-size (100-500 μ m) (Torrey 1978). The majority of the particles fall within the silt-size range. Most large particles (>200-300 μ m) do not become entrained in the flue gases, but rather fall to the bottom

of the boiler-furnace with the bottom ash fraction. This mechanism limits the inclusion of large ash particles in the fly ash fraction. The quantity of very small fly ash particles collected is mainly determined by the ability of the individual ESP to collect fine particles.

The inability to efficiently collect very small fly ash particles is the major drawback of ESPs. Usually >40% of the fly ash particles produced through pulverized-coal combustion are <10 μ m in diameter (White 1977b). ESP efficiencies begin to decline with decreasing particle size fractions below 20 μ m (Biermann and Ondov 1980) and are highly inefficient at collecting particles of <1 μ m. Increasing the efficiency of submicron-sized particle collection is a major concern of the electrical power industry (White 1977a). Combining ESPs with other collection devices (e.g. wet scrubbers) usually improves the collection efficiency of finer particle sizes; however, no device has yet been developed which is extremely efficient at retaining submicron particles (Vandegrift et al. 1973).

The labeling of fly ash with respect to its collection status has caused some confusion. Fly ash removed from flue gas streams is usually specifically referred to as fly ash in North America and is differentiated from "stack-emitted" or "emitted" fly ash by utilizing these qualifying terms. In some European countries collected fly ash may be referred to as "precipitator ash" or "coal ash" while emitted or uncollected fractions are referred to as "fly ash". In the

present study fly ash or ash will be utilized in the North American context and meant to refer to the collected variety unless specified otherwise.

D. The Mineralogy of Fly Ash

Fly ash particles are composed primarily of amorphous glass. Watt and Thorne (1965) estimated the glass content of British fly ashes to range between 71% and 80%. Similar estimates have been made for United States fly ashes (Hulett et al. 1979). The glass content of particles tends to increase with decreasing particle size (Torrey 1978). Crystalline mineral species occurring either dispersed within the matrix of amorphous glass particles or as discrete particles comprise the remainder of the ash. A variety of crystalline species have been reported; however, only a few are observed consistently.

Quartz

The crystalline mineral most commonly found in fly ash is α -quartz (α -SiO₂). Quantities range from 10 to 6.5% (Simons and Jeffery 1960). It is generally thought that the quartz in fly ash is derived directly from quartz inclusions in the parent coals. The melting point of α -quartz (1387°C) and its phase transition point to β -quartz (573°C) are well within the operational temperature range of most boiler-furnaces. Small quartz particles in the parent coals seem to undergo fusion since only large discrete mineral

grains (>50um) are commonly observed in fly ash. Larger quartz grains exhibit partial fusion of sharp edges. Residence time in the furnace, particularly in the high temperature zone, is apparently not sufficient enough to produce total fusion of the larger particles (Raask 1969). Phase transformations of α -quartz may occur in the boiler-furnace but are not apparent since β -quartz or the high temperature polymorphs, cristobolite and tridymite, have not been observed in fly ash. Hulett and Weinberger (1980) found quartz exhibiting a coral-like morphology inside some spherical fly ash particles. The external glass had been removed with 1% HF. Recrystallization of the quartz was not ruled out in this case because traces (2%) of Al were detected in the material.

Mullite

Mullite ($3\text{Al}_2\text{O}_3 \cdot 2\text{SiO}_2$) is also a commonly reported mineral species in fly ash. Simons and Jeffery (1960) determined, by X-ray diffraction methods, the amount of mullite in most British ashes to be in the range of 9% to 35% while eastern United States ashes of similar composition contained a maximum of only 16% mullite. Mullite does not occur naturally in coal. Its presence in fly ash is a result of crystallization during rapid cooling of aluminosilicate melts (Hansen et al. 1981).

Fisher and co-workers (1978) observed "quench crystals" located on the surface and/or in the interior of a number of

transparent spherical particles. Hulett and co-workers (1979) later found mullite crystals located within the glass matrix of most solid spherical fly ash particle as a network of interlaced acicular crystals. These crystal networks were found to retain the overall shape of the original fly ash spheres after the surrounding amorphous glassy material was selectively dissolved with a 1% HF solution. Mullite crystals displaying a chunky crystal habit were also observed in some etched particles (Hulett et al. 1979). The amount of mullite found in the ashes ranged from 28% to 41% by weight of the spherical ash particles (Hulett et al. 1980; Hulett and Weinberger 1980). Mullite therefore constitutes a significant fraction of most fly ashes.

Magnetic Spinels

A third mineral species commonly mentioned among the crystalline suites found in fly ashes is an iron-rich spinel. Spinels in fly ash generally take the form of discrete black opaque spheres that are ferromagnetic in nature and yield X-ray diffraction patterns commonly identified as magnetite (Fe_3O_4). The occurrence of spinel in fly ash seems highly correlated with the pyrite content of the parent coal (Lauf et al. 1982). Hulett et al. (1979) found approximately 10% hematite ($\alpha\text{-Fe}_2\text{O}_3$) and smaller amounts of another unidentified mineral, most likely maghemite ($\gamma\text{-Fe}_2\text{O}_3$) as reported by Hansen et al. (1981), in the magnetically separated fractions of an iron-rich fly

ash. This magnetically separable material was further found to be highly substituted in Al with an approximate composition of $\text{Fe}_{2.3}\text{Al}_{0.7}\text{O}_4$, corresponding more closely to the composition of a ferrite than magnetite. Lattice constants for the particles were also found to closely resemble ferrite (Hulett et al. 1979). Lauf and co-workers (1982) used the term "ferrosphere" to describe magnetically separable fly ash particles; however, the term has not gained wide acceptance.

Other Crystalline Species

Mullite, α -quartz and spinel are the crystalline minerals most commonly reported in almost all fly ashes. Identification is achieved mostly by X-ray diffraction of bulk ash samples. Spinel is only observed in bulk samples containing extremely high Fe contents. Low Fe samples require prior separation of ferromagnetics before the spinels can be detected by X-ray diffraction. Hematite and maghemite are reported consistently only in samples containing large quantities of spinels.

Simons and Jeffery (1960) reported the presence of minor amounts of gypsum ($\text{CaSO}_4 \cdot 2\text{H}_2\text{O}$), anhydrite (CaSO_4), lime (CaO), dicalcium ferrite ($2\text{CaO} \cdot \text{Fe}_2\text{O}_3$), anatase (TiO_2), and γ -alumina ($\gamma\text{-Al}_2\text{O}_3$) in fly ashes. Mattigod (1982) recently identified discrete zircon (ZrSiO_4) and lime (CaO) particles in the heavy mineral fraction of a fly ash. Occurrence of these and other miscellaneous mineral species

appear to be limited to individual ashes or they may constitute only extremely minor fractions of most ashes and cannot be detected by X-ray diffraction methods.

Coal Fragments

One of the components of fly ash often overlooked is unburnt coal. Combustion of all the carbonaceous material in coal is seldom achieved. Incomplete combustion results in the inclusion of carbon fragments as part of the ash. A slight increase in fly ash carbon content tends to darken the overall colour of the ash although the total carbon content does not usually exceed a few percent (Torrey 1978). Most unburnt coal particles are found in the larger size fractions (10 to 300um) and appear mostly as miniature coal particles or low density sponge-like or lace-like fragments (White 1977b).

E. The Chemistry of Fly Ash

Bulk Chemistry

Fly ash contains quantities of every naturally occurring element. The components constituting the bulk (>90%) of most fly ashes are the oxides of Si, Al, Fe, and Ca. The oxides of Mg, K, Na, Ti, and in some cases S, constitute minor components. All other elements occur in trace quantities (parts per million) and together rarely exceed one percent of the bulk ash (Natusch et al. 1975;

Torrey 1978).

The concentration of major and minor elements in fly ash (O, Si, Al, Fe, Ca, Mg, Na, K, Ti, S) are usually close to crustal abundances (Block and Dams 1975a). SiO_2 and Al_2O_3 make up the largest fraction (>50%) of most ashes. SiO_2 generally exceeds Al_2O_3 in quantity. The Al:Si ratio of the bulk ash usually reflects the composition of the prominent clay mineral in the source coal. Fe_2O_3 and CaO usually occur in lower concentrations than SiO_2 and Al_2O_3 , but in some cases Fe_2O_3 will exceed Al_2O_3 contents. Iron and Ca are generally associated with the chemical reactivity of fly ashes (Theis and Wirth 1977). Ash derived from subbituminous and lignite coals generally contain larger quantities of Ca and related alkali and alkaline earth elements and are alkaline in reaction while ashes derived from bituminous coals are richer in Fe and associated metals and semimetals and are acidic in reaction.

Unlike the major components, the content of trace elements in fly ash are substantially enriched with respect to crustal abundances. The main reason for enrichment is that coal itself is usually enriched in a large number of trace elements (Kronberg et al. 1981). Of the elements that normally occur in trace levels in terrestrial material the most abundant in fly ash are Ba and Sr. Concentrations of these two elements in many cases exceed 0.1% of the bulk ash. Concentrations of $>100\text{ug}\cdot\text{g}^{-1}$ are often obtained for B, Ce, Cr, Cu, Mn, Rb, and V. The elements As, Cl, Co, Ga, Mo,

Ni, Pb, Sc, Se, Sm, Sn, Th, and Zn are usually present in the 10-100 $\mu\text{g}\cdot\text{g}^{-1}$ range and Br, Cd, Cs, F, Hf, I, La, Sb, Ta, U, W, and Yb fall within the 1-10 $\mu\text{g}\cdot\text{g}^{-1}$ range. Levels of Au, Hg, In, and Lu do not commonly exceed 1 $\mu\text{g}\cdot\text{g}^{-1}$ (Furr et al. 1977).

Elemental Distribution

The major and minor elements in fly ash are heterogeneously distributed among the particles. Many elements are preferentially concentrated in some particles; for example Fe in ferromagnetic particles (Hayes et al. 1978; Smith 1980). Chemical heterogeneity is derived mainly from the differences in compositions of the individual minerals forming the ash particles (Smith 1980). Heterogeneity also exists within individual fly ash particles. For example much of the Al_2O_3 may be located within the mullite ($3\text{Al}_2\text{O}_3\cdot 2\text{SiO}_2$) crystals contained within most spherical ash particles. Incongruent crystallization of the mullite within the molten ash droplets leaves the glassy matrix Al_2O_3 poor and SiO_2 rich (Hulett et al. 1979).

It has also been determined that many elements, particularly volatile trace elements, are preferentially enriched in small fly ash particles. Davidson et al. (1974) found particles in the range of 1.1 to 2.1 μm diameter to be preferentially enriched by a number of orders of magnitude over >54 μm diameter particles in As, Cd, Cr, Ni, Pb, Sb, Se, Tl, and Zn. High temperature volatilization and

either condensation or sorption onto entrained particle surfaces were outlined as the reason for enrichment. Smaller fly ash particles have larger surface areas per unit mass than larger particles. The smaller particle fractions therefore contain a greater quantity of volatilized constituents, assuming even distribution on all particle surfaces during condensation.

Several observations have supported and/or developed on the volatilization-condensation theory of Davidson et al. (1974). Many authors have also observed concentration dependence on particle size (e.g. Natusch and Wallace 1974; Kaakinlen et al. 1975; Klein et al. 1975; Lee et al. 1975; Schwitzgerbel et al. 1975; Block and Dams 1976; Gladney 1976; Coles et al. 1978). Special surface characterization techniques have determined that a number of elements (Be, Ca, Cr, K, Na, Pb, S, V, and Zn) are enriched on fly ash particle surfaces (Linton et al. 1976; Linton et al. 1977). Natusch et al. (1975) estimated the surface enrichment layer on most particles to be approximately 1000Å thick. Smith et al. (1979a) speculated that some extremely small (<0.1µm) fly ash particles may even be composed exclusively of volatilized elements. Formation of these minute particles is believed due to homogeneous nucleation and condensation of volatilized elements from the gas stream as supersaturation levels are reached with respect to temperature during cooling (Markowski et al. 1980; Quann et al. 1982).

The elements most frequently reported as being surface enriched and to exhibit decreasing particle size concentration dependence are As, Cd, Pb, Sb, Se, Th, and Zn. These elements or their compounds all have boiling points of $<1600^{\circ}\text{C}$ (Natusch et al. 1975). Sarofim et al. (1977) found that up to 4% of the total Si in fly ash may also be volatilized, possibly through the formation of volatile silicon monoxide (SiO) from Si-C reactions. All elements exhibit some degree of volatilization during coal combustion; the extent is determined by the physiochemical properties of the elements and/or the compounds in which they occur in the coal (Kaakinen et al. 1975).

The distribution of elements in fly ash in relation to volatilization can be classified into four categories:

1. Elements that are extremely volatile and to a large degree do not condense onto fly ash particle surfaces at flue gas temperatures.

These include the elements Hg and Se of which approximately 10% and 50% respectively of the total in the parent coal become associated with the fly ash. The remainders are emitted as vapours (Billings and Matson 1972; Billings et al. 1973; Andren et al. 1975; Kalb 1975; Anderson and Smith 1977).

2. Elements that are easily volatilized, but condense on particle surfaces, and are highly enriched in fine particle fractions.

These elements include As, Cd, Cu, Ga, Mo, Pb, Sb, and Zn

(Klein et al. 1975; Natusch et al. 1975; Kaakinin et al. 1975).

3. Elements that are only partially volatilized and are located both within the ash matrix and on particle surfaces.

These elements include Ca, Cr, K, Mg, Na, Ni, Sc, U, and V (Klein et al. 1975).

4. Non-volatile refractory elements located mostly within the matrix of fly ash particles.

These elements include Al, Ce, Co, Fe, Hf, La, Mn, and Si (Natusch et al. 1975; Abel and Rancitelli 1975; Hansen and Fisher 1980).

A few investigators have suggested that volatilization/condensation is not the only means of surface enrichment. Stinespring and Stewart (1981) indicated that elemental segregation of elements within particle melts also contribute to surface predominance. Hulett et al. (1979) demonstrated how the presence of mullite crystals within spherical particles indicate some degree of element mobility within the melt. Elemental migration within the melt to particle surfaces would be driven by the decrease in surface free energy associated with excess surface solutes as predicted by Gibb's adsorption isotherm (Hulett and Weinberger 1980).

Other minor types of concentration segregation involve isomorphous substitution. Various degrees of isomorphous substitution of a number of metals into the structures of

magnetic spinels have been reported by various investigators (Abel and Rancitelli 1975; Hulett et al. 1980; Hansen et al. 1981; Lauf et al. 1982). Hulett et al. (1979) found evidence for enrichment of +3 and +4 valence elements such as Cr, Ga, Fe, Ti, V, and Zr in mullite by substitution for Al and Si as well as enrichment of Co, Cr, Cu, Mn, Ni, and Zn in the spinel structure.

Dissolution Characteristics

Only a small fraction (4-7%) of fly ash is dissolved easily (Rohrman 1971). Aqueous extracts of fly ash are usually extremely alkaline ($\text{pH} > 12.0$) and highly saline ($\text{EC} = 8-12 \text{ mmho/cm}$) (Townsend and Hodgson 1973; Page et al. 1979). The majority of the soluble constituents tend to be released during initial dissolution stages.

The initial dissolution stages of fly ash are characterized by the release of high concentrations of soluble salts. Shannon and Fine (1974) found Ca and Na to constitute the mass of the soluble material (>80%) released from fly ash derived from lignite. Smaller amounts of K, Mg, Fe, Al, and Si are released from most fly ashes (Talbot et al. 1978). Generally, Ca^{2+} and OH^- are initially responsible for most of the salinity and the extreme alkalinity. Hydrolysis of CaO produces the Ca^{2+} and OH^- . Concentrations are maintained near saturation with respect to $\text{Ca}(\text{OH})_2$ (Talbot et al. 1978). Moderate amounts of Na and K are also usually dissolved but solution concentrations are

not maintained as dilutions increase (Elseewi et al. 1980). Initial Na and K dissolution is mainly due to surface sulfate salts which are not usually present in sufficient quantities to maintain concentrations near saturation levels (Green and Manahan 1978; Dudas 1981).

Theis and Wirth (1977) found that the initial pH of hydrated fly ash was determined by the relative amounts of lime (CaO) and amorphous iron oxides found on the surfaces of fly ash particles. A 3:1 ratio Fe:Ca determined the boundary as to acid-base reaction. Ashes high in iron produced acidic hydrolysis reactions, while high Ca ashes produced alkaline reactions. Most ashes tended to be alkaline in nature.

The dissolution of alkaline fly ash constituents increases substantially with acidification. Three or four buffer zones can be observed as acidification proceeds. An initial buffer zone is usually observed above pH 10.5 for fly ashes with very high calcium contents (Green and Manahan 1978; Hodgson et al. 1982). It is generally agreed that the buffering in this zone is primarily due to the hydrolysis of CaO. Smaller amounts of Ca, Na, and K sulfates are usually also found to be dissolve along with the CaO (Green and Manahan 1978). Hodgson et al. (1982) observed a second buffer zone between pH 9.2 and 8.5, and contributed it to Mg hydrolysis. Green and Manahan (1978) observed a similar zone but credited it to the dissolution of less soluble alkali salts located within the silicate matrix. A third

and sometimes a fourth buffer zone both occurring below pH 4.2 are also frequently observed after the dissolution and removal of alkaline salts. These zones are mainly attributed to the dissolution of various Al compounds located in the glass matrix and/or partial dissolution of an iron phase (Green and Manahan 1978; Hodgson et al. 1982).


The release of most elements from fly ash during dissolution cannot be predicted on the basis of bulk ash composition. Prediction is not reliable because of variation in the distribution of the elements among soluble and sparingly soluble fractions. Shannon and Fine (1974) found most (80-90%) of the soluble Na but only 31-36% of the soluble Ca in lignite fly ash was released during initial dissolution stages. High initial release of many trace elements have also been observed (Dreesen et al. 1977; Phung et al. 1979; Harris and Silberman 1983). Kopsick and Angino (1981) observed three distinct patterns of release for fly ash constituents with leaching; namely: (1) a pattern of large initial release followed by the concentration levelling off to a constant release rate, (2) constant (steady state) release and (3) delayed release. Most elements followed the first release pattern indicating association with at least two distinct solubility phases.

Residue Characteristics

The dissolution and removal of the highly soluble fly ash constituents leaves a residue of different bulk

composition and characteristics compared to unreacted ash. Heterogeneous distribution of elemental constituents between soluble and sparingly soluble phases primarily account for preferential enrichment and depletion of given elements in the residue. After leaching for two years with distilled water and lowering the leachate pH values of an alkaline fly ash to approximately 8.0, Dudas (1981) found Ca, B, Sr, and V to be preferentially removed resulting in negative enrichment of elements such as Al, Ba, Fe, K, Na, Mn, Pb, and Zn in the ash residue. Hansen and Fisher (1980) found more than 70% of Ti, Na, K, Mg, Th, and Fe in fly ash to be associated with the acid insoluble aluminosilicate matrix while more than 70% of the Ca, Sc, Sr, La, Ni, and rare earths were soluble. The characteristics of the less soluble residue are also a function of heterogeneous elemental distribution. Talbot et al. (1978) found fly ash, which had been equilibrated as a slurry, to display amphoteric properties and a pH dependent charge over the pH range 1.0 to 12.0. The isoelectric pH value was 7.55. Hydration of Fe and Al oxides and Al substitution for Si in the silicate matrix were suggested as determinant factors in controlling surface characteristics of the residue.

Leached or hydrated fly ash exhibits some pozzolanic and cementitious properties dependent on its chemistry. Fly ash is a pozzolan. It has little cementitious value itself but, in the presence of moisture, will chemically react with Ca(OH)_2 to form compounds possessing cementitious properties



(Berry and Malhotra 1980). The pozzolanic properties of fly ash tend to increase proportional to SiO_2 or $\text{SiO}_2 + \text{Al}_2\text{O}_3$ contents (Thorne and Watt 1965). Some fly ashes display some weak self-hardening properties. Alberta fly ashes generally exhibit a small degree of self cementation and hardening on exposure to moisture and subsequent drying (Joshi 1981). Cope (1962) and Townsend and Gillham (1975) observed horizontal cemented layers in large fly ash deposits which restricted vertical, but not horizontal movement of water. Self-hardening is likely due to the pozzolanic reactions of $\text{Ca}(\text{OH})_2$, produced on hydrolysis of CaO , with aluminosilicate components of the ash.

Other products, formed as a result of hydration and/or leaching of fly ash, appear to be similar to some hydration products found in cement. Ettringite ($\text{Ca}_3\text{Al}(\text{SO}_4)_3 \cdot 32\text{H}_2\text{O}$) forms in cement in the presence of soluble sulfate, saturated with respect to gypsum (CaSO_4) (Mindess and Young 1981). Needle-like crystals, identified as ettringite, have been observed in hydrated fly ash (Joshi 1981). Other needle-like acicular crystals, observed in fly ash taken from a non-operational power plant, have been identified as gypsum or anhydrite (Fisher et al. 1976; Fisher et al. 1978). In the presence of low sulfate contents, irregular platy crystals or rosette clusters of calcium sulfoaluminate hydrate (no known mineral name) ($\text{Ca}_3\text{Al}(\text{SO}_4)_3 \cdot 12\text{H}_2\text{O}$) tend to develop in place of ettringite in cement pastes (Mindess and Young 1981). Crystals of similar platy structure were noted

in the leached fly ash of Dudas (1981); however such crystals also resemble amorphous Si (Blatt et al. 1980) and gypsum displaying a platy morphology. CaCO_3 might also form as a precipitate in hydrated fly ash due to the reaction of dissolved Ca with atmospheric CO_2 which is readily adsorbed by alkaline solutions (Talbot et al. 1979; Elsewi et al. 1980; Dudas 1981).

III. METHODS AND MATERIALS

A. Sample Selection

Two Alberta produced fly ashes derived from Alberta coal were selected from a number of available samples. Selection was based on preliminary scanning electron and light microscope observations. The two selected fly ash samples contained spherical shaped particles typical of those described in most fly ash studies. The second criterion for selection was dissimilarity in the chemical compositions of the two ashes. The two samples selected were not drastically dissimilar in chemical composition but they do represent the extremities of the range in chemical compositions of fly ashes produced in Alberta. Both ashes were alkaline in reaction.

One of the selected samples was taken from Alberta Power's Battle River power plant located near Forestburg Alberta. This fly ash was derived from coal of the Forestburg Deposit of the Battle River coal field. The coal was formed in Upper Cretaceous sediments, is Subbituminous-C in rank, and contains approximately 7.0% ash and 0.4% sulfur (ERCB 1980). This ash sample exhibited the highest iron content of all the ashes available while containing relatively low calcium levels. This sample will be referred to as the Forestburg ash.

The other selected sample originated from Transalta Utilities' Highvale Mine power plant. This mine is located

on the Southern shore of Lake Wabamun, approximately 50km due west of Edmonton Alberta. The coal used in this utility is mined from the Sundance deposit of the Wabamun coal field. The coal is Subbituminus-B in rank, formed in Tertiary and Upper Cretaceous sediments and contains approximately 13.6% ash and 0.2% sulfur (ERCB 1980). The sample contained the highest calcium level of all the available samples and a relatively low iron content. This sample will be referred to as the Sundance ash.

Approximately 4kg of each fly ash was required for the study. One large bulk sample was taken from each respective power plant. Samples were taken directly from the electrostatic precipitator hoppers during normal plant operation, homogenized, and stored in a dry state until use.

B. Artificial Leaching

Leaching Column Construction

A total of thirty identical columns were constructed to contain the fly ash during leaching. Columns were constructed entirely of transparent plexiglass to facilitate easy observation of the contents.

The leaching columns consisted of three parts: body, base, and drainage spout. The body consisted of a 21cm length of 7.7cm outside diameter plexiglass tubing. The tubes had a wall thickness of approximately 0.3cm. The inside diameter of the tubes were found to vary from 6.7cm

to 7.0cm. , The base of the columns consisted of 10cm square, 0.5cm thick plexiglass plates. Holes of diameter 1.27cm were drilled in the centre of each plate for drainage spouts. The spouts consisted of 3.5cm long, 1.28cm outside diameter, 1.25cm inside diameter pieces of plexiglass tubing sanded to fit the drainage hole.

Columns were assembled using 2,2-dichloroethane to bond the plexiglass pieces together with water tight seals. With the drainage holes centred the bases were secured to one end of the tubular bodies. Spouts was inserted into the drainage holes extruding from the bottoms of the assemblies.

Column Packing

A series of five plexiglass leaching columns packed with increasing amounts of fly ash served as the basic experimental unit. The first column in the series was packed with 50.0g of fly ash. Each succeeding column in the series received 25.0g more ash than the previous column so that columns one through five contained 50.0, 75.0, 100.0, 125.0, and 150.0g of fly ash, respectively. Triplicate series were set up for each fly ash sample for each leaching regime.

All columns were packed in the same manner. The bottom of each column was first lined with two successive layers of glass wool to retain the ash. The appropriate mass of fly ash was placed on top of the glass wool using a funnel to facilitate even distribution. The top of each fly ash core

was covered with a circular piece of 11.0cm diameter filter paper. Filter papers were crimped to cover the top of the ash cores and extend up the inside wall of the columns. Filter papers were held in place with 3.5cm wide, 6.4cm outside diameter, 5.7cm inside diameter transparent plexiglass rings. The filter paper coverings served to minimize surface disturbances of the ash cores during solution addition. The top of each column was covered with a 9.0cm diameter plastic petridish lid to minimize contamination of the ash cores with atmospheric particulates or other contaminants. The ash packed columns were then set on top of 600mL Nalgene beakers used to contain the leaching solutions.

Leaching

Two acid solutions were employed to leach the fly ash samples. Each type acid solution was used to leach both fly ash samples during two separate leaching experiments. Both experiments extended for a period of approximately three months. The first experiment involved the use of 0.005 M H_2SO_4 as the leaching solution. The second involved the use of an aqueous-organic solution (AASA solution) containing 0.01 M acetic acid (CH_3COOH) and 0.002 M salicylic acid (2-Hydroxybenzoic acid). The initial pH values of the H_2SO_4 and AASA solutions were 2.1 and 3.0, respectively. Both solutions were made from reagent grade chemicals and distilled water.

The five prepared columns in each series were leached in sequential order with consecutive increments of leaching solution. Leaching of a series began by adding a solution increment of 500mL to the first (50.0g) column in the series. Channeling of solutions within the cores was minimized by gently rapping the columns while the ash was wetting up. After all of the solution had leached through the 50.0g core a 50.0mL aliquot was removed from the Nalgene collection beaker for analysis. The remainder of the increment (450mL) was added to the second (75.0g) column in the series and a second 500mL increment of solution would then be added to the first column. Each increment of solution was passed sequentially through each of the five columns of the series and a 50.0mL aliquot removed after it had passed through each column.

Solutions percolated through the columns at a rate governed by the hydraulic conductivity of the individual ash cores. Initially the solutions passed through all columns within 24hr but after approximately 15 increment additions 48hr were required. Transfer of solutions from one column to the next was not begun until all solutions in all columns had entirely leached through. By increasing the quantity of ash in successive columns while decreasing volumes of solution passing through each, the number of pore volumes generated per leaching increment per column decreased exponentially (Table 1). The degree of weathering achieved by the ash was therefore highest in the first column,




Table 1. Quantity and core thickness of fly ash, volume of leaching solution, and corresponding number of pore volumes generated per increment addition for each leaching column.

Column #	Quantity of Ash g	Ash Core Thickness mm	Volume of Increment mL	Pore Volumes per Addition
1	50.0	15	500	14.8
2	75.0	23	450	8.8
3	100.0	28	400	6.7
4	125.0	35	350	4.9
5	150.0	40	300	3.7

exponentially decreasing in a stepwise fashion to a minimal degree of weathering in the fifth column.

Leaching was terminated in each experiment when the widest diversity in leachate pH measurements was obtained among the five columns of a series. Leaching with 0.005 M H_2SO_4 required a total of 52 increment additions to obtain the widest diversity in leachate pH values for both ashes. The Sundance ash required 47 solution increment additions, when leached with the AASA solution, while the Forestburg ash required only 38 additions.

Leachate Analysis

Aliquots of the leachate solutions were immediately monitored for pH and concentration of eight cationic constituents. The pH was determined to the nearest 0.05 pH unit for every aliquot taken. Concentrations of Ca, Na, Mg, K, Mn, Fe, Al, and Si were directly determined in the

leachate solutions by flame atomic absorption spectrophotometry. Concentrations were determined for every aliquot taken from each of the first eight to twelve increments for columns five to one, respectively, and for every second or third aliquot taken from the remainder of the increments.

C. Sectioning of the Core Residues

Immediately after the last leachate increment passed through the ash cores the entire column assemblies were placed in a freezer. After 48hr the columns were removed and the ash cores quickly thawed around the edges. The intact frozen cores, including filter paper and glass wool, were forced out of the columns with compressed air. The cores were then oven-dried for 48hr at 60°C and retained for sectioning.

The oven-dried cores were sectioned horizontally on a somewhat arbitrary basis. The ash cores from the first columns were divided into three layers designated "surface", "middle" and "bottom" core sections. The surface core section consisted of a very thin (15mm) layer of the ash from the top of the core located immediately below the filter paper covering. The remainder of the first ash core was split evenly between the two remaining core sections (middle and bottom).

The remaining column cores were sectioned essentially in the same manner as the first except for the inclusion of

a fourth layer designated "subsurface" (Table 2). The extra core section was added because of the increased size of the cores. A fifth layer, designated "base", was also added in the case of column five, again due to the increased core size.

In addition to the above-mentioned layers, samples were also taken of materials precipitated onto the surfaces of the covering filter paper (designated "surface precipitate") and of the surface edges next to the plastic where some mixing of precipitates and ash samples occurred (designated "surface-edges") (Table 2).

D. Analysis of the Core Sections

Total Chemical Analysis

All triplicate core section samples, surface-edge samples, and surface precipitate samples were mixed into composite samples. Chemical composition was determined for all composite core section and surface-edge samples. The quantities of surface precipitate samples were not great enough to allow destructive analysis. Triplicate aliquots of the unleached ash samples and single aliquots from each composite core section and surface-edge samples were dissolved in concentrated HF and HCl according to the procedure of Pawluk (1967). All digests were analysed for Al, Ca, Mg, Na, K, Fe, Mn, Cr, Pb, Ni, Co, Cu, Ba, and Sr by flame atomic absorption spectrophotometry.

Table 2. Designated names and descriptions of the core sections of the weathered ash residues.

Ash core where name is used	Designation	Description
Column #		
1 2 3 4 5		
X X X X X	Surface Precipitate	Precipitates collected from the filter paper surfaces.
X X X X X	Surface-Edges	Edges of the ash core adjacent to the container walls where the filter paper did not cover the ash and mixing of ash and precipitate occurred.
X X X X X	Surface	Very thin top layer of the ash core (5mm) located immediately below the filterpaper.
X X X X X	Subsurface	The layer located immediately below the surface in columns 2-5 equal to one-third of the remainder* in columns 2-4 and one-quarter of the remainder* in column 5.
X X X X X	Middle	The layer located immediately below the surface in column 1 and immediately below the subsurface in all other columns.
X X X X X	Bottom	The layer located next to the glass wool in columns 1-4.
X	Base	The layer located next to the glass wool in column 5 only.

* Note: After removal of surface layer.

X-Ray Diffraction

X-ray diffractograms were obtained for both unleached samples and their ferromagnetic fractions, all composite core section samples, surface-edge samples and surface precipitate samples. Diffractograms were obtained using a Philips diffractometer equipped with a LiF curved crystal monochromator using $\text{CuK}\alpha$ radiation generated at 40kV and 20mA. Samples were scanned as random powders at ambient temperature and humidity ($\approx 10\%$ RH) at a scanning rate of $1^\circ 2\theta$ per minute. Samples were scanned from $4^\circ 2\theta$ to $30^\circ 2\theta$ using a 1° divergence slit and from $20^\circ 2\theta$ to $72^\circ 2\theta$ using a 4° divergence slit.

Differential Thermal Analysis

Differential thermal analysis (DTA) patterns were obtained for 43 selected composite samples. Patterns were obtained on a Perkin-Elmer Model 1700 differential thermal analyzer coupled with a Perkin-Elmer system 7/4 thermal analysis controller. Samples were equilibrated for at least 12hr at 54% RH then mixed in approximately a 1:1 ratio v/v with Al_2O_3 and heated at a rate of 15° per minute from near ambient temperature to 1050°C in an atmosphere of N_2 gas. Differential thermal grade Al_2O_3 was used as the reference material.

Electron Microscopy

Scanning electron micrographs of unleached, selected leached, and unleached etched samples were obtained on a Cambridge Steroscan 250 scanning electron microscope. The instrument was coupled with a Kevex 7000 energy dispersive X-ray analyzer to aid in the identification of components. Unleached etched fly ash samples were prepared by the procedure outlined by Hulett et al. (1979).

Transmission electron micrographs were obtained for one sample suspected of containing aluminosilicate material of short-range order. Five mg of the sample were suspended in approximately 10mL H₂O and sonified at 375W for about 2 minutes. A drop of the suspension was placed on a 200 mesh copper microgrid coated with *Formvar* and dried at 60°C for 30 minutes to evaporate the excess water. Micrographs of the sample were obtained at an accelerating voltage of 80kV.

Infrared Analysis

Fifteen composite samples were selected for infrared analysis. Samples were equilibrated at 54% RH for at least 48hr, mixed with oven-dried infrared grade KBr at a ratio of approximately 1%, and pressed into transparent discs. Infrared patterns were produced as % transmittance vs wavenumbers (cm⁻¹). Samples were scanned over the range of 4000cm⁻¹ to 200cm⁻¹ at a rate of approximately 2 minutes per scan. After the initial fifteen patterns were obtained one disc of exceptional interest was heated at 350°C for 4hr,

repressed, and a second pattern obtained.

Extractions

Composite core section samples and surface-edge samples were extracted with citrate-bicarbonate-ithionite (CBD) solution. A second set of the same samples were extracted with acid ammonium oxalate (AAO) (McKeague 1978). All extracts were analysed for Fe, Mn, Al, and Si by flame atomic absorption spectrophotometry.

Total Inorganic Carbon

Total inorganic carbon content was determined for duplicate samples of composite mixtures of each core section and surface-edge sample according to the procedure of Bundy and Bremner (1972)

E. Ferromagnetic Particle Analysis

Ferromagnetic Separation

Ferromagnetic particles were separated from the unleached fly ash samples using a wet separation method. For both unweathered ashes four replicate samples of 100.00g each were weighed into 600mL beakers. Distilled water was added at a water to fly ash ratio of approximately 4:1. A large teflon coated magnetic stirring bar was introduced and the slurries stirred at high speed on a magnetic stirring device for a period of over two minutes.

Beakers were then removed from the stirrer and the suspension allowed to settle. The stirring bar was retrieved and particles adhering to it were washed off into a clean beaker. After removal of all adhering particles the bar was then reintroduced into the ash suspension and subsequently retrieved an additional nine times.

After completion of the bar retrieval process the collected particles were washed to remove any nonmagnetic particles incidentally retrieved with the stirring bar. This was accomplished by holding a strong magnet to the outside of the bottom of the beaker containing the retrieved particles and washing the sample free of all particles not strongly held to the beaker bottom. After all weakly held particles were removed the strongly held particles were released and retained in another beaker. The washing process was repeated on the removed fraction until only insignificant quantities of particles were held in the washing beaker. The strongly ferromagnetic particles were then oven-dried at 105°C and weighed to determine the content of ferromagnetic particles.

Chemical Analysis

Chemical composition of the ferromagnetic fraction was determined by sample dissolution. Aliquots were taken from each homogenized oven-dried separated fraction and ground to a very fine powder. From each ground aliquot, 0.250g was weighed in a crucible and fired in a muffle furnace at 800°C

for 8 hr. After cooling samples were quantitatively transferred into 100 mL teflon beakers. Solutions were evaporated to dryness at 80°C after each of three additions of 15 mL concentrated HCl. After the third evaporation, 10 mL concentrated HCl, 5 mL concentrated HNO₃, and 5 drops HF were added and the beaker contents again evaporated to dryness. A final addition of 10 mL concentrated HCl was made to ensure removal of any excess HF. The dried residues were then dissolved in 6 mL concentrated HCl and 25 mL H₂O and heated at 80°C for 4 hr. The remaining solution was quantitatively transferred into a 50 mL volumetric flask and made up to volume with distilled H₂O. All digests were analysed for Fe, Al, Mg, Mn, Co, Cr, Cu, Ni, Ca, K, and Na by flame atomic absorption spectrophotometry.

IV. RESULTS AND DISCUSSION

The fly ash cores of each leaching series can be considered analogous to two kinds of weathering profiles or weathering gradients. Each five-core sequence can be regarded as a single unit consisting of five overlying, although not necessarily adjacent, "horizons" similar to a soil or geologic profile. Solutions percolating downwards through a core sequence (columns one through five) dissolved and leached constituents from the uppermost cores. Constituents translocated with the solutions subsequently interacted with the solid phases of ash materials in the latter columns of each sequence. Hence, the upper column cores (columns one and two) might be considered eluvial cores, while the lower cores (columns three, four, and five) might be considered illuvial.

Each individual core might also be considered as a single "profile" in itself. Solutions percolating through each core within a sequence would not only transport materials from one ash core to the next but also translocate materials within each individual core. Hence, the tops of each ash core would be considered eluvial and the bottoms illuvial. Both intercore and intracore translocation will be discussed in subsequent sections.

A. Leachate Chemistry

The two acid leaching solutions, 0.005 M H_2SO_4 and AASA, were chosen because of their close resemblances to natural weathering solutions. Precipitation is naturally acidic having a theoretical pH of 5.6 based on equilibrium absorption of atmospheric CO_2 (Stumm and Morgan 1980). Anthropogenic H_2SO_4 is primarily responsible for additional acidity observed in most rainwaters (Cogbill and Likens 1974). Geologic materials experiencing chemical weathering will therefore undergo progressive acidification and in the most extreme circumstances the active agent is most likely H_2SO_4 . Accordingly, H_2SO_4 was employed in this study.

The aqueous-organic mixture of acetic and salicylic acids (AASA) was designed to simulate the weathering conditions imposed by natural organic acids. Both acetic acid and salicylic acid have been used in other simulated weathering studies (e.g. Huang and Keller 1970; Huang and Kiang 1972). Organic compounds possessing the ortho-hydroxybenzoic acid structure of salicylic acid have been identified in soil organic matter. These compounds are known to form stable complexes with Fe^{3+} , Al^{3+} , and other inorganic soil components (Schnitzer and Skinner 1965; Schnitzer 1969). Acetic acid and salicylic acid therefore simulate the chemistry of soluble soil organic compounds that form highly soluble complexes and/or salts with inorganic soil constituents (De Coninck 1980). The concentrations of both the organic and inorganic leaching

solutions were elevated above normal field levels simply to speed the weathering process.

Mean data from the analyses of column leachates were plotted against leachate increment using the TEKTRONIX PLOT-10 APL GRAPH-II graphing package (Textronix 1977) available from the University of Alberta's Computing Services. Leachate increment units were employed to facilitate easy comparison of leachate chemistries among columns. The generated graphs illustrate the major trends in the leachate chemistries of the ashes with increasing chemical weathering. Trend lines of pH values and concentrations of elements for the column leachates were constructed from a series of means calculated from three (two in the case of AASA leached Sundance ash) individually determined data points. Each trend line represents from 50 to 156 individually determined data points (Appendix, Tables 1-36).

The pH values of all initial leachates were extremely alkaline. Acidification of the ash cores in each column series progressed in a stepwise fashion through up to three buffer stages as indicated by the leachate pH values (Figures 1 & 2). The first ash cores in each series were rapidly acidified. The leachate pH values dropped into the acid range (below pH 7.0) within the first ten solution increment additions. The leachates from the second columns remained in the alkaline range for a longer period but also eventually dropped into the acid range. Acidification of

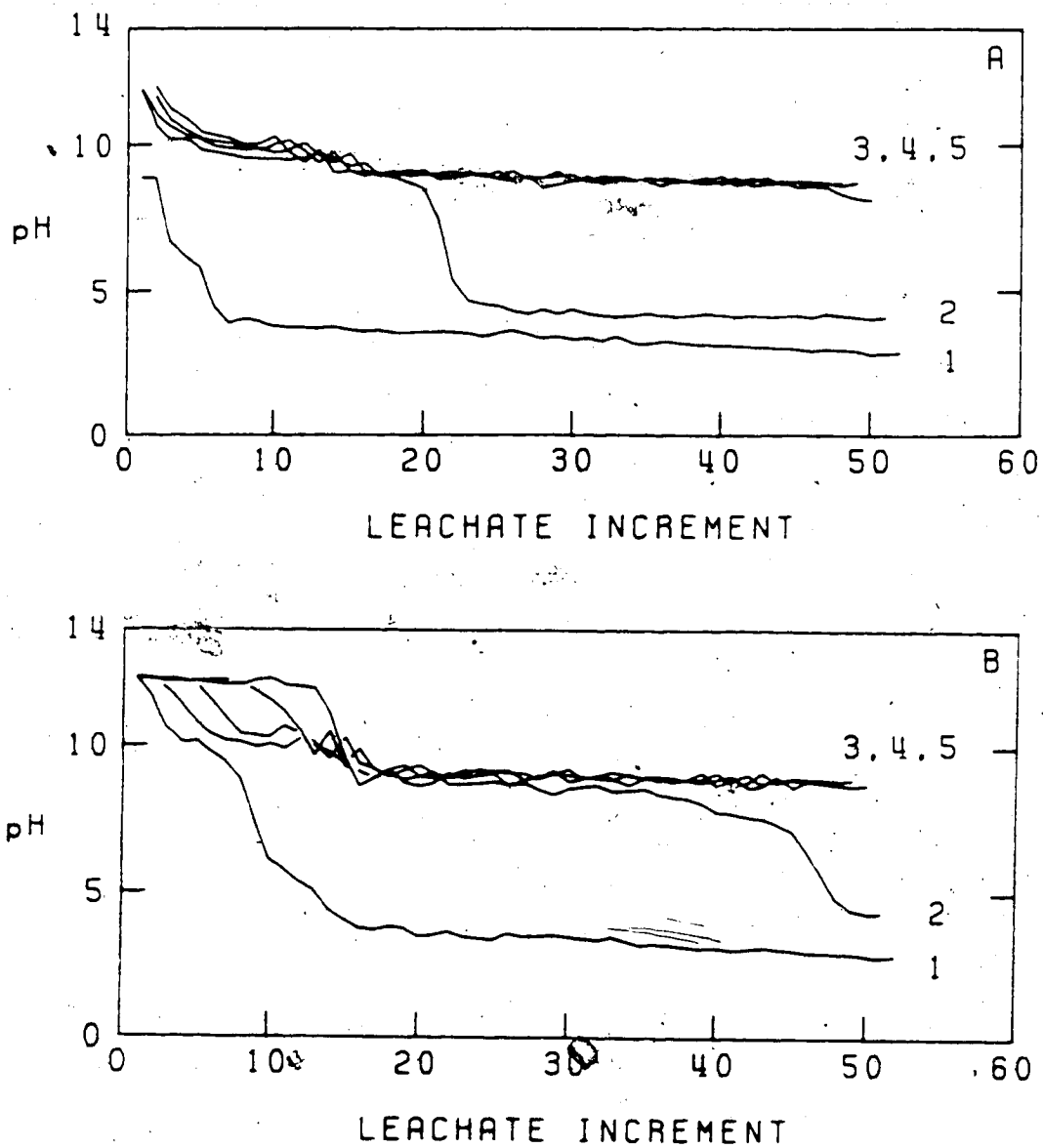


Figure 1. Leachate pH values of the Forestburg (A) and Sundance (B) fly ashes leached with 0.005 M H_2SO_4 . The numbers one to five indicate the respective columns.

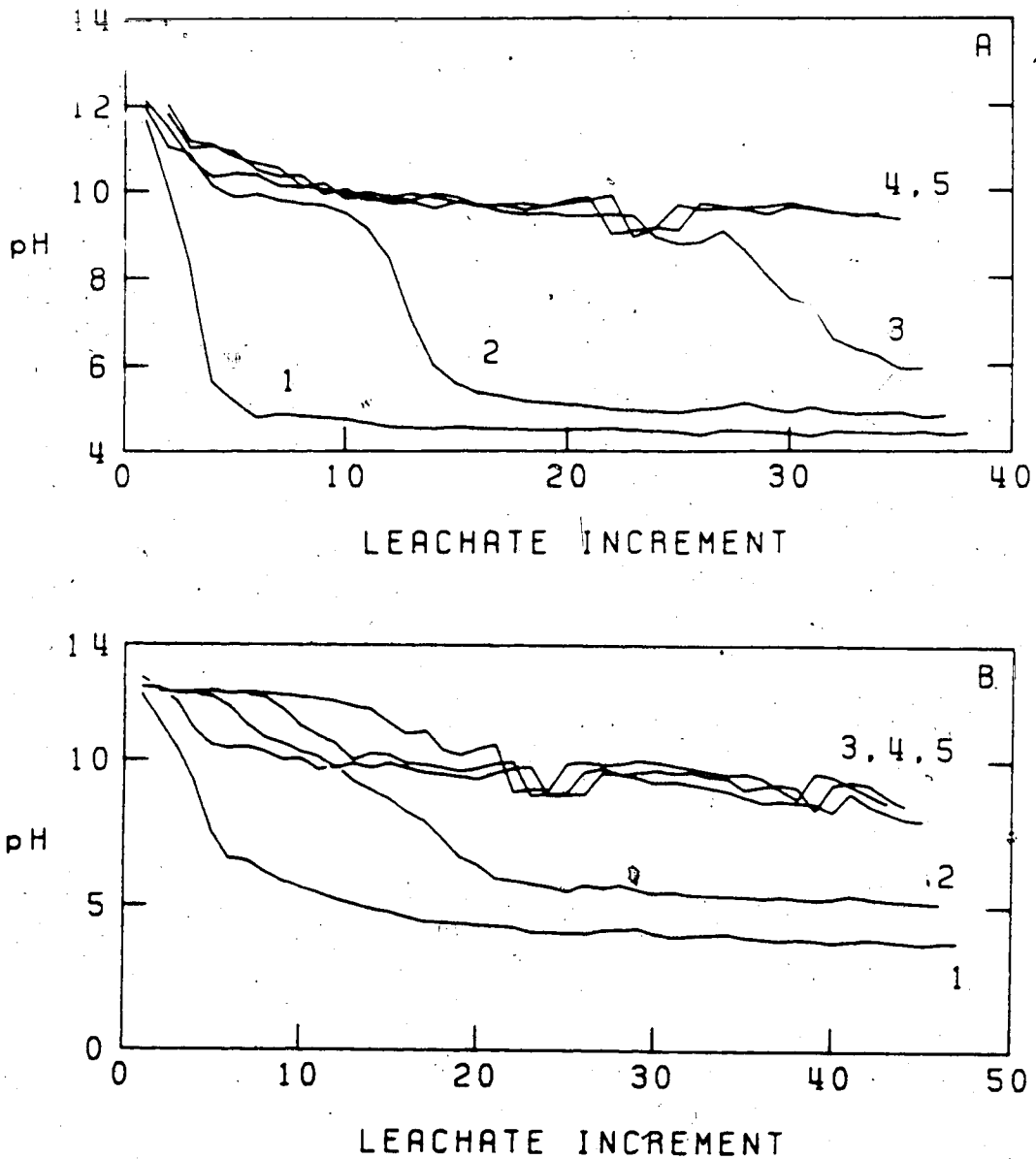


Figure 2. Leachate pH values of the Forestburg (A) and Sundance (B) fly ashes leached with AASA solution. The numbers one to five indicate the respective columns.

the second columns required from 2.5 to 7 times the number of increments required to acidify the ash in the corresponding first columns. In general the AASA solution was more efficient at acidifying the ash cores but did not produce as abrupt changes in the pH values as did the mineral acid (cf., Figures 1 & 2).

Leaching was terminated for each series when the pH values of the third column leachates began to drop towards neutrality. At termination, leachate pH values for the first two columns (1 & 2) in each series were in the acid range and values for the last two columns (4 & 5) were in the alkaline range. Values for most middle (3) columns were also in the alkaline range but nearer neutrality than columns four and five.

The two fly ashes differed slightly in their buffering capacities. Buffering was observed in all columns. Two buffer zones common to both ashes and a third zone, unique to the Sundance ash, were observed (cf. Figures 1A, 2A & 1B, 2B). One of the buffer zones common to both ashes occurred in the alkaline range between pH 8.5 and 9.0. The pH values for the other common buffer region were located in the acid range. The pH values for the acidic buffer region were dependent on the type of leaching solution and the particular leaching column. In the case of the first columns, buffering in the acid region occurred within 1.5 pH units above that of the unreacted leaching solutions. In the case of the second columns, buffering occurred within

one pH unit above that of the first columns.

The additional buffer zone, generated only by the Sundance ash, occurred in extreme alkaline ranges. During initial leaching of the Sundance ash, buffering was observed in the alkaline region above pH 12.0 in all columns but the first. The pH values of the leachates from the second columns were maintained above pH 12.0 for the first three increment additions. Each subsequent column in the sequence required three to four further increment additions over that of the respective previous column before the leachate pH values decreased from above 12.0. The fifth column in each column sequence for the Sundance ash maintained pH values above 12.0 for more than twelve increment additions before the values dropped to the next buffer level (Figures 1B & 2B).

The patterns of release of Ca from the ash cores (Figures 3 & 4) closely followed the respective pH patterns. High concentrations of Ca were released from all columns at the onset of leaching. The patterns more closely resembled the "initial flush release" pattern rather than the "constant release" pattern of Kopsick and Angino (1981). Concentrations of Ca in the initial leachate increments were the highest of all monitored elements. Reduction in the concentration of Ca in the leachates corresponded to declines in the pH patterns. Concentrations of Ca in the initial leachates of the Forestburg fly ash declined almost immediately. The levels of Ca in the initial leachates of

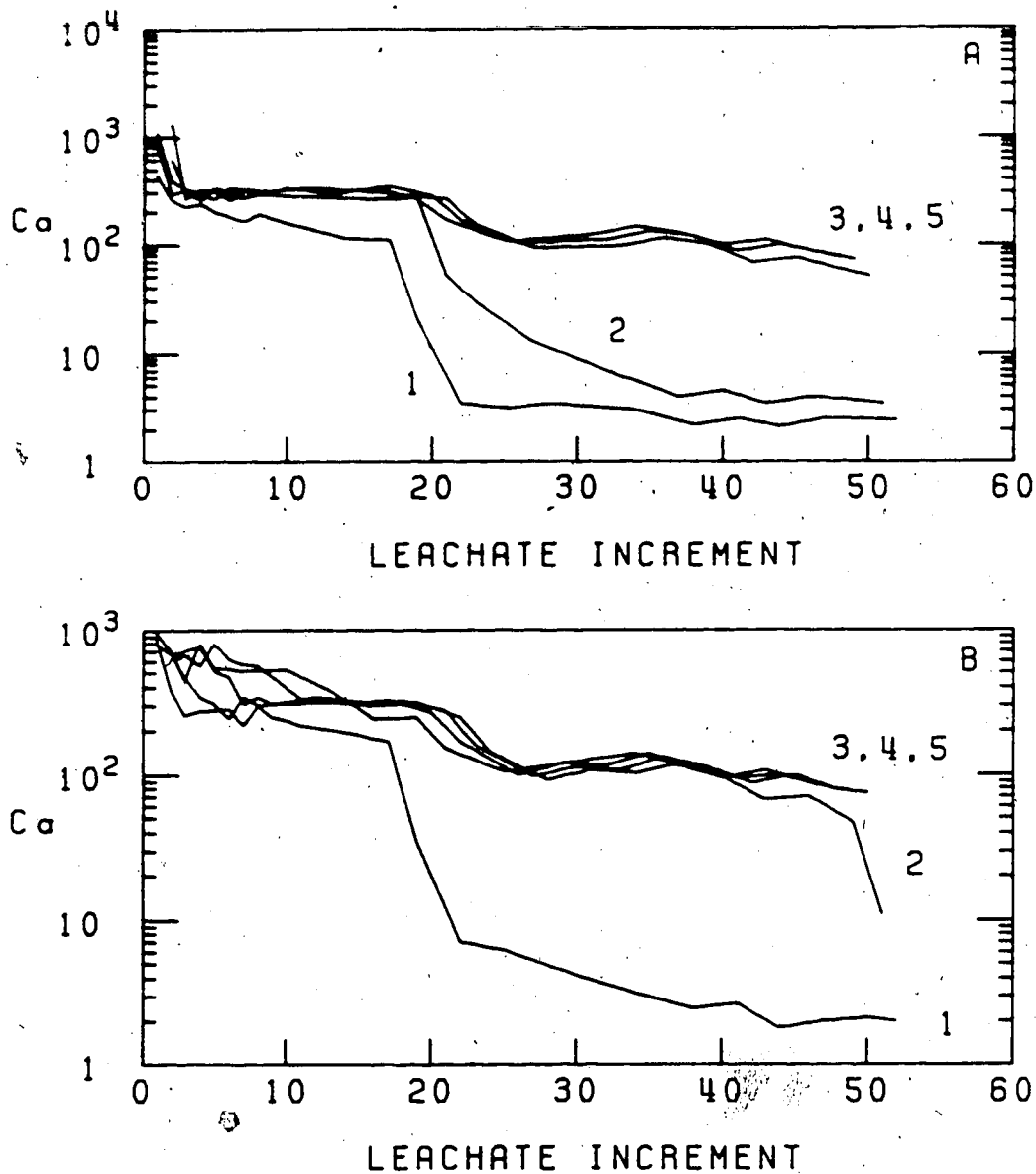


Figure 3. Concentration of Ca (ug/mL) in the leachates of the Forestburg (A) and Sundance (B) fly ashes leached with 0.005 M H₂SO₄. The numbers one to five indicate the respective columns.

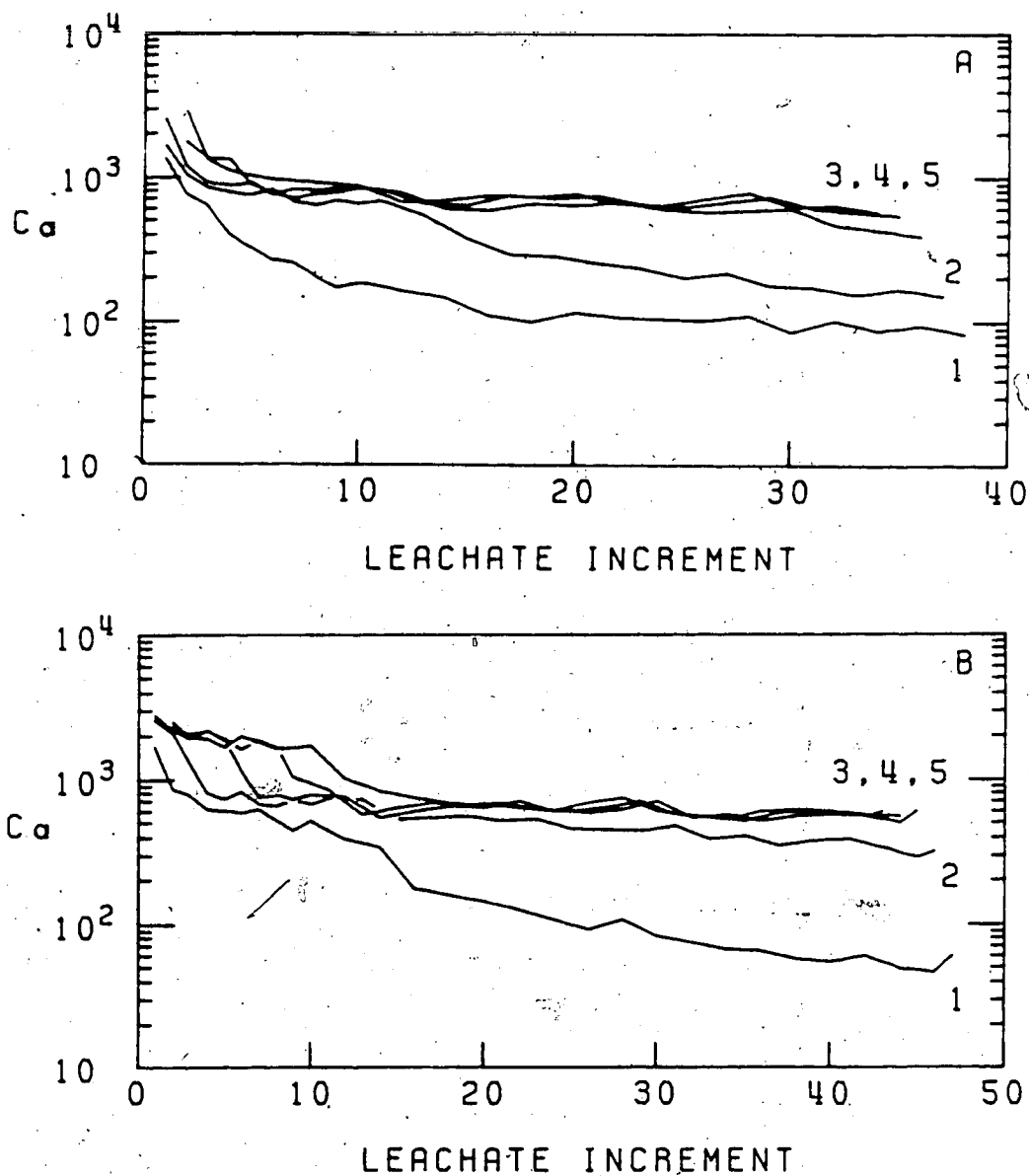


Figure 4. Concentration of Ca (ug/mL) in the leachates of the Forestburg (A) and Sundance (B) fly ashes leached with AASA solution. The numbers one to five indicate the respective columns.

the Sundance ash were maintained briefly, following patterns similar to the pH values for each column, then declined concomitant with the drop in pH values. Levels of Ca remained uniform while the pH values were buffered between 8.5 and 9.0. The overlapping Ca release patterns and pH value patterns in alkaline regions suggested that dissolution of Ca-bearing phases in the ash control alkaline buffering during initial weathering stages. While column leachates of both ashes were buffered between pH 8.5 and 9.0, the release of Ca decreased slightly with time. The concentrations of Ca in the leachates of the AASA leached columns were approximately 0.5 orders of magnitude above those of the 0.005 M H_2SO_4 leached columns (cf. Figures 2 & 3). The difference the levels of Ca in solution between the two leaching regimes is likely related to the formation of highly soluble Ca-organic complexes which enhance dissolution of Ca in the AASA leaching series. Precipitation of Ca-sulfates in the mineral acid leaching series could also contribute to the difference. Declines in the levels of released Ca lagged after the rapid drop in leachate pH values from alkaline to acid ranges. As with the pH value patterns, changes in the leachate concentrations of Ca were more abrupt with 0.005 M H_2SO_4 leaching than with AASA leaching (cf. Figures 1, 2 & 3, 4).

The patterns of dissolution of Mg from the column cores were similar for both ashes and both leaching regimes (Figure 5). Magnesium exhibited a delayed release pattern

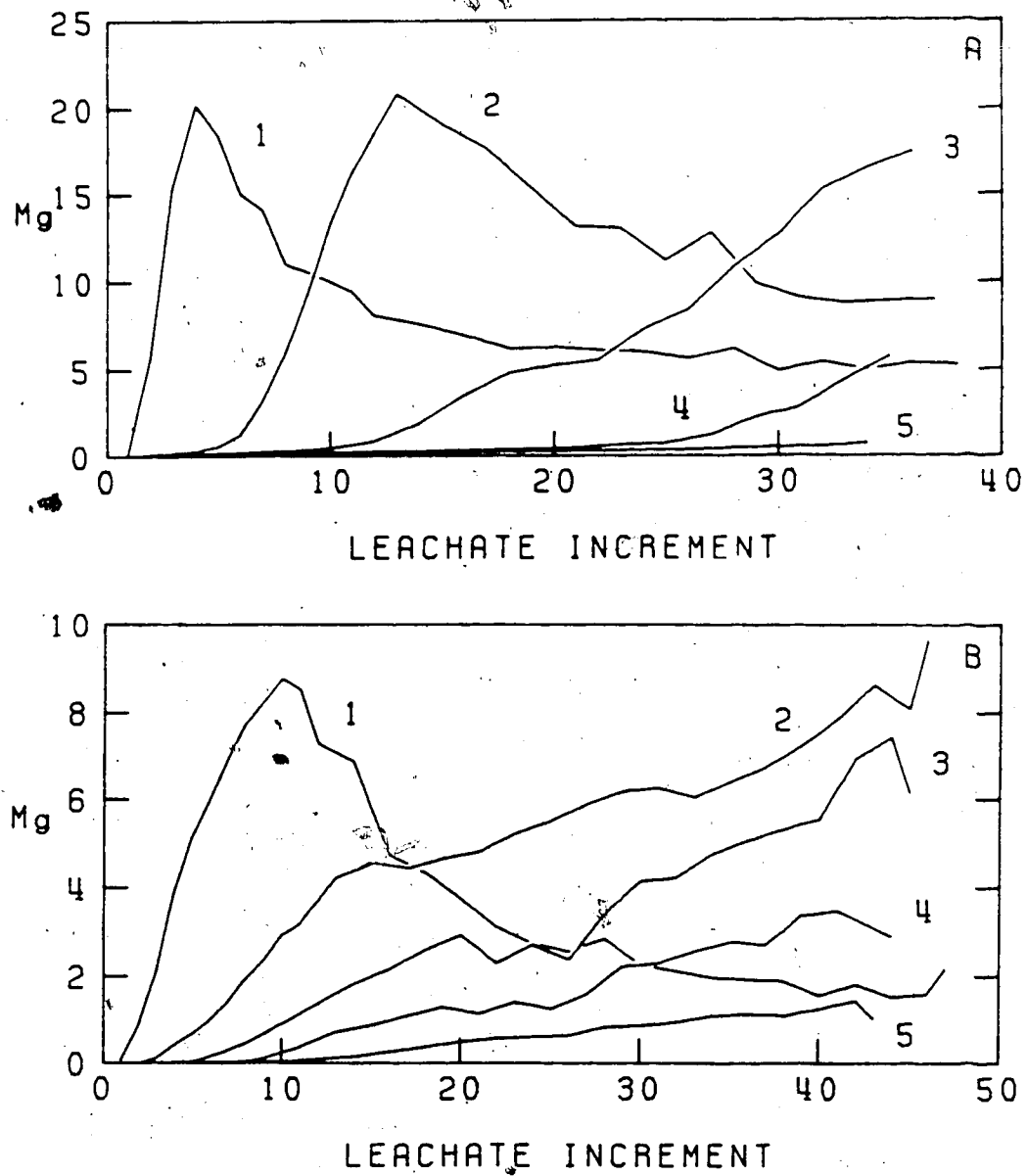


Figure 5. Concentration of Mg (ug/mL) in the leachates of the Forestburg (A) and Sundance (B) fly ashes leached with AASA solution. The numbers one to five indicate the respective columns.

similar to that observed by Kopsick and Angino (1981). Initial leachates from all columns contained very minor or undetectable quantities of Mg. Significant release of Mg began only after the leachate pH values of a column dropped below 10.0 (cf. Figures 5A & 5B). A peak in the release of Mg was observed only in the leachates of columns one and two. The peak concentrations of Mg in the leachates coincided with the major drop in pH values from alkaline to acid ranges. The magnitude of the peak concentration of Mg for all acidified columns was approximately the same for each ash. The Forestburg ash released higher overall levels of Mg (approximately double) compared to the Sundance ash (cf. Figures 5A & 5B). AASA leaching tended to produce patterns with sharper release peaks for Mg than did leaching with the mineral acid. Leachate concentrations of Mg tended to stabilize at relatively low levels for the duration of leaching after passing the concentration maximums. The low levels of Mg released from the second columns of each series were consistently 50% higher than the levels for the respective first columns.

The patterns for release of Na and K from the ash columns were similar for both ashes and both leaching regimes. All patterns displayed two distinct release stages (Figures 6 & 7). Concentrations of Na and K were highest in the initial leachate increments. Within the first few increment additions to all columns, concentrations quickly fell to relatively low nearly constant levels which were

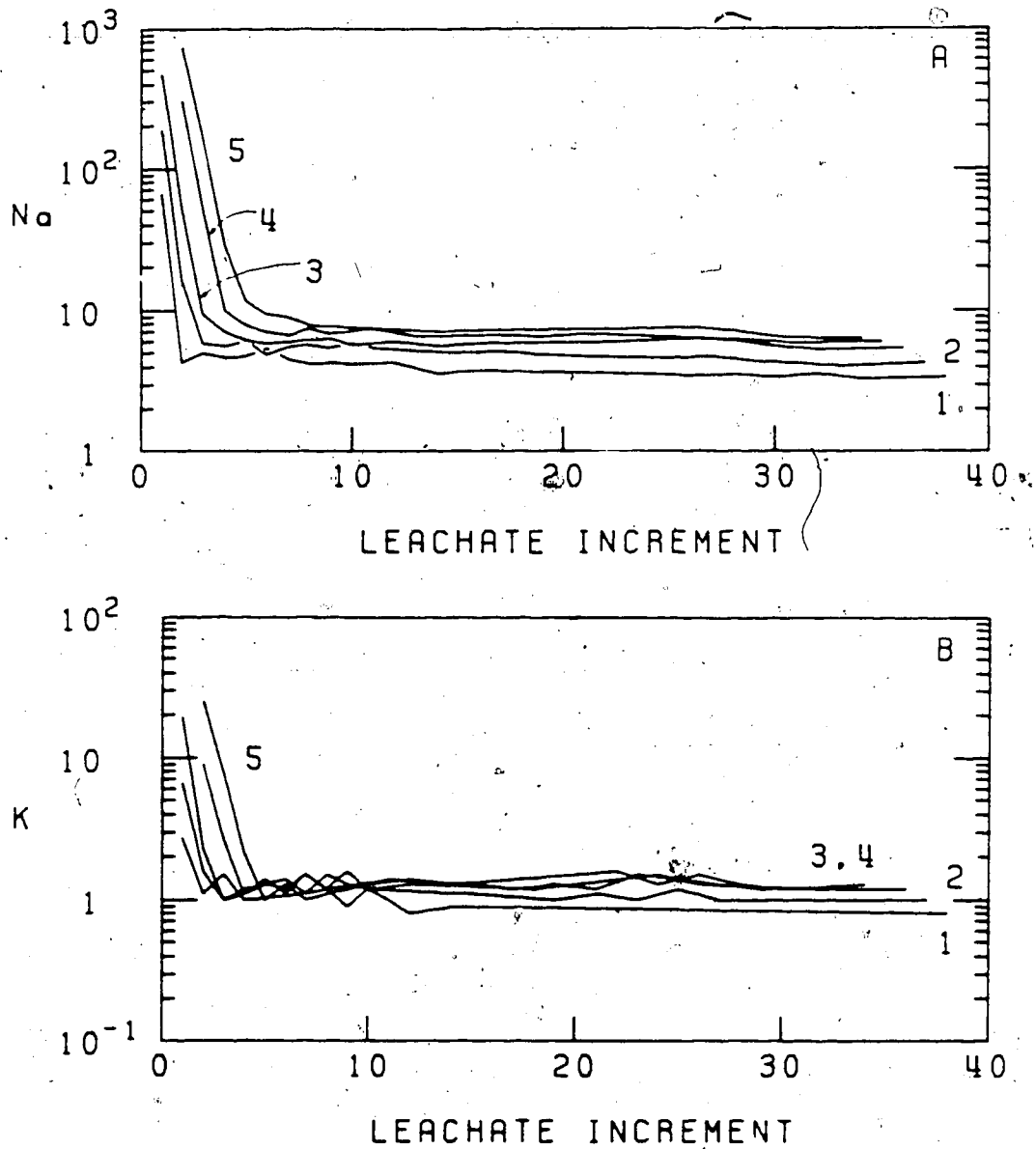


Figure 6. Concentration (ug/mL) of Na (A) and K (B) in the leachates of the Forestburg fly ash leached with AASA solution. The numbers one to five indicate the respective columns.

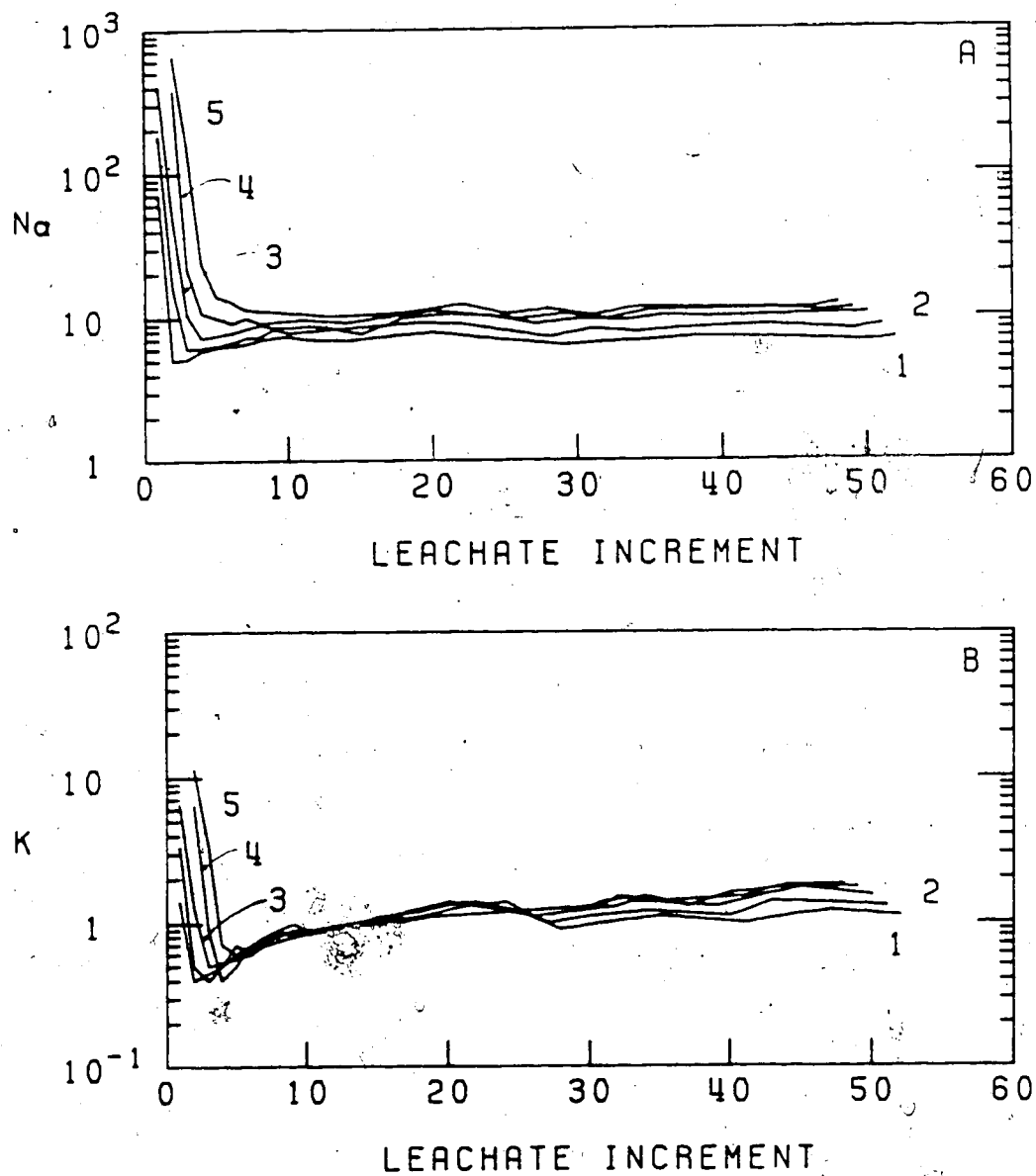


Figure 7. Concentration (ug/mL) of Na (A) and K (B) in the leachates of the Forestburg fly ash leached with 0.005 M H₂SO₄. The numbers one to five indicate the respective columns.

maintained for the duration of leaching. The majority of the Na and K released during the latter leaching stages was derived primarily from the first columns. The remainder of the columns in each series contributed only slight amounts of Na and K to the leachate solutions. The greatest quantities of K and Na were therefore removed from the first column cores of each series.

The overall concentrations of Na in the leachates were approximately one-half to one order of magnitude above the overall leachate concentrations of K. The type of leaching solution did not appear to alter the concentration of Na released at the onset of leaching; however, AASA leaching enhanced the initial release of K compared to H₂SO₄ leaching (cf. Figures 6B & 7B). From leachate increment number 16 onward the concentrations of both Na and K were enhanced by H₂SO₄ leaching, compared to AASA leaching (Table 3).

Table 3: Mean concentrations (ug/mL) of Na and K in leachate increments 16 to 30 for the first columns of the Forestburg and Sundance fly ash leaching series.

Leachate Inc. #	Na				K			
	Forestburg		Sundance		Forestburg		Sundance	
	H ₂ SO ₄ 2-4	AASA	H ₂ SO ₄ 2-4	AASA	H ₂ SO ₄ 2-4	AASA	H ₂ SO ₄ 2-4	AASA
16	-	3.8	-	3.0	1.0	0.9	1.3	0.7
17	7.5	-	11.4	-	-	-	-	-
18	-	3.8	-	2.8	-	0.9	-	0.7
19	-	-	-	-	1.1	-	1.4	-
20	7.9	3.8	11.3	2.6	-	0.9	-	0.5
21	-	-	-	-	-	-	-	-
22	-	3.8	-	2.3	1.1	0.9	1.5	0.4
23	7.3	-	10.5	-	-	-	-	-
24	-	3.6	-	1.9	-	0.9	-	0.4
25	-	-	-	-	1.2	-	1.4	-
26	7.3	3.5	10.6	1.8	-	0.9	-	0.6
27	-	-	-	-	-	-	-	-
28	-	3.6	-	2.1	0.9	0.9	1.2	0.4
29	6.3	-	8.9	-	-	-	-	-
30	-	3.4	-	2.0	-	0.9	-	0.5

Enhancement of release of Na and K from the ash cores by H₂SO₄ leaching versus AASA leaching was observed in all columns.

Dissolution of Al and Si occurred mainly in the first two leaching columns of each series after leachate pH values decreased from alkaline to acid values (cf. Figures 8,9 & 10A,B). Leachate concentrations of Si began to increase approximately five increment additions before the major pH drop occurred for each column. Increases in the concentrations of Al corresponded almost exactly with the decline in pH values. The highest levels of dissolved Al and Si (50ug mL⁻¹ and 35ug mL⁻¹, respectively) occurred with the 0.005 M H₂SO₄ leaching regime. In the first column leachates, the concentrations of Si, and to some extent the concentrations of Al, declined slightly with progressive leaching under acidic conditions. Levels of Si released from the first and second column ash cores were consistently 25% to 30% lower than the levels of Al (cf. Figs 3A,9A & 8B,9B). Consistently lower levels of Si and Al were released under acidic conditions with AASA leaching (approximately 30ug mL⁻¹ and 40ug mL⁻¹, respectively) compared with 0.005 M H₂SO₄ leaching. Neither the leachate levels nor the patterns of release for either Al or Si differed significantly between leaching regimes while leachates were alkaline.

The elevated and parallel release of Al and Si from the first two columns of each series under acid leaching

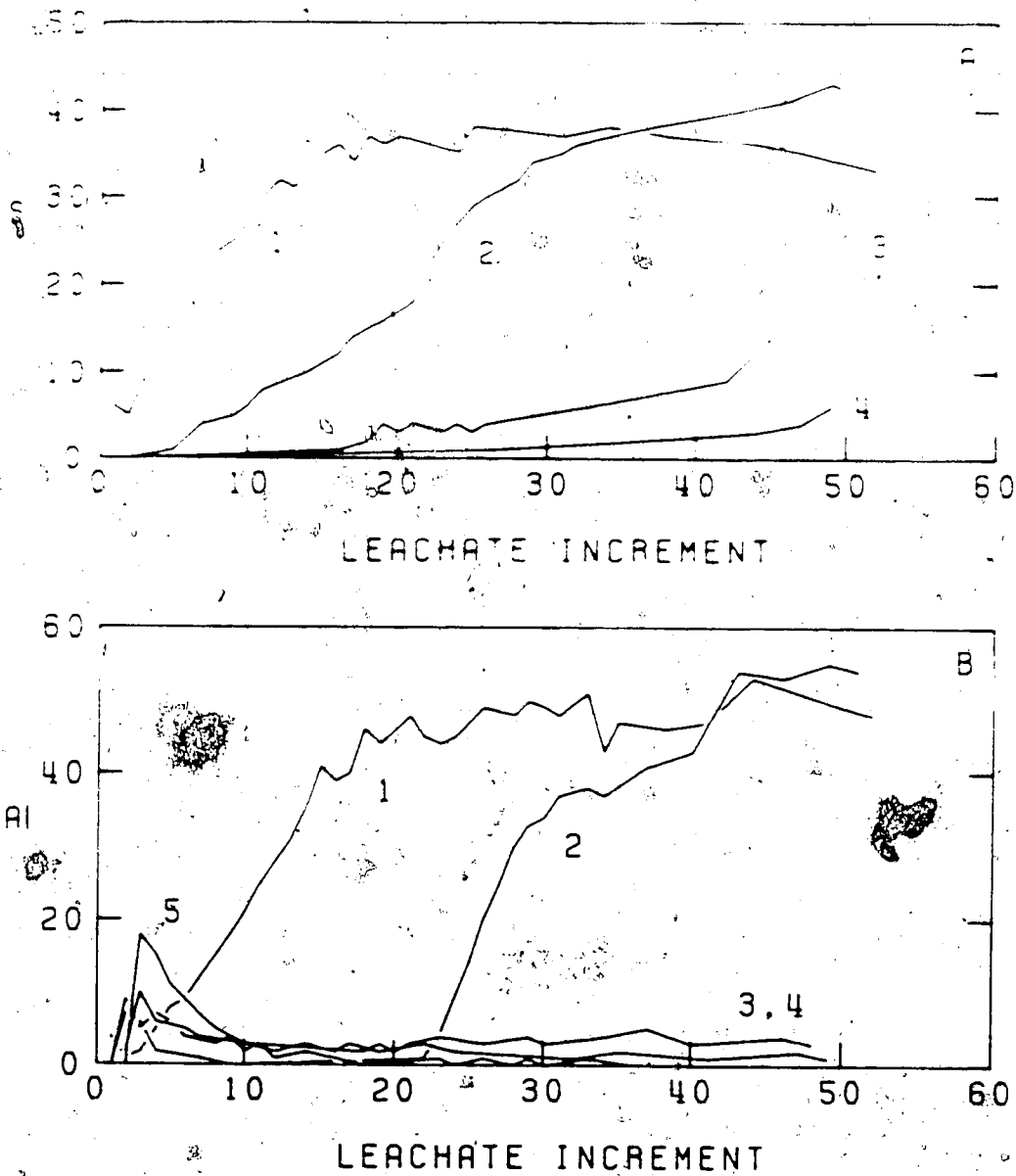


Figure 8. Concentration ($\mu\text{g/mL}$) of Si (A) and Al (B) in the leachates of the Forestburg fly ash leached with $0.005 \text{ M H}_2\text{SO}_4$. The numbers one to five indicate the respective columns.

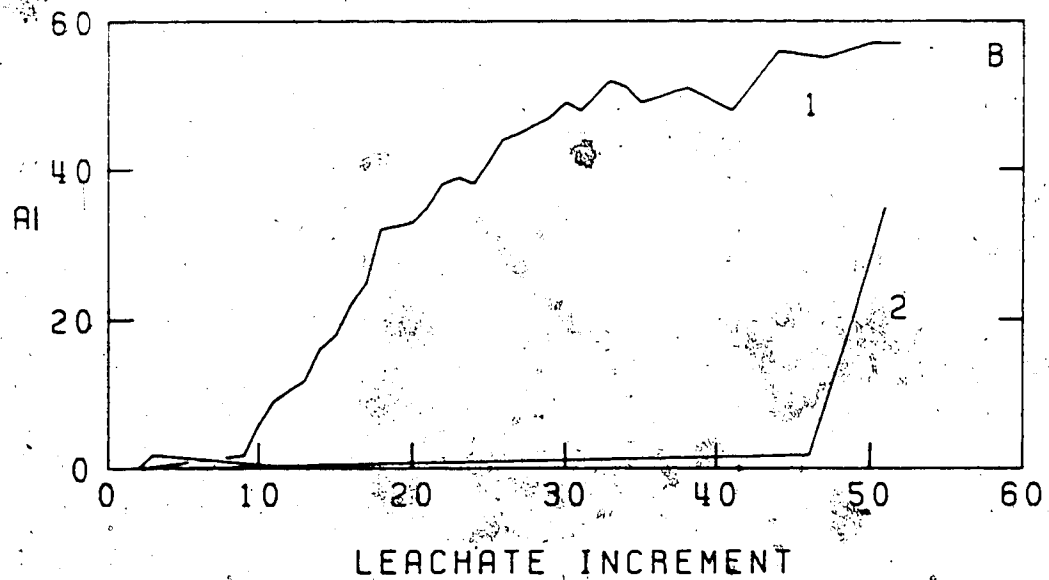
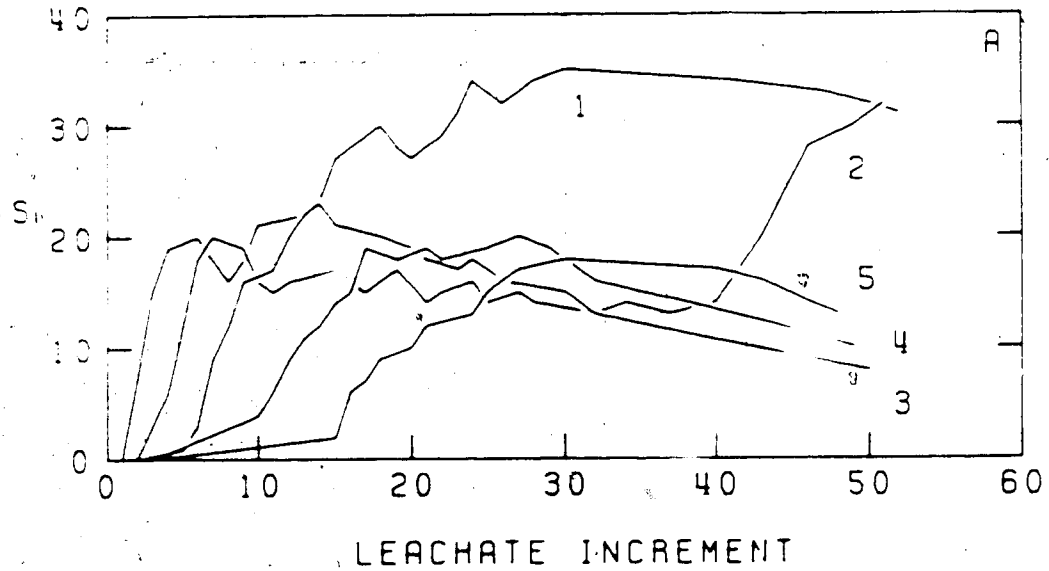


Figure 9. Concentration (ug/mL) of Si (A) and Al (B) in the leachates of the Sundance fly ash leached with 0.005 M H_2SO_4 . The numbers one to five indicate the respective columns.

conditions indicates that dissolution of Si is likely dependent on dissolution of Al. Extensive rapid dissolution of Si from rock-forming minerals is least favoured under acidic conditions (Brownlow 1979). Silicon is therefore likely co-released from fly ash particles under acidic conditions as a monomer and/or a polymer during acid hydrolysis of Al in the aluminosilicate matrix. Similar acid-accentuated dissolution of Si can occur during the weathering of natural aluminosilicate minerals (Huang and Keller 1970; Huang and Kiang 1972). Other elements (i.e. Na, K, Ca, Mg, and Fe) are also dissolved from the ash matrix, as indicated by the low level release of these elements paralleling acid release of Al and Si from the ash cores. Inclusion of these elements in the matrix likely contributed to the instability of the aluminosilicate structure in the ash, further enhancing dissolution of Si. The slowness of the precipitation kinetics of Si would allow metastability and supersaturation in acidic solution (Krauskopf 1956).

The release patterns for Si and Al differed between the ashes under alkaline leaching conditions. The concentrations of Si in all leachates of the Sundance ash series increased rapidly to levels of just under $20\text{ug}\cdot\text{mL}^{-1}$ as soon as the leachate pH values dropped from above 12.0 (Figure 9A). As leachates were buffered between pH 8.5 and 9.0, levels of Si declined slightly with time (cf. Figures 1B & 9A). Only minor levels of Si were released from the

Forestburg ash columns (3 & 4) while leachate pH values were alkaline (Figure 8A). Indeed, the sum quantities of Si in the Forestburg ash leachates decreased with each column in the series. Silicon was not detected in the fifth column leachates of the Forestburg ash.

In contrast to the behaviour of Si, small bursts of Al were released from the Forestburg ash during initial alkaline leaching (concentrations increasing with each column in the series). Aluminum was not detected in the comparable leachates of the Sundance fly ash (cf. Figures 8B & 9B). The Forestburg ash also continued to release low levels ($<5\mu\text{g}\cdot\text{mL}^{-1}$) of Al under sustained alkaline conditions from the third, fourth, and fifth columns (concentrations decreasing slightly with time) after subsidence of the initial bursts of Al. The sum quantities of Al released under alkaline conditions were minor compared to quantities dissolved under acidic conditions from the first and second columns.

Differences between the two ashes in the release patterns for Si under alkaline leaching conditions were likely due to differences in dissolution and/or precipitation reactions. The concentrations of Si in the Forestburg ash leachates decreased after passing through the nonacidified leaching columns of the series. This indicated deposition of Si in the alkaline ash of the latter columns. Co-precipitation of Si with Al, on encountering alkaline conditions, is indicated by the massive decreases in the

concentrations of both elements on passing through the third columns of each series (Figures 8 & 9). Co-precipitation would account for much of the removal of Si and Al from the third column leachates of the Forestburg ash. Precipitation of remnant Si transferred in the leachates to the fourth and fifth columns might occur through reaction with various electrolytes (concentrations increased in the latter columns) similar to precipitation of Si dissolved in river-water on meeting with sea-water at river-mouths (Biem et al. 1958).

Similar precipitation mechanisms for Si also likely occurred in the Sundance ash; however, the effects were apparently masked by a Si release mechanism(s) not manifest in the Forestburg ash. Silicon was released rapidly from the Sundance ash under alkaline conditions but not until pH values declined to below 12.0. Dissolution of Si alone is not likely since it is increasingly favoured as pH values increase above 9.0 (Kranskopf 1956; Brownlow 1979). Dissolved levels of Ca paralleled alkaline pH values for the weathering of the Sundance ash. This behaviour suggested that the dissolution of Si under alkaline conditions from the Sundance ash may be related either directly or indirectly to the dissolution of Ca.

The patterns of release for Fe and Mn were similar for both ashes and both leaching regimes (Figure 10). Iron was detected in the leachates of the first, second, and in some cases, the third columns of each series only after the

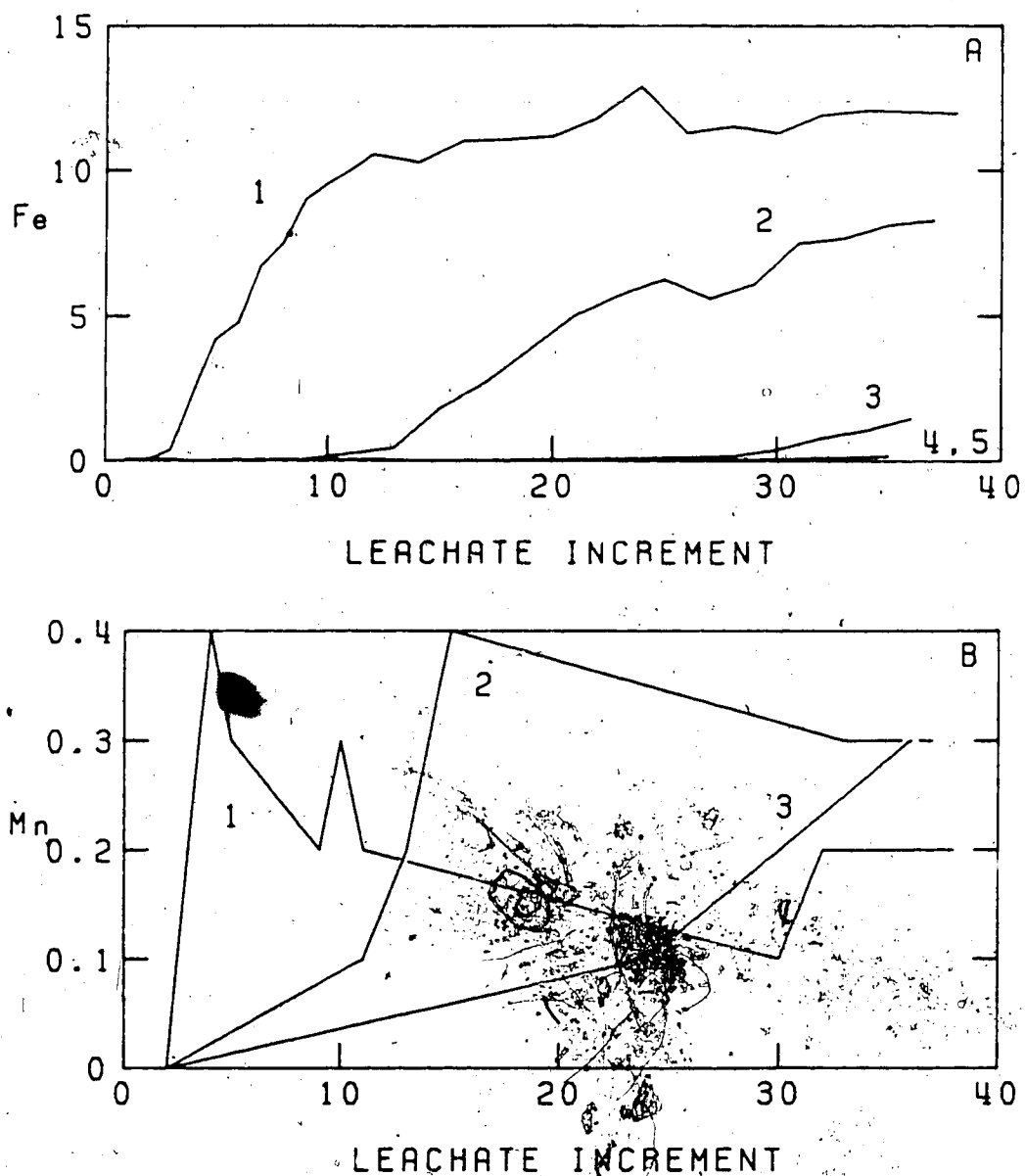


Figure 10. Concentration (ug/mL) of Fe (A) and Mn (B) in the leachates of the Sundance fly ash leached with AASA solution. The numbers one to five indicate the respective columns.

leachate pH values had decreased to below 7.0. Stabilization of the pH value levels in the acid range coincided with the highest levels of Fe in solution. AASA leaching elevated soluble Fe in the acidified first column leachates to levels over double those of 0.005 M H₂SO₄ leaching. Manganese levels in the leachates were barely above AAS detection limits; however, they were monitored because of the usual geochemical association of Mn with Fe. Manganese displayed a delayed flush pattern similar to Mg, although the delay peaks were not as intense (cf. Figures 10B & 5). Contrary to Fe, Mn concentrations were depressed by AASA leaching compared to H₂SO₄.

A. Residue Chemistry

Bulk Chemistry

The chemical analyses of the unleached (unweathered) Forestburg and Sundance fly ash samples are shown in Table 4. Major and minor components are expressed in percent as the oxide. Both ashes are Si-rich with abundant quantities of Al and Ca. Only slight differences occur between the compositions of the two ashes; however, these compositional differences may account for differences in the magnitude of release of some elements and the ash buffering capacities. The Sundance ash contained 36% more Ca than the Forestburg ash which corresponded with the greater buffering capacity of the Sundance ash. Conversely, the Forestburg

Table 4. Chemical composition of the unweathered fly ash samples.

Component	Forestburg Fly Ash	Sundance Fly Ash
SiO ₂	56 %	51 %
Al ₂ O ₃	19 %	22 %
CaO	11 %	15 %
Fe ₂ O ₃	5.9 %	4.5 %
Na ₂ O	3.7 %	3.7 %
MgO	2.4 %	1.3 %
K ₂ O	1.8 %	1.3 %
L.O.I. ^{**}	0.2 %	0.9 %
Ba	2400 ug/g	1400 ug/g
Sr	230 ug/g	190 ug/g
Mn	340 ug/g	500 ug/g
Cr	140 ug/g	100 ug/g
Pb	70 ug/g	120 ug/g
Ni	40 ug/g	40 ug/g
Co		30 ug/g
Cu		40 ug/g

* Determined by difference.

** Loss on ignition.

ash contained approximately 30%, 38%, and 84% more Fe, K, and Mg, respectively, than the Sundance ash corresponding with higher overall concentrations of Fe, K, and Mg released in the Forestburg ash leachates.

Based on major element composition and initial hydration reactions both fly ashes are classified as *Alkaline Modic* according to the proposed classification system outlined by Roy and Griffin (1982) for coal produced fly ash. *Alkaline Modic* fly ashes may be the most common type of fly ash produced from eastern U.S. bituminous coals (Roy and Griffin 1982). The Forestburg ash can be subclassified as an *Alkaline Barium-Modic* fly ash, as it contains an exceptionally high level ($>0.2\%$) of Ba. The Sundance ash cannot be subclassified as it did not contain levels greater than 0.2% for constituents normally occurring in trace quantities in terrestrial materials.

The changes in the chemical compositions of the leached (weathered) fly ashes, compared to the respective unweathered ashes, are shown in Tables 5 to 8 (for actual compositions see Appendix, Tables 37-40). Various depletion and enrichment patterns were evident for some components within some individual cores in each of the four leaching series. The differences in the enrichment/depletion patterns among the various constituents reflects both diversity of phases within the unweathered ashes and differences in the chemical behaviour of components.

Table 5. Percentage change in the chemical composition of weathered Forestburg fly ash relative to unweathered ash, for the 0.005 M sulfuric acid leaching regime.

Sample	SiO ₂	Al ₂ O ₃			FeO	CaO	MgO	Na ₂ O		K ₂ O	Ba	Co	Cr	Cu	Mn	Ni	Pb	Sr
		2	3	2				3										
Column 1																		
Surface	16	-10	-24	-69	-38	0	17	33	0	-36	-33	-32	0	14	-83			
Middle	9	-5	8	-58	-25	0	17	0	7	0	-21	0	28	-52				
Bottom	5	-5	29	-52	-25	-5	11	8	0	-7	0	-24	0	14	-48			
Column 2																		
Surface-Edges	4	-5	27	-41	-20	0	0	0	0	0	33	-15	0	14	-52			
Surface	0	5	7	-33	-12	0	0	4	0	0	0	15	0	14	-65			
Subsurface	-2	10	2	-20	-12	-5	0	-8	0	0	33	-6	0	14	-43			
Middle	-5	16	-2	-16	-8	0	0	4	0	0	33	3	0	0	-39			
Bottom	4	5	-2	-22	-8	0	0	-4	0	-7	33	0	0	0	-48			
Column 3																		
Surface-Edges	0	10	-12	-25	-12	-8	-5	-17	0	-14	33	-9	0	0	-52			
Surface	-4	10	-3	-14	-8	3	0	-17	0	-14	33	-6	0	0	-39			
Subsurface	-2	10	-2	-17	-8	-3	-5	-8	0	-14	33	-6	0	0	-48			
Middle	0	5	-2	-23	-4	-5	-5	-21	0	-14	33	3	0	0	-52			
Bottom	-4	5	3	-15	8	0	-5	-12	0	-14	0	0	0	0	-43			
Column 4																		
Surface-Edges	-4	0	-10	0	-12	-11	-5	-8	0	-21	0	6	0	0	0			
Surface	0	5	-3	-9	-4	-3	0	-4	0	-14	0	3	0	14	-30			
Subsurface	0	0	0	-9	0	3	5	-4	0	-14	0	6	0	14	-30			
Middle	-2	0	2	-9	0	0	5	-4	0	-14	0	3	0	0	-30			
Bottom	-2	0	-2	-9	8	-5	5	-8	0	-21	0	3	0	0	-30			
Column 5																		
Surface-Edges	-5	0	-10	9	-8	-8	0	-4	0	-21	0	9	0	0	0			
Surface	0	5	-5	-9	-8	-3	5	17	0	-14	0	3	2	14	-22			
Subsurface	-2	5	-2	-9	-4	0	5	4	0	-14	0	3	0	14	-30			
Middle	-2	0	0	0	0	-3	0	-17	0	-21	0	0	0	0	-30			
Bottom	-2	0	0	0	0	-3	0	-17	0	-14	0	3	0	0	-26			
Base	-4	5	-2	0	0	-3	0	-21	0	-14	0	0	0	0	-26			

Table 6. Percentage change in the chemical composition of weathered Forestburg fly ash relative to unweathered ash, for the AASA leaching regime.

Sample	SiO ₂			Al ₂ O ₃			Fe ₂ O ₃			CaO	MgO	Na ₂ O		K ₂ O	Ba	Co	Cr	Cu	Mn	Ni	Pb	Sr
	2	3	2	2	3	2	2	2														
Column 1	Surface	5	-12	45	-17	8	17	-50	0	-28	0	-21	0	0	-74							
	Middle	-2	10	2	-4	5	6	-38	0	-28	33	-6	0	0	-52							
	Bottom	-4	16	5	-4	8	6	-29	0	-28	33	-3	0	0	-52							
Column 2	Surface-Edges	-2	10	2	-12	11	6	0	0	-21	33	-21	0	0	-65							
	Surface	-2	10	5	-28	11	6	-12	0	-21	33	-12	0	0	-60							
	Subsurface	-2	10	7	-24	3	0	-4	0	-21	33	-3	0	0	-48							
	Middle	-2	10	7	-24	4	0	-4	0	-21	33	-3	0	-14	-48							
Column 3	Bottom	-4	10	7	-21	0	0	-8	0	-14	33	0	0	0	-48							
	Surface-Edges	-4	16	-3	-18	3	0	-4	0	-21	0	0	0	0	-43							
	Surface	-4	16	0	-19	3	0	-8	0	-14	0	0	0	0	-39							
	Subsurface	-4	16	3	-21	4	0	-8	0	-21	0	0	0	0	-43							
Column 4	Middle	-4	16	0	-24	4	0	-4	0	-14	0	0	0	0	-48							
	Bottom	-5	16	2	-21	8	0	0	0	-7	0	0	0	0	-39							
	Surface-Edges	-2	5	-8	-9	0	-6	8	0	-28	0	0	0	0	-26							
	Surface	-2	10	-3	-9	4	0	0	0	-28	0	3	0	0	-35							
Column 5	Subsurface	-4	10	-3	-9	0	0	-4	0	-21	0	-12	0	0	-26							
	Middle	-5	5	-8	-9	4	0	-8	0	-21	0	3	0	0	-26							
	Bottom	-4	5	-5	0	4	0	-4	0	-21	0	3	0	0	-30							
	Surface-Edges	-7	10	-5	0	-8	0	4	0	-28	0	-12	0	0	-17							
Column 5	Surface	-4	10	-2	-9	0	3	0	0	-28	0	-3	0	-14	-22							
	Subsurface	-5	10	-2	0	0	-6	-4	0	-36	0	0	0	0	-26							
	Middle	-4	5	2	0	0	-6	-4	0	-28	0	0	0	0	-26							
	Bottom	-5	5	-2	0	-4	0	0	0	-36	0	3	0	0	-22							
Column 5	Base	-4	5	-2	0	-4	-6	-4	0	-36	0	0	0	0	-22							

Table 7. Percentage change in the chemical composition of weathered Sundance fly ash relative to unweathered ash, for the 0.005 M sulfuric acid leaching regime.

Sample	SiO ₂			Al ₂ O ₃			Fe ₂ O ₃			CaO	MgO	Na ₂ O		K ₂ O	Ba	Co	Cr	Cu	Mn	Ni	Pb	Sr
	2	2	3	2	2	3	2	2														
Column 1																						
Surface	33	-18	-35	-79	-54	-27	8	185	-33	-60	-50	-43	-25	33	-89							
Middle	27	-18	-2	-76	-54	-24	0	150	0	-50	0	-41	-25	33	-84							
Bottom	16	-9	42	-66	-38	-13	0	100	0	-20	0	-33	0	17	-84							
Column 2																						
Surface-Edges	8	4	9	-47	-31	-3	0	43	0	-20	25	-10	0	0	-78							
Surface	12	4	16	-52	-31	-3	8	78	0	-20	0	-14	0	8	-84							
Subsurface	4	9	2	-38	-15	-3	0	57	0	-30	25	-2	0	-8	-68							
Middle	8	9	0	-39	-8	-3	0	7	0	-20	50	0	0	-8	-68							
Bottom	2	14	-2	-40	0	-5	0	36	33	-30	50	4	25	-8	-74							
Column 3																						
Surface-Edges	2	-4	-2	-13	-15	-8	-8	86	33	-20	0	20	25	0	-21							
Surface	2	9	-2	-20	0	-3	0	86	33	-30	0	18	25	0	-42							
Subsurface	6	0	-4	-20	0	-3	-8	71	0	-30	0	10	25	0	-37							
Middle	4	0	-2	-20	15	-5	-8	50	0	-20	0	2	25	0	-42							
Bottom	0	4	-2	-13	8	-3	-8	14	0	-10	0	0	25	0	-37							
Column 4																						
Surface-Edges	8	-9	-13	13	-15	-11	0	57	0	-20	0	-12	0	-17	-26							
Surface	2	4	-7	-20	-15	-3	0	64	0	-20	0	2	0	0	-47							
Subsurface	4	4	-7	-20	-8	-5	0	64	0	-20	0	2	0	58	-47							
Middle	-2	9	-2	-13	0	0	0	64	0	-30	0	2	0	0	-42							
Bottom	2	4	-7	-13	-8	-5	0	-14	0	-20	0	2	0	0	-37							
Column 5																						
Surface-Edges	-6	-4	-9	7	-8	-3	0	86	0	-30	0	-6	0	-25	-21							
Surface	0	4	-2	-13	0	-3	0	86	0	-30	0	0	0	-17	-47							
Subsurface	0	0	-4	-7	0	3	0	64	0	-30	0	0	0	-8	-42							
Middle	0	0	-2	-7	8	3	0	14	0	-30	0	-2	0	-17	-37							
Bottom	2	-4	-4	-7	0	-3	-8	-28	0	-30	0	-2	0	-8	-37							
Base	0	0	-9	-7	0	0	-8	-28	0	-30	0	-2	0	-25	-37							

Table 8. Percentage change in the chemical composition of weathered Sundance fly ash relative to unweathered ash, for the AASA leaching regime

Sample	SiO ₂		Al ₂ O ₃		Fe ₂ O ₃		CaO	MgO	Na ₂ O		K ₂ O	Ba	Co	Cr	Cu	Mn	Ni	Pb	Sr
	2	1	2	1	2	1			2										
Column 1	Surface	10	9	-4	-57	-31	11	15	7	0	-30	25	-14	0	0	-84			
	Middle	6	9	4	-42	-23	5	0	-7	33	-30	25	2	25	0	-73			
	Bottom	4	14	2	-40	-15	5	0	93	0	-30	25	2	0	-8	-68			
Column 2	Surface-Edges	10	9	-7	-57	-31	5	15	50	0	-30	25	-18	0	8	-84			
	Surface	6	14	2	-52	-23	19	15	57	0	-30	25	-14	0	8	-84			
	Subsurface	0	18	9	-42	-15	8	0	86	0	-20	50	-6	0	0	-73			
	Middle	0	18	4	-40	-8	5	0	86	0	-30	50	-2	0	0	-73			
Column 3	Bottom	-2	18	4	-33	8	5	0	93	0	-10	25	8	25	0	-68			
	Surface-Edges	-2	18	2	-33	-8	5	0	143	0	40	50	-2	0	0	-58			
	Surface	2	14	2	-33	-8	3	0	114	0	-20	50	2	0	-8	-47			
	Subsurface	4	9	-2	-33	0	3	-8	100	33	0	25	2	0	0	-42			
Column 4	Middle	-2	9	-7	-13	0	3	0	78	33	-10	0	6	0	0	-37			
	Bottom	-2	9	-4	-13	0	3	-8	78	33	-10	0	4	0	-8	-32			
	Surface-Edges	-10	-9	-13	13	-15	8	-8	107	0	-30	0	-6	0	-8	0			
	Surface	-4	4	-7	-7	-8	-3	0	121	33	-30	0	0	0	0	-32			
Column 5	Subsurface	-2	9	-4	-13	0	3	0	86	33	-30	0	0	0	0	-32			
	Middle	2	4	-4	-13	-8	0	0	86	33	-30	0	0	0	-8	-32			
	Bottom	-4	9	-4	-7	-8	3	0	64	33	-20	0	2	0	-8	-32			
	Surface-Edges	-4	-4	-9	0	-32	-8	-8	93	0	-40	0	-8	0	-8	-16			
Column 5	Surface	-6	9	-4	-7	-8	3	0	93	33	-40	0	0	0	0	-32			
	Subsurface	-2	9	-2	-13	-8	3	0	71	0	-40	0	0	0	0	-37			
	Middle	-6	14	-2	-7	0	3	0	57	0	-30	0	-2	0	0	-32			
	Bottom	-6	14	-4	-7	0	3	0	64	0	-20	0	-2	0	0	-32			
Column 5	Base	-4	9	-4	-7	0	3	0	50	0	-20	0	-2	0	0	-32			

Reduction in the concentration of a constituent in a core section, with respect to the content in the unweathered ash, indicates preferential net removal of the constituent from the core section. Most large decreases in the content of some elements, such as Ca, Mg, and Fe in the first column cores, give a good indication of the magnitude of element removal. Minor differences of a few percent among core sections, such as the Si values of the lower core sections of the third, fourth, and fifth columns of all series, probably reflect only the intrinsic variability of the ashes.

Increases in the content of an element in a core section with respect to the unweathered ash indicate either negative enrichment or net deposition. Negative enrichment occurred primarily in the first column cores where no components were added and only dissolution and leaching of select components took place. Increases (positive numbers) or no change (zeros) in the quantity of a component not extensively dissolved from the first column cores, compared to the unweathered ash samples, indicates negative enrichment. An exception is the case of Na in the AASA leached samples (Tables 6 & 8) where considerable quantities of the element were removed from the first column (Figures 6 & 7) but negative enrichment primarily due to Ca removal was greater than or equal to the magnitude of Na removal.

Net deposition of constituents took place in all column cores after the first where the quantity of a component

deposited was greater than the quantity removed from a given core section. Net deposition of an element in a core section was generally indicated by an increase in the amount of an element in the sample with respect to the unweathered ashes. Enrichment of a core section in a given component may also have occurred through deposition of a certain phase while being preceded by removal of a larger quantity of the same component through dissolution of another ash phase. Enrichment of this type is indicated by the elevation in compositional levels of a core section, compared to adjacent core sections. For example, Ca was deposited in the surface-edge samples of the latter leaching columns but in some cases the enrichment values of all core sections were negative with respect to the unweathered ashes (Tables 5-8). Enrichment of Ca in the surface-edge samples was indicated only through the increases in the content of Ca in the core section with respect to adjacent core sections. These core sections are therefore actually enriched in Ca while displaying a decrease in total composition with respect to the unweathered ash.

Calcium and Magnesium

Ca and Mg were depleted from both ashes in quantities that exceeded all other major and minor constituents (Tables 5-8). Calcium appeared to be more extensively leached than Mg, with respect to the unweathered ashes; however, the apparent lower relative dissolution of

Mg (minor component), compared to Ca (major component), could arise from negative enrichment of Mg due to the massive overall removal of Ca.

Depletions of Ca and Mg were greatest in the ash of the first and second columns (Tables 5-8). Depletions decreased asymptotically within the core sections of each leaching series. The surface layers of the first columns sustained the greatest losses. The lower core sections of the fourth and fifth columns were not substantially different from the respective unweathered ashes.

Similar asymptotic depletion patterns for Ca and Mg were also evident within some of the individual ash cores. The surface core sections (excluding the surface-edge samples) of most column cores usually contained less Ca and Mg than the lower core sections. The magnitude of differences among the core sections of each column core were generally less pronounced in the latter columns of each series. Leaching with 0.005 M H_2SO_4 removed more Ca and Mg from the ash than did leaching with AASA solution (cf. Tables 5, 7 & 6, 8).

The initial mobilization of Ca from the ash is most likely due to the hydrolysis of CaO and dissolution of the hydroxide products ($Ca(OH)_2$) as suggested by many investigators (Theis and Wirth 1977; Talbot et al. 1978; Elseewi et al. 1980; Dudas 1981; Hodgson et al. 1982). Comparatively minor amounts might also be dissolved from anhydrite ($CaSO_4$) in the ash (Dudas 1981). The formation of

Ca(OH)_2 was most evident in the trends for leachate pH values and release patterns of Ca of the Sundance ash (Figures 1-4). While the column leachates of the Sundance ash were buffered in the extreme alkaline ranges above pH 12.0, solution levels of Ca remained within the range of $500\text{ug}\cdot\text{mL}^{-1}$ to $950\text{ug}\cdot\text{mL}^{-1}$ with $0.005\text{ M H}_2\text{SO}_4$ leaching, and from $1500\text{ug}\cdot\text{mL}^{-1}$ to $2500\text{ug}\cdot\text{mL}^{-1}$ with AASA leaching. The high levels of Ca in solution coinciding with extremely alkaline pH values indicates the presence of a large quantity of a discrete soluble Ca phase in the ash controlling the solution parameters. The stable phase under these conditions (extremely high solution levels of Ca and extremely alkaline pH values) is Ca(OH)_2 (portlandite) (Lindsay 1979). This mineral likely formed through the hydrolysis of a large amount of available CaO and remained temporarily undissolved in the case of the Sundance ash. Continuous leaching did not allow its formation in the Forestburg ash and quickly removed it from the Sundance ash. Exposure to less acidic solutions than those employed in this study, such as water (Dudas 1981), may not elevate levels of Ca high enough to facilitate Ca(OH)_2 formation as occurred in the Sundance ash.

Availability of most of the Ca in the ashes to the leaching solutions is evident in the removal of considerable quantities of Ca from the ash of the first columns (Tables 5-8). Much of the Ca in the ashes was therefore associated with the particle surfaces. The extremely high solubility

of Ca(OH)_2 would account for the short duration of highly alkaline buffering in the Sundance ash. The disappearance of the portlandite (Ca(OH)_2) from the ash cores is indicated by the sharp decrease in the pH values of the leachates of each column from above 12.0 to below 9.0 and the corresponding decrease in the leachate concentrations of Ca. Conversely, even though Ca was also dissolved in large quantities from the Forestburg ash, a similar buffer zone above pH 12.0 did not occur (Figures 1-4). The unweathered Forestburg ash contained less Ca than the Sundance ash (Table 4); however, the difference in content of Ca between the ashes was not likely great enough to account for differences in the ash buffering capacities. Instead, differences in the buffering capacity likely reflect differences in the physical forms of Ca in the ashes (i.e. percentage of Ca which occurs as CaO) rather than simply differences in total quantities. The possible forms of Ca in the ashes will be discussed at length in the mineralogy section.

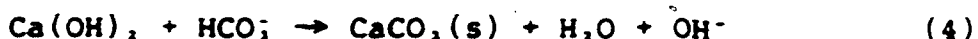
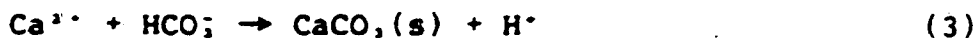
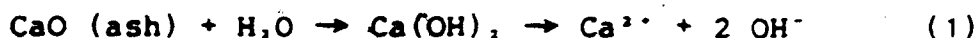
The removal of much of the Mg from the ashes was comparable to the removal of Ca and consistent with the chemistry of a MgO phase. The hydrolysis of MgO results in the formation of Mg(OH)_2 , which is generally less soluble than Ca(OH)_2 and only sparingly soluble in excess alkali (pH > 10.0) (Cotton and Wilkinson, 1972). The formation of Mg(OH)_2 in the ashes would account for the very low or undetectable concentrations of Mg in the first few leachate

increments in which leachate pH values remained above 10.0. Magnesium dissolved from any highly soluble Mg-salts (e.g. MgSO_4) present in the ash, under alkaline conditions, would also contribute to a solid Mg(OH)_2 phase. The "delayed flush" pattern observed for the release of Mg corresponded to acidification of the respective ash cores (cf. Figures 2 & 4). The peak concentrations were likely caused by rapid dissolution of Mg(OH)_2 previously formed under the initially extreme alkaline conditions. Magnesium oxide in the unweathered ash likely occurs in solid solution with CaO , but unlike Ca, Mg does not dissolve until pH values drop from extreme alkaline ranges to moderate alkaline or acidic ranges. Further discussion of the physical forms of Mg is also reserved for subsequent sections.

A white (10YR 8/1)d precipitate was found on the filter papers on the surfaces of the fourth, fifth, and in some cases, the third columns of each leaching series. The surface-edge samples of most fourth and fifth columns were either enriched or did not differ in Ca content from the composition of the respective unweathered ashes (Tables 5-8). The concentrations of all other major elements in the surface-edge samples, including Mg, were considerably diluted with respect to the unweathered ash contents (Tables 5-8). This indicated that the white precipitate was composed essentially of Ca. Core section samples adjacent to the surface-edge samples (bottom core sections of the previous column cores and the surface core sections of the

same column cores) were usually lower in content of Ca. Therefore, although content of Ca in the surface-edge samples (columns 3, 4 & 5) was less than the content of Ca in the unweathered ashes, Ca was still enriched in the sample with respect to adjacent core sections. Calcium accumulations in the surface-edge samples corresponded well with inorganic carbon contents (Table 9), indicating precipitation of a carbonate phase. Transport and precipitation of other Ca phases also occurred under the specific conditions imposed during these leaching experiments. Discussion of these phases is reserved for subsequent sections.

Precipitation of CaCO_3 on the core surfaces of the latter columns of each series likely occurred through the following reactions:



Some of the Ca^{2+} and/or Ca(OH)_2 , derived from the hydrolysis of CaO , native to the ash (equation 1), would react with atmospheric CO_2 dissolved in solution (accentuated by excess OH^- , equation 2) to form a CaCO_3 precipitate under the prevailing alkaline conditions (equations 3 & 4). Formation of CaCO_3 would be at the expense of Ca(OH)_2 (solid phase or

Carbonate ion (CO_3^{2-}) would also be present in solution and participate in similar reactions; however, the bicarbonate ion (HCO_3^-) is the dominant species in solution under the prevalent pH conditions (Stumm and Morgan 1981).

Table 9 Calcium carbonate equivalent of leached and unleached samples.

Sample	Forestburg Fly Ash		Sundance Fly Ash		% Equivalent Calcium Carbonate
	Sulfuric Acid Leached	AASA Leached	Sulfuric Acid Leached	AASA Leached	
Unleached	0.0	0.0	0.7	0.7	0.7
Column 1					
Surface	0.0	0.0	0.0	0.0	0.0
Middle	0.0	0.0	0.1	0.0	0.0
Bottom	0.0	0.0	0.0	0.0	0.0
Column 2					
Surface-Edges	0.3	0.0	0.0	0.0	0.0
Surface	0.0	0.0	0.0	0.0	0.0
Subsurface	0.0	0.0	0.0	0.0	0.0
Middle	0.0	0.0	0.1	0.0	0.0
Bottom	0.0	0.0	0.1	0.1	0.2
Column 3					
Surface-Edges	0.2	0.0	7.5	0.2	0.2
Surface	0.1	0.0	1.3	0.2	0.2
Subsurface	0.1	0.0	2.0	1.4	1.4
Middle	0.1	0.0	1.8	1.6	1.6
Bottom	0.4	0.1	1.4	1.5	1.5
Column 4					
Surface-Edges	4.5	0.9	8.4	11.0	11.0
Surface	0.4	0.3	1.9	3.5	3.5
Subsurface	0.4	0.5	1.7	1.6	1.6
Middle	0.9	0.9	1.4	1.5	1.5
Bottom	0.7	0.5	1.5	1.4	1.4
Column 5					
Surface-Edges	4.2	1.7	8.9	8.4	8.4
Surface	0.4	0.5	2.1	3.1	3.1
Subsurface	0.5	0.5	2.0	1.5	1.5
Middle	0.8	0.5	1.4	1.3	1.3
Bottom	0.6	0.5	1.6	1.4	1.4
Base	0.4	0.5	1.6	1.4	1.4

solution species) which is metastable in the presence of dissolved CO_2 (Lindsay 1979).

Precipitated CaCO_3 was redissolved along a front corresponding to the acidification front within the ash cores of each series. Carbonates were present in the core sections of those columns which had not undergone acidification and absent in those where the leachate pH values had dropped into the acid range (cf. Table 9 with Figures 1 & 2). Some redissolved CaCO_3 would again precipitate further down each leaching series. Redissolution of precipitated CaCO_3 and reprecipitation in latter columns would account for the buffering observed for all nonacidified columns in each series in the 8.5 to 9.0 pH range. This would also account for the sustained levels of Ca released prior to acidification, and the corresponding decrease in the leachate concentrations of Ca from high levels following acidification of the ash cores.

Precipitation of Mg in the ash was not identical to Ca precipitation. The sum quantity of Mg in the leachates decreased with successive columns in each leaching series (Figure 5), indicating that Mg precipitated in the latter columns of each series. Accumulation of Mg did not occur in the surface-edge samples, as did Ca, but rather over a broad range of core sections, mostly in the middle and/or bottom layers of the fourth, fifth and in some series, the third columns (Tables 5 to 8). Most salts of Mg (e.g. chlorides and sulfates) are highly soluble (Lindsay 1979) and are not

likely to precipitate under the leaching conditions imposed during this experiment. Most carbonates of Mg are also highly soluble and do not usually precipitate as separate phases. Magnesium does however commonly form solid solutions with CaCO_3 (Lindsay 1979). Carbonates were present in all core sections of the nonacidified columns (Table 9). Precipitation of MgCO_3 in solid solution with CaCO_3 is therefore the most probable mode of Mg accumulation in the lower ash columns.

A number of factors may have contributed to the dispersal of Mg precipitates among the lower core sections of the nonacidified columns. The $\text{Mg}^{2+}:\text{Ca}^{2+}$ solution ratio plays an important role in the incorporation of Mg into CaCO_3 structures (St. Arnaud and Herbillon 1973). Precipitation of CaCO_3 from a solution containing both Mg and Ca, such as occurred on the core surfaces of the third, fourth, and fifth columns, would effectively increase the $\text{Mg}^{2+}:\text{Ca}^{2+}$ ratios of the leaching solutions. Removal of Ca from solution at the beginning of core infiltration would therefore promote precipitation of Mg-bearing CaCO_3 in the lower core sections, similar to the formation of Mg-bearing calcites in soils (St. Arnaud 1979). Other factors such as formation of stable sulfates, acetates, or salicylate complexes with Mg in leaching solutions might hinder MgCO_3 precipitation. The solution species MgSO_4^0 would likely form in the H_2SO_4 leaching solutions and would account for a significant portion of the total dissolved Mg (Lindsay

1979). Precipitation of Mg in solid solution with CaCO_3 might therefore also be limited by transformation kinetics of Mg solution species. This would also result in the greater dispersal of precipitated Mg among the ash core sections, compared to Ca.

Sodium and Potassium

Of the minor univalent constituents examined, K displayed trends of negative enrichment in the leached residues while Na displayed both negative enrichment (AASA leached samples) and depletion (0.005 M H_2SO_4 leached samples) (Tables 5-8). Changes in the compositions of K and Na, with respect to the unweathered ashes, were most pronounced in the first column cores. Changes in the compositions of K and Na in subsequent column cores were minimal except in some cases for the surface and surface-edge samples of the second columns. Negative enrichment of K in the first column cores was primarily due to removal of Ca and Mg. Sodium also displayed negative enrichment in the first column cores of the AASA leached ashes and depletion or no change in content, with respect to the unweathered ash in the H_2SO_4 leached first columns. The mineral acid solution removed considerably more Na from the ashes than the organic acid solution.

The two stages of Na and K release observed in the leachate patterns (Figures 6 & 7) reflect dissolution from two distinct phases in the unweathered ash. Similar trends

have been reported elsewhere (Dudas 1981). The initial stage of Na and K release is characterized by a rapid decline in initially high leachate concentrations. The drop in concentrations is consistent with dissolution of a limited quantity of readily soluble salts, most likely sulfate salts, associated with particle surfaces as suggested by Green and Manahan (1978) and Dudas (1981). Negative enrichment of K in the residue core sections, primarily in the first column cores, (Tables 5-8) indicates that most of the K in the ash is not associated with the soluble salt fraction. The much higher concentrations of Na than K in the initial leachates (Figures 6 & 7), compared to the Na:K ratios of the unweathered ashes (Table 4), suggests that a much greater percentage of the total Na than the total K is associated with the soluble salt fraction of the ash.

The low levels of Na and K in the leachates detected after the initial flushes indicates that Na and K were dissolved during latter weathering stages from forms far less soluble than the forms that account for the initial flush. The majority of the Na and K dissolved from the ash after reaction of the highly soluble forms was derived almost entirely from the ash of the first leaching columns. Levels of Na and K in the leachates increased only slightly after passing through each of the subsequent columns of each series (Figures 6 & 7). Concomitant high levels of Si and Al were also maintained in the leachates of the acidified

columns (cf. Figures 6,7 & 8,9) suggesting that Na and K released at low levels from the ash was likely derived from the aluminosilicate matrix of the ash.

The mechanism of univalent element removal from fly ash may be more complex than the dissolution of particle surfaces. Differential depletion of Na from the ashes with respect to K, was most notable in the 0.005 M H₂SO₄ leached Sundance series (Table 7). The overall levels of Na released from the ashes were also much higher than the levels of K released during the later leaching stages (Table 3). Differential removal of the univalent elements from the near-surface locale of the aluminosilicate glass phase of the ashes may be possible. Univalent cations (Li, Na, K, Rb, Cs, etc.), unlike other glass constituents, are capable of solid state migration within glass which is in contact with aqueous acid solutions (Boksay et al. 1968). The removal rates of Na, K, and other alkali cations from glass depend on solution acidity, temperature, atomic radius of the dominant diffusing ion (increasing with decreasing ionic radius) and the activities of the respective ions in solution (Jambon and Carron 1976; White 1983). Migration and escape of univalent elements occurs at a decreasing rate independent of a dissolving glass surface (White 1983). The slight decrease in the concentration of both Na and K in the first column leachate solutions during the later stages of leaching (Table 3), suggests that migration of the univalent elements within the aluminosilicate glass of fly ash

particles does occur. The increased acidity of the mineral acid, compared to the organic acid mixture, would be responsible for the enhancement of the migration mechanism in the 0.005 M H_2SO_4 leached samples. Hence, the greater removal of Na from the ash compared to K, may be due to both greater association of Na than K with a more soluble phase of the ash and greater solid state removal of Na from the less soluble glass phase of the ash.

Silicon and Aluminum

Silicon displayed the greatest degree of negative enrichment of the major ash constituents (Tables 5-8). In all four leaching series Si was negatively enriched in the ash of the first columns, and in some cases, the surface core sections of the second columns. Negative enrichment of Si in the first column was greatest in the surface core sections, then decreased with core depth. The remaining ash core sections from all other columns were not significantly changed in content of Si from the unweathered ashes except for the surface-edge samples of some of the latter columns of each leaching series. The moderate depletion of Si in these samples would be due to dilution through carbonate additions.

The percentage of the total Al represented by the amount of Al removed from the first column ash was much greater than the percentage of the total Si removed from the column. The total quantities of Si in the ashes was much

greater than the quantities of Al (Table 4). Aluminum was depleted in the ash of the first columns leached with 0.005 M H₂SO₄, but negatively enriched in the first column ash of the AASA leached series (Tables 5-8). Increases in the content of Si in the first columns of each leaching series corresponded well with negative enrichment primarily due to Ca removal. Negative enrichment of Al in the first columns of the AASA leached series was also due to the removal of Ca. The same effect was nullified due to an equal or greater magnitude of Al removal from the ash of the H₂SO₄ leached first columns. The greater acidity of the mineral acid and its longer reaction period in this experiment was apparently more effective in removal of Al than the organic leaching solution. The acidified H₂SO₄ leached ash cores released higher levels of Al than did the AASA leached columns. Under acidic conditions, the levels of Al in the first column leachates also exceeded the levels of Si (Figures 8 & 9). The sum quantities of Al released from the first column ash cores were greater than the sum quantities of Si. Silicon was therefore primarily residual in the ash while Al was primarily depleted from the eluvial ash columns.

The lower core sections of the second columns and/or the upper core sections of some of the third column cores were generally enriched in Al compared to the unweathered ash (Tables 5-8). The moderate increases in the content of Al in these core sections were likely due to precipitation

of Al from solution as indicated by the sharp decreases in concentrations of Al in the leachates passing through the second and third columns of each series (Figures 8B & 9B). Dissolved Si was removed from the leachates similar to Al (Figures 8A & 9A) Precipitation of Si must have therefore also occurred in the second and third column cores. Increases in the content of Si in the core sections, parallel to increases in the content of Al, were not evident (Tables 5-8). The percentage of Si added to the cores through precipitation from solution, compared to the total content of Si in the ash, was very small and therefore likely not detectable. Errors introduced through determination of Si by difference would also contribute to errors in detection of the small percentage increase in the content of Si in each core section. Although increases in the content of Si in the ash cores were not discernable, precipitation of Al and Si within the same column and increases contents of Al in the respective column core sections suggested that translocated Al and Si could have precipitated in the ash cores as an aluminosilicate.

Iron

The highly visible movement of Fe within the ash cores was related to declining pH values. Soon after acidification of the ash in the first columns (after the first few incremental additions) a brownish yellow (10YR 6/8)m to yellowish red (5YR 4/8)m band of approximately

0.5cm thickness developed within the ashes near the top of the cores. Similar bands also developed within the ash of the second and third columns soon after their acidification. With additional acidic leaching, the bands slowly moved down the ash cores in chromatographic fashion. Over the entire leaching period the bands did not reach the bottoms of any of the cores. Isolated pockets of similar colour were also observed surrounding a few large bubbles which had formed against the column walls within some of the acidified ash cores. Formation of the colours adjacent to the bubbles indicate that oxidation-reduction conditions also have an important role in the translocations of Fe during fly ash weathering.

The enrichment of Fe in the core sections closely matched the positions of the coloured bands in each of the columns. The surface and middle core sections of the first columns were extensively depleted of Fe (Tables 5-8). Iron was most highly enriched in the bottom of the first column cores which corresponded to the location of the band at the termination of leaching. Iron enrichment also occurred in the surface and surface-edge samples of the second columns of each series. Iron dissolved from the surface and middle core sections of the first columns by the mineral acid was immediately precipitated either in the bottom of the first columns or on the surfaces of the ash of the second columns before acidification of the latter. Columns which were not acidified showed no evidence of translocation (cf.

Figures 1B & 10A). However, these columns were slightly depleted in Fe (Tables 5-8). Iron depletion in these latter columns was likely due to dilution through the addition of other phases.

Iron dissolved from the ash by the organic acid solutions tended to diffuse into the ash of the second column cores more readily compared to the mineral acid leachates. In general the coloured bands produced from AASA leaching were more diffuse and not as intense in chroma as those produced through mineral acid leaching. Infiltration of the AASA dissolved Fe into the ash of second column cores is indicated by the Fe enrichment of most of the ash core sections (Tables 6 & 8). Enrichment of Fe was limited to only the surface layers of the second columns of the 0.005 M H_2SO_4 leached series (Tables 5 & 7).

The more diffuse Fe enrichment pattern in the second column cores of the AASA leached series suggested that the formation of the stable Fe-salicylate complexes inhibited Fe precipitation. Complex Fe-salicylate salts tend to be reddish in colour (Windholtz 1976). The organic leaching solutions, after passing through the acidified first and second columns, ranged in colour from burgundy to dark purple which changed to clear on addition of alkali. Similar colours involving organic- Fe^{2+} complexes were observed by Bloomfield (1953) in pine needle extracts used to leach soil material in a study of podzolization. Formation of Fe^{2+} -salicylate complexes would inhibit Fe

precipitation. Similar inhibition of Fe precipitation has been observed for soil organic compounds (Schwertmann 1966).

The ferromagnetic fractions of the unweathered fly ashes were primarily composed of Fe and represented only a small fraction of the bulk ashes (Table 10). Of the major elements, only Fe was enriched in the ferromagnetic fraction, compared to the bulk ash. The ferromagnetic fraction comprised 8.8% and 13% of the Fe in the Sundance and Forestburg bulk ashes, respectively. The elements capable of substitution for Fe in spinel structures include Al, Ca, Mg, Mn, Ni, Cr, Cu, and Co, (Deer et al. 1966; Brimblecombe and Spedding 1975; Sidue et al. 1978). These elements did not exceed 10% of the ferromagnetic fractions. Silicon was the second most abundant constituent (after Fe) in the ferromagnetic fraction, but it likely occurs as discrete inclusions of quartz and/or amorphous material physically fused with the ferromagnetic particles. Some of the Al and Ca in the ferromagnetic fractions may be associated with Si.

The majority of the Fe removed from the bulk ash was derived from a source other than the ferromagnetic fraction. Dissolution of magnetite or ferrite is very slow even under extreme acid conditions. The percentage of the total Fe contained in the ferromagnetic fraction is considerably less than the percentage of Fe removed from the surface and middle core sections (Fe depleted) of the first column cores. The ferromagnetic fraction could therefore not

Table 10. Chemical characteristics of the ferromagnetic fractions separated from the unleached fly ash.

Component	Forestburg Fly Ash			Sundance Fly Ash		
	Content	Enrichment Factor	% of Bulk Composition	Content	Enrichment Factor	% of Bulk Composition
SIO ₂	24.4 %	0.4	0.3 %	17.9 %	0.4	0.2 %
FeO ₂₃	58 %	9.8	13 %	66 %	14.7	8.8 %
AlO ₂₃	7 %	0.4	0.5 %	6 %	0.3	0.2 %
CaO	5.9 %	0.5	0.7 %	6.2 %	0.4	0.2 %
MgO	1.8 %	0.8	1.0 %	1.3 %	1.0	0.6 %
NaO ₂	1.1 %	0.3	0.4 %	0.7 %	0.2	0.1 %
KO ₂	0.4 %	0.2	0.2 %	0.2 %	0.1	0.1 %
MnO	1.0 %	29.4	40 %	1.3 %	26.0	16 %
Ni	270 ug/g	6.8	9.0 %	140 ug/g	3.1	1.9 %
Cr	120 ug/g	0.8	1.2 %	80 ug/g	0.8	0.5 %
Cu	70 ug/g	2.3	3.2 %	80 ug/g	1.8	1.1 %
Co	80 ug/g	2.7	4.0 %	70 ug/g	2.0	1.2 %

* Determined by difference.

account for all Fe dissolved from the first column cores. Since the percentage of all other elements in the ferromagnetic fraction represent negligible fractions of the bulk ash compositions (except Mn), the quantity of these elements released through dissolution of the ferromagnetic fraction compared to the bulk ash would also likely be negligible.

Trace Elements

Most of the trace elements displayed enrichment and depletion patterns within each series of weathered ash similar to those for the major and minor elements (Tables 5-8). Significant positive and negative correlations occurred among three main groups of elements (Table 11 and/or Appendix, Tables 41 & 42). The elements Sr and Ba (in the case of AASA leaching) were highly correlated only with Ca and Mg. Correlations also suggest that the trace elements Mn, Ni, Cr, Co, and Cu act similar to Fe, Al, Ca, and/or Mg. The concentrations of Pb in the core section samples exhibited a high positive correlation with Si, K, and in the case of 0.005 M H₂SO₄ leaching, Ba. The content of some trace elements in the weathered residue digests were in some instances very close to AAS detection limits. Differences in trace element compositions among the weathered core sections and the unweathered ashes may therefore in some cases be questionable.

Table 11. Elements with concentrations in the weathered ash residues exhibiting significant correlations

Element	H 88		AASA		H 88		AASA	
	Positive	Negative	Positive	Negative	Positive	Negative	Positive	Negative
Al	Mn, Mg, Co, Si, Cu	Si, K, Pb, Ba	Cr, Mg	Si	Mo, Co, Cu, Si, Mg, Mn, Cr	Be, Si, Pb	Pb, Cu, Mn	Sr, Co
Ca	Mn, Ni, Mg, Al, Sr, Cu	Si, K, Pb, Ba	Sr, Mn, Ba, Mg	K, Na, Si	Sr, Ni, Mn, Mg, Cr, Ba, Co	Si, Pb, K, Ba	Sr, Mn, Mg, Ba	K, Na, Si, Sr, Pb
Pb	Cr, Co		Ni, Cu, Mg	Si	Cr	Al, Cu	Al, Cu	Sr
K	Si, Pb, Ba	Co, Mg, Mn, Si, Al, Cu, Sr	Si, Ba, Co	Be, Co, Sr, Mn, Mg, Cr	Si	Sr, Co, Mg, Mn, Si	Si, Na, Pb	Mn, Co, Mg, Sr, Ba, Cr
Mg	Si, Mn, Co, Al, Cu, Sr	Si, K, Pb, Ba	Mn, Sr, Co, Al, Pb, Cr	Si, K, Ba	Si, Mn, Co, Al, Mg, Ba, Cr, Cu	Sr, Pb, Ba, K	Mn, Cr, Ba, Co	Si, K
Na			K	Mn, Sr, Co, Mg	Al, Ni, Co, Cr, Mn, Mg, Cu, Co	Al, K	Sr, Co	
Si	K, Ba, Pb	Co, Mn, Mg, Al, Si, Cu, Sr	K	Co, Sr, Mg, Al, Mn, Ba, Pb	Pb, Ba, K	K, Mn, Na, Mg, Co, Ba, Cr, Si, Sr	K, Pb	Mg, Co, Mn, Sr, Ba, Cr
Be	K, Si, Pb	Mn, Co, Mg, Al, Ni, Sr	Ca, Sr, Cr	K, Co, Si	Pb, Si	Mo, Al, Cr, Cu, Ni, Mg, Co, Mn, Co	Mg, Co, Ba	Si, K
Co	Cu, Cr, Fe		K	Be, Cr	Si, Al, Mn, Mo, Cu, Mg, Cr, Co	Si, Pb, Ba	Mg, Mn	
Cr	Fe, Co, Cu		Be, Al, Mg	Co, K	Mo, Ni, Co, Cr, Al, Mn, Mg, Fe, Cu	Si, Pb, Ba		Si, K
Cu	Al, Mn, Co, Ca, Cr, Mg	Si, K, Pb	Pb, Si		Al, Co, Ba, Si, Mg, Mn, Cr	Be, Pb, Si	Pb, Al	K, Si, Pb
Mn	Mg, Ni, Co, Al, Cu, Sr	Si, K, Ba	Mg, Sr, Co	Na, K, Si	Si, Mg, Co, Ni, Ba, Al, Cr, Cu	Si, Pb, Ba, K	Mg, Cr	
Ni	Mg, Mn, Co, Al, Sr, Cu	Si, K, Pb, Ba	Fe, Cu		Mn, Mg, Co, Ba, Cr, Al, Ni, Sr, Cu	Si, Pb, Ba, K		
Pb	K, Si, Ba	Mg, Ni, Co, Al, Mn, Cu			Si, Ba	Mn, Mg, Ni, Ba, Co, Cu, Cr, Sr	K, Na, Si	Sr, Co, Mn
Sr	Co, Mn, Ni, Mg	Si, Ba, K	Co, Mn, Ba	K, Si, Na	Co, Mn, Ni, Mg	K, Si, Pb	Co, Ba	Mo, K, Al, Si, Pb, Fe

© 1980 U.S. Geological Survey, Reston, Virginia

Barium and Sr are chemically similar to Ca and Mg and act accordingly during fly ash weathering. Barium displayed two enrichment/depletion patterns. A negative enrichment pattern, similar to that of Si and K, in the 0.005 M H_2SO_4 leached series and a depletion pattern, similar to that of Ca, in the AASA leached samples. Strontium exhibited depletion in all leached ash residues and overall was the most extensively depleted of all the monitored elements. Both Ba and Sr were slightly enriched, with respect to adjacent core sections, in the carbonate enriched surface-edge samples.

Negative enrichment of Ba in the first column cores of the H_2SO_4 leached series was very likely due to the immediate precipitation of dissolved Ba as sparingly soluble $BaSO_4$ (barite). The high concentration of SO_4^{2-} maintained in solution through H_2SO_4 additions would depress $BaSO_4$ dissolution for the duration of leaching. The concentrations of SO_4^{2-} were apparently not high enough to induce $SrSO_4$ (celestite) precipitation. Depletion of Ba in the AASA leached samples displays the dissolution trend of Ba in the presence of the organic ligands. The exceptionally high enrichment values for Ba in all core sections of the Sundance ash leaching series are not realistic, suggesting some analytical problems with Ba determination.

The substantial removal of Sr suggests that the largest percentage of this element is associated with the highly

soluble phases of the unweathered ash. The high correlation of Sr with Ca indicates association with CaO, most likely as SrO in solid solution with CaO. Dreesen et al. (1978) also observed similarities in behaviour of soluble Sr and Ca. Strontium association with Ca is likely, since the solubility of alkaline earth oxides increases with increasing cationic radii whereas other compounds (e.g. sulfates) exhibit the opposite trend (Cotton and Wilkinson 1972). Barium also probably occurs in solid solution with CaO, but not to the extent of Sr. After leaching fly ash for two years with distilled water, Dudas (1981) also found Ba negatively enriched and Sr depleted in leached ash residues. Lower overall removal of Ba from the ash, (considering the Forestburg data only) compared to Sr, suggest that a significant portion of the total Ba in the unweathered ashes is associated with a less soluble phase than an oxide.

The degree of enrichment of the trace elements Co, Cr, Cu, Mn, and Ni in the ferromagnetic fractions of the unweathered ashes was very diverse (Table 10). Compared to the bulk ashes, the ferromagnetic fractions contained slightly elevated concentrations of Co, Cu, and Ni, consistent with the results of Hansen et al. (1981). Contrary to the results of Hansen et al. (1981), Cr contents of the ferromagnetic fractions were lower than the bulk ash contents while Mn displayed extreme enrichment. Except in the case of Mn, the low ferromagnetic yield

suggests that this fraction does not contain major percentages of any elements in the bulk ash. Dissolution of the ferromagnetic fraction would substantially influence only the translocation of Mn among the trace elements in the ash.

The concentrations of the trace elements Co, Cr, Cu, Mn, and Ni in the weathered core sections displayed various correlations with the major elements Fe and Al, and the minor constituent Mg. Differences were notable between the two leaching regimes. Only Cr in the 0.005 M H_2SO_4 leached samples and Cu in the AASA leached samples were significantly correlated with Fe. Conversely, Cu exhibited positive correlations with Al, and Cr with Mg in the 0.005 M H_2SO_4 and AASA leaching regimes, respectively. Manganese was highly correlated with Mg in all four leaching series while Ni was positively correlated with Mg (and Mn) only in the H_2SO_4 leached samples. No consistent correlations were found for Co, or in the case of the AASA leached samples, for Ni.

The parallel depletion/enrichment patterns for Cr with Fe in the H_2SO_4 leached samples indicates that these elements are translocated in a similar fashion during leaching with the mineral acid solution. Chromium enrichment in the same core sections as Fe indicates co-precipitation. Depletion of Cr in almost all core sections (Tables 5-8) suggests that a significant percentage of the total Cr is easily leached from the ash under

alkaline conditions. In an anionic form (such as an oxyanion or as a negatively charged complex) Cr would remain soluble under alkaline conditions and could be transferred through the column cores. In a cationic form, Cr would likely precipitate (Eggett and Thorpe 1978).

Lead (Pb) was the only trace element to exhibit a consistently high positive correlation in the weathered core residues with the elements Si and K. Some precipitation of Pb as $PbSO_4$, similar to the formation of $BaSO_4$, may have occurred in the H_2SO_4 leached samples. Since enrichment of Pb in the first column cores also occurred in the AASA leached series, inhibition of Pb mobilization strictly by sulfate precipitation is unlikely. Negative enrichment of Pb in the first column cores is therefore likely due to the association of the majority of the total Pb in the ash with sparingly soluble aluminosilicate phases.

The similarity of other trace element depletion/enrichment patterns with major and minor components, as indicated by the significant correlations among the components of the weathered ash (Table 11), generally indicated removal and precipitation of the elements within the same core sections. Copper enrichment in the same ash samples as Al and Fe may indicate association of Cu with precipitated Fe and/or Al phases. Correlation of Ni with Mg suggests that Ni may precipitate as a carbonate, similar to Mg, in solid solution with $CaCO_3$. The chemistries of many of the remaining correlated elements

are not highly compatible and explanations for the remaining positive correlations are not readily apparent.

C. Residue Mineralogy

Unweathered Ash

The X-ray diffractograms of the bulk unweathered ash samples revealed the presence of some crystalline material and a large quantity of X-ray amorphous material (Figure 11). Only two crystalline minerals were found in the unweathered bulk samples: mullite ($3\text{Al}_2\text{O}_3 \cdot 2\text{SiO}_2$) and α -quartz ($\alpha\text{-SiO}_2$). The broad humps located between $15^\circ 2\theta$ and $35^\circ 2\theta$ in both patterns indicate the presence of large quantities of amorphous glass in both fly ashes.

The quantities of mullite and α -quartz in the two unweathered ashes were different. The intensities of the various peaks in the X-ray diffraction patterns give an indication of the relative quantities of crystalline minerals in each ash. The 101 peak (3.343\AA) of α -quartz was consistently more intense in the patterns for the unweathered Forestburg ash than in the patterns for the Sundance ash indicating a larger quantity of α -quartz in the former ash. Conversely, the most intense diffraction peaks for mullite (3.390\AA and 3.428\AA) were much lower in intensity and many of the smaller diffraction peaks absent in the Forestburg ash patterns compared to the Sundance ash patterns.

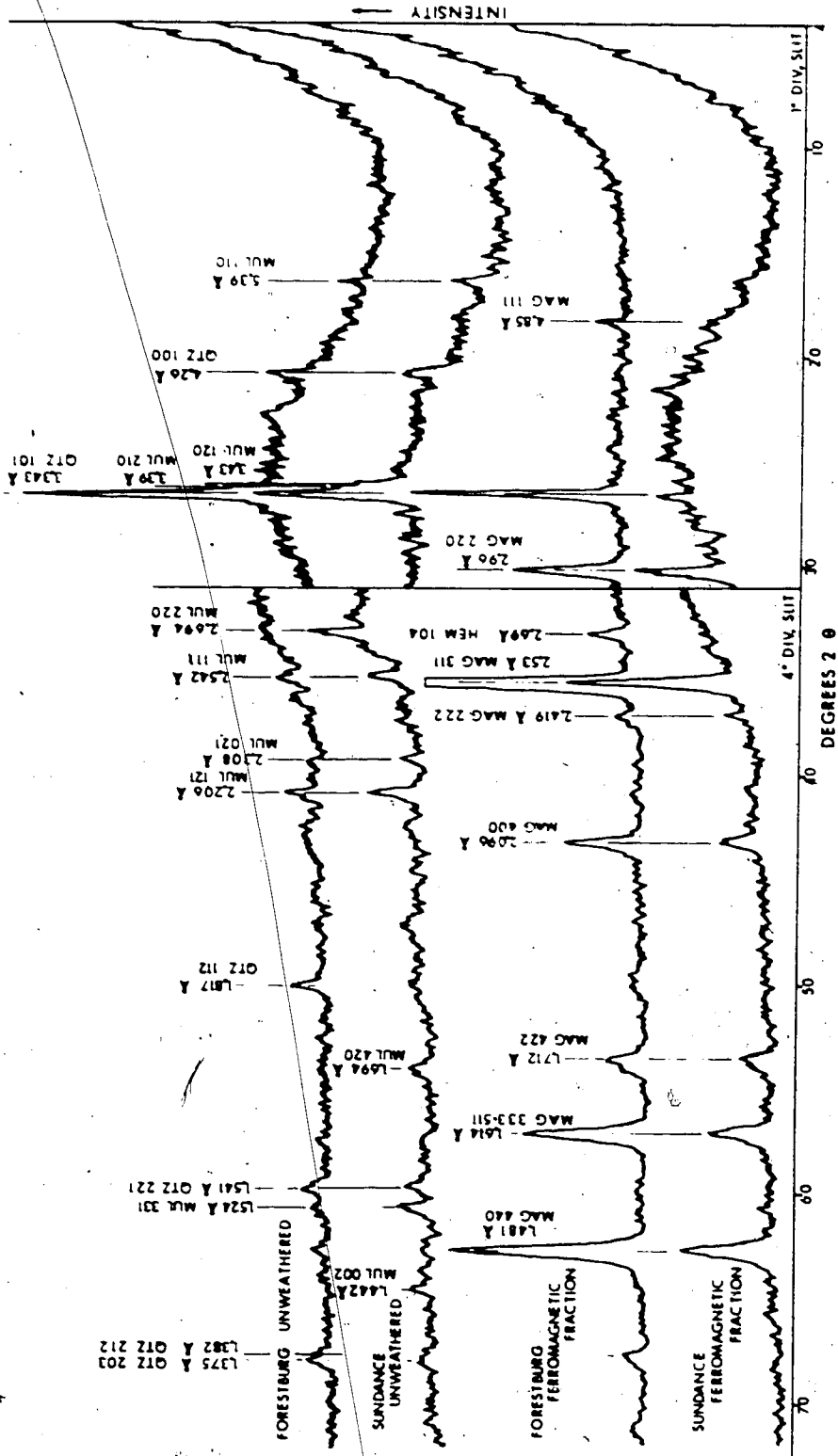


Figure 11. X-ray diffractograms of the unweathered Forestburg and Sundance fly ash samples and their respective ferromagnetic fractions.

The unweathered ash samples also contained magnetic spinels. The diffraction patterns for the two unweathered bulk samples did not exhibit peaks for magnetite. Considering the very low content of ferromagnetic material in the bulk samples (Table 10) detection of magnetite by X-ray diffraction methods is unlikely. The X-ray diffraction patterns for the magnetically separated fractions were typical of magnetite (Figure 11). In addition to magnetite, the ferromagnetic fraction of the Sundance ash also contained some amorphous material, as indicated by the broad humps in the pattern. The ferromagnetic fraction of the Forestburg ash contained some α -quartz. The most intense peak for hematite (2.69Å) was also evident in the Forestburg ferromagnetic pattern; however, the absence of other diffraction peaks for the mineral precluded positive identification.

Almost all the particles comprising both unweathered fly ashes were spherical (Plate 1A) which is typical of the dominant particle morphologies of most fly ashes. Particles of other morphologies, including cenospheres and plerospheres, were also identified in both ashes (Plate 1B). The Forestburg ash contained more cenospheres and plerospheres and had a higher content of Fe than the Sundance ash which is consistent with the findings of Raask (1968). Energy dispersive spectra revealed Fe as the third most abundant element (after Si and Al) in most spherical Forestburg ash particles, while Ca was the third most

7
Plate 1. Scanning electron micrographs and energy dispersive spectra of the unweathered fly ash samples.

A: The "typical" spherical morphologies of the particles of the unweathered fly ash samples.

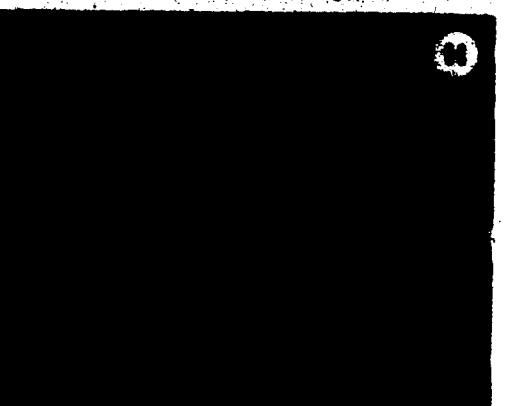
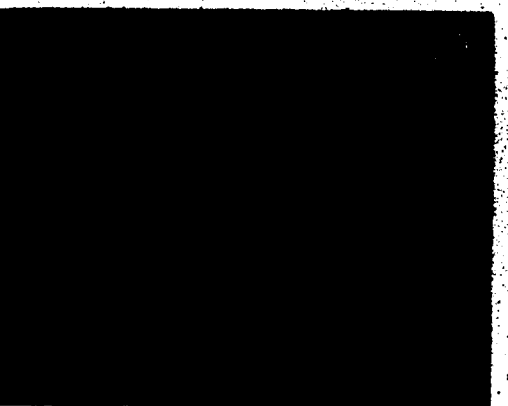
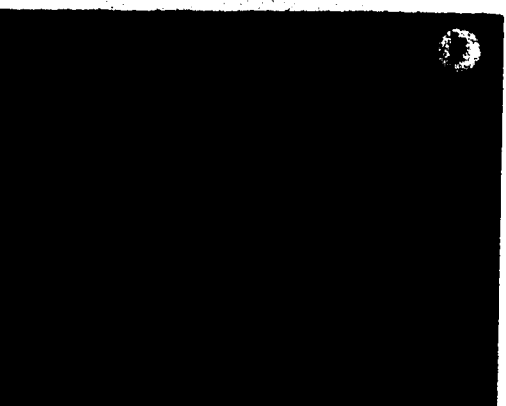
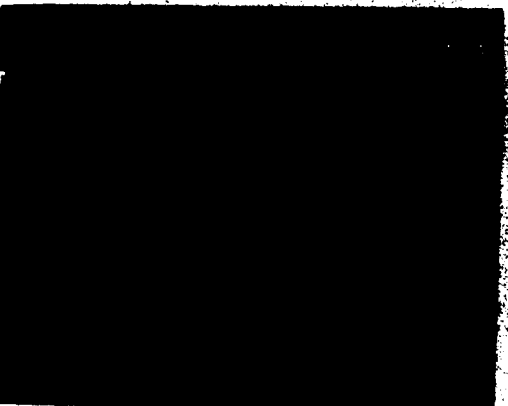
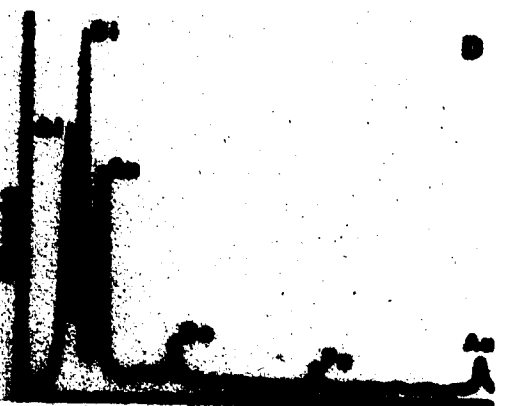
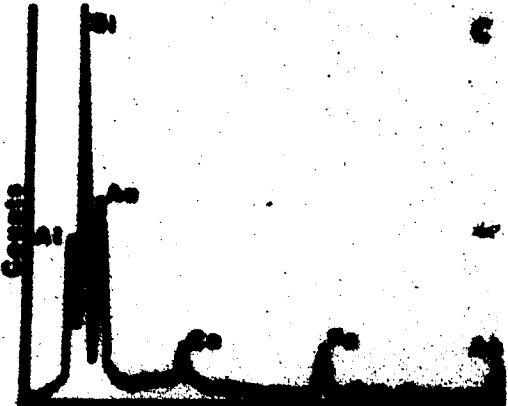
B: A plerosphere in the unweathered Forestburg ash.

C: Energy dispersive spectrum of a "typical" spherical particle of the Forestburg ash.

D: Energy dispersive spectrum of a "typical" spherical particle of the Sundance ash.

E,F: Surface morphology of the spherical particles of the unweathered Forestburg fly ash.

G,H: Surface morphology of the spherical particles of the unweathered Sundance fly ash.



abundant element in most Sundance particles (Plate 1C & 1D). The surfaces of all spherical particles in both unweathered ash samples appeared smooth, although the Forestburg ash particles tended to be much "cleaner" in appearance than the Sundance particles (cf. Plate 1E & 1G). Most Sundance ash particles were covered with extremely small (submicron) dust-like fragments (Plate 1G & 1H). The Forestburg ash also contained these fragments (Plate 1E & 1F) but in lower quantities compared to the Sundance ash.

The infrared spectra of the unweathered fly ash samples contained major absorption bands of various intensities located within the wavenumber regions of $3200-3700\text{cm}^{-1}$, $2850-2900\text{cm}^{-1}$, $1600-1800\text{cm}^{-1}$, $900-1200\text{cm}^{-1}$, $650-850\text{cm}^{-1}$, and $300-500\text{cm}^{-1}$ (Figure 12). The three small sharp peaks located in the $2850-2900\text{cm}^{-1}$ region indicate the presence of a small quantity of coal in the ash (van der Marel and Beutelspacher 1967). The bands within the $3200-3700\text{cm}^{-1}$ and $1600-1800\text{cm}^{-1}$ regions correspond to vibrations for structural OH groups and strongly absorbed water, respectively (Lyon 1964). The largest absorption band in the unweathered fly ash spectra was a very broad featureless band located between 900cm^{-1} and 1200cm^{-1} with a maxima at approximately 1025cm^{-1} . Such bands are common to aluminosilicates and are usually well developed in spectra for glassy materials (Leonard et al. 1964, Farmer 1974). These bands are usually loosely assigned to (Si-O)- and (Al-O)- stretching modes (Farmer 1974). The small broad

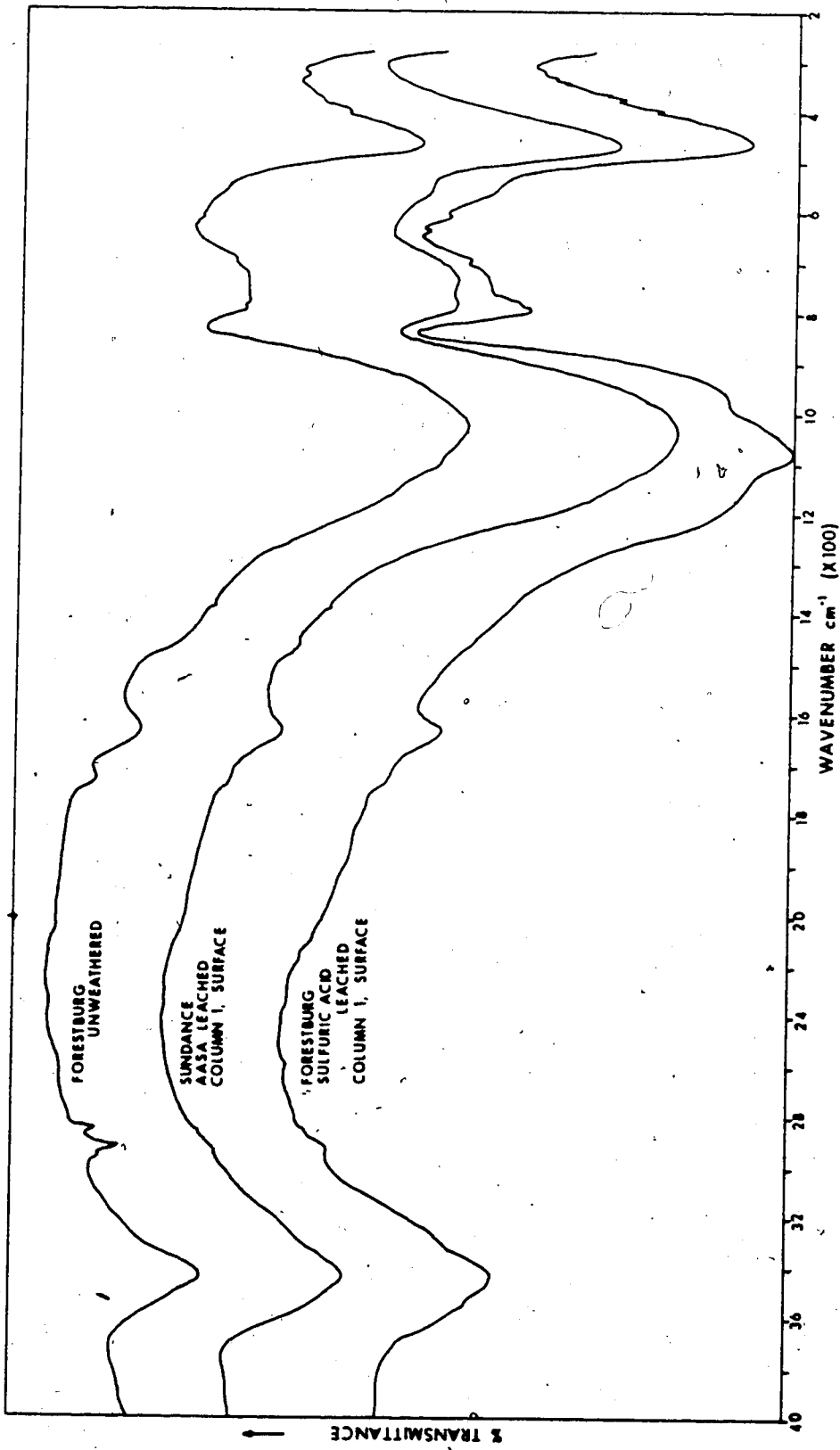


Figure 12. Infrared spectra of the unweathered Forestburg ash and surface core sections from the first columns of the AASA leached Sundance ash and the 0.005 M sulfuric acid leached Forestburg ash.

band in the $650-850\text{cm}^{-1}$ region corresponds to Si-O-Al vibrations and the larger maxima at about 450cm^{-1} is generally assigned to Si-O bending frequencies (Stubican and Roy 1961a,b). Absorption bands at 630cm^{-1} , 670cm^{-1} , 740cm^{-1} , and 950cm^{-1} , characteristic of CaO (Jacobson and Nixon 1968), were not evident in the spectra for any of the samples. These bands may have been masked by the large broad bands for aluminosilicate materials located in the same regions.

Leached Residues

The results of the leachate analyses and other data presented to this point indicate that the dissolution of the fly ash samples occurred in essentially two transient stages. These stages are dominated by specific solution characteristics. The first stage was characterized by extreme solution alkalinity and the release of Ca, Na, and K from the ash in high concentrations. The first leaching stage gave way fairly quickly to the latter leaching stage involving the release of lower levels of Ca, Na, and K along with Si, Al, and Fe under acidic conditions. The dissolution of these and other constituent elements will now be related to the mineralogical characteristics of the weathered ash residues and the dissolution of spherical ash particles.

The extremely small (submicron) dust-like fragments located on, or slightly imbedded in, the surfaces of the

unweathered particles (Plate 1F & 1H) have been noted elsewhere (Fisher et al. 1978; Dudas 1981). The precise composition of these surface dust fragments is not known. The composition of individual dust-like flecks could not be determined by energy dispersive analysis in this study. Most fragments are somewhat similar in appearance to individual physical components of aggregate particles described elsewhere as CaO (Mattigod 1982). The dissolution behaviour of the two ashes employed in this study also strongly implies that the composition of these fragments is indeed CaO.

The Sundance ash contained a greater quantity of dust-like flecks and fragments, compared to the Forestburg ash, and also displayed an additional buffering zone in the pH region above 12.0 not produced during the weathering of the Forestburg ash (Figures 1 & 2). The larger quantity of small fragments present in the Sundance ash would have effectively increased the amount of surface area per unit mass of ash exposed to the leaching solutions. Supersaturation of the Sundance ash leachates with Ca, with respect to Ca(OH)_2 , was due to the very rapid dissolution of a large quantity of Ca. Supersaturation with respect to Ca(OH)_2 created the additional alkaline buffer region above pH 12.0 at the onset of leaching of the Sundance ash (Figures 1B & 2B). The difference in contents of Ca between the two unweathered ashes was not substantial (Table 4). The greater quantity of Ca dissolved from the Sundance ash,

compared to the Forestburg ash, could have been derived directly from the additional surface area provided by the small fragments. The small flecks were not obvious on the surfaces of particles in the leached Sundance ash residues (cf. Plates 1H & 2D). The small dust-like fragments observed in the unweathered ash samples could therefore have been the source of CaO in the ashes.

Such fragments of CaO composition could have been produced in the ashes through the decarbonation of limestone and/or dolomite impurities in the parent coal. Most boiler-furnace temperatures do not exceed the melting point of CaO (2900°C) (Robie 1979). Fragments of CaO formed from the decarbonation of carbonates in the parent coal would not likely admix with coalescing molten material but would rather be expelled, due to surface tension, to the surface of the molten ash droplets. Thus the fragments would be concentrated on particle surfaces and maintain their integrity.

The highly soluble fraction of the unweathered ash samples also contained a variety of elements other than Ca. Alkaline earth elements (Mg, Sr, Ba, etc.) are common impurities in natural carbonate rocks and would very likely occur in solid solution with such CaO fragments formed in fly ash. During weathering, dissolution of CaO would also involve the release of Mg, Sr, and Ba components contained in the oxide. These elements were depleted in the ash similar to Ca (Tables 5-8) indicating that they dissolved

Plate 2. Scanning electron micrographs and energy dispersive spectra of some 1% HF etched fly ash particles and some weathered fly ash particles.

A,B: Spherical fly ash particles etched with 1% HF.

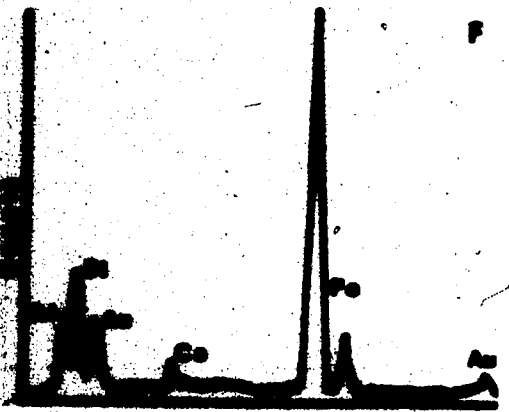
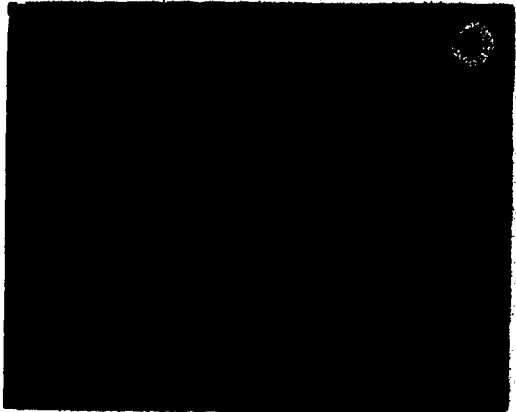
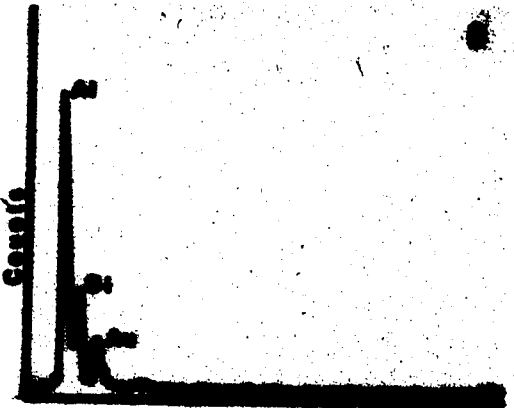
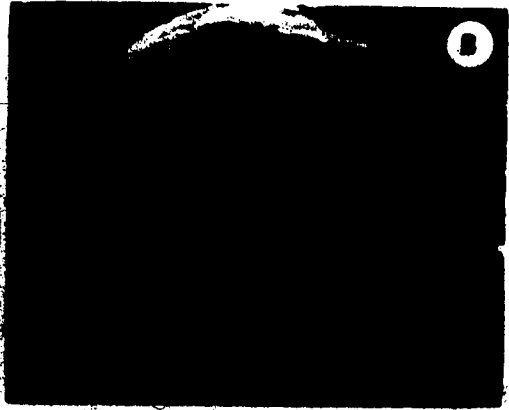
C: Energy dispersive spectra of mullite crystals found in the 1% HF etched fly ash particles.

D,E: Fly ash particles found in the surface core section of the first column of the AASA leached and the 0.005 M H_2SO_4 leached Sundance ash series. Note the surface morphologies.

F: Energy dispersive spectra of a ferromagnetic particle separated from the unweathered Forestburg fly ash.

G: A ferromagnetic particle from the unweathered Forestburg fly ash.

H: A ferromagnetic particle separated from the surface core section of the first column of the 0.005 M H_2SO_4 leached Forestburg ash.



from a common source in the ashes.

The high concentrations of Na and K released from the ashes at the onset of leaching indicates that these constituents are also associated with the CaO phase. Sodium and K could either substituted into the oxide or occur as distinct phases such as sulfates (Green and Manahan 1978; Dudas 1981). The precise forms of the highly soluble Na and K constituents is not evident from the data. As discussed previously, much more of the total Na than the total K in the unweathered ashes is associated with a highly soluble portion of the ash. The very low levels of Al released under alkaline conditions from the latter columns of the Forestburg ash (Figure 8B) suggests that small amounts Al may also be an elemental component of the highly soluble fraction of the Forestburg ash only.

Analysis of the weathered ash residues by XRD and IR methods and examination of the particles by scanning electron microscopy indicate that the Al and Si dissolved from the ash of the first columns of each leaching series under acidic conditions was derived from the glassy matrix of the fly ash particles. The X-ray diffractograms and IR spectra of the ash residue samples from the first column cores indicate that mullite crystals, located in the interior of spherical fly ash particles, become enriched in the ash with weathering. The weathered particles examined by scanning electron microscopy displayed direct evidence that the exterior portion of glassy particles are indeed

removed during weathering.

The preferential dissolution of the glassy material from the fly ash particles was evident in the presence of outlines of numerous acicular crystals on the surfaces of spherical particles from the surface core sections of the first columns of each leaching series (Plate 2, D & E). The surfaces of the spherical particles in the unweathered ashes were essentially smooth (Plate 1). Most spherical particles in both fly ashes etched with 1% HF contained an internal network of acicular mullite crystals (Al:Si ratio = 3:1) enclosed within a matrix composed of amorphous glass (Plate 2, A-C) very similar to the structures reported by Hulett et al. (1979, 1980) and Hulett and Weinburger (1980). Mullite displaying other crystal habits (Hulett et al. 1979) were not observed in the 1% HF etched samples. Exposure of the mullite crystals on the surfaces of the weathered ash particles indicates that the enveloping glassy material was removed during weathering.

The X-ray diffraction patterns for the core section samples from the first leaching columns displayed differences in intensities of the diffraction peaks for α -quartz and mullite. The intensities of the diffraction peaks for mullite and quartz in the patterns for the three core sections for the first leaching columns increased from the bottom to the surface (Figure 13). The intensities of the diffraction peaks for α -quartz increased markedly in the patterns for the first column ash residues compared to the

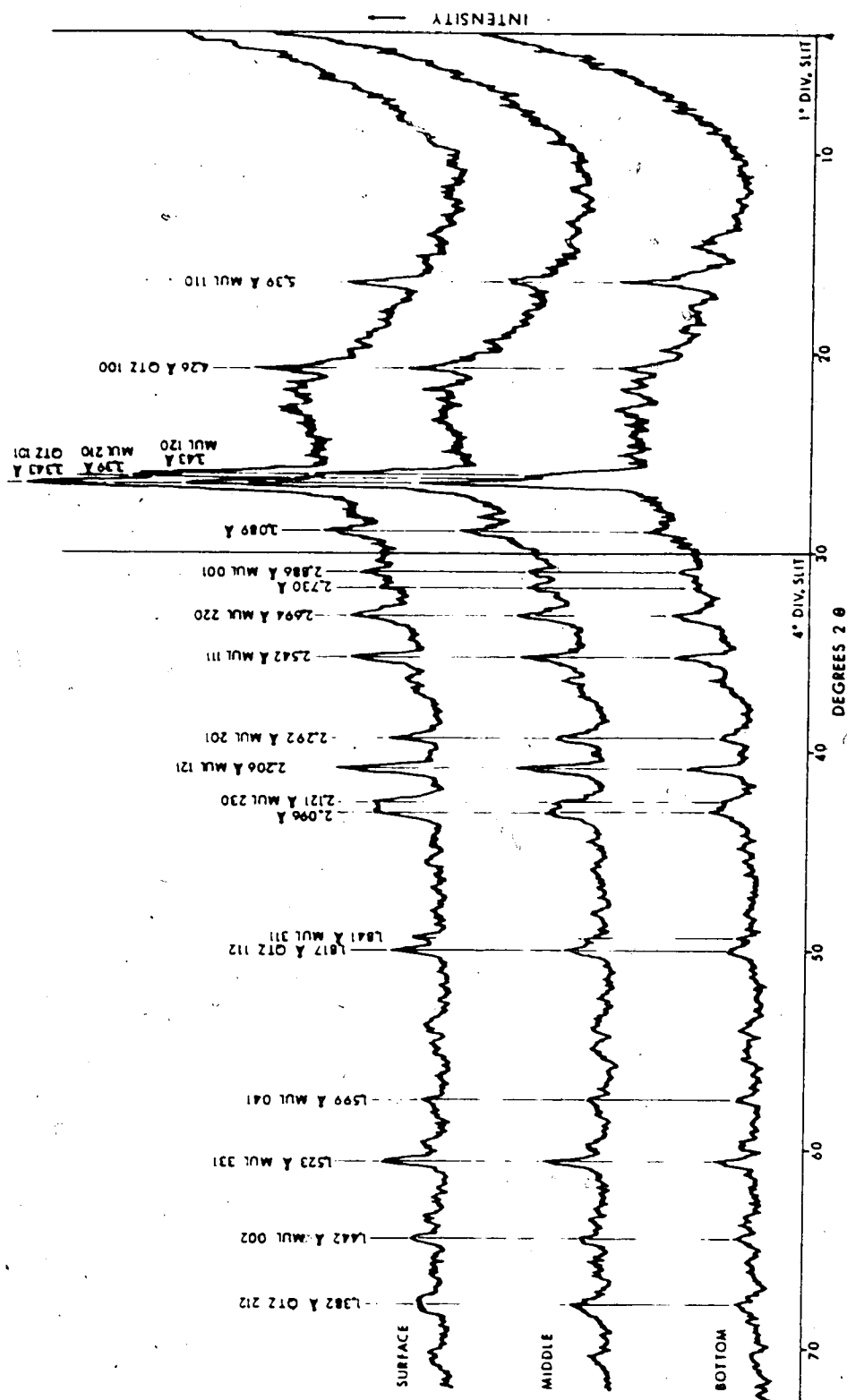


Figure 13. X-ray diffractograms of the three ash core sections from column one of the Sundance ash leached with 0.005 M sulfuric acid.

unweathered ashes (cf. Figures 11 & 13). The intensities of the mullite peaks also increased, but not in proportion to the α -quartz peaks. The ratios of the intensities of the 210 mullite peak (3.390Å) to the 100 α -quartz peak (3.343Å) for the surface, middle and bottom core sections from the first columns of the 0.005 M H_2SO_4 leached Sundance ash were 0.67, 0.62, and 0.53, respectively (Figure 13). The same peak ratio for the unweathered Sundance ash was 0.47 (Figure 11). The diffractograms for the core sections from the first columns of all other leaching series were similar but displayed less pronounced differences in the peak ratios.

The differences in the diffraction peak intensities indicate that dissolution of the glassy material from the ash particles decreased with depth in the ash core according to the chemical dissolution gradient within the core. Alpha-quartz occurs in fly ash essentially as discrete nonfused mineral fragments and possibly as recrystallized inclusions inside some solid spherical particles (Hulett and Weinburger 1980). The solubility of α -quartz is very low, approximately $10\mu g \cdot mL^{-1}$ at low pH values (Brownlow 1979), and therefore it should not dissolve rapidly under the acidic leaching conditions of the first columns. The increases in the intensities of all diffraction peaks with weathering indicate either negative enrichment of the crystalline material in the ashes or removal of amorphous coatings covering them.

The disproportionate increase in the intensity of the mullite peaks, compared to the peaks for α -quartz, indicate that the exposure of mullite on particle surfaces increases from the bottom to the top of the ash core. These increases reflected an increase in the amount of glass removed from the ash from bottom to surface of the first column core. The intensity of the weathering gradient decreased within the first column as the solution percolating through became saturated with respect to the solubility of the glass. Solutions were saturated with Si and Al on leaving the first columns as indicated by the levels of the elements in the leachates (Figures 8 & 9). The amount of glass removed from the particles therefore decreased with depth in response to the weathering gradient.

The major differences between the infrared spectra of the weathered and unweathered samples occurred mainly at wavenumbers of less than 1400cm^{-1} that involve vibration frequencies for Al and Si. Changes in the absorption bands corresponding to vibrations for Al and Si bonds indicate dissolution and removal of the glassy matrix of the ash particles. The 1025cm^{-1} maxima of the large band in the unweathered ash spectra shifted to slightly higher wavenumbers and broadened in the spectra for the surface core sections from the first column of the H_2SO_4 leaching series (Figure 12). The spectra for the corresponding AASA leached sample displayed the same tendencies but the bands were less developed (Figure 12). The broadening of the

largest band was primarily due to two shoulders in the 1100-1200 cm^{-1} and 900-1000 cm^{-1} ranges, most obvious in the H_2SO_4 leached sample. The shoulder in the higher wavenumber region and the band maxima of the large band both correspond to Si-O stretch vibrations while the lower wavenumber shoulder is usually assigned to H-O-(Al) liberation (bending of O-H co-ordinated with Al) vibrations (Stubican and Roy 1961a,b; Farmer 1974). Increases in the intensity of the 460 cm^{-1} band maxima and separation of the broad band in the 1200-1000 cm^{-1} region into sharper more distinct bands generally corresponds with negative enrichment of Si in the weathered samples and possibly the purification of Si phases. Increases in the intensities of the Si-O-Al stretch absorption bands between 650 cm^{-1} and 850 cm^{-1} suggest a greater predominance of Si-O-Al bonds in the weathered ash samples. These bonds would be present in mullite more so than in glass. The small broad 650-850 cm^{-1} band separated into sharper individual bands with weathering. The maxima at 800 cm^{-1} , specifically corresponding to a Si-O-Al stretch vibration (Al in 4-fold coordination) (Stubican and Roy 1961), further indicated that the weathered samples contained a greater quantity of crystalline material compared to the unweathered samples. The appearance of the distinct absorption bands for mullite for the weathered samples instead of the broad non-specific absorption bands of glassy material in the unweathered ash spectra further indicated that the amorphous glass enveloping the mullite

crystals was removed selectively.

Differences in the levels of acid ammonium oxalate extractable Al and Si between most of the first column core sections and the respective unweathered ashes suggested that the amorphous glass of the ash is composed of two major phases: a highly reactive glass phase associated with the exterior of ash particles and a less soluble glass phase associated with the interior regions. Oxalate extractable levels of Al and Si were much lower in most of the first column core sections compared to the values for other samples from the same leaching series and the respective unweathered ashes (Tables 12 & 13). Most of the Si and Al dissolved from the first column was derived from the glassy matrix of the surfaces of the spherical particles. The lower AAO extractable levels of Al and Si only in the first column cores indicated that the residual glassy material remaining after weathering is much less soluble than the reactive glassy material that initially coated the particles. Comparable levels of AAO extractable Si and Al in the weathered samples (other than from the first column), and in respective unweathered ashes, indicated that reaction of the exterior glass was restricted to the samples of the first columns (greatest weathering intensity). The H₂SO₄ weathering regime was more effective in dissolving the reactive glassy phase than was the organic acid regime.

Other alterations with respect to the unweathered ash, not obvious in the SEM photographs or the infrared spectra

Table 12. Acid ammonium oxalate extractable Fe, Al, Si, and Mn in the leached Forestburg fly ash samples expressed as percent of the total elemental content of each core section.

Sample	Sulfuric Acid Leached				AASA Leached			
	Si	Al	Fe	Mn	Si	Al	Fe	Mn
Unleached	10	17	22	9.7	10	17	22	9.7
Column 1								
Surface	0.2	0.9	8.9	15	2.5	7.2	22	18
Middle	1.8	6.5	30	11	8.3	16	29	12
Bottom	4.2	11	35	15	11	19	28	12
Column 2								
Surface-Edges	6.0	18	43	18	10	20	33	19
Surface	8.7	21	37	12	9.1	22	35	13
Subsurface	10	23	30	10	9.1	22	32	14
Middle	12	25	24	11	11	22	30	14
Bottom	10	27	23	8.4	11	22	27	14
Column 3								
Surface-Edges	12	31	33	29	12	19	23	12
Surface	10	29	24	10	11	20	22	11
Subsurface	11	27	24	11	11	23	22	14
Middle	12	30	29	17	14	19	23	17
Bottom	12	26	26	21	13	21	23	15
Column 4								
Surface-Edges	5.8	14	15	8.8	10	21	24	13
Surface	10	21	25	13	10	22	24	13
Subsurface	10	18	22	13	9.3	18	23	13
Middle	10	22	22	12	9.2	21	25	13
Bottom	9.0	22	23	14	10	19	21	13
Column 5								
Surface-Edges	12	24	27	17	10	18	28	10
Surface	9.1	19	26	11	10	22	30	11
Subsurface	11	26	25	11	11	20	25	11
Middle	12	23	25	13	11	24	23	13
Bottom	11	25	18	11	11	18	30	13
Base	11	29	20	11	11	23	30	13

Table 13. Acid ammonium oxalate extractable Fe, Al, Si, and Mn in the leached Sundance fly ash samples expressed as percent of the total elemental content of each core section.

Sample	Sulfuric Acid Leached				AASA Leached			
	Si	Al	Fe	Mn	Si	Al	Fe	Mn
Unleached	13	30	22	5.7	13	30	22	5.7
Column 1								
Surface	0.2	0.6	14	14	8.9	21	53	13
Middle	0.2	1.7	32	16	14	25	55	8.8
Bottom	1.6	13	47	17	16	23	47	8.8
Column 2								
Surface-Edges	12	28	64	27	8.0	19	41	21
Surface	8.9	18	38	10	12	21	43	13
Subsurface	13	22	34	7.5	15	21	44	11
Middle	12	26	32	8.5	18	22	30	12
Bottom	14	31	31	9.0	16	24	29	12
Column 3								
Surface-Edges	14	30	26	8.5	14	30	44	7.1
Surface	14	24	27	10	14	26	38	7.6
Subsurface	14	34	23	9.2	14	27	39	8.4
Middle	13	27	21	9.2	15	21	33	7.7
Bottom	14	25	27	7.3	13	21	31	7.4
Column 4								
Surface-Edges	15	30	31	7.4	16	28	26	8.3
Surface	15	26	26	7.2	16	28	26	7.8
Subsurface	15	26	23	7.2	16	22	31	7.3
Middle	15	24	20	7.2	14	27	28	7.3
Bottom	15	24	26	7.2	15	23	25	6.8
Column 5								
Surface-Edges	14	32	30	7.8	14	28	35	8.9
Surface	16	30	25	9.0	18	26	37	8.6
Subsurface	15	32	29	9.0	18	26	32	8.2
Middle	14	30	25	8.0	16	28	27	7.9
Bottom	12	31	23	7.5	15	25	27	7.5
Base	14	30	27	8.5	16	29	25	7.1

of the first column surface core sections, were detected in the DTA patterns (Figure 14). The broad absorption bands in the infrared spectra of the first column surface core sections of the mineral acid leached and the organic acid leached samples located within the $3200-3700\text{cm}^{-1}$ and $1600-1800\text{cm}^{-1}$ regions, correspond with vibrations for structural OH groups and strongly adsorbed water, respectively (Lyon 1964). These absorption bands did not differ substantially in size, shape, or spectral location from the unweathered ash spectra (Figure 12). The DTA pattern for the first column surface core section of the $0.005\text{ M H}_2\text{SO}_4$ leached series displayed a broad endotherm at 125°C while a similar endotherm was not observed in the patterns for the companion AASA leached samples and the unweathered ashes (Figure 14). DTA patterns for the remaining core sections of the H_2SO_4 leached and AASA leached first columns were similar to their respective surface core sections. This indicated that the mineral acid leached ash contained more adsorbed water and/or OH groups, than the ash of the companion AASA leached series and the unweathered ash. Greater hydration of the first column ash samples due to leaching with H_2SO_4 is also indicated in the loss on ignition (LOI) values (Table 14). The LOI values for the first column core sections of the H_2SO_4 leached series were considerably greater than those for the comparable AASA leached samples. These data indicate that a larger amount of adsorbed water was associated with the

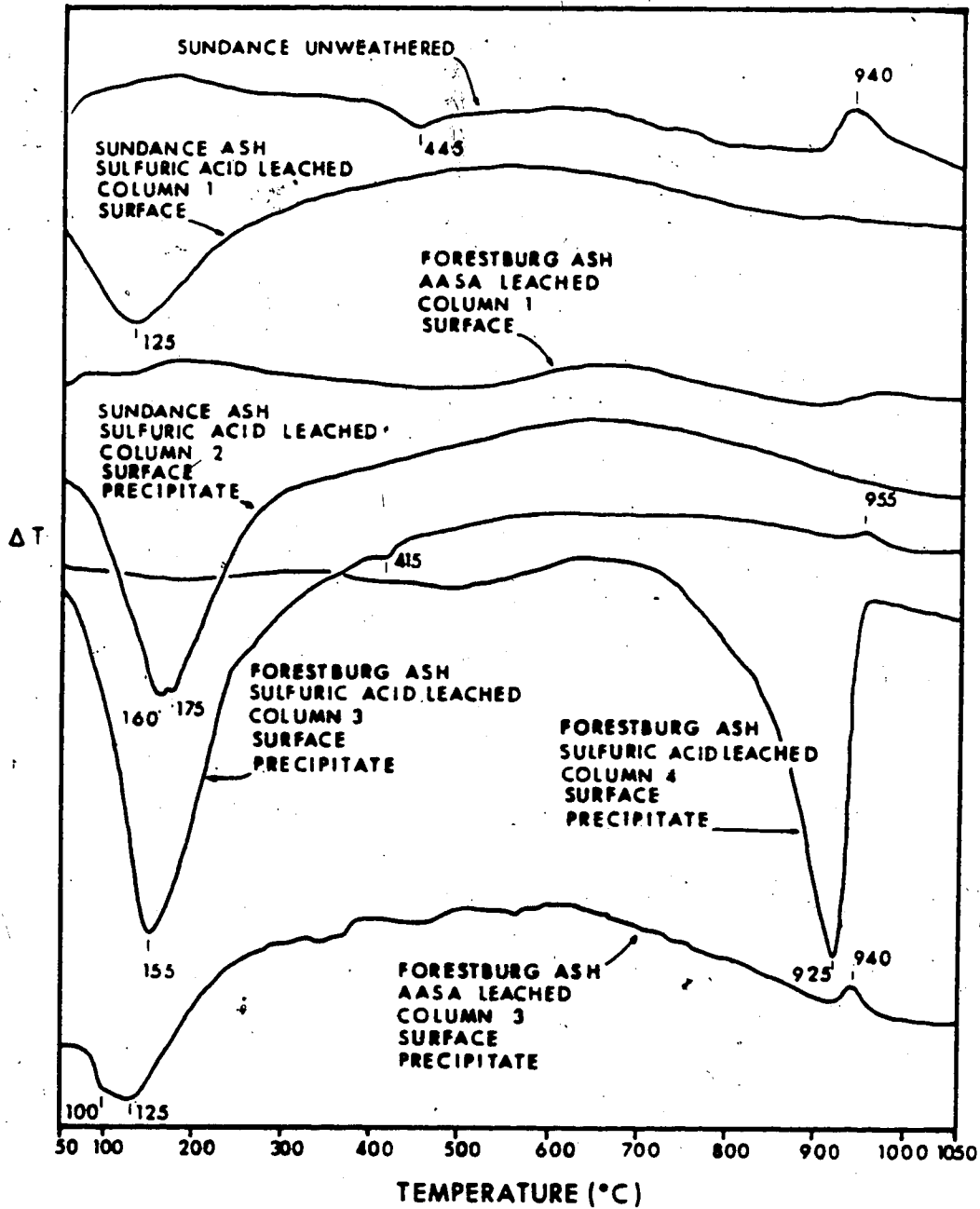


Figure 14. DTA patterns for selected weathered and unweathered fly ash samples.

Table 14. Percent loss on ignition (LOI) for all leached and unleached fly ash samples.

Sample	Forestburg Fly Ash			Sundance Fly Ash		
	Sulfuric Acid Leached	AASA Leached	AASA Leached	Sulfuric Acid Leached	AASA Leached	AASA Leached
Unleached	0.2	0.2	0.2	0.9	0.9	0.9
Column 1						
Surface	2.0	1.2	1.2	3.4	1.7	1.7
Middle	1.6	1.1	1.1	3.6	1.9	1.9
Bottom	2.6	1.1	1.1	3.8	1.9	1.9
Column 2						
Surface-Edges	2.2	2.0	2.0	3.0	2.5	2.5
Surface	1.9	1.4	1.4	2.7	2.1	2.1
Subsurface	1.5	0.9	0.9	2.4	2.3	2.3
Middle	1.6	1.5	1.5	2.7	2.4	2.4
Bottom	1.9	1.7	1.7	2.9	2.4	2.4
Column 3						
Surface-Edges	2.4	1.6	1.6	3.3	2.6	2.6
Surface	1.3	1.3	1.3	1.6	2.2	2.2
Subsurface	1.4	1.4	1.4	1.8	2.1	2.1
Middle	2.0	1.8	1.8	1.9	2.0	2.0
Bottom	2.1	1.7	1.7	1.8	1.9	1.9
Column 4						
Surface-Edges	2.7	2.0	2.0	6.0	6.9	6.9
Surface	0.8	1.0	1.0	2.0	3.4	3.4
Subsurface	1.0	1.0	1.0	1.9	1.8	1.8
Middle	1.4	1.4	1.4	1.9	1.7	1.7
Bottom	1.6	1.4	1.4	1.9	1.7	1.7
Column 5						
Surface-Edges	2.7	2.2	2.2	5.0	5.2	5.2
Surface	1.1	1.1	1.1	2.3	2.7	2.7
Subsurface	1.1	1.1	1.1	2.2	1.8	1.8
Middle	1.4	1.2	1.2	1.8	1.7	1.7
Bottom	1.4	1.4	1.4	1.8	1.7	1.7
Base	1.3	1.4	1.4	1.9	1.7	1.7

H₂SO₄ leached residue samples.

The presence of adsorbed water in the weathered samples may be explained by more than one mechanism. The presence of adsorbed water only in the H₂SO₄ leached samples may possibly be related to the greater degree of solid state migration of univalent elements. The appearance of the H-O-(Al) shoulder between 930 and 980cm⁻¹ on the large absorption band in the IR spectra for the H₂SO₄ leached sample (Figure 12) suggested the presence of OH groups within the aluminosilicate matrix of the ash in co-ordination with Al. Formation of structural OH groups may possibly be due to proton substitution for cations. As discussed in previous sections, the first column cores of the H₂SO₄ leached series were more depleted in Na compared to the first column core AASA leached samples (Tables 5-8). The larger amount of absorbed water might also be due to hydration of the ash particle surfaces through reactions with the mineral acid. The differences definitely indicate some basic dissimilarity in the dissolution mechanisms of the two types of acidic leaching solutions.

The ferromagnetic particles in the ash were also selectively dissolved during leaching. Ferromagnetic particles are usually spherical. They are very similar to non-magnetic aluminosilicate spheres, except that in many cases they can be visually distinguished by the rough appearance of parts of their surfaces (Plate 2G). During weathering, portions of the ferromagnetic particles

associated with smooth surface patches tended to be selectively dissolved leaving a skeleton-like structure (Plate 2H). The internal skeletons of ferromagnetic particles were composed of many small cubic components reflecting the cubic crystal structure of spinels. The smoother appearing surface patches were more soluble than the interior skeletons. The dissolved portions of the particles were likely composed of the elements included in the bulk composition of the ferromagnetic fractions (Table 10) but are not commonly substituted into spinel structures (e.g. Ca, Na, K). Hulett et al. (1979, 1980) found HCl extracts of ferromagnetic fractions to contain high levels of Na and K. Since Mn likely substitutes for Fe in the spinel structure, both elements would not likely be extensively dissolved from ferromagnetic particles.

Precipitation Products

A variety of discrete mineral species and other mineral materials were found in the illuvial ash columns. Three groups of precipitates were distinguished: those associated with Ca, those associated with Fe, and those of aluminosilicate nature. Calcium precipitates were formed under a variety of conditions and were widely dispersed within the ash cores. Translocation of Fe was limited to the acidified cores. Precipitation products of Fe accumulated primarily within the same column cores from which the Fe was derived. Aluminosilicate precipitates

occurred in limited quantities within a range of core sections.

The white (10 YR 8/1)d precipitate deposited in greatest quantities on the surfaces of the ash of the fourth and fifth columns for all four leaching series was composed primarily of CaCO_3 in the form of calcite (Figures 15 & 16). The X-ray diffraction patterns of the fourth and fifth column surface precipitates for both the AASA leached and 0.005 M H_2SO_4 leached series were typical of calcite. DTA patterns for the same samples all displayed large endotherms at 925°C (Figure 14) also diagnostic of calcite (Webb and Fruger 1970). Calcite was also detected by XRD in the surface precipitates and surface-edge samples nonacidified third columns, the surface-edge samples of all fourth and fifth columns and in the surface core sections of the fifth columns of some leaching series. Small rhombohedral crystals of calcite were identified in many of the third, fourth, and fifth surface precipitate samples (Plate 3A & 3B). Other core sections contained carbonate (Table 9) but calcite or other carbonate minerals were not detected by XRD, DTA, or IR methods in these samples. Calcite is the most stable phase of Ca at pH values greater than 7.5-8.0 and atmospheric CO_2 partial pressure (Lindsay 1979). The mineral precipitated under alkaline conditions in the leaching columns regardless of the type of leaching solution.

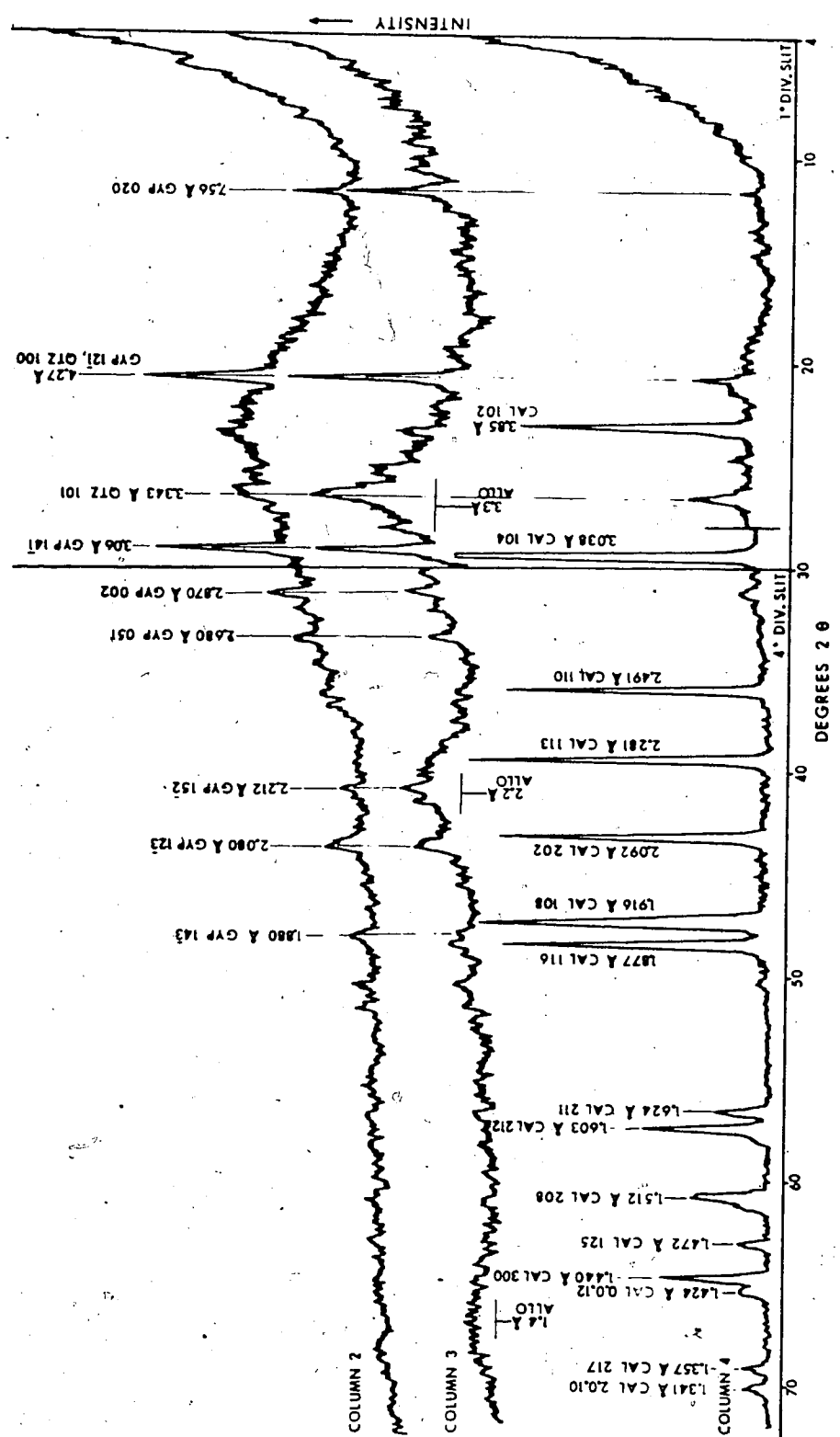


Figure 15. X-ray diffractograms of the surface precipitates from columns two, three, and four of the 0.005 M sulfuric acid leached Forestburg ash.

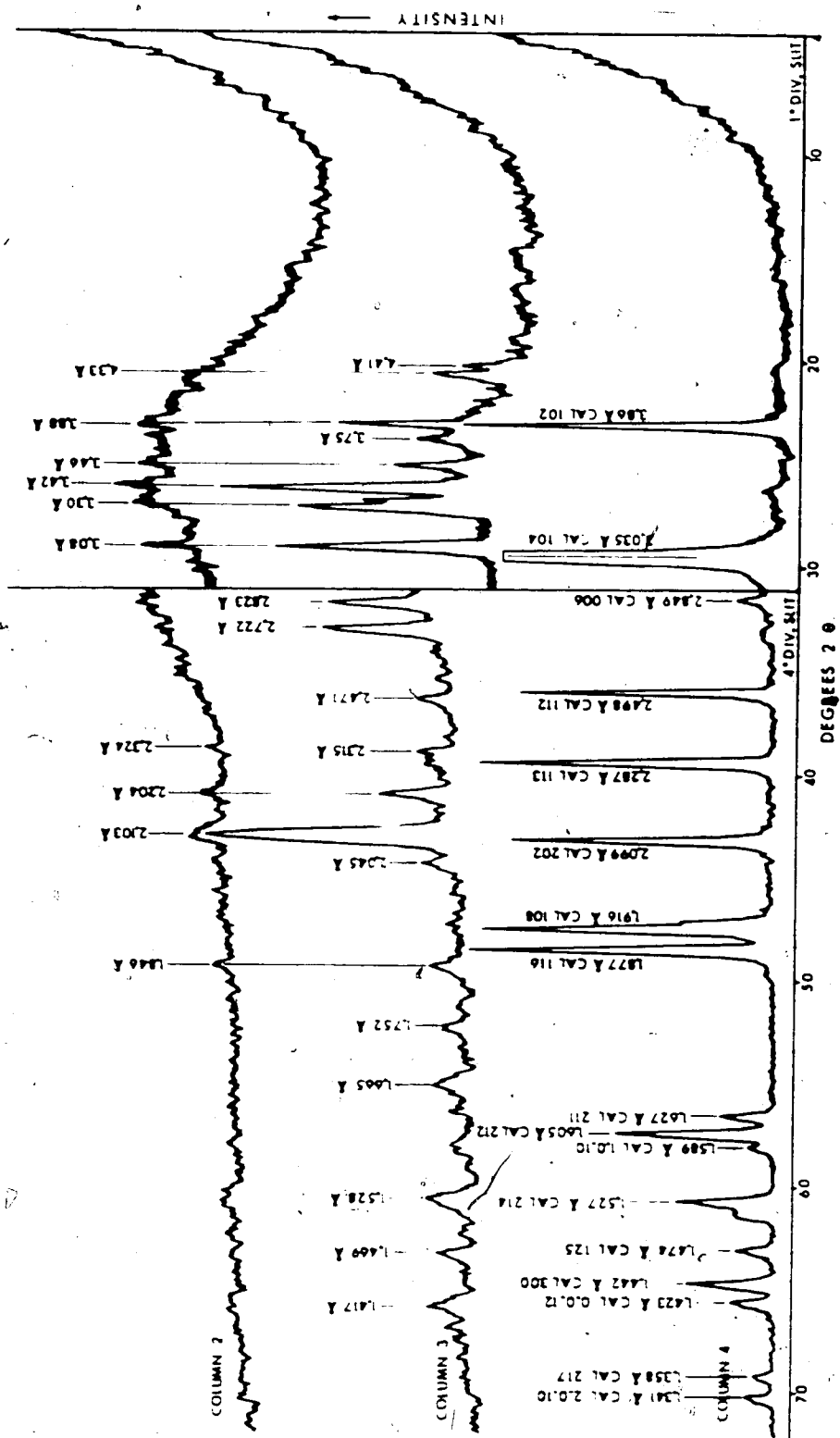
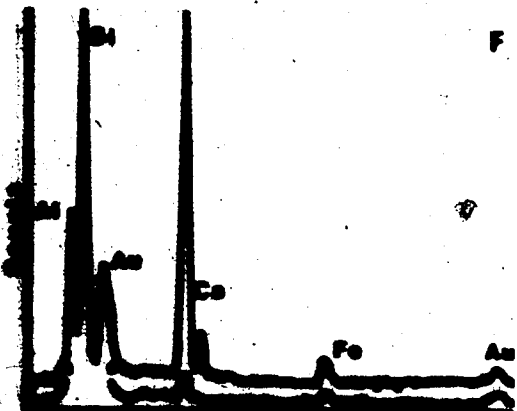
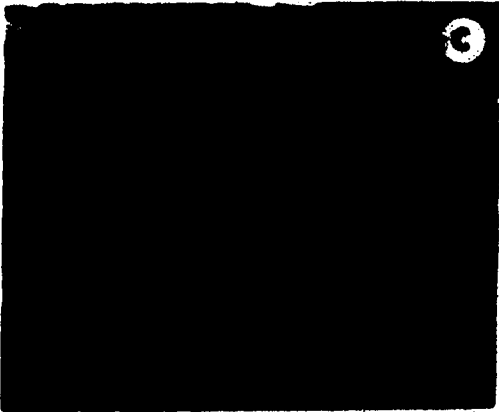
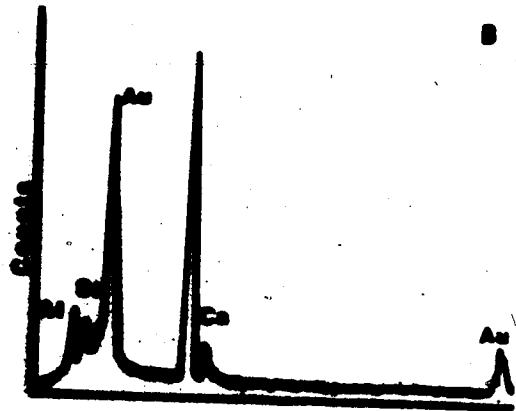


Figure 16. X-ray diffraction patterns of the surface precipitates from columns two, three, and four of the AASA leached Sundance ash.

Plate 3. Scanning electron micrographs of some calcium-rich precipitates from selected weathered ash samples.

- A: Rhombohedral crystals of calcite (CaCO_3) in the surface precipitate from the fourth column of the 0.005 M H_2SO_4 leached Sundance ash series.
- B: Energy dispersive spectra of A.
- C: Bladed gypsum ($\text{CaSO}_4 \cdot 2\text{H}_2\text{O}$) crystals in the surface precipitate from the second column of the 0.005 M H_2SO_4 leached Forestburg ash series.
- D: Orthorhombic Ca-rich crystals (aragonite?) in a fibrous interwoven mass of submicron sized acicular crystals covering the surface of a spherical fly ash particle; from the bottom core section, column four, AASA leached Forestburg ash series.
- E: Discrete orthorhombic Ca-rich crystals (aragonite?) admixed with some fly ash particles; from the surface core section, column four, 0.005 M H_2SO_4 leached Sundance ash series.
- F: Energy dispersive spectra of the crystals in E. Upper spectra = crystals, lower spectra = spherical particles.
- G,H: Orthorhombic Ca-rich crystals (aragonite?) covering the entire surface of a large fly ash particle. Note the tangential orientation of the crystals to the particles surface. Found in the bottom core section, column four, AASA leached Forestburg ash series.



With changing pH conditions other Ca-bearing minerals were formed in the leaching columns. Gypsum ($\text{CaSO}_4 \cdot 2\text{H}_2\text{O}$) was detected by XRD in the surface precipitates of the acidified columns of each 0.005 M H_2SO_4 leaching series (Figure 15). The infrared spectra of the surface precipitates of the second column of the H_2SO_4 leached Forestburg ash (Figure 17) displayed absorption bands typical of naturally occurring gypsum (van der Marel and Beutalspacher 1976). Bladed gypsum crystals were identified by SEM in the same sample (Plate 3C). The DTA pattern for the comparable Sundance ash sample (Figure 14) exhibited two dehydration endotherms at 160°C and 175°C indicative of gypsum, but lacked the small exothermic peak in the $320\text{-}280^\circ\text{C}$ range which is usually also present in DTA patterns of pure samples of gypsum (Berg 1970). Absence of the small exotherm is likely due to dilution of the sample with the Al_2O_3 necessary for sample preparation for DTA.

Instead of gypsum, an unidentified crystalline material was detected by XRD in the companion AASA leached samples (Figure 16). X-ray diffraction characteristics of the surface precipitates from the second and third columns leached with AASA could not be matched with any available XRD standards. DTA patterns of the samples displayed minor reaction in the $200\text{-}700^\circ\text{C}$ range (Figure 14) which could arise from organic materials in the sample (Mitchell and Birnie 1971). The infrared spectra of the sample (Figure 18) displayed a number of sharp narrow absorption bands

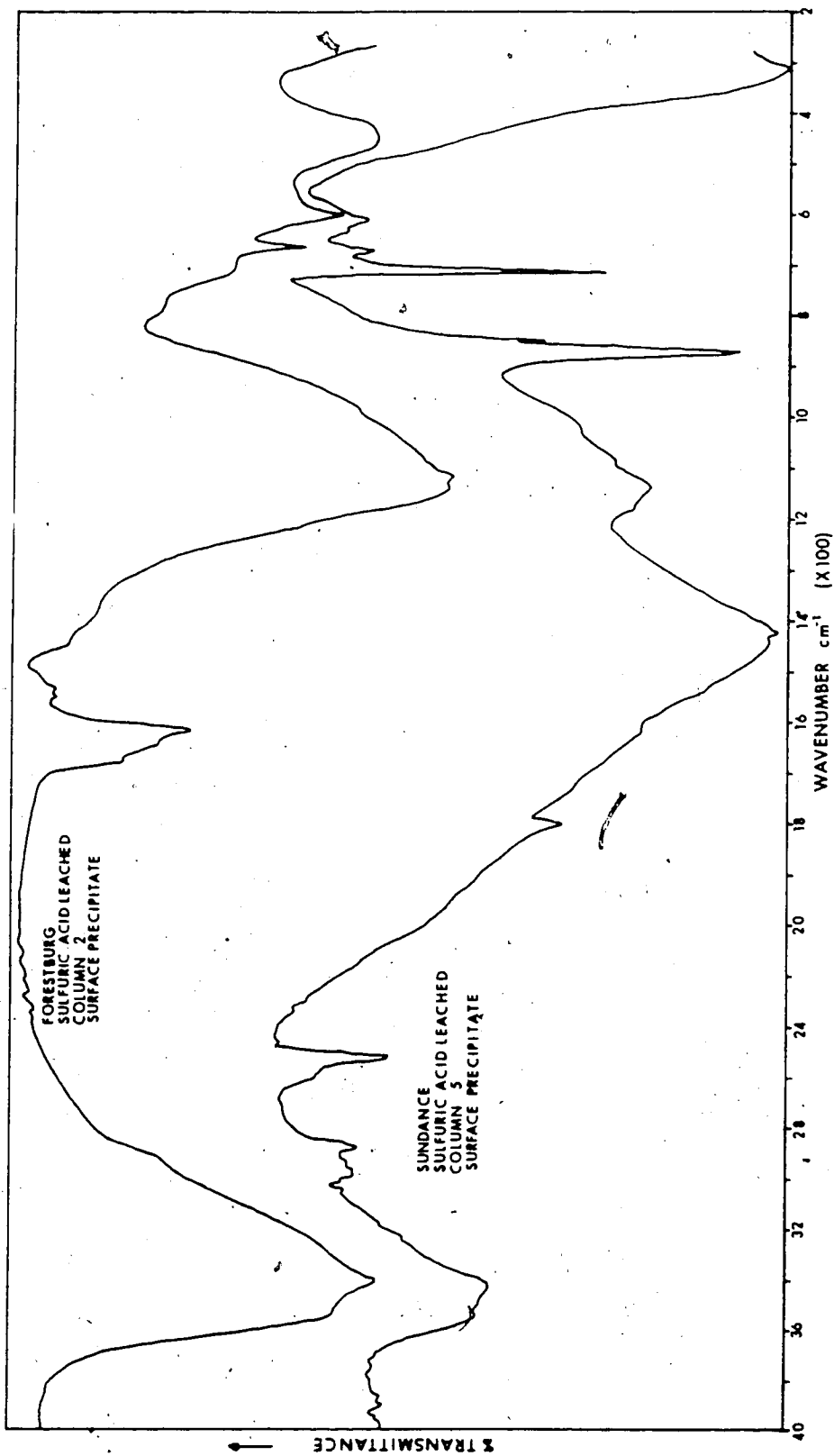


Figure 17. Infrared spectra of the surface precipitates from the second column of the Forestburg ash and the fifth column of the Sundance ash for the sulfuric acid weathering regime.

normally associated with organic compounds (Alpert et al. 1970). The two infrared absorption maxima at 1610cm^{-1} and 1580cm^{-1} (Figure 18) specifically identify the compound(s) as containing conjugated o-hydroxyl phenol groups (Randall 1949) suggesting that salicylate complexes formed part of the precipitate. The small absorption band at 760cm^{-1} further implicated the ortho-substituted benzene ring structure of salicylate (Randall 1949).

The salicylate compounds present in the acidified surface precipitates are undoubtedly derived from salicylic acid from the AASA leaching solution. Salicylate is capable of forming numerous complexes with many of the elemental constituents of fly ash. Salicylate complexes in general are less soluble than salicylic acid (Chaberk and Martell 1959). The organic compounds in the surface precipitates of the acidified AASA leached columns are therefore likely a mixture of salicylate compounds formed from the reaction of salicylic acid with numerous major and minor ash constituents (e.g. Ca, Mg, Fe, Al).

Calcite was replaced by gypsum in the surface precipitates of the acidified columns of the H_2SO_4 leached series. The transformation from calcite to gypsum is evident in the XRD patterns of the surface precipitates from the second, third, and fourth columns of the $0.005 \text{ M } \text{H}_2\text{SO}_4$ leached Forestburg ash series (Figure 15). Gypsum was the only crystalline Ca phase in the surface precipitate of the acidified second column. Calcite was the dominant mineral

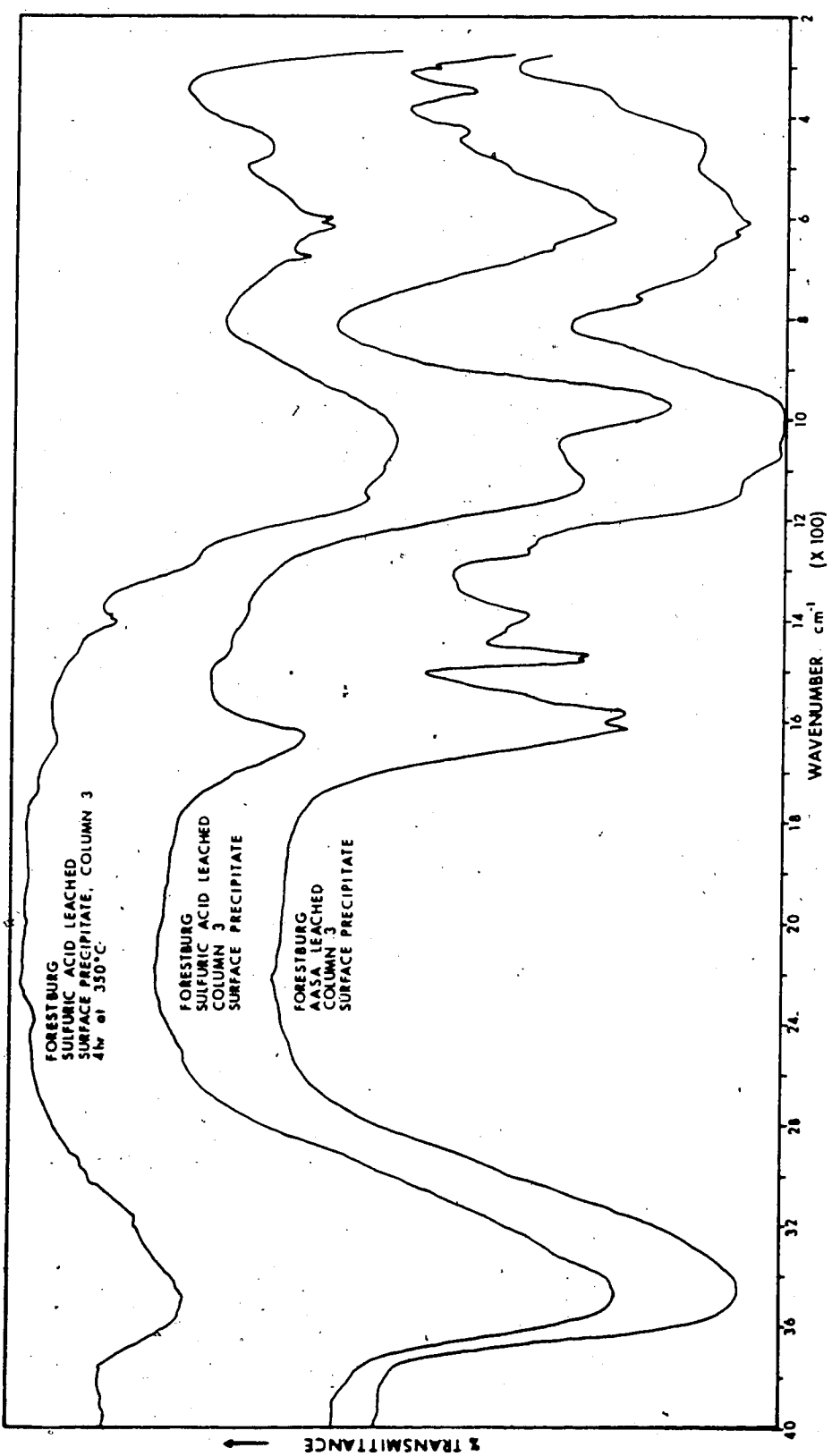


Figure 18. Infrared spectra of the surface precipitates from the third columns of the sulfuric acid leached, and AASA leached Forestburg ash.

in the nonacidified fourth (and fifth) column surface precipitate. Both calcite and gypsum were evident in the surface precipitate of the third column in which pH values of the leachates were just beginning to drop from alkaline to acid ranges. Gypsum is the most stable Ca phase when SO_4^{2-} activities are greater than 0.001 M and pH values are less than 7.5 (Lindsay 1979). Calcite formed in the surface precipitate under alkaline conditions would redissolve in acidic solution. Gypsum likely precipitated through the reaction of Ca, redissolved from calcite, with SO_4^{2-} derived from H_2SO_4 . The gypsum would be persistent in the surface precipitate because of high concentrations of SO_4^{2-} in solution.

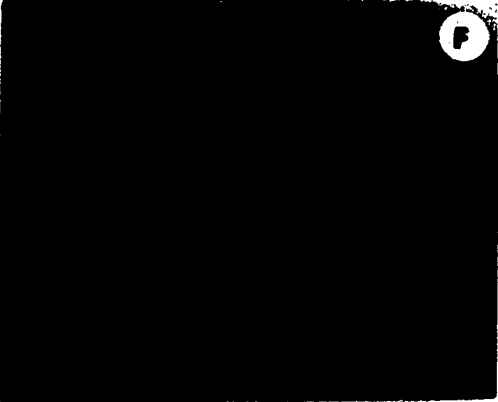
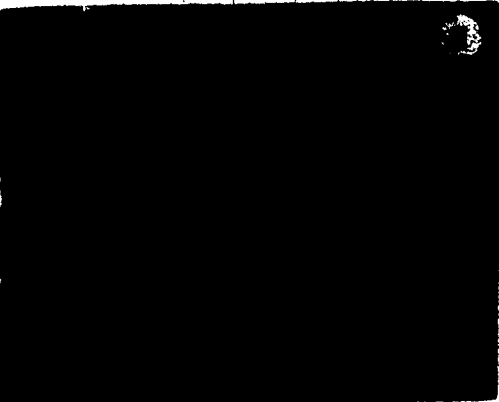
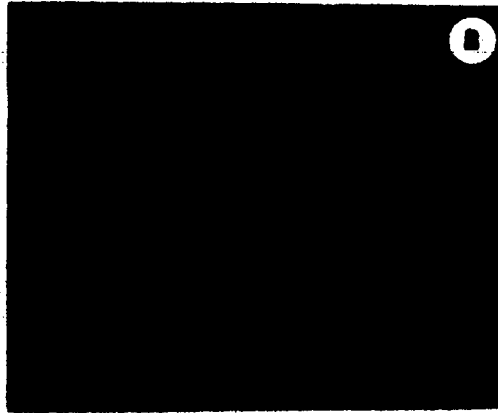
Small amounts of gypsum were also detected in the calcite-rich surface precipitate samples of the nonacidified columns. Absorption bands at 1135cm^{-1} , 675cm^{-1} , and 615cm^{-1} (Figure 17) were evident in the IR spectra of the fifth column surface precipitate of the 0.005 M H_2SO_4 leached Sundance ash series. These bands are indicative of gypsum (van der Marel and Beutelspacher 1976). The presence of these bands in this sample indicate that gypsum formed with calcite under highly alkaline conditions. Formation of gypsum in the nonacidified columns likely occurred during initial leaching stages when Ca concentrations were very high and in excess of gypsum solubility. Gypsum would be persistent in the latter columns also because of high concentrations of SO_4^{2-} in solution.

Precipitation of the salicylate compounds in the companion AASA leached surface precipitates (Figure 16) likely occurred in a manner similar to gypsum formation in the H_2SO_4 leached samples. This implies that the main inorganic component of the salicylate precipitate(s) was Ca. No salicylate was detected by IR analysis in the surface precipitates of the nonacidified columns of the AASA leached series, indicating that the Ca-salicylate is more soluble than gypsum. The higher levels of Ca released from the AASA leached columns compared to the H_2SO_4 leached columns after acidification reflects the much greater solubility of Ca-salicylate complexes compared to the solubility of Ca dissolved from the ash by H_2SO_4 (Figures 3 & 4).

Carbonates deposited within the nonacidified ash of the latter columns of each leaching series (Table 9) did not occur in sufficient quantities to be detected by XRD, IR, or DTA analysis. Examination of samples containing carbonates by scanning electron microscopy (SEM) revealed the presence of a variety of Ca-rich crystals (Plates 3 & 4). Most Ca-rich crystals were less than a few microns in length. Most formed fibrous interwoven mesh-like coatings on the surfaces of fly ash particles (Plates 3D & 4C). The size of the crystals comprising the coatings was generally uniform for any given particle but varied for particles in different locations in the core sections (cf. Plates 3D & 4C). Larger crystals which formed coatings were oriented tangentially to the spherical particle surfaces (Plate 3G & 3H), similar to

Plate 4. Scanning electron micrographs of precipitation products from selected weathered ash core sections.

- A: Long acicular crystals formed on the surface of a large fly ash particle from the surface core section of the fifth column of the AASA leached Sundance ash series.
- B: Large acicular crystals admixed with spherical fly ash particles from the same core section as A.
- C: A mesh-like network of interwoven fibrous Ca-rich material forming a continuous coating over a number of spherical ash particles from the fourth column bottom core section of the 0.005 M H₂SO₄ leached Forestburg ash.
- D: Platy crystals formed among spherical fly ash particles from the surface core section of the fourth column of the 0.005 M H₂SO₄ leached Sundance ash series.
- E,F: Cementitious material forming a bridge between two spherical fly ash particles from the bottom core section of the fourth column of the AASA leached Forestburg ash series.
- G,H: Coatings, possibly composed of amorphous Fe, covering spherical fly ash particles from a selected Fe-rich pocket in the first column bottom core section of the 0.005 M H₂SO₄ leached Forestburg ash series.



the orientation of aragonite (CaCO_3) crystals which form as coatings on oolitic particles in marine environments (Blatt et al. 1980). Some dissolved material also formed platy shaped crystals and bridges which cemented some particles together (Plate 4, D-F). Many, larger discrete crystals resembled orthorhombic or hexagonal rods (Plates 3E, 4A & 4B) which were either associated with particle surfaces (Plate 3D) or admixed with the spherical ash particles (Plate 3E). The morphologies of many of the crystals are not typical of calcite; they are believed to be aragonite.

The formation of Fe precipitates in the weathered ash was evident in the development of rust coloured bands. The form of the Fe precipitates in the bands was not determined by XRD, DTA, or IR analyses. Instead, acid ammonium oxalate (AAO) and sodium citrate-bicarbonate-dithionite (CBD) extractants were employed to establish the mineral form(s) of the Fe precipitates.

Oxalate and CBD extractants are frequently used to distinguish relative amounts of amorphous and crystalline forms of Fe and Al in soils (McKeague et al. 1971). Citrate-bicarbonate-dithionite extraction dissolves both amorphous and crystalline phases. Oxalate extraction primarily dissolves amorphous forms. The difference in quantities dissolved with the two extractants gives an estimate of crystalline forms (McKeague and Day 1966).

The quantities of Fe extracted from the unweathered ashes and most of the weathered ash core sections using CBD

were consistently less than the quantities extracted using AAO. The high alkalinity of most of the samples likely raised the pH values of the CBD extraction solutions to levels considerably higher than the optimum range (pH=7.3) for Fe dissolution (Mehra and Jackson 1960). The quantities of Si, Al, and Mn dissolved from most of the ash samples using CBD were also much less than the values for AAO extraction (Appendix, Tables 43-46). Since it was not possible to meaningfully interpret the CBD data, discussion will be restricted to the AAO data.

Data for acid ammonium oxalate extractable Fe (Tables 12 & 13) indicate that at least some of the Fe translocated during weathering was deposited in an X-ray amorphous form. The proportions of total Fe as AAO extractable Fe were highest in core sections that contained rust coloured bands (Tables 12 & 13). The same samples also contained the highest content of total Fe (Tables 5-8). These increases in AAO extractable levels indicate that Fe deposited in the Fe enriched core sections precipitated in an amorphous form. Particles from small localized pockets enriched in Fe (based on colour) from the first column bottom core section of the H₂SO₄ leached ashes were coated with material that may be amorphous Fe (Plate 4G & 4H). Particle coatings with this particular appearance were not observed in other samples.

The acid ammonium oxalate extractable Fe values (Tables 12 & 13) also reflected differences between the two leaching regimes. Acid ammonium oxalate extractable levels of Fe in

the first column surface core sections were much lower than in the unweathered ashes while values for the AASA leached samples were equal to or greater than the unweathered ash values. This difference is related to the greater depletion of total Fe in the H_2SO_4 leached samples compared to the AASA leached samples (Tables 5-8). The mineral acid removed the AAO extractable forms of Fe from the ash while the AASA leaching increased the AAO extractable percentage of the total Fe in the ashes.

Acid ammonium oxalate extractable levels of Fe in all nonacidified ash cores were generally slightly greater than the values for the respective unweathered ash samples (Tables 12 & 13). Translocation of Fe into the nonacidified columns did not occur as the leachates entering these columns contained no detectable levels of Fe (Figure 10). The slight increase in the quantities of AAO extractable Fe in the core sections of these columns compared to the unweathered ashes were likely due to the differences in the efficacy of the extractant. Unreacted CaO in the fresh ash would tend to neutralize the acidity of the AAO thereby diminishing Fe extraction.

The patterns of AAO extractable levels of Mn in each leaching series were similar to Fe except that no differences occurred between the two leaching regimes for the first column surface core sections (Tables 12 & 13). The percentage of Mn extractable with AAO in all core sections of all leaching regimes were greater than in the

unweathered ashes. Extractable percentages of Mn were similar for the two leaching regimes. Dissimilarities in the extraction patterns for Mn and Fe suggested they do not originally occur in the same fraction of the ash. Similarities in the patterns of extractable Mn and Fe for the other core sections suggests that Mn shares a solid phase form with Fe in the precipitation products.

Analyses of weathered ash samples by XRD, DTA, and IR methods indicate that Al and Si precipitated in the ashes as an aluminosilicate clay mineral having short-range order. The occurrence of such materials has not previously been documented in weathered fly ash. Most of the clay material occurred in surface precipitate samples of the third columns in each series. The XRD pattern for the surface precipitate sample from one of the leaching series displayed broad peaks indicative of allophane. DTA patterns for the sample displayed endotherms indicative of both allophanic and imogolite material. The IR spectra for surface precipitate samples from the AASA and H₂SO₄ leached series displayed absorption bands indicative of allophane and imogolite, respectively. Gel-like material similar in appearance to allophane and some thread-like strands characteristic of imogolite were observed in transmission electron micrographs of the precipitated material.

The XRD pattern for the surface precipitate from the third column of the 0.005 M H₂SO₄ leached Forestburg ash series (Figure 15) displayed evidence for the presence of

two minerals. Along with sharp diffraction peaks corresponding to the crystalline structure for gypsum, three very broad reflections with d-spacings of approximately 3.3Å, 2.2Å, and 1.4Å were also evident in the pattern (Figure 15). These broad peaks correspond well with most d-spacings documented for allophane (Wada and Yoshingaga 1969) and some of the more intense spacings for imogolite (Wada and Yoshingaga 1969, Brown 1980). The most intense reflection (11-20Å) usually observed in XRD patterns for allophane and imogolite and other minor reflections associated mostly with imogolite were not discernable in the pattern. The broadness of the reflections are typical of allophane.

The DTA pattern for the same sample displayed one very large endotherm at 150°C, a small endotherm at 415°C, and a small exotherm at 955°C (Figure 14). These deflections also appear in DTA patterns documented for imogolite (Wada 1977). DTA patterns for allophane are very similar to those for imogolite except that patterns for allophane do not display small endotherms in the 390-420°C range which occur due to loss of structural OH groups in imogolite (Wada 1977). The disproportionately large size of the first endotherm (150°C) in the sample pattern (Figure 14), compared to the smaller endothermic and exothermic deflections, is likely due to the loss of structural water from gypsum in the sample.

The infrared spectra for the surface precipitate samples from the third columns of both the AASA and H₂SO₄

leached Forestburg ash series also exhibited absorption bands characteristic of imogolite (Figure 18). The IR spectra for the third column surface precipitate from the H_2SO_4 leached Forestburg ash series displayed strong absorption bands with maxima at wavenumbers of approximately $3480cm^{-1}$, $1625cm^{-1}$, $1125cm^{-1}$, $975cm^{-1}$, $605cm^{-1}$, $430cm^{-1}$, and $345cm^{-1}$ (Figure 18). The IR spectra for the companion AASA leached samples displayed weaker bands of similar wavenumber, indicative of allophane rather than imogolite (Farmer et al. 1977, 1979). Other less developed bands in the mineral acid leached sample spectra appeared as shoulders around the $605cm^{-1}$ maxima at $665cm^{-1}$, $560cm^{-1}$, and $500cm^{-1}$. An IR spectrum for imogolite also generally displays major bands in three regions: $2800-3800cm^{-1}$, $1400-1600cm^{-1}$, and $650-1200cm^{-1}$ (Wada 1977). Gypsum was evident in the sample with the appearance of the large absorption maxima at $1125cm^{-1}$ and the weakly expressed shoulder at $665cm^{-1}$. The absorption bands for gypsum at $1685cm^{-1}$, $1620cm^{-1}$, and $605cm^{-1}$ would overlap with bands for imogolite (van der Marel and Beutelspacher 1976). As described earlier, the sharp narrow bands in the AASA leached sample spectra corresponded to frequencies for organic compounds.

Changes in the IR spectra between heated and nonheated samples have been used to determine the presence of imogolite in soils. Farmer and co-workers (1977, 1978) indicated disappearance the $346-348cm^{-1}$ absorption band with

heating to 350°C is diagnostic of imogolite. Heating the sample of the third column surface precipitate to 350°C caused the 345cm⁻¹ band observed in the untreated sample spectrum to disappear along with all other bands corresponding to imogolite (Figure 18). The bands remaining in the spectra after the heat treatment, located at wavenumbers of 600cm⁻¹, 615cm⁻¹, 675cm⁻¹, 1110cm⁻¹, 1155cm⁻¹, 1640cm⁻¹, and 3415cm⁻¹, corresponded to anhydrite (CaSO₄) (van der Marel and Beutelspacher 1976). The two very broad bands at approximately 1035cm⁻¹ and 445cm⁻¹ can be assigned to (Si-O)- and (Al-O)- stretching modes (Farmer 1974).

The occurrence and formation of allophane and imogolite in soils formed in material of volcanic origin is well documented (e.g. Fieldes 1966; Wada et al. 1972; Aomine and Mizota 1973; Wada and Aomine 1973; Wada and Harward 1973; Dudas and Harward 1975). Allophanes are members of a series of naturally occurring hydrous aluminosilicates of somewhat variable composition (van Ophen 1971). Allophane is generally assigned the composition Al₂O₃ · 2SiO₂ · nH₂O (Wada 1977). Allophanes may occur alone or with imogolite, but imogolite always occurs with allophane. Allophane is generally thought to be a precursor to imogolite (Wada 1977). Imogolite (Al₂O₃ · SiO₂ · 2.5H₂O) has a slightly different composition and more highly ordered structure than allophane. Imogolite is visually characterized by smooth, usually curved strands or threads approximately 100-300Å in

diameter that may extend up to a few microns in length. Allophane occurs as 35-50Å diameter spherical units which are commonly found grouped together as irregular aggregates or gels (Wada 1977).

The formation of materials characterized by allophane and imogolite during the weathering of fly ash could occur similar to their formation in volcanic ash soils. Allophane and imogolite form through a process of component dissolution and reprecipitation as opposed to direct alteration (Eswaran 1972). The process requires the presence of an easily weatherable form of aluminosilicate lacking ordered structure (Fieldes 1966). Precipitation of allophanic material can occur from solutions containing dissolved $\text{SiO}_2:\text{Al}_2\text{O}_3$ in ratios ranging from one to three (Wada 1977). Imogolite tends to form when $\text{SiO}_2:\text{Al}_2\text{O}_3$ ratios are close to one (Aomine and Mizota 1973). The $\text{SiO}_2:\text{Al}_2\text{O}_3$ ratios of the leachate solutions after passing through the acidified first and second ash columns of the H_2SO_4 leached Forestburg ash series were approximately 0.8 (Figures 8 & 9). Silicon was therefore in excess of the above mentioned ratios but incorporation of excess Si or Al into allophanic structures is possible (Farmer et al. 1979). In soils, allophane and imogolite form as dispersed complexes in acid solution ($\text{pH} < 5.0$) which precipitate as solution pH values rise into the 5.5-8.0 range (Wada and Kubo 1975; Farmer et al. 1979; Anderson et al. 1982). Similar conditions would be encountered when leaching solutions containing Si and Al

dissolved from the acidified first and second columns percolated through the alkaline ash columns within each series. Increases in the acid ammonium oxalate extractable levels of Al in the bottom of the second columns and much of the third columns of each leaching series (Tables 12 & 13) also suggested that some aluminosilicate material precipitated within this broad range of core sections.

Structures observed by transmission electron microscopy in the third column surface precipitate samples of the 0.005 M H_2SO_4 leached Forestburg ash series confirmed that aluminosilicate materials of short-range order were indeed formed during the weathering of the ash. Transmission electron micrographs of the surface precipitate material in the 0.005 M H_2SO_4 leached Forestburg ash series are shown in Plate 5. Much of the material was filmy and gelatinous in appearance (Plate 5A-D) similar to amorphous materials that coat the surfaces of weathered soil minerals (Jones and Uehara 1973) or aggregate globules formed in weathered pumice beds (Kitigasa 1971; Sudo et al. 1981). Material displaying the long thread-like morphology characteristic of imogolite (Wada et al. 1970) was not apparent; however, some gel-like clumps did contain parallel structures which may be the initial development of imogolite threads (Plate 5E & 5F).

The amorphous aluminosilicate material formed during the mineral acid weathering of the ashes may best be described as proto-imogolite. Proto-imogolite resembles

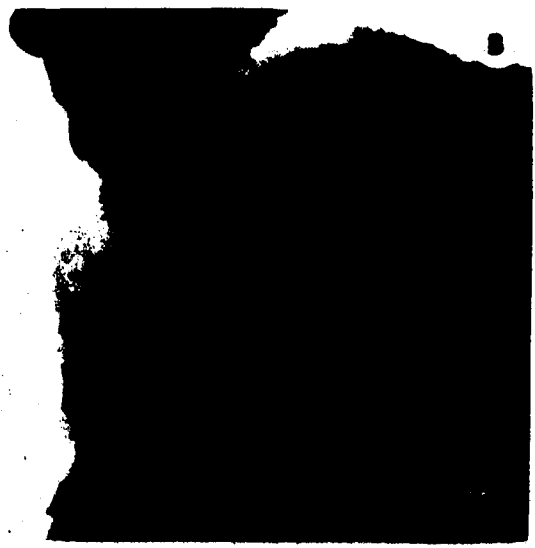
Plate 5. Transmission electron micrographs of material in the surface precipitate sample from the third column of the 0.005 M H₂SO₄ leached Forestburg ash series.

A,B: Gelatinous material similar in appearance to amorphous silicate and aluminosilicate gels commonly associated with weathered volcanic ash and pumice deposits.

C,D: Gel-like material formed as discrete globs and as coatings on some solid opaque fragments.

E,F: Gelatinous material containing some very small uniformly separated filiform structures orientated parallel to each other. These units are possibly the beginning of the development of imogolite strands.

The bar in each photo equals 0.1um.



imogolite in composition, analytical behaviour, and likely structure on a molecular scale, but it does not exhibit the tubular morphology of imogolite (Farmer et al. 1978, 1980). X-ray amorphous material more characteristic of allophane was found in the organic acid leached ashes. The presence of the organic compounds are known to inhibit the formation of imogolite in soils (Wada 1977). The presence of proto-imogolite and allophane in the weathered fly ash samples indicates that after the alkali producing components of fly ash are depleted, weathering apparently proceeds in manner very similar to the weathering of volcanic ash or materials of volcanic origin.

V. SUMMARY AND CONCLUSIONS

The present investigation was initiated to ascertain the chemical processes and mineralogical transformations accompanying the artificial weathering of fly ash. In this study the chemical weathering of fly ash was accomplished through accelerated leaching, simulating weathering as it might occur over a very long period of time in a large fly ash disposal site located at or near the land's surface. The decomposition and dissolution of fly ash was evaluated in terms of association of the major chemical elements with phases and physical components of fly ash. The results were also evaluated in terms of the formation and redissolution of secondary phases in response to a simulated weathering gradient.

The results of this investigation can be used to construct a conceptual model of the chemical nature of spherical fly ash particles. This model elaborates on previous concepts outlined elsewhere. Most "typical" fly ash particles are micron-sized spheres composed primarily of Si and Al with lesser and varying amounts of Ca and Fe. The two ashes employed in this study were alkaline in reaction with Ca as the third most abundant constituent. The results of this study indicated the surfaces of unweathered fly ash particles are coated with varying quantities of very small (submicron) fragments composed primarily of CaO. A considerable portion of the interior of fly ash spheres

contain networks of small acicular crystals of mullite ($3\text{Al}_2\text{O}_3 \cdot 2\text{SiO}_2$) which incongruently crystallized during cooling of the precursor molten droplets (Hulett et al. 1979). The residual interstitial melt forms a Si-rich, Al-poor glass enriched in a variety of elements that were excluded from the mullite crystals.

The results obtained here suggest that the glass matrix is comprised of two phases characterized by different solubilities. The nature of the two glass phases is dictated by their elemental compositions. Glass in the external regions of the particles tended to contain higher concentrations of many elements (e.g. Ca, Mg, Fe, Al) compared to the Si-rich interior regions. The exterior glass was also considerably more reactive than glass of the interior. Enrichment of some elements in the exterior glass region is likely a result of element migration within the glass melt during solidification. Mechanisms for such migration have been suggested previously (Hulett et al. 1979). The diversity and quantity of elements associated with the exterior glass (compared to a purer Si glass of the interior) enhanced its solubility compared to the interior. The concentration gradients from surface to interior may be element specific. The central regions of most spherical particles are apparently composed essentially of Si admixed with the major portions of some minor and trace constituents such as K, Na, and Pb.

The aforementioned conceptual model is in agreement with the weathering characteristics observed in this study. The initial weathering stages of the fly ashes were in part characterized by the dissolution of Na and K salts. Both K and particularly Na were dissolved in high concentrations from the ashes at the onset of leaching. This study revealed that the proportion of the total Na associated with the highly soluble salt fraction, most likely sulfate salts as suggested by Green and Manahan (1978) and Dudas (1981), is much greater than the percentage of total K associated with the highly soluble fraction (i.e. Na was more leachable than K). The results did not aid in identification of discrete Na or K phases that might comprise part of the fly ash particles. These soluble phases were likely incorporated into the exterior glassy matrix of the particles or they may have occurred as discrete fragments, indistinguishable from CaO, located on the surfaces. Most of the Na and K in the ashes tended to be associated with the internal glassy matrix. Solid state migration of Na from the internal matrix to the surface under acidic conditions may be a significant mechanism in the removal and depletion of Na in fly ash.

Initial weathering stages were also characterized by the hydrolysis of CaO and the subsequent development of extremely alkaline leaching solutions. The hydrolysis of CaO and the dissolution of the hydrolysis product, $\text{Ca}(\text{OH})_2$, accounted for the extreme alkalinity of the initial leachate

solutions. The alkaline reactivity of fly ash has previously been related to high contents of Ca (Theis and Wirth 1977). The two ashes employed in this study did not differ greatly in contents of Ca but the buffering capacities were notably different. The percentage of total Ca in fly ash in the form of CaO occurring as discrete fragments on particle surfaces appeared to be more critical than total content of Ca in dictating ash reactivity and degree of sustained alkalinity.

After soluble Na and K salts and CaO are removed from the ash, weathering causes selective dissolution of particle surfaces. Selective dissolution of the glassy matrix was evident in the exposure of mullite crystals contained within fly ash particles. Chemical analysis of the weathered ash residues suggested that much of the Ca and Mg not associated with the oxide phase are contained in the surface glass. Other major elements, including Al not associated with mullite and Fe not associated with ferromagnetic particles, were also associated with the exterior glass phase. The occurrence of an external glass phase of higher solubility than glass of the interior portion was suggested by data for extractable Al, Fe, and Si.

Significant differences were observed between the two ashes in the elemental release patterns for Si under alkaline conditions. Under moderate alkaline conditions the levels of Si in the leachates of the Sundance ash were much greater than levels in the Forestburg ash leachates. These

differences indicate the distribution of each element (like Si) among soluble salt phases, crystalline phases, and more-soluble and less-soluble glass phases partially dictates its dissolution and release characteristics.

Ferromagnetic particles occur in very low abundances in most fly ashes of alkaline character and are therefore of minor importance with respect to the weathering of such ashes. The weathering behaviour of ferromagnetic particles, may, however be significant in the weathering of Fe-rich ashes such as those produced by some eastern U.S. utilities. The interior of the ferromagnetic particles of the ashes used in this study contained agglomerates of small cubes, each reflecting the crystal habit of Fe spinels. These cube agglomerates were very resistant to the imposed weathering regimes. The outer surfaces of the ferromagnetic particles were composed of material that readily dissolved with acid leaching. The data of this investigation suggested dissolution of ferromagnetic particles will not likely involve extensive release of first row transition elements (notably Mn in this case) which normally are concentrated in the ferromagnetic fraction as substituted elements in the spinel structure.

A sequence of secondary phases formed during the artificial weathering of the ash in this study. An initial secondary phase to form was Ca(OH)_2 (portlandite). It formed only in the Sundance ash through the hydrolysis of large quantities of CaO and was persistent for only a very

limited time. The presence of $\text{Ca}(\text{OH})_2$ in the ash was not observed directly but inferred by comparison of the elevated pH values and concentration of Ca in the initial leachates with known thermodynamic stability relationships. A large percentage of the total Ca in the unweathered ash must occur as CaO in order for $\text{Ca}(\text{OH})_2$ to form. Dissociation of $\text{Ca}(\text{OH})_2$ was primarily responsible for the alkaline reaction of the ashes.

The main Ca precipitation product in the ashes was CaCO_3 . It formed through the reaction of Ca, redissolved from $\text{Ca}(\text{OH})_2$ or dissolved from the external glass phase of the ash, with CO_2 which dissolved readily in the alkaline leaching solutions. The presence of CaCO_3 in the ash accounted for most of the alkaline buffering that occurred within the pH range of 8.5-9.0. Much of the CaCO_3 formed calcite on the core surfaces. The CaCO_3 which precipitated within the ash cores formed crystals resembling aragonite in crystal habit. Other Ca precipitates included gypsum in the H_2SO_4 leached columns and a Ca-salicylate in the organically leached series. Formation of gypsum and Ca-salicylate was essentially a function of the high concentrations of Ca, SO_4^{2-} , and salicylate in the initial leaching solutions.

Acidification of the ashes occurred after all carbonates were redissolved and removed from the ash cores. The acidic pH levels generated in the ash cores were dictated primarily by the initial pH of the unreacted acidic leaching solutions. Dissolution of the external glass of

the particles occurred following acidification and accounted for the release of high levels of Si and Al, along with lower levels of Fe, Mg, Ca, Na, K, and other elements. Silicon and Al translocated during mineral acid leaching was deposited in alkaline environments, evidently as protohemogolite. Material more characteristic of allophane was detected in the organic acid leached ashes. Sodium and K did not precipitate in the ash cores. Dissolved Ca and Mg became incorporated into carbonates in the alkaline ash columns. Iron experienced limited translocation and precipitated almost entirely in an amorphous form, likely as coatings on ash particles. No crystalline forms of Fe were detected in the precipitates. Iron precipitates in the organically leached series were more dispersed among the ash columns than those formed in the inorganically leached series.

In conclusion, the weathering of fly ash of alkaline reaction takes place in a predictable sequence. Initially, highly soluble salts are dissolved and leached from the ash. The hydrolysis of CaO generates initial high alkalinity and high levels of soluble Ca. Some of the leached Ca becomes incorporated into CaCO_3 on reaction with dissolved CO_2 under alkaline conditions. Calcium carbonate is the major buffering agent in the ash under alkaline conditions. After dissolution of CaCO_3 , the acidity of the weathering environment is dictated primarily by the nature of the leaching solution. Under acidic conditions Al, Si and Fe

rapidly dissolved from the glass of the external regions of the ash particles. Dissolved Fe is minimally translocated and precipitates in an X-ray amorphous form. Dissolved Si and Al precipitate when translocated into a more alkaline environment as noncrystalline clay minerals. This weathering sequence is very similar to the natural weathering of glassy materials of volcanic origin.

REFERENCES

- Abel, K.H. and Randitelli, D.A. 1976. Major, minor and trace element composition of coal and fly ash as determined by instrumental neutron activation analysis. Pages 178-188 in S.P. Babo, ed. Trace elements in fuel. Adv. Chem. Ser. 141. Am. Chem. Soc. Pub. Washington, D.C.
- Adriano, D.C., Page, A.L., Siseewi, A.A., Chan, A.C. and Straughan, J. 1960. Utilization and disposal of fly ash and other coal residues in terrestrial ecosystems: A review. *J. Environ. Qual.* 9:333-344.
- Alder, H.H. and Kerr, P.F. 1962. Infrared study of aragonite and calcite. *Am. Min.* 47:700-717.
- Alpert, H.L., Keiser, W.E., and Szymanski, H.A. 1970. Theory and practice of infrared spectroscopy. 2nd ed. Plenum press. New York N.Y. 380pp.
- Anderson, H.A., Berrow, M.L., Farmer, V.C., Hepburn, A., Russel, J.D. and Walker, A.D. 1982. A reassessment of podzol formation processes. *J. Soil Sci.* 33:125-136.
- Anderson, W.L. and Smith, K.E. 1977. Dynamics of Mercury at coal-fired power plant and adjacent cooling lake. *Environ. Sci. Tech.* 11:75-80.
- Andren, A.W., Klein, D.H. and Taimi, Y. 1975. Selenium in coal-fired steam plant emissions. *Environ. Sci. Tech.* 9:856-858.
- Aomine, S. and Mizota, C. 1973. Distribution and genesis of imogolite in volcanic ash soils of Northern Kanto, Japan. Pages 207-213 in J.M. Serratosa, ed. Proceedings International Clay Conf. Madrid, Spain.
- Baril, R. and Bitton, G. 1967. Anomalous values of free iron in some Quebec soils containing magnetite. *Can. J. Soil Sci.* 47:261.
- Bauer, C.F. and Natusch, D.F.S. 1981. Identification and quantification of carbonate compounds in coal fly ash. *Environ. Sci. Tech.* 15:783-788.
- Berg, L.G. 1970. Salt Minerals. Pages 463-475. in R.C. Mackenzie, ed. Differential thermal analysis: I Fundamental aspects. Academic Press. New York. N.Y.

- Bern, J. 1976. Residues from power generation: Processing, recycling and disposal. Pages 226-248 in Land applications of waste materials. Soil Conserv. Soc. Am. Pub. Ankeny, Iowa.
- Berry, E.E. and Malhotra, V.M. 1980. Fly ash for use in concrete: A critical review. J. Am. Concrete Inst. 77:59-73.
- Bertine, K.K. and Goldberg, E.D. 1971. Fossil fuel combustion and the major sedimentary cycle. Sci. 173:233-235.
- Bien, G.S., Contois, D.E. and Thomas, W.H. 1958. The removal of soluble silica from fresh water entering the sea. Geochim. Cosmochim. Acta 14:35-54.
- Biermann, A.H. and Ondov, J.M. 1980. Application of surface-deposition models to size-fractionated coal fly ash. Atmos. Environ. 14:289-295.
- Billings, C.E. and Matson, W.R. 1972. Mercury emissions from coal combustion. Sci. 176:1232-1233.
- Billings, C.E., Sacco, A.M., Matson, W.R., Griffin, R.M., Caniglio, W.R. and Harley, R.A. 1973. Mercury balance on a pulverized coal-fired furnace. J. Air Polln. Cont. Assn. 23:773-777.
- Blakemore, L.C. 1968. Determination of iron and aluminum in Tamm's soil extracts. N.Z. J. Agr. Res. 11:515-520.
- Blatt, H., Middleton, G. and Murry, R. 1980. Origin of sedimentary rocks. 2nd edition. Prentice-Hall Inc. Englewood Cliffs, N.J. 782pp.
- Block, C. and Dams, R. 1975a. Inorganic composition of Belgian coals and coal ashes. Environ. Sci. Tech. 9:146-150.
- Block, C. and Dams, R. 1975b. Lead contents of coal, coal ash, and fly ash. Water Air and Soil Polln. 5:207-211.
- Block, C. and Dams, R. 1976. Study of fly ash emissions during combustion of coal. Environ. Sci. Tech. 10:1011-1017.
- Bloomfield, C. 1953. A study of podzolization I: The mobilization of iron and aluminum by scots pine needles. J. Soil Sci. 4:5-16.

- Bloomfield, C. 1955. A study of podzolization VI: The immobilization of iron and aluminum. *J Soil Sci.* 6:284-292.
- Blume, H.P. and Schwertmann, U. 1969. Genetic evaluation of profile distributions of aluminum, iron, and manganese oxides. *Soil Sci. Soc. Am. Proc.* 33:438-444.
- Boksay, Z., Bouquet, G. and Dobos, S. 1968. The kinetics of the formation of leached layers on glass surfaces. *Phys. and Chem. of Glasses.* 9:69-71.
- Brindley, G.W. and Brown, G. eds. 1980. Crystal structures of clay minerals and their X-ray identification. Mineralogical Society Pub. Monograph 5 London. 495pp.
- Brown, G. 1980. Associated minerals. Pages 361-410 in G.W. Brindley and G. Brown, eds. Crystal structures of clay minerals and their X-ray identification. Mineralogical Society Pub. Monograph 5 London.
- Brownlow, A.H. 1979. *Geochemistry.* Prentice-Hall Inc. Englewood Cliffs, N.J. 498pp.
- Bundy, L.G. and Bremner, J.M. 1972. A simple titrimetric method for determination of inorganic carbon in soils. *Soil Sci. Soc. Am. Proc.* 36:273-275.
- Buol, S.W., Hole, F.D. and McCracken, R.J. 1980. Soil genesis and classification. 2nd edition. Iowa State University Press. Ames, Iowa. 406pp.
- Campbell, J.A., Laul, J.C., Nielson, K.K. and Smith, R.D. 1978. Separation and chemical characterization of finely-sized fly-ash particles. *Anal. Chem.* 50:1032-1040.
- Campbell, J.A., Smith, R.D. and Davis, L.E. 1978. Application of X-ray photoelectron spectroscopy to the study of fly ash. *Appl. Spec.* 32:316-319.
- Cameron, W.E. 1977a. Composition and cell dimensions of mullite. *Ceramic Bull.* 56:1003-1016.
- Cameron, W.E. 1977b. Mullite: A substituted alumina. *Am. Min.* 62:747-755.
- Carpenter, R.L., Clark, R.D. and Su, Y. 1980. Fly ash from electrostatic precipitators: Characterization of large spheres. *J. Air Polln. Cont. Assn.* 30:679-681.

- Chaberk, S. and Martell, A.E. 1959. Organic sequestering agents. Wiley Pub. New York, N.Y. 616pp.
- Cherry, D.S. and Guthrie, R.H. 1977. Trace metals in surface waters from coal ash. Water Resour. Res. Bull. 13:1227-1236.
- Churey, D.J., Gutenmann, W.H. Kabata-Pendias, A. and Lisk, D.J. 1979. Element concentrations in aqueous equilibrates of coal and lignite fly ashes. J. Agr. Food Chem. 27:910-911.
- Cogbill, C.V. and Likens, G.E. 1974. Acid precipitation in the Northeastern United States. Water Resour. Res. 10:1133-1137.
- Coles, D.G., Ragaini, R.C. and Ondov, J.M. 1978. Behavior of natural radionuclides in western coal-fired power plants. Environ. Sci. Tech. 12:442-446.
- Coles, D.G., Ragaini, R.C. and Ondov, J.M., Fisher, G.L., Silberman, D. and Prentice, B.A. 1979. Chemical studies of stack fly ash from a coal-fired power plant. Environ. Sci. Tech. 13:455-459.
- Cope, F. 1962. The development of a soil from an industrial waste ash. Pages 859-863 in Inter. Soc. Soil Sci Trans. Comm. IV and V. Palmerston, N.Z. 1962.
- Cotton, F.A. and Wilkinson, G. 1972. Advanced inorganic chemistry: A comprehensive text. John Wiley and Sons. Toronto. 1145pp.
- Csakvari, B., Boksay, Z. and Bouquet, G. 1971. Investigation of surface layers on electrode glasses for pH measurement. Anal. Chim. Acta 56:279-284.
- Daniels, R.B., Brasfield, J.F. and Riecken, F.F. 1962. Distribution of sodium hydrosulfite extractable manganese in some Iowa soil profiles. Soil Sci. Soc. Am. Proc. 26:75-78.
- Davidson, R.L., Natusch, D.F.S., Wallace, J.R. and Evans, C.A. 1974. Trace elements in fly ash: Dependence of concentration on particle size. Environ. Sci. Tech. 8:1107-1112.
- De Coninck, F. 1980. Major mechanisms in formation of spodic horizons. Geoderma. 24:101-128.

- Deer, W.A., Howie, R.A. and Zussman, J. 1966. An introduction to the rock-forming minerals. Longman, London. 528pp.
- Doner, H.E. and Lynn, W.C. 1977. Carbonate, halide, sulfate, and sulfide minerals. Pages 75-98 in J.B. Dixon and S.B. Weed, eds. Minerals in soil environments. Soil Sci. Soc. Am. Pub. Madison, Wisconsin.
- Dreesen, D.R., Gladney, E.S., Owens, J.W., Perkins, B.L., Wienke, C.L. and Wangen, L.E. 1977. Comparison of levels of trace elements extracted from fly ash and levels found in effluent waters from a coal-fired power plant. Environ. Sci. Tech. 11:1017-1019.
- Dreesen, D.R., Wangen, L.E. and Gladney, E.S. 1978. Solubility of trace elements in coal fly ash. Pages 240-252 in D.C. Adriano and I.L. Brisbin, eds. Environmental chemistry and cycling processes. Min. Cycl. Sym. U.S. Dept. Energy Conf-760427.
- Dudas, M.J. and Harward, M.E. 1975. Weathering and authigenic halloysite in soil developed in Mazama ash. Soil Sci. Soc. Am. Proc. 39:561-566.
- Dudas, M.J. 1981. Long-term leachability of selected elements from fly ash. Environ. Sci. Tech. 15:840-843.
- Eggett, J.M. and Thorpe, T.M. 1981. Mobilization of chromium from fly ash particulates by aqueous systems modeling natural waters. J. Environ. Soil Health. A 13:295-318.
- Elsewi, A.A., Page, A.L. and Griffin, S.R. 1980. Chemical characterization of fly ash aqueous systems. J. Environ. Qual. 9:424-427.
- Energy Resources Conservation Board. 1980. Reserves of coal, Province of Alberta at 31 Dec. 1979. 5th edition. ERCB Report #80-31. Calgary, Alberta.
- Energy Resources Conservation Board. 1982a. Alberta coal industry: Annual statistics, 1981. 9th edition. ERCB Report #82-29. Calgary, Alberta. 35pp.
- Energy Resources Conservation Board. 1982b. Energy requirements in Alberta, 1981-2005. 6th edition. ERCB Report #82-F Calgary, Alberta. 153pp.
- Eswaran, H. 1972. Morphology of allophane, imogolite, and halloysite. Clay Mins. 9:281-285.

- Farmer, V.C. ed. 1974. The infrared spectra of minerals. Mineralogical Soc. Pub. Monograph #4, London, 539pp.
- Farmer, V.C., Fraser, A.R., Russell, J.D. and Yoshinaga, N. 1977. Recognition of imogolite structures in allophanic clays by infrared spectroscopy. *Clay Mins.* 12:55-57.
- Farmer, V.C., Fraser, A.R., Tait, J.M., Palmieri, F., Violate, P., Nakai, M. and Yoshinaga, N. 1978. Imogolite and proto-imogolite in an Italian soil developed on volcanic ash. *Clay Mins.* 13:271-274.
- Farmer, V.C., Fraser, A.R. and Tait, J.M. 1979. Characterization of the chemical structures of natural and synthetic aluminosilicate gels and sols by infrared spectroscopy. *Geochim. Cosmochim. Acta* 43:1417-1420.
- Farmer, V.C., Russell, J.D. and Berrow, M.L. 1980. Imogolite and proto-imogolite allophane in spodic horizons: Evidence for a mobile aluminium silicate complex in podzol formation. *J. Soil Sci.* 31:673-684.
- Fieldes, M. 1966. The nature of allophane in soils: I Significance of structural randomness in pedogenesis. *N.Z. J. Sci.* 9:599-607.
- Fisher, G.L., Chang, D.P.Y. and Brummer, M. 1976. Fly ash collected from electrostatic precipitators: Microcrystalline structures and the mystery of the spheres. *Sci.* 192:553-555.
- Fisher, G.L. and Natusch, D.F.S. 1979. Size dependence of the physical and chemical properties of fly ash. Pages 489-541 in C. Karr Jr., ed. *Analytical methods for coal and coal products*. Vol. 3, Academic Press. N.Y.
- Fisher, G.L., Prentice, B.A., Silberman, D., Ondov, J.M., Biermann, A.H., Ragaini, R.C. and McFarland, A.R. 1978. Physical and morphological studies of size-classified coal fly ash. *Environ. Sci. Tech.* 12:447-451.
- Furr, A.K., Parkinson, T.F., Hinrichs, R.A., van Campen, D.R., Bache, C.A., Gutenmann, W.H., St. John, L.E., Pakkala, I.S. and Lisk, D.J. 1977. National survey of elements and radioactivity in fly ashes: Absorption of elements by cabbage grown in fly ash-soil mixtures. *Environ. Sci. Tech.* 11:1194-1199.

- Gladney, E.S. 1976. Composition and size distribution of in-stack particulate material at a coal-fired power plant. *Atmos. Environ.* 10:1071-1077.
- Glover, E.D. and Sippel, R.F. 1967. Synthesis of magnesium calcites. *Geochim. Cosmochim. Acta* 31:603-613.
- Gluskoter, H.J. 1975. Mineral matter and trace elements in coal. Pages 1-22 in S.P. Babu, ed. Trace elements in fuel. *Adv. Chem. Series* 141. Am Chem. Soc. Pub. Washington, D.C.
- Gluskoter, H.J. 1978. An introduction to the occurrence of mineral matter in coal. Pages 3-19 in R.W. Bryes, ed. Ash deposits and corrosion due to impurities in combustion gases. *Proc. Inter. Conf. 1977.* Hemisphere Pub. Co. Washington, D.C.
- Gordon, R.L. 1978. The hobbling of coal: Policy and regulatory uncertainties. *Sci.* 200:153-158.
- Green, J.B. and Manahan, S.E. 1978. Determination of acid-base and solubility behaviour of lignite fly ash by selective dissolution by mineral acids. *Anal. Chem.* 50:1975-1980.
- Greene, R.P. and Galagher, J.M. 1980. Future coal prospects: Country and regional assessments. Ballinger Pub. Co. Cambridge, Mass. 577pp.
- Gutenmann, W.H., Bache, C.A., Youngs, W.D. and Lisk, D.J. 1976. Selenium in fly ash. *Sci.* 191:966-967.
- Guthrie, R.K. and Cherry, D.S. 1976. Pollutant removal from coal-ash basin effluent. *Water Resour. Bull.* 12:889-902.
- Hansen, L.D. and Fisher, G.L. 1980. Elemental distribution in coal fly ash particles. *Environ. Sci. Tech.* 14:1111-1117.
- Hansen, L.D., Silberman, P. and Fisher, G.L. 1981. Crystalline components of size-fractionated coal fly ash. *Environ. Sci. Tech.* 15:1057-1062.
- Harris, W.R. and Silberman, D. 1983. Time-dependent leaching of coal-fly ash by chelating agents. *Environ. Sci. Tech.* 17:139-145.

- Hayes, B.S., Neville, M., Quann, R.J. and Sarofim, A.F. 1982. Factors governing the surface enrichment of fly ash in volatile trace species. *J. Colloid Interface Sci.* 87: 266-278.
- Hayes, T.L., Pawley, J.B. and Fisher, G.L. 1978. The effect of chemical variability of individual fly ash particles on cell exposure. *Scanning Electron Microscopy* 1978(1):239-244.
- Henmi, T. and Wada, K. 1976. Morphology and composition of allophane. *Am. Min.* 61:379-390.
- Hodgson, D.R. and Buckley, G.P. 1975. A practical approach towards the establishment of trees and shrubs on pulverized fuel ash. Pages 305-329 in M.J. Chadwick and G.T. Goodman, eds. *The ecology of resource degradation and renewal.* Blackwell Sci. Pubs. Oxford.
- Hodgson, L. Dyer, D. and Brown, D.A. 1982. Neutralization and dissolution of high-calcium fly ash. *J. Environ. Qual.* 11:93-98.
- Huang, W.H. and Keller, W.C. 1976. Dissolution of rock-forming silicate mineral organic acids: Simulated first-stage weathering of fresh mineral surfaces. *Am. Min.* 55:2076-2094.
- Huang, W.H. and Keller, W.D. 1972. Geochemical mechanics for the dissolution, transport, and deposition of aluminum in the zone of weathering. *Clays and Clay Mins.* 20:69-74.
- Huang, W.H. and Kiang, W.C. 1972. Laboratory dissolution of plagioclase feldspars in water and organic acids at room temperature. *Am. Min.* 57:1849-1859.
- Hulett, L.D., Weinberger, A.J., Ferguson, N.M., Northcutt, K.J. and Lyon, W.S. 1979. Chemical speciation studies of fly ash I: Characterization of solids. Electric Power Res. Instit. Palo Alto, Calif. Report #RP1061. Final Report. 63pp.
- Hulett, L.D., Weinburger, A.J., Northcutt, K.J. and Ferguson, M. 1980. Chemical species in fly ash from coal-burning power plants. *Sci.* 210:1356-1358.

- Hulett, L.D. and Weinburger, A.J. 1980. Some etching studies of the microstructure and composition of large aluminosilicate particles in fly ash from coal-burning power plants. *Environ. Sci. Tech.* 14:965-970.
- Jacobson, J.L. and Nixon, E.R. 1968. Infrared dielectric response and lattice vibrations of calcium and strontium oxides. *J. Physics Chem. Solids* 29:967-976.
- Jambon, A. and Carron, J.D. 1976. Diffusion of Na, K, Rb, and Cs in glasses of albite and orthoclase composition. *Geochim. Cosmochim. Acta* 40:897-903.
- James, W.D., Janghorbani, M. and Baxter, T. 1977. Leachability of neutron irradiated fly ash. *Anal. Chem.* 49:1994-1997.
- Joint Committee on Powder Diffraction Standards. Powder Diffraction File. Joint Committee on Powder Diffraction Standards Pub. Swarthmore, Penn.
- Jones, L.H. and Lewis, A.V. 1960. Weathering of fly ash. *Nature.* 185:404-405.
- Jones, R.C. and Uehara, G. 1973. Amorphous coatings on mineral surfaces. *Soil Sci. Soc. Am. Proc.* 37:792-798.
- Joshi, R.C. 1981. Geotechnical aspects of coal ash production, disposal, and utilization. Pages 3-27 in P.F. Ziemkiewicz, R. Stein, R. Leitch, and G. Lutwick, eds. Coal ash and reclamation. Alberta Land Conservation and Reclamation Council. Report# RRTAC 81-3.
- Kaakinen, J.W., Jorden, R.M., Lawasani, M.H. and West, R.E. 1975. Trace element behavior in coal-fired power plant. *Environ. Sci. Tech.* 9:862-869.
- Kalb, G.W. 1975. Total mercury mass balance at a coal-fired power plant. Pages 154-174. in S.P. Babu, ed. Trace elements in fuel. *Adv. Chem. Ser.* 141., Am. Chem. Soc. Pub. Washington, D.C.
- Kitagawa, Y. 1971. The unit particle of allophane. *Am. Min.* 56:465-475.
- Klein, D.H. and Russell, P. 1973. Heavy metals: Fallout around a power plant. *Environ. Sci. Tech.* 7:357-358.

- Klein, D.H., Andren, A.W., Carter, J.A., Emery, J.F., Feldman, C., Fulkerson, W., Lyon, W.S., Talmi, Y., van Hook, R.I. and Bolton, N. 1975. Pathways of thirty-seven trace elements through coal-fired power plant. *Environ. Sci. Tech.* 9:979.
- Kopsick, D.A. and Angino, E. Effect of leachate solutions from fly ash bottom ash on groundwater quality. *J. Hydrol.* 54:34.
- Krauskopf, K.B. 1956. Dissolution and precipitation of silica at low temperatures. *Geochim. Cosmochim. Acta* 10:1-26.
- Kronberg, B.I., Brown, J.R., Fyfe, W.S., Peirce, M. and Winder, C.G. 1981. Distribution of trace elements in Western Canadian coal ashes. *Fuel* 60:59-63.
- Landau, S.I. ed. 1976. Funk and Wagnalls standard college dictionary: Canadian edition. Fitzhenry and Whiteside Ltd. Toronto. 1590pp.
- Landau, S.I. ed. 1977. The Doubleday Roget's thesaurus in dictionary form. Doubleday and Co. Inc. Garden City, N.Y. 804pp.
- Lauf, R.J., Lawrence, A.H. and Rawlston, S.S. 1982. Pyrite framboids as a source of magnetite spheres in fly ash. *Environ. Sci. Tech.* 16:218-220.
- Lee, R.E., Crist, H.L., Riley, A.E. and Macleod, K.E. 1975. Concentration and size of trace metal emissions from a power plant, a steel plant, and a cotton gin. *Environ. Sci. Tech.* 9:643-647.
- Leonard, A., Suzuki, S., Fripiat, J.J. and De Kimpe, C. 1964. Structure and properties of amorphous silicoaluminas. I: Structure from X-ray fluorescence spectroscopy and infrared spectroscopy. *J. Phys. Chem.* 68:2608-2617.
- Levy, A., Barrett, R.E., Stamma, R.D. and Hazard, H.R. 1980. Coal combustion residues 359-433 in R.A. Meyers, ed. *Coal handbook*. Marcel Dekker. New York, N.Y.
- Linton, R.W., Loh, A., Natusch, D.F.S., Evans, C.A. and Williams, P. 1976. Surface predominance of trace elements in airborne particles. *Sci.* 191:852-854.

- Lihton, R.W., Williams, P., Evans, C.A. and Natusch, D.F.S. 1977. Determination of the surface predominance of toxic elements in airborne particles by ion microprobe mass spectrometry and auger electron spectrometry. *Anal. Chem.* 49:1514-1521.
- Lindsay, W.L. 1979. Chemical equilibria in soils. Wiley-Interscience Pub. New York, N.Y. 449pp.
- Lyon, R.J.P. 1964. Infrared analysis of soil minerals. Pages 170-199 in C.I. Rich and G.W. Kunze, eds. Soil clay mineralogy: A symposium. University of North Carolina Press, Chapel Hill, N.C.
- Mackenzie, R.C. ed. 1970. Differential thermal analysis. I: Fundamental aspects. Academic press New York, N.Y. 775pp.
- Markowski, G.R., Ensor, D.S. and Hodder, R.G. 1980. A submicron aerosol mode in flue gas from a pulverized coal utility boiler. *Environ. Sci. Tech.* 14:1400-1402.
- Mattigod, S.V. 1982. Characterization of fly ash particles. *Scanning Electron Microscopy* 1982(2):611-617.
- McKeague, J.A. and Day, J.H. 1966. Dithionite and oxalate-extractable Fe and Al as an aid in differentiating various classes of soils. *Can. J. Soil Sci.* 46:13-22.
- McKeague, J.A. 1967. An evaluation of 0.1 M pyrophosphate and pyrophosphate-dithionite in comparison with oxalate as extractants of the accumulation products in podzols and some other soils. *Can. J. Soil Sci.* 47:95-99.
- McKeague, J.A. and Day, J.H. 1969. Oxalate-extractable Al as a criterion for identifying podzol B horizons. *Can. J. Soil Sci.* 49:161-163.
- McKeague, J.A., Brydon, J.E. and Miles, N.M. 1971. Differentiation of forms of extractable iron and aluminum in soils. *Soil Sci. Soc. Am. Proc.* 35:33-38.
- McKeague, J.A. ed. 1978. Manual of soil sampling and methods of analysis. 2nd edition. Can. Soc. Soil Sci. Pub. Ottawa. 212pp.

- Mehra, O.P. and Jackson, M.L. 1960. Iron oxide removal from soils and clays by a dithionite-citrate system buffered with sodium carbonate. Pages 317-327. In A. Swineford, ed. Seventh national conference on Clays and Clay Minerals.
- Meikle, P.G. 1975. Fly ash. Pages 727-752 in C.L. Mantell, ed. Solid wastes: Collection, processing, and disposal. Wiley-Interscience. New York, N.Y.
- Mindess, S. and Young, J.F. 1981. Concrete. Prentice-Hall Inc. Englewood Cliffs, N.J. 691pp.
- Mitchell, B.D., Farmer, V.C. and McHardy, W.J. 1964. Amorphous inorganic materials in soils. Adv. Agron. 16:327-383.
- Mitchell, B.D. and Birnie, A.C. 1970. Organic Compounds. Pages 611-641 in R.C. Mackenzie, ed. Differential thermal analysis: Fundamental aspects. Academic Press. New York, N.Y.
- Munsell Color. 1975. Munsell soil color charts. Macbeth Division, Kollmorgen Corp. Baltimore, Maryland.
- Natusch, D.F.S., Bauer, C.F., Matusiewicz, H., Evans, C.A., Baker, J., Loh, A., Linton, R.W. and Hopke, P.K. 1975. Characterization of trace elements in fly ash. Pages 553-575 in T.E. Hutcheson, ed. Symposium proceedings: International conference on heavy metals in the environment. Toronto, Canada. Vol. 2, Pt. 2.
- Natusch, D.F.S. and Wallace, J.R. 1974. Urban aerosol toxicity: The influence of particle size. Sci. 186:695-699.
- Natusch, D.F.S., Wallace, J.R. and Evans, C.A. 1974. Toxic trace elements: Preferential concentration in respirable particles. Sci. 183:202-204.
- Olson, R.V. 1947. Iron solubility in soils as affected by pH and free iron oxide content. J. Soil Sci. 33:125-136.
- Page, A.L., Elsewi, A.A. and Straughan, I.R. 1979. Physical and chemical properties of fly ash from coal-fired power plants with reference to environmental impacts. Residue Rev. 71:83-120.

- Paulson, C.A.J. and Ramsden, A.R. 1970. Some microscopic features of fly-ash particles and their significance in relation to electrostatic precipitation. *Atmos. Environ.* 4:175-185.
- Paulson, L.E., Beckering, W. and Fowkes, W.V. 1972. Separation and identification of minerals from northern great plains province lignite. *Fuel* 51:224-227.
- Pawluk, S. 1967. Soil analysis by atomic absorption spectrophotometry. *At. Absorp. Newslett.* 6:53-67.
- Pawluk, S. 1972. Measurement of crystalline and amorphous iron removal in soils. *Can J. Soil Sci.* 52:119-123.
- Phung, H.T., Lund, L.J. and Page, A.L. 1978. Potential use of fly ash as a liming material. Pages 504-515 in D.C. Adriano and I.L. Brisbin, eds. *Environmental cycling and cycling processed.* Min. Cycl. Sym. U.S. Dept. Energy Conf-760427.
- Phung, H.T., Lund, L.J., Page, A.L. and Bradford, G.R. 1979. Trace elements in fly ash and their release in water and treated soils. *J. Environ. Qual.* 8:171-175.
- Quann, R.J., Neville, M., Janghorbani, M., Mims, C.A. and Sarofim, A.F. 1982. Mineral matter and trace element vaporization in a laboratory pulverized coal combustion system. *Environ. Sci. Tech.* 16:776-781.
- Raad, A.T., Protz, R. and Thomas, R.L. 1969. Determination of Na-dithionite and NH_4 -oxalate extractable Fe, Al, and Mn in soils by atomic absorption spectroscopy. *Can J. Soil Sci.* 49:89-94.
- Raask, E. 1968. Censopheres in pulverized fuel ash. *J. Inst. Fuel* 41:339-344.
- Raask, E. 1969. Fusion of silicate particles in coal flames. *Fuel* 48:366-374.
- Ramsden, A.R. 1968. Application of electron microscopy to the study of pulverized coal combustion and fly-ash formation. *J. Inst. Fuel* 41:451-454.
- Ramsden, A.R. 1969. A microscopic investigation into the formation of fly-ash during combustion of a pulverized bituminous coal. *Fuel* 48:121-127.

- Randall, H.M., Fower, R.G., Fuson, N., and Dangi, J.R. 1949. Infrared determination of organic structures. D. Van Nostrand Co. Toronto, 239pp.
- Rippon, J.E. and Wood, M.J. 1975. Microbiological aspects of pulverized fuel ash. Pages 331-349 in M.J. Chadwick and G.T. Goodman, eds. The ecology of resource degradation and renewal. Blackwell Sci. Pubs. Oxford.
- Robie, R.A., Hemingway, B.S. and Fisher, J.R. 1979. Thermodynamic properties of minerals and related substances at 298.15°K and 1 bar (10⁵ pascals) pressure and at higher temperatures. U.S. Geol. Survey Bull. 1452. Washington, D.C. 456 pp.
- Rohrman, F.A. 1971. Analyzing the effect of fly ash on water pollution. Power 115(8):76-77.
- Ross, G.T. 1980. Mineralogical, physical, and chemical characteristics of amorphous constituents in some podzolic soils from B.C. Can. J. Soil Sci. 60:31-43.
- Roy, R.W. and Griffin, R.A. 1982. A proposed classification system for coal fly ash in multidisciplinary research. J. Environ. Qual. 11:563-568.
- St. Arnaud, R.J. and Herbillon, A.J. 1973. Occurrence and genesis of secondary magnesium-bearing calcites in soils. Geoderma 9:279-298.
- St. Arnaud, R.J. 1979. Nature and distribution of secondary soil carbonates within landscapes in relation to soluble Mg²⁺/Ca²⁺ ratios. Can. J. Soil Sci. 59:87-98.
- Sarofim, A.F., Howard, J.B. and Padia, A.S. 1977. The physical transformation of mineral matter in pulverized coal under simulated combustion conditions. Comb. Sci. Tech. 16:187-204.
- Schnitzer, M. and Skinner, S.I.M. 1965. Organo-metallic interactions in soils. IV: Carbonyl and hydroxyl groups in organic matter and metal retention. Soil Sci. 99:278-284.
- Schnitzer, M. 1969. Reactions between fulvic acid, a soil humic compound and inorganic soil constituents. Soil Sci. Soc. Am. Proc. 33:75-81.

- Schwertmann, U. 1966. Inhibitory effect of soil organic matter on the crystallization of amorphous ferric hydroxide. *Nature* 212:645-646.
- Schwertmann, U. 1973. Use of oxalate for Fe extraction from soils. *Can. J. Soil Sci.* 53:244-246.
- Schwitzgerbel, K., Meserole, F.B., Oldham, R.G., Magee, R.A., Mesich, F.G. and Thoem, T.L. 1975. Trace element discharge from coal-fired power plants. Pages 533-551 in T.E. Hutchison, ed. Symposium proceedings: International conference on heavy metals in the environment. Toronto, Canada. Vol. 2, Pt. 2.
- Shannon, D.G. and Fine, L.O. 1974. Cation solubilities of lignite fly ashes. *Environ. Sci. Tech.* 8:1026-1028.
- Sherman, G.D., Schultz, F. and Alway, F.J. 1962. Dolomitization in soils of the Red River valley, Minnesota. *Soil Sci.* 94:304-313.
- Shibaoka, M. and Ramsden, A.R. 1978. Microscopic investigation of the behaviour of inorganic material in coal during combustion. Pages 67-75 in R.W. Bryers, ed. Ash deposits and corrosion due to impurities in combustion gases. Proc. Inter. Conf. 1977. Hemisphere Pub. Co. Washington, D.C.
- Simons, H.S. and Jeffery, J.W. 1960. An X-ray study of pulverized fuel ash. *J. Appl. Chem.* 10:328-336.
- Singer, A. and Novrot, J. 1976. Extraction of metals from basalt by humic acids. *Nature* 262:479-480.
- Smith, J.V. ed. 1967. Index (inorganic) to the powder diffraction file. ASTM Pub #PD1S-17i, American Society for Testing and Materials. Philadelphia, Penn. 566pp.
- Smith, R.D. 1980. The trace element chemistry of coal during combustion and the emissions from coal-fired plants. *Proc. Ener. Comb. Sci.* 6:53-119.
- Smith, R.D., Campbell, J.A. and Neilson, K.K. 1979a. Characterization and formation of submicron particles in coal-fired plants. *Atmos. Environ.* 13:607-617.

- Smith, R.D., Campbell, J.A. and Neilson, K.K. 1979b. Concentration dependence upon particle size of volatilized elements in fly ash. Environ. Sci. Tech. 13:553-558.
- Smith, R.D., Campbell, J.A. and Neilson, K.K. 1980. Volatility of fly ash and coal. Fuel 59:661-665.
- Steel, R.G.D. and Torrie, J.H. 1980. Principles and procedures of statistics: A biometrical approach. 2nd edition. McGraw-Hill, New York, N.Y. 632pp.
- Stinespring, C.D. and Stewart, G.W. 1981. Surface enrichment of aluminosilicate minerals and coal combustion ash particles. Atmos. Environ. 15:307-313.
- Stubican, V. and Roy, R. 1961a. Isomorphous substitution and infra-red spectra of the layer lattice silicates. Am. Min. 46:32-51.
- Stubican, V. and Roy, R. 1961b. A new approach to assignment of infrared absorption bands in layer-structure silicates. Zeitz. Kristallogr. 155:200-214.
- Stumm, W. and Morgan, J.J. 1981. Aquatic chemistry: An introduction emphasizing chemical equilibria in natural waters. 2nd edition. Wiley-Interscience N.Y. 780pp.
- Sudo, T., Shimoda, S., Yutsumoto, H. and Aita, S. 1981. Electron micrographs of clay minerals. Developments in sedimentology 31. Kodansha Ltd. Tokyo. 203pp.
- Talbot, R.W., Anderson, M.A. and Anders, W.A. 1978. Quantitative model of heterogeneous equilibria in a fly ash pond. Environ. Sci. Tech. 12:1056-1062.
- Tektronix Inc. 1977. TEKTRONIX PLOT-10 APL GRAPH-II, User's manual. Tektronix, Inc. Beaverton, Oregon.
- Theis, T.L. and Wirth, J.L. 1977. Sorptive behavior of trace metal ion fly ash in aqueous systems. Environ. Sci. Tech. 11:1096-1100.
- Theis, T.L., Westrich, J.D., Hsu, C.L. and Marley, J.J. 1978. Field investigation of trace metals in groundwater from fly ash disposal. J. Water Polln. Contr. Fed. 50:2457-2469.

- Thorne, D.J. and Watt, J.D. 1965. Composition and possolanic properties of pulverized fuel ashes. II: Possolanic properties of fly ashes as determined by crushing strength tests on lime mortars. *J. Appl. Chem.* 15:595-604.
- Torrey, S. ed. 1978. Coal ash utilization: Fly ash, bottom ash and slag. *Polln. Tech. Rev.* #48. Noyes Data Corp. Park Ridge, N.J. 370pp.
- Townsend, W.N. and Hodgson, D.R. 1973. Edaphological problems associated with deposits of fuel ash. Pages 45-56 *in* R.J. Huntick and G.Davis, eds. *Ecology and reclamation of devastated land* Vol. 1. Gordon and Breach, New York, N.Y.
- Townsend, W.N. and Gillham, E.W.F. 1975. Pulverized fuel ash as a medium for plant growth. Pages 287-304 *in* M.J. Chadwick and G.T. Goodman, eds. *The ecology of resource degradation and renewal*. Blackwell Sci. Pubs. Oxford.
- Turner, R.R. 1981. Oxidation of arsenic in coal ash leachate. *Environ. Sci. Tech.* 15:1062-1066.
- Vandergrift, A.E., Shannon, J. and Gorman, P.G. 1973. Collecting fine particles. *Chem. Eng.* 80(6):107-114.
- van der Marel, H.W. and Beutelspacher, H. 1976. Atlas of infrared spectroscopy of clay minerals and their admixtures. Elsevier Sci. Pub. Amsterdam. 396pp.
- van Olphen, H. 1971. Amorphous clay materials. *Sci.* 171:91-92.
- Voina, N.I. and Todor, D.N. 1978. Thermal analysis of coal and coal ashes. Pages 619-648 *in* C. Karr Jr., ed. *Analytical methods of coal and coal products*. Vol 2. Academic press. New York, N.Y.
- Wada, K. and Yoshinaga, N. 1969. The structure on imogolite. *Am. Min.* 54:50-71.
- Wada, K., Yoshinaga, N., Yotsumoto, H., Ibe, K. and Aida, S. 1970. High resolution electron micrographs of imogolite. *Clay Mins.* 8:487-489.
- Wada, K. and Tokashiki, Y. 1972. Selective dissolution and difference infrared spectroscopy in quantitative mineralogical analysis of volcanic ash soil clays. *Geoderma* 7:199-213.

- Wada, K., Henmi, T., Yoshinaga, N. and Patterson, S.H. 1972. Imogolite and allophane formed in saprolite of basalt on Maui, Hawaii. *Clays and Clay Mins.* 20:375-380.
- Wada, K. and Aomine, S. 1973. Soil developed on volcanic materials during the quaternary. *Soil Sci.* 116:170-177.
- Wada, K. and Harward, M.E. 1974. Amorphous clay constituents of soils. *Adv. Agron.* 26:211-260.
- Wada, K. and Kubo, H. 1975. Precipitation of amorphous aluminosilicates from solutions containing monomeric silica and aluminum ions. *J. Soil Sci.* 26:100-111.
- Wada, K. 1977. Allophane and imogolite. Pages 603-638 in J.B. Dixon and S.B. Weed, eds. *Minerals in soil environments.* Soil Sci. Soc. Am. Pub. Madison, Wisconsin.
- Watt, J.D. and Thorne, D.J. 1965. Composition and pozzolanic properties of pulverized fuel ashes. I: Composition of fly ashes from some British power stations and properties of their component particles. *J. Appl. Chem.* 15:585-594.
- Watt, J.D. and Thorne, D.J. 1966. The composition and pozzolanic properties of pulverized fuel ashes. III: Pozzolanic properties of fly ashes as determined by chemical methods. *J. Appl. Chem.* 16:33-39.
- Weast, R.C. ed. 1974. *Handbook of chemistry and physics.* 55th edition. Chemical Rubber Pub. Co. Cleveland, Ohio.
- Weaver, R.M., Syers, J.K. and Jackson, M.L. 1968. Determination of silica in citrate-bicarbonate-dithionite extracts of soils. *Soil Sci. Soc. Am. Proc.* 32:497-501.
- Webb, T.L. and Kruger, J.E. 1970. Carbonates. Pages 303-341 in R.C. Mackenzie, ed. *Differential thermal analysis.* I: Fundamental aspects. Academic press. New York, N.Y.
- White, A.F. 1983. Surface chemistry and dissolution kinetics of glassy rock at 25°C. *Geochim. Cosmochim. Acta* 47:805-815.
- White, H.J. 1977a. Electrostatic precipitation of fly ash. *J. Air Polln. Cont. Assn.* 27:15-21.

- White, H.J. 1977b. Electrostatic precipitation of fly ash: Fly ash and furnace gas characteristics. J. Air Polln. Cont. Assn. 27:114-120.
- Windholtz, M. ed. 1976. The Merck index: An encyclopedia of chemicals and drugs. 9th edition. Merck and Co. Inc. Rahway, N.J.
- Wray, J.L. and Daniels, F. 1957. Precipitation of calcite and aragonite. J. Am. Chem. Soc. 79:2031-2034.
- Young, A.W., Campbell, A.S. and Walker, T.W. 1980. Allophane isolated from a podzol developed on a non-vitric parent material. Nature 284:46-48.

APPENDIX

Table 1. Leachate pH values of the Forestburg fly ash leached with 0.005 M sulfuric acid

Inc #	Rep 1 Column Number					Rep 2 Column Number					Rep 3 Column Number				
	1	2	3	4	5	1	2	3	4	5	1	2	3	4	5
1	11.88	11.80	11.88			11.70	11.80	11.88			3.88	11.88	11.80		
2	10.20	10.80	11.28	11.88	12.00	9.88	10.88	10.80	11.88	12.08	8.80	10.88	11.00	11.80	12.00
3	9.70	10.20	10.40	10.78	11.00	8.80	10.20	10.80	10.80	11.28	4.70	10.18	10.88	10.80	11.40
4	8.30	10.20	10.80	10.80	10.78	4.48	10.20	10.20	10.80	11.00	4.70	10.20	10.28	10.40	10.88
5	8.88	9.80	10.18	10.18	10.80	4.18	9.88	10.10	10.20	10.48	4.18	9.80	10.28	10.20	10.80
6	8.08	9.80	9.80	10.10	10.40	3.78	9.88	10.88	10.18	10.30	3.80	9.78	10.00	10.18	10.28
7	4.80	3.88	3.80	10.00	10.80	3.88	8.88	9.88	10.10	10.28	3.80	9.80	9.88	10.08	10.40
8	4.28	3.88	3.80	10.18	8.88	3.80	8.80	9.80	10.00	10.08	4.28	8.80	9.80	10.08	10.18
9	4.18	3.88	3.88	8.80	10.20	3.70	9.80	10.88	9.70	10.08	3.90	9.80	9.80	10.00	10.08
10	4.10	3.80	3.88	10.10	10.20	3.80	9.80	9.80	9.88	10.30	3.88	9.80	9.78	10.08	10.28
11	3.10	3.80	3.80	10.20	9.88	3.88	9.78	9.80	10.10	9.80	3.80	9.40	9.80	10.20	9.80
12	4.10	3.80	3.88	9.88	9.80	3.88	9.80	10.08	9.88	9.80	3.80	9.88	10.18	9.80	9.80
13	4.18	3.80	3.88	8.80	9.80	3.80	9.80	9.78	9.48	9.88	3.88	9.78	9.80	9.20	9.88
14	4.10	3.88	3.80	9.88	9.10	3.88	9.88	9.28	9.78	9.00	3.80	9.48	9.28	9.78	9.10
15	4.10	3.20	3.40	9.20	9.20	3.20	3.28	9.78	9.18	9.10	3.80	9.30	9.70	9.10	9.18
16	4.20	3.48	3.10	9.08	9.00	3.20	3.48	9.10	9.10	9.00	3.40	9.38	9.10	9.08	9.00
17	4.18	3.08	3.08	9.88	9.10	3.80	3.08	9.10	9.88	9.08	3.38	9.88	9.00	9.88	9.10
18	4.18	3.88	3.80	9.10	9.10	3.28	3.88	9.08	9.10	9.18	3.20	3.80	9.00	9.08	9.18
19	4.10	3.88	3.08	9.10	9.00	3.20	3.80	9.10	9.28	9.88	3.28	3.88	9.00	9.20	9.80
20	4.08	3.78	3.20	9.08	9.00	3.20	3.88	9.20	9.00	9.88	3.20	3.20	9.18	9.88	9.00
21	4.10	3.80	3.80	9.00	9.88	3.40	7.28	9.80	9.88	9.00	3.20	7.28	9.80	9.08	9.88
22	4.18	3.80	3.88	9.00	9.00	3.40	8.00	9.88	9.88	9.18	3.20	8.10	9.88	9.80	9.18
23	4.08	4.70	3.80	9.10	9.00	3.20	4.88	9.88	9.18	9.08	3.20	4.70	9.88	9.10	9.88
24	3.88	4.80	3.80	9.00	9.80	3.20	4.80	9.88	9.00	9.00	3.18	4.88	9.10	9.80	9.88
25	4.00	4.48	3.88	9.80	9.20	3.18	4.80	9.80	9.88	9.18	3.18	4.88	9.88	9.88	9.10
26	4.18	4.20	3.78	9.18	9.10	3.48	4.28	9.80	9.10	9.88	3.40	4.28	9.80	9.10	9.88
27	4.08	4.20	3.80	9.88	9.80	3.20	4.28	9.00	9.88	9.80	3.18	4.28	9.88	9.80	9.08
28	3.88	4.20	3.88	9.00	9.88	3.10	4.40	9.88	9.00	9.88	3.10	4.28	9.88	9.88	9.88
29	4.00	4.20	3.70	9.00	9.10	3.18	4.28	9.70	9.00	9.10	3.20	4.20	9.88	9.88	9.18
30	3.88	4.28	3.78	9.00	9.78	3.00	4.28	9.78	9.00	9.88	3.10	4.48	9.88	9.00	9.78
31	3.80	4.20	3.80	9.70	9.80	3.10	4.20	9.88	9.78	9.88	3.20	4.20	9.00	9.70	9.78
32	3.80	4.20	3.78	9.80	9.80	3.00	4.20	9.88	9.78	9.08	3.00	4.10	9.88	9.78	9.88
33	3.88	4.10	3.80	9.88	9.88	3.20	4.10	9.70	9.88	9.80	3.20	4.08	9.70	9.88	9.80
34	3.70	4.18	3.80	9.88	9.80	3.00	4.18	9.80	9.88	9.80	2.88	4.08	9.88	9.88	9.78
35	3.88	4.20	3.88	9.80	9.88	2.88	4.20	9.78	9.78	9.80	2.88	4.20	9.70	9.78	9.80
36	3.80	4.18	3.88	9.80	9.88	3.20	4.18	9.88	9.88	9.88	3.00	4.18	9.88	9.80	9.88
37	3.80	4.18	3.80	9.88	9.70	3.20	4.18	9.78	9.80	9.80	2.88	4.10	9.88	9.80	9.78
38	3.80	4.18	3.78	9.78	9.70	3.08	4.20	9.70	9.70	9.78	2.88	4.20	9.78	9.78	9.80
39	3.40	4.20	3.70	9.78	9.80	3.10	4.20	9.80	9.70	9.88	2.08	4.20	9.80	9.80	9.80
40	3.40	4.20	3.88	9.88	9.88	2.08	4.20	9.78	9.88	9.70	2.00	4.18	9.80	9.88	9.88
41	3.38	4.18	3.88	9.70	9.88	2.00	4.18	9.80	9.80	9.70	2.80	4.10	9.80	9.88	9.70
42	3.20	4.10	3.80	9.88	9.88	3.00	4.20	9.80	9.80	9.80	2.80	4.20	9.80	9.88	9.80
43	3.20	4.10	3.80	9.80	9.70	2.88	4.10	9.80	9.80	9.78	2.80	4.10	9.80	9.88	9.70
44	3.28	4.10	3.88	9.70	9.78	2.80	4.18	9.80	9.78	9.80	2.88	4.18	9.80	9.80	9.70
45	3.20	4.18	3.80	9.88	9.70	2.80	4.18	9.80	9.88	9.80	2.88	4.10	9.80	9.88	9.78
46	3.20	4.18	3.70	9.70	9.70	2.80	4.18	9.80	9.88	9.80	2.88	4.10	9.80	9.88	9.78
47	3.18	4.18	3.88	9.70	9.70	2.88	4.20	9.80	9.78	9.88	2.88	4.20	9.80	9.78	9.70
48	3.18	4.10	3.40	9.70	9.70	2.88	4.18	9.80	9.88	9.70	2.88	4.20	9.80	9.88	9.78
49	3.08	4.08	3.28	9.88		2.80	4.10	9.30	9.70		2.80	4.10	9.00	9.80	9.80
50	3.00	4.08	3.18			2.80	4.08	9.18			2.70	4.08	7.80		
51	3.00	4.10				2.78	4.10				2.78	4.18			
52	3.00					2.80					2.78				

Table 2 Concentration of Ca (ug/ml) in the leachates of the Forestburg fly ash leached with 0.005 M sulfuric acid.

Inc #	Rep 1				Rep 2				Rep 3			
	1	2	3	4	1	2	3	4	1	2	3	4
1	510	370	1100	870	900	1100	840	1300	220	810	1100	1200
2	200	270	410	270	300	330	300	280	200	300	420	480
3	210	300	250	270	340	330	310	280	200	320	330	310
4	210	280	210	210	340	330	280	330	280	310	340	350
5	200	310	280	270	310	320	320	320	220	310	280	250
6	200	280	320	270	310	320	320	320	220	310	280	330
7	150	220	320	180	280	320	320	320	210	280	320	320
8	150	220	320	180	280	320	320	320	140	220	320	300
9	150	220	320	180	280	320	320	320	220	300	320	250
10	150	220	320	180	280	320	320	320	220	300	320	310
11	150	220	320	180	280	320	320	320	180	300	310	340
12	150	220	320	180	280	320	320	320	180	280	310	340
13	150	220	320	180	280	320	320	320	180	280	310	340
14	150	220	320	180	280	320	320	320	180	280	310	340
15	150	220	320	180	280	320	320	320	180	280	310	340
16	150	220	320	180	280	320	320	320	180	280	310	340
17	150	220	320	180	280	320	320	320	180	280	310	340
18	150	220	320	180	280	320	320	320	180	280	310	340
19	150	220	320	180	280	320	320	320	180	280	310	340
20	150	220	320	180	280	320	320	320	180	280	310	340
21	2	47	280	180	82	210	270	270	22	280	340	280
22	2	28	150	110	37	180	180	180	3	82	240	170
23	2	28	150	110	37	180	180	180	3	82	240	170
24	2	28	150	110	37	180	180	180	3	82	240	170
25	2	28	150	110	37	180	180	180	3	82	240	170
26	2	28	150	110	37	180	180	180	3	82	240	170
27	2	28	150	110	37	180	180	180	3	82	240	170
28	2	28	150	110	37	180	180	180	3	82	240	170
29	2	28	150	110	37	180	180	180	3	82	240	170
30	2	28	150	110	37	180	180	180	3	82	240	170
31	2	28	150	110	37	180	180	180	3	82	240	170
32	2	28	150	110	37	180	180	180	3	82	240	170
33	2	28	150	110	37	180	180	180	3	82	240	170
34	2	28	150	110	37	180	180	180	3	82	240	170
35	2	28	150	110	37	180	180	180	3	82	240	170
36	2	28	150	110	37	180	180	180	3	82	240	170
37	2	28	150	110	37	180	180	180	3	82	240	170
38	2	28	150	110	37	180	180	180	3	82	240	170
39	2	28	150	110	37	180	180	180	3	82	240	170
40	2	28	150	110	37	180	180	180	3	82	240	170
41	2	28	150	110	37	180	180	180	3	82	240	170
42	2	28	150	110	37	180	180	180	3	82	240	170
43	2	28	150	110	37	180	180	180	3	82	240	170
44	2	28	150	110	37	180	180	180	3	82	240	170
45	2	28	150	110	37	180	180	180	3	82	240	170
46	2	28	150	110	37	180	180	180	3	82	240	170
47	2	28	150	110	37	180	180	180	3	82	240	170
48	2	28	150	110	37	180	180	180	3	82	240	170
49	2	28	150	110	37	180	180	180	3	82	240	170
50	2	28	150	110	37	180	180	180	3	82	240	170
51	2	28	150	110	37	180	180	180	3	82	240	170
52	2	28	150	110	37	180	180	180	3	82	240	170

Table 3. Concentration of Na (ug/mL) in the leachates of the Forestburg fly ash leached with 0.005 M sulfuric acid.

Inc. #	Rep. 1					Rep. 2					Rep. 3				
	Column Number	1	2	3	4	1	2	3	4	5	1	2	3	4	5
1	72	170	390	-	-	81	210	400	-	-	58	170	420	-	-
2	8.1	18	53	370	680	4.5	15	41	420	530	4.4	17	53	340	570
3	8.3	7.0	12	23	170	4.5	5.1	9.1	21	140	4.9	5.1	11	22	140
4	8.1	6.7	8.3	12	28	4.1	5.3	8.4	10	22	7.2	5.5	7.3	11	22
5	8.5	7.2	8.2	11	18	5.2	5.4	8.3	8.7	13	5.3	5.5	7.5	10	14
6	8.7	7.5	9.2	10	14	5.5	5.4	8.5	7.8	12	7.1	5.7	8.1	10	13
7	7.3	8.3	8.9	11	13	5.3	5.1	8.7	8.6	10	6.9	7.5	7.9	10	11
8	8.0	8.0	9.5	10	-	5.8	5.4	7.5	8.2	-	7.4	8.1	9.5	8.4	-
9	7.7	8.9	8.4	-	-	8.3	7.5	7.7	-	-	7.3	8.4	8.6	-	-
10	8.2	8.4	-	-	11	8.5	7.2	-	-	10	7.4	8.0	-	-	11
11	7.8	-	-	10	-	8.3	-	-	8.8	-	7.2	-	-	-	-
12	-	-	10	-	-	-	-	8.0	-	-	-	-	8.5	-	-
13	-	8.8	-	-	11	-	7.8	-	-	9.5	-	8.4	-	-	10
14	7.4	-	-	10	-	6.1	-	-	8.6	-	7.1	-	-	8.3	-
15	-	-	8.8	-	-	-	-	8.2	-	-	-	-	8.8	-	-
16	-	8.3	-	-	8.4	-	7.5	-	-	11	-	9.1	-	-	11
17	8.2	-	-	10	-	6.8	-	-	8.4	-	7.8	-	-	-	11
18	-	-	10	-	-	-	-	8.0	-	-	-	-	10	-	-
19	-	9.3	-	-	11	-	8.3	-	-	10	-	10	-	-	12
20	8.4	-	-	12	-	7.1	-	-	10	-	8.1	-	-	11	-
21	-	-	12	-	-	-	-	10	-	-	-	-	10	-	-
22	-	8.2	-	-	13	-	7.9	-	-	11	-	8.2	-	-	13
23	7.9	-	-	12	-	8.5	-	-	10	-	7.4	-	-	12	-
24	-	-	11	-	-	-	-	9.2	-	-	-	-	11	-	-
25	-	8.4	-	-	12	-	8.0	-	-	8.4	-	-	-	-	10
26	8.1	-	-	11	-	8.8	-	-	8.8	-	7.2	-	-	10	-
27	-	-	8.5	-	-	-	-	8.1	-	-	-	-	8.0	-	-
28	-	7.8	-	-	12	-	8.8	-	-	10	-	7.5	-	-	11
29	7.0	-	-	11	-	5.7	-	-	8.5	-	5.2	-	-	11	-
30	-	-	11	-	-	-	-	8.6	-	-	-	-	10	-	-
31	-	8.0	-	-	11	-	7.1	-	-	9.4	-	8.4	-	-	11
32	7.5	-	-	11	-	5.7	-	-	8.7	-	5.5	-	-	10	-
33	-	-	10	-	-	-	-	8.7	-	-	-	-	8.1	-	-
34	-	8.1	-	-	13	-	7.2	-	-	11	-	8.2	-	-	12
35	7.7	-	-	12	-	6.1	-	-	10	-	5.8	-	-	11	-
36	-	-	11	-	-	-	-	8.4	-	-	-	-	10	-	-
37	-	8.5	-	-	12	-	7.8	-	-	11	-	8.5	-	-	12
38	7.9	-	-	12	-	6.7	-	-	10	-	7.1	-	-	11	-
39	-	-	10	-	-	-	-	8.3	-	-	-	-	10	-	-
40	-	8.3	-	-	12	-	7.5	-	-	11	-	8.8	-	-	12
41	8.1	-	-	12	-	8.4	-	-	10	-	7.1	-	-	11	-
42	-	-	10	-	-	-	-	8.4	-	-	-	-	10	-	-
43	-	9.4	-	-	12	-	17.8	-	-	11	-	8.8	-	-	12
44	8.1	-	-	12	-	8.1	-	-	10	-	5.0	-	-	11	-
45	-	-	11	-	-	-	-	9.2	-	-	-	-	10	-	-
46	-	9.3	-	-	12	-	8.1	-	-	10	-	8.8	-	-	11
47	7.8	-	-	12	-	8.3	-	-	10	-	7.1	-	-	10	-
48	-	-	10	-	13	-	-	10	-	11	-	-	10	-	12
49	-	8.4	-	-	12	-	7.4	-	-	11	-	8.3	-	-	11
50	7.3	-	11	-	-	5.0	-	-	10	-	5.8	-	-	10	-
51	-	9.0	-	-	-	-	8.1	-	-	-	-	8.9	-	-	-
52	8.0	-	-	-	-	6.2	-	-	-	-	6.7	-	-	-	-

Table 4 Concentration of K (ug/mL) in the leachates of the Verontburg fly ash leached with 0.005 M sulfuric acid

Inc #	Rep 1					Rep 2					Rep 3					
	Column Number	1	2	3	4	1	2	3	4	5	1	2	3	4	5	
1		1.5	3.3	5.5	-	1.4	3.5	5.4	-	1.4	3.1	5.8	-	-		
2		0.5	0.7	1.4	5.5	11	0.4	0.4	1.2	7.2	11	0.3	0.5	1.4	5.2	11
3		0.5	0.5	0.7	1.4	3.5	0.3	0.3	0.4	0.8	3.5	0.4	0.5	0.4	0.5	2.5
4		0.5	0.7	0.7	0.5	0.5	0.4	0.4	0.4	0.5	0.5	0.5	0.5	0.4	0.5	0.5
5		0.7	0.7	0.7	0.7	0.7	0.5	0.5	0.4	0.5	0.5	0.7	0.5	0.5	0.5	0.5
6		1.0	0.4	0.5	0.5	0.5	0.5	0.5	0.5	0.5	0.7	0.7	0.5	0.7	0.5	0.5
7		0.5	0.5	1.0	1.0	0.5	0.5	0.5	0.5	0.5	0.7	0.7	0.5	0.5	0.5	0.5
8		1.0	1.0	1.1	0.5	-	0.5	0.5	0.7	0.5	-	0.5	1.0	1.0	0.5	-
9		1.0	1.1	0.5	-	0.5	0.5	0.5	-	0.7	0.5	0.5	1.0	0.5	-	0.5
10		1.1	0	-	1.0	-	0.5	0.5	-	0.7	-	1.0	1.0	-	1.0	-
11		0.5	-	1.1	-	-	0.5	-	0.5	-	-	1.0	-	1.0	-	-
12		-	1.0	-	-	1.0	-	0.5	-	-	0.5	-	0.5	-	-	1.0
13		0.5	-	-	1.1	-	0.5	-	-	0.5	-	1.0	-	-	1.0	-
14		-	-	1.1	-	-	-	0.5	-	-	-	-	1.1	-	-	-
15		0	-	-	-	1.0	-	0.5	-	-	1.0	-	-	-	-	1.2
16		-	-	-	1.1	-	0.5	-	-	1.0	-	1.0	-	-	1.1	-
17		-	1.2	-	-	-	-	1.1	-	-	-	-	1.2	-	-	-
18		-	1.2	-	-	1.4	-	0.5	-	-	1.1	-	1.2	-	-	1.3
19		-	-	1.5	-	-	0	-	-	1.1	-	1.2	-	-	1.4	-
20		-	-	1.5	-	-	-	1.1	-	-	-	-	1.4	-	-	-
21		-	1.5	-	-	1.5	-	1.1	-	-	1.2	-	-	-	-	1.5
22		1.2	-	-	1.5	-	1.0	-	-	1.2	-	1.2	-	-	1.4	-
23		-	-	1.5	-	-	-	1.2	-	-	-	-	1.5	-	-	-
24		-	1.5	-	-	1.4	-	1.1	-	-	1.0	-	1.5	-	-	1.3
25		1.5	-	-	-	1.4	-	0.5	-	-	1.1	-	1.2	-	-	1.2
26		-	-	1.2	-	-	-	1.0	-	-	-	-	1.2	-	-	-
27		-	1.1	-	-	1.4	-	0.5	-	-	1.1	-	1.1	-	-	1.3
28		1.0	-	-	1.3	-	0.7	-	-	1.1	-	0.5	-	-	1.3	-
29		-	-	1.2	-	-	-	-	1.0	-	-	-	1.2	-	-	-
30		-	1.1	-	-	1.4	-	0.5	-	-	1.1	-	1.2	-	-	1.3
31		1.1	-	-	1.4	1.5	0.4	-	-	1.2	1.2	1.1	-	-	1.3	1.3
32		-	-	1.5	1.5	-	-	-	1.2	1.3	-	-	-	1.3	1.5	-
33		-	1.2	1.5	-	-	-	0.5	1.2	-	-	-	1.1	1.4	-	-
34		1.1	1.3	-	-	1.5	0.5	1.1	-	-	1.3	1.0	1.3	-	-	1.5
35		1.3	-	-	1.5	-	0.5	-	-	1.2	-	1.1	-	-	1.4	-
36		-	1.5	-	-	-	-	-	1.2	-	-	-	1.4	-	-	-
37		-	1.4	-	-	1.5	-	1.1	-	-	1.2	-	1.2	-	-	1.3
38		1.3	-	-	1.5	-	1.0	-	-	1.3	-	1.0	-	-	1.3	-
39		-	-	1.4	-	-	-	-	1.2	-	-	-	1.3	-	-	-
40		-	1.2	-	-	1.5	-	1.0	-	-	1.4	-	1.1	-	-	1.5
41		1.2	-	-	1.7	-	0.5	-	-	1.3	-	1.0	-	-	1.5	-
42		-	-	1.5	-	-	-	-	1.4	-	-	-	-	1.5	-	-
43		-	1.5	-	-	1.5	-	1.2	-	-	1.5	-	1.4	-	-	1.7
44		1.3	-	-	1.5	-	0.5	-	-	1.5	-	1.1	-	-	1.5	-
45		-	-	1.5	-	-	-	-	1.4	-	-	-	-	1.7	-	-
46		-	1.5	-	-	2.0	-	1.3	-	-	1.5	-	1.5	-	-	1.9
47		1.4	-	-	2.0	-	1.0	-	-	1.5	-	1.1	-	-	1.7	-
48		-	-	1.5	-	1.5	-	-	1.4	-	-	1.5	-	1.5	-	1.5
49		-	1.5	-	-	1.5	-	1.2	-	-	1.5	-	1.4	-	-	1.5
50		1.4	-	-	1.7	-	1.1	-	1.3	-	-	1.2	-	1.5	-	-
51		-	1.4	-	-	-	-	1.2	-	-	-	-	1.4	-	-	-
52		1.2	-	-	-	-	0.5	-	-	-	-	1.1	-	-	-	-

Table 5 Concentration of Mg (ug/mL) in the leachates of the Forestburg fly ash leached with 0.005 M sulfuric acid.

Inc #	Rep 1					Rep 2					Rep 3				
	Column	Number	1	2	3	Column	Number	1	2	3	Column	Number	1	2	3
1	0.1	0.0	0.0	0.0	0.0	0.3	0.0	0.0	0.0	0.0	5.0	0.1	0.0	0.0	0.0
2	1.2	0.1	0.0	0.0	0.0	5.5	0.1	0.0	0.0	0.0	2.8	0.1	0.0	0.0	0.0
3	5.8	0.1	0.0	0.0	0.0	5.5	0.1	0.0	0.0	0.0	2.1	0.2	0.1	0.0	0.0
4	12	0.1	0.1	0.0	0.0	10	0.1	0.1	0.0	0.0	2.5	0.3	0.1	0.0	0.0
5	15	0.3	0.1	0.1	0.0	10	0.3	0.1	0.1	0.0	3.7	0.5	0.1	0.0	0.0
6	17	0.8	0.1	0.1	0.0	10	0.8	0.1	0.1	0.0	4.8	0.9	0.1	0.1	0.0
7	18	2.0	0.1	0.1	0.0	12	1.6	0.1	0.1	0.0	8.8	1.5	0.1	0.1	0.0
8	18	3.3	0.1	0.1	0.0	12	2.8	0.1	0.1	0.0	9.2	2.5	0.1	0.1	0.0
9	18	5.1	0.2	0.1	0.0	13	4.2	0.1	0.1	0.0	11	3.7	0.1	0.1	0.0
10	15	6.4	0.1	0.1	0.0	13	5.4	0.1	0.1	0.0	11	5.1	0.1	0.1	0.0
11	15	0.1	0.1	0.1	0.0	14	0.1	0.1	0.1	0.0	11	0.1	0.1	0.1	0.0
12	13	0.2	0.1	0.1	0.0	14	0.2	0.1	0.1	0.0	13	0.3	0.1	0.1	0.0
13	11	0.1	0.1	0.1	0.0	11	0.1	0.1	0.1	0.0	12	0.1	0.1	0.1	0.0
14	11	0.2	0.1	0.1	0.0	11	0.2	0.1	0.1	0.0	12	0.2	0.1	0.1	0.0
15	11	0.5	0.1	0.1	0.0	11	0.4	0.1	0.1	0.0	12	0.5	0.1	0.1	0.0
16	18	0.1	0.1	0.1	0.0	12	0.1	0.1	0.1	0.0	13	0.1	0.1	0.1	0.0
17	11	0.2	0.1	0.1	0.0	12	0.3	0.1	0.1	0.0	13	0.3	0.1	0.1	0.0
18	21	2.2	0.1	0.1	0.0	22	1.0	0.1	0.1	0.0	22	1.9	0.1	0.1	0.0
19	21	3.0	0.1	0.1	0.0	22	1.8	0.1	0.1	0.0	22	2.8	0.1	0.1	0.0
20	10	0.3	0.1	0.1	0.0	10	0.3	0.1	0.1	0.0	11	0.3	0.1	0.1	0.0
21	21	3.0	0.1	0.1	0.0	20	1.8	0.1	0.1	0.0	21	2.8	0.1	0.1	0.0
22	8.2	0.3	0.1	0.1	0.0	8.2	0.3	0.1	0.1	0.0	10	0.3	0.1	0.1	0.0
23	2.4	0.2	0.1	0.1	0.0	1.5	0.1	0.1	0.1	0.0	2.2	0.2	0.1	0.1	0.0
24	8.4	0.2	0.1	0.1	0.0	10	0.1	0.1	0.1	0.0	10	0.2	0.1	0.1	0.0
25	4.3	0.4	0.1	0.1	0.0	4.8	0.5	0.1	0.1	0.0	4.5	0.4	0.1	0.1	0.0
26	3.7	0.2	0.1	0.1	0.0	2.9	0.2	0.1	0.1	0.0	3.5	0.2	0.1	0.1	0.0
27	7.7	0.2	0.1	0.1	0.0	8.1	0.2	0.1	0.1	0.0	8.8	0.2	0.1	0.1	0.0
28	4.3	0.5	0.1	0.1	0.0	4.1	0.5	0.1	0.1	0.0	4.1	0.5	0.1	0.1	0.0
29	8.4	0.2	0.1	0.1	0.0	3.2	0.2	0.1	0.1	0.0	3.8	0.2	0.1	0.1	0.0
30	7.7	0.2	0.1	0.1	0.0	8.0	0.2	0.1	0.1	0.0	7.9	0.2	0.1	0.1	0.0
31	4.4	0.7	0.1	0.1	0.0	4.0	0.7	0.1	0.1	0.0	4.2	0.7	0.1	0.1	0.0
32	5.8	0.3	0.1	0.1	0.0	4.2	0.3	0.1	0.1	0.0	5.4	0.3	0.1	0.1	0.0
33	7.7	0.3	0.1	0.1	0.0	7.5	0.2	0.1	0.1	0.0	7.4	0.3	0.1	0.1	0.0
34	4.5	0.8	0.1	0.1	0.0	4.2	0.8	0.1	0.1	0.0	4.3	0.8	0.1	0.1	0.0
35	7.1	0.3	0.1	0.1	0.0	5.8	0.3	0.1	0.1	0.0	6.5	0.3	0.1	0.1	0.0
36	7.0	0.3	0.1	0.1	0.0	7.0	0.2	0.1	0.1	0.0	6.7	0.3	0.1	0.1	0.0
37	4.3	1.1	0.1	0.1	0.0	4.2	1.0	0.1	0.1	0.0	4.1	1.1	0.1	0.1	0.0
38	8.0	0.3	0.1	0.1	0.0	8.7	0.3	0.1	0.1	0.0	9.2	0.3	0.1	0.1	0.0
39	7.1	0.3	0.1	0.1	0.0	7.0	0.3	0.1	0.1	0.0	6.5	0.3	0.1	0.1	0.0
40	4.4	1.0	0.1	0.1	0.0	4.1	1.3	0.1	0.1	0.0	4.2	1.0	0.1	0.1	0.0
41	10	0.4	0.1	0.1	0.0	10	0.3	0.1	0.1	0.0	8.4	0.4	0.1	0.1	0.0
42	5.8	0.4	0.1	0.1	0.0	5.8	0.3	0.1	0.1	0.0	5.4	0.4	0.1	0.1	0.0
43	3.7	1.2	0.1	0.1	0.0	3.2	1.2	0.1	0.1	0.0	3.4	1.2	0.1	0.1	0.0
44	11	0.4	0.1	0.1	0.0	11	0.4	0.1	0.1	0.0	11	0.4	0.1	0.1	0.0
45	8.5	0.4	0.1	0.1	0.0	8.5	0.4	0.1	0.1	0.0	8.2	0.4	0.1	0.1	0.0
46	3.5	2.0	0.1	0.1	0.0	3.2	2.1	0.1	0.1	0.0	3.2	2.1	0.1	0.1	0.0
47	17	0.5	0.1	0.1	0.0	18	0.4	0.1	0.1	0.0	16	0.5	0.1	0.1	0.0
48	5.7	2.4	0.1	0.1	0.0	5.3	2.5	0.1	0.1	0.0	5.4	2.5	0.1	0.1	0.0
49	2.6	1.6	0.1	0.1	0.0	3.3	1.7	0.1	0.1	0.0	3.4	1.6	0.1	0.1	0.0
50	5.8	0.1	0.1	0.1	0.0	5.5	0.1	0.1	0.1	0.0	5.5	0.1	0.1	0.1	0.0
51	3.6	0.1	0.1	0.1	0.0	3.2	0.1	0.1	0.1	0.0	3.4	0.1	0.1	0.1	0.0
52	3.6	0.1	0.1	0.1	0.0	3.2	0.1	0.1	0.1	0.0	3.4	0.1	0.1	0.1	0.0

Table 8 Concentration of Fe (ug/mL) in the leachates of the Forestburg fly ash leached with 0.005 M sulfuric acid

Inc #	Rep. 1 Column Number					Rep. 2 Column Number					Rep. 3 Column Number				
	1	2	3	4	5	1	2	3	4	5	1	2	3	4	5
1	0.51	0.1	0.2	-	-	0.1	0.1	0.2	-	-	3.1	0.1	0.2	-	-
2	0.0	0.1	0.0	0.0	0.0	0.1	0.1	0.0	0.0	0.0	0.2	0.1	0.0	0.1	0.0
3	0.1	0.0	0.0	0.0	0.0	0.2	0.0	0.0	0.0	0.0	0.3	0.0	0.0	0.0	0.0
4	0.0	0.0	0.0	0.0	0.0	2.0	0.0	0.0	0.0	0.0	0.4	0.0	0.0	0.0	0.0
5	0.0	0.0	0.0	0.0	0.0	1.1	0.0	0.0	0.0	0.0	0.8	0.0	0.0	0.0	0.0
6	0.1	0.0	0.0	0.0	0.0	2.1	0.0	0.0	0.0	0.0	1.2	0.0	0.0	0.1	0.0
7	0.4	0.0	0.0	0.0	0.0	2.7	0.0	0.0	0.0	0.0	1.0	0.0	0.0	0.0	0.0
8	0.7	0.0	0.0	0.0	0.0	2.4	0.0	0.0	0.0	0.0	0.8	0.0	0.0	0.0	0.0
9	0.9	0.0	0.0	-	-	2.2	0.0	0.0	-	-	1.1	0.0	0.0	-	-
10	1.2	0.0	-	-	0.0	2.9	0.0	-	-	0.0	1.3	0.0	-	-	0.0
11	1.3	-	-	0.1	-	2.8	-	-	0.0	-	1.4	-	-	0.0	-
12	-	-	0.0	-	-	-	-	0.0	-	-	-	-	0.0	-	-
13	-	0.0	-	-	0.0	-	0.0	-	-	0.0	-	0.1	-	-	0.0
14	1.8	-	-	0.0	-	3.4	-	-	-	-	1.8	-	-	0.0	-
15	-	0.0	0.0	-	0.0	-	0.0	0.0	-	-	-	0.0	-	-	-
16	-	-	-	-	-	-	0.0	-	-	0.0	-	0.0	-	-	0.0
17	1.2	-	-	0.0	-	2.8	-	-	0.0	-	1.8	-	-	0.0	-
18	-	-	0.0	-	-	-	-	0.0	-	-	-	0.0	-	-	-
19	-	0.0	-	-	0.0	-	0.0	-	-	0.0	-	0.0	-	-	0.0
20	1.8	-	-	0.0	-	3.2	-	-	0.0	-	2.2	-	-	0.0	-
21	-	-	0.0	-	-	-	-	0.0	-	-	-	-	0.0	-	-
22	-	0.1	-	-	0.0	-	0.1	-	-	0.0	-	0.1	-	-	0.0
23	1.8	-	-	0.0	-	4.3	-	-	0.0	-	2.8	-	-	0.0	-
24	-	-	0.0	-	-	-	-	0.0	-	-	-	-	0.0	-	-
25	-	0.8	-	-	0.0	-	0.2	-	-	0.0	-	0.3	-	-	0.0
26	1.3	-	-	0.0	-	2.8	-	-	0.0	-	1.8	-	-	0.0	-
27	-	-	0.0	-	-	-	-	0.0	-	-	-	-	0.0	-	-
28	-	0.8	-	-	0.0	-	0.4	-	-	0.0	-	0.8	-	-	0.0
29	1.2	-	-	0.0	-	4.3	-	-	0.0	-	2.0	-	-	0.0	-
30	-	-	0.0	-	-	-	-	0.0	-	-	-	-	0.0	-	-
31	-	0.4	-	-	0.0	-	0.2	-	-	0.0	-	0.3	-	-	0.0
32	1.7	-	-	0.0	-	3.8	-	-	0.0	-	2.4	-	-	0.0	-
33	-	-	0.0	-	-	-	-	0.0	-	-	-	-	0.0	-	-
34	-	0.7	-	-	0.0	-	0.4	-	-	0.0	-	0.8	-	-	0.0
35	2.3	-	-	0.0	-	4.1	-	-	0.0	-	2.8	-	-	0.0	-
36	-	-	0.0	-	-	-	-	0.0	-	-	-	-	0.0	-	-
37	-	0.8	-	-	0.0	-	0.8	-	-	0.0	-	0.7	-	-	0.0
38	2.7	-	-	0.0	-	4.8	-	-	0.0	-	3.1	-	-	0.0	-
39	-	-	0.0	-	-	-	-	0.0	-	-	-	-	0.1	-	-
40	-	0.8	-	-	0.0	-	0.8	-	-	0.0	-	0.8	-	-	0.0
41	3.1	-	-	0.0	-	8.0	-	-	0.0	-	3.4	-	-	0.0	-
42	-	-	0.0	-	-	-	-	0.0	-	-	-	-	0.0	-	-
43	-	0.8	-	-	0.0	-	0.4	-	-	0.0	-	0.8	-	-	0.0
44	2.8	-	-	0.0	-	8.2	-	-	0.0	-	2.8	-	-	0.0	-
45	-	-	0.0	-	-	-	-	0.0	-	-	-	-	0.0	-	-
46	-	0.8	-	-	0.0	-	0.8	-	-	0.0	-	0.8	-	-	0.0
47	3.4	-	-	0.0	-	8.0	-	-	0.0	-	3.1	-	-	0.0	-
48	-	-	0.0	-	0.0	-	-	0.0	-	0.0	-	-	0.0	-	0.0
49	-	0.8	-	-	0.0	-	0.8	-	-	0.0	-	0.7	-	-	0.0
50	3.7	-	-	0.0	-	8.7	-	-	0.0	-	3.3	-	-	0.0	-
51	-	1.1	-	-	-	-	0.8	-	-	-	-	1.0	-	-	-
52	4.3	-	-	-	-	8.2	-	-	-	-	3.8	-	-	-	-

Table 10 Lead:ate pH values of the Sunders fly ash leached with 0.005 M sulfuric acid

Inc #	Rep 1					Rep 2					Rep 3				
	Column	Number	1	2	3	Column	Number	1	2	3	Column	Number	1	2	3
1	12.30	12.40	12.38			12.30	12.40	12.30			12.30	12.30	12.30		
2	11.80	12.30	12.30	12.28	12.30	11.85	12.30	12.28	12.30	12.30	11.80	12.25	12.25	12.25	12.25
3	10.45	12.00	12.30	12.25	12.25	10.50	12.00	12.30	12.30	12.15	10.40	11.95	12.30	12.30	12.15
4	10.15	11.50	12.25	12.20	12.20	10.05	11.40	12.30	12.25	12.15	10.25	11.40	12.25	12.25	12.15
5	10.30	10.85	12.15	12.20	12.15	10.10	10.90	12.05	12.20	12.30	10.10	10.70	12.00	12.20	12.20
6	9.85	10.50	11.75	12.15	12.15	9.80	10.55	11.60	12.20	12.20	9.70	10.25	11.45	12.15	12.25
7	9.80	10.25	11.05	12.05	12.25	9.85	10.30	11.00	12.20	12.25	9.05	10.05	10.80	12.05	12.20
8	9.85	10.10	10.70	12.10	12.05	9.05	10.15	10.45	12.25	12.10	7.75	10.15	10.15	12.10	12.15
9	9.45	9.80	10.85	12.00	12.10	7.45	10.05	10.35	11.70	12.30	5.10	10.00	10.15	11.85	12.30
10	9.20	9.95	10.30	11.60	12.35	4.85	10.05	10.40	11.50	12.20	4.85	10.15	10.20	11.80	12.45
11	9.00	9.85	10.50	11.20	12.10	3.80	9.80	10.90	11.25	12.00	4.50	10.00	10.60	11.15	12.20
12	8.15	10.30	10.85	10.40	12.20	3.45	10.15	10.70	10.25	12.15	4.40	10.25	10.65	10.50	11.70
13	7.30	10.35	10.10	9.85	12.00	3.25	10.20	10.00	9.80	12.00	4.45	10.25	10.35	9.75	11.85
14	6.40	9.40	9.85	10.55	11.15	3.20	9.20	9.80	10.45	11.60	4.50	10.00	9.80	10.55	10.60
15	4.80	9.40	10.30	9.30	9.25	3.25	9.30	10.30	9.30	10.15	4.00	9.45	10.25	9.20	9.40
16	4.80	9.35	9.50	9.15	8.85	3.10	9.00	9.20	9.10	8.75	3.70	9.05	9.35	9.10	8.50
17	4.30	9.20	9.30	8.85	8.85	3.15	9.15	9.25	9.05	9.10	3.75	9.15	9.15	8.80	8.80
18	4.20	8.05	9.10	9.25	9.00	3.05	9.05	9.00	9.15	9.50	4.20	8.00	8.80	9.10	9.10
19	4.15	8.80	9.25	8.40	8.85	2.85	8.80	9.20	9.55	9.10	4.20	8.85	9.00	9.10	8.50
20	4.15	8.85	9.30	8.85	8.80	2.80	8.90	9.25	9.00	8.90	3.80	9.10	9.25	8.80	8.55
21	4.15	9.05	9.10	8.80	8.70	2.85	9.10	9.05	8.95	8.80	3.80	9.20	9.00	8.80	8.70
22	4.20	8.75	9.05	8.95	8.85	2.90	8.85	8.95	8.95	9.30	3.80	8.70	8.75	8.85	8.95
23	4.05	8.75	9.10	9.25	8.75	2.85	8.85	9.10	9.15	9.30	3.80	8.80	8.80	9.10	8.70
24	4.10	8.85	9.25	9.20	8.85	2.80	8.85	9.40	9.10	9.30	3.25	8.80	9.10	9.05	8.80
25	4.10	8.85	9.15	9.15	9.00	2.70	8.85	9.10	9.10	9.25	3.20	8.75	9.05	9.05	9.00
26	4.25	8.70	9.20	9.30	8.45	2.80	8.85	9.20	9.10	9.00	3.85	8.70	9.05	9.20	8.60
27	4.10	8.80	9.20	8.85	8.80	2.75	8.85	8.90	8.85	9.00	3.80	8.70	9.10	8.85	8.85
28	4.15	8.85	8.90	9.00	8.80	2.85	8.75	8.85	8.95	9.25	3.45	8.85	9.00	8.95	8.80
29	4.20	8.40	9.10	9.10	9.00	2.85	8.20	9.15	9.00	9.50	3.80	8.80	8.90	9.10	9.10
30	4.15	8.50	9.10	9.35	8.70	2.85	8.60	9.10	9.20	9.00	3.45	8.85	9.05	9.15	8.70
31	4.20	8.70	9.05	8.80	8.70	2.80	8.85	9.10	8.85	9.00	3.25	8.70	9.10	8.90	8.60
32	4.05	8.85	8.90	8.95	8.95	2.75	8.85	8.90	8.85	9.30	3.25	8.75	8.85	8.85	8.80
33	4.15	8.40	8.95	9.10	8.85	2.95	8.45	9.00	9.20	9.15	3.40	9.05	8.75	8.15	8.75
34	3.85	8.45	9.10	9.05	8.85	2.80	8.25	9.20	9.05	8.95	3.20	8.50	9.05	8.95	8.80
35	3.80	8.80	9.05	8.95	8.90	2.75	8.50	9.00	9.00	9.15	3.05	8.50	9.00	8.90	8.70
36	3.85	8.40	8.85	8.95	8.80	2.80	8.25	8.85	9.05	9.40	3.15	8.50	8.75	9.00	8.70
37	3.70	8.20	9.00	8.95	8.75	2.80	8.15	8.95	9.10	9.10	3.10	8.45	8.90	8.85	8.50
38	3.60	8.20	8.90	8.85	8.80	2.80	7.85	9.00	8.85	9.25	3.00	8.55	8.70	8.80	8.65
39	3.80	8.00	8.80	8.80	9.00	2.75	7.80	8.90	9.00	9.45	2.85	8.45	8.75	8.90	8.65
40	3.60	7.70	8.90	9.15	8.70	2.80	7.60	8.90	9.15	8.90	3.00	8.05	8.90	9.05	8.40
41	3.85	7.75	9.05	8.80	8.80	2.75	7.60	9.10	8.70	8.90	2.85	7.00	8.95	8.70	8.50
42	3.80	7.85	8.85	8.80	9.00	2.85	7.80	8.85	8.70	9.30	2.90	7.50	8.80	8.80	8.85
43	3.85	7.85	8.70	9.15	8.85	2.80	7.65	8.70	9.15	9.00	2.95	7.45	8.85	9.10	8.85
44	3.70	7.80	9.00	8.80	8.80	2.85	7.50	9.05	8.80	9.20	2.80	7.00	9.00	8.70	8.70
45	3.45	7.70	8.85	9.00	8.80	2.80	7.40	8.85	8.85	9.10	2.80	6.20	8.80	8.85	8.75
46	3.40	7.50	8.75	8.95	8.80	2.80	8.75	9.00	9.05	9.10	2.70	6.00	8.80	8.85	8.70
47	3.45	8.75	8.80	8.80	8.80	2.80	8.65	8.90	8.95	9.10	2.95	4.85	8.80	8.85	8.85
48	3.30	8.15	8.85	8.80	8.80	2.80	8.30	8.85	8.80	9.05	2.80	4.50	8.75	8.80	8.80
49	3.30	4.55	8.85	8.95		2.85	4.45	8.75	8.90		2.85	4.20	8.80	8.85	
50	3.20	4.25	8.85			2.75	4.20	8.80			2.85	4.25	8.70		
51	3.25	4.40				2.75	4.40				2.80	4.25			
52	3.20					2.80					2.85				

Table II. Concentration of Co (ug/mL) in the leachates of the Sundnes fly ash leached with 0.005 M sulfuric acid

Inc. #	Rep. Number 1		Rep. Number 2		Rep. Number 3		Rep. Number 4		Rep. Number 5	
	1	2	1	2	1	2	1	2	1	2
1	800	1000	850	1000	820	800	800	800	800	820
2	280	400	270	720	370	800	300	720	300	800
3	350	400	310	500	400	600	300	450	300	500
4	200	310	200	300	200	300	200	300	200	300
5	200	310	200	300	200	300	200	300	200	300
6	200	310	200	300	200	300	200	300	200	300
7	200	310	200	300	200	300	200	300	200	300
8	200	310	200	300	200	300	200	300	200	300
9	200	310	200	300	200	300	200	300	200	300
10	200	310	200	300	200	300	200	300	200	300
11	270	300	200	300	200	300	200	300	200	300
12	320	320	300	300	300	300	300	300	300	300
13	320	320	300	300	300	300	300	300	300	300
14	320	320	300	300	300	300	300	300	300	300
15	320	320	300	300	300	300	300	300	300	300
16	180	200	180	200	180	200	180	200	180	200
17	180	200	180	200	180	200	180	200	180	200
18	31	310	32	300	300	300	41	330	300	300
19	3	200	14	200	200	200	7	200	200	160
20	3	200	14	200	200	200	7	200	200	160
21	3	200	14	200	200	200	7	200	200	160
22	3	200	14	200	200	200	7	200	200	160
23	3	200	14	200	200	200	7	200	200	160
24	3	200	14	200	200	200	7	200	200	160
25	3	200	14	200	200	200	7	200	200	160
26	3	200	14	200	200	200	7	200	200	160
27	3	200	14	200	200	200	7	200	200	160
28	3	200	14	200	200	200	7	200	200	160
29	3	200	14	200	200	200	7	200	200	160
30	3	200	14	200	200	200	7	200	200	160
31	3	200	14	200	200	200	7	200	200	160
32	3	200	14	200	200	200	7	200	200	160
33	3	200	14	200	200	200	7	200	200	160
34	3	200	14	200	200	200	7	200	200	160
35	3	200	14	200	200	200	7	200	200	160
36	3	200	14	200	200	200	7	200	200	160
37	3	200	14	200	200	200	7	200	200	160
38	3	200	14	200	200	200	7	200	200	160
39	3	200	14	200	200	200	7	200	200	160
40	3	200	14	200	200	200	7	200	200	160
41	3	200	14	200	200	200	7	200	200	160
42	3	200	14	200	200	200	7	200	200	160
43	3	200	14	200	200	200	7	200	200	160
44	3	200	14	200	200	200	7	200	200	160
45	3	200	14	200	200	200	7	200	200	160
46	3	200	14	200	200	200	7	200	200	160
47	3	200	14	200	200	200	7	200	200	160
48	3	200	14	200	200	200	7	200	200	160
49	3	200	14	200	200	200	7	200	200	160
50	3	200	14	200	200	200	7	200	200	160
51	3	200	14	200	200	200	7	200	200	160
52	3	200	14	200	200	200	7	200	200	160
53	3	200	14	200	200	200	7	200	200	160

Table 12 Concentration of Na (ug/ML) in the leeches of the Sumneria fly ash leached with 0.005 N sulfuric acid

Inc #	Rep 1					Rep 2					Rep 3							
	Column	Number	1	2	3	Column	Number	1	2	3	Column	Number	1	2	3			
1	25	00	220	-	-	40	110	240	-	-	30	00	220	-	-			
2	7	2	14	37	100	7	0	15	20	230	400	7	0	14	20	220	400	
3	6	6	10	14	22	160	6	0	10	13	21	140	6	0	11	14	23	160
4	0	0	11	12	18	20	0	0	11	12	14	40	10	12	14	18	20	40
5	10	11	14	18	10	-	10	11	12	17	23	10	12	18	21	22	-	10
6	12	11	17	10	21	-	10	11	14	16	21	11	11	16	10	23	-	10
7	10	13	18	21	23	-	10	12	13	17	20	10	13	14	21	26	-	10
8	12	12	18	20	-	-	11	11	12	16	-	11	12	18	20	-	-	11
9	11	14	14	-	-	-	10	12	12	-	-	11	13	14	-	-	-	10
10	12	12	-	-	23	-	10	12	-	-	21	11	12	-	-	-	-	10
11	11	-	-	17	-	-	10	-	-	18	-	10	-	-	18	-	-	10
12	-	-	14	-	-	-	-	-	12	-	-	-	-	13	-	-	-	-
13	-	12	-	-	21	-	0	3	11	-	-	10	12	-	-	-	-	10
14	11	-	-	18	-	-	-	-	-	14	-	10	-	-	18	-	-	10
15	-	-	12	-	-	-	-	-	12	-	-	-	-	13	-	-	-	-
16	-	14	-	-	22	-	-	11	-	-	18	-	13	-	-	-	-	11
17	12	-	-	18	-	-	10	-	-	16	-	12	-	16	-	-	-	10
18	-	-	16	-	-	-	-	-	14	-	-	-	-	16	-	-	-	-
19	-	15	-	-	21	-	-	-	12	-	-	-	-	16	-	-	-	-
20	12	-	-	10	-	-	0	2	-	-	16	-	-	-	16	-	-	0
21	-	-	17	-	-	-	-	-	14	-	-	-	-	18	-	-	-	-
22	-	14	-	-	23	-	-	-	12	-	-	20	-	14	-	-	-	-
23	12	-	-	10	-	-	6	7	-	-	18	-	11	-	16	-	-	6
24	-	-	17	-	-	-	-	-	16	-	-	-	-	17	-	-	-	-
25	-	14	-	-	20	-	-	-	12	-	-	-	14	-	-	-	-	-
26	12	-	-	16	-	-	0	0	-	-	14	-	11	-	18	-	-	0
27	-	-	18	-	-	-	-	-	13	-	-	-	-	14	-	-	-	-
28	-	12	-	-	18	-	-	-	11	-	-	20	-	12	-	-	-	-
29	10	-	-	10	-	-	7	3	-	-	17	-	0	4	-	-	-	7
30	-	-	17	-	-	-	-	-	16	-	-	-	-	18	-	-	-	-
31	-	16	-	-	19	-	-	-	13	-	-	17	-	16	-	-	-	-
32	12	-	-	18	-	-	0	4	-	-	18	-	11	-	16	-	-	0
33	-	-	14	-	-	-	-	-	12	-	-	-	-	12	-	-	-	-
34	-	12	-	-	23	-	-	-	12	-	-	20	-	12	-	-	-	-
35	11	-	-	10	-	-	0	0	-	-	10	-	10	-	20	-	-	0
36	-	-	17	-	-	-	-	-	16	-	-	-	-	17	-	-	-	-
37	-	14	-	-	22	-	-	-	13	-	-	21	-	14	-	-	-	-
38	12	-	-	10	-	-	0	0	-	-	18	-	10	-	19	-	-	0
39	-	-	18	-	-	-	-	-	16	-	-	-	-	11	-	-	-	-
40	-	14	-	-	21	-	-	-	13	-	-	21	-	14	-	-	-	-
41	12	-	-	10	-	-	6	7	-	-	18	-	0	6	-	-	-	6
42	-	-	18	-	-	-	-	-	10	-	-	-	-	16	-	-	-	-
43	-	12	-	-	22	-	-	-	13	-	-	21	-	12	-	-	-	-
44	12	-	-	18	-	-	0	1	-	-	18	-	0	4	-	-	-	0
45	-	-	17	-	-	-	-	-	16	-	-	-	-	18	-	-	-	-
46	-	14	-	-	21	-	-	-	14	-	-	20	-	12	-	-	-	-
47	11	-	-	18	-	-	0	4	-	-	17	-	0	8	-	-	-	0
48	-	-	18	-	21	-	-	-	16	-	-	20	-	18	-	-	-	-
49	-	12	-	17	-	-	-	-	12	-	-	18	-	12	-	-	-	-
50	11	-	-	18	-	-	0	7	-	-	16	-	7	6	-	-	-	0
51	-	12	-	-	-	-	-	-	13	-	-	-	-	18	-	-	-	-
52	11	-	-	-	-	-	0	8	-	-	-	-	7	7	-	-	-	0

Table 13 Concentration of K (ug/ml) in the leachates of the Sundance Fly ash leached with 0.005 M sulfuric acid

Inc #	Rep 1					Rep 2					Rep 3				
	Column	Number	1	2	3	1	2	3	4	5	1	2	3	4	5
1	0.8	0.8	1.8	-	-	0.8	0.8	2.0	-	-	0.4	1.0	2.8	-	-
2	0.4	0.4	0.7	2.1	4.0	0.4	0.4	0.8	3.0	4.8	0.4	0.4	0.7	2.8	4.7
3	0.7	0.7	0.8	0.8	2.1	0.8	0.8	0.8	0.8	1.8	0.8	0.8	0.8	0.8	2.0
4	1.1	1.1	0.8	0.8	0.8	0.8	0.8	0.7	0.7	0.7	0.8	0.8	0.8	0.8	0.8
5	1.1	1.0	1.0	1.1	1.2	1.0	1.0	1.0	1.2	1.0	1.1	1.0	1.0	1.0	1.0
6	1.1	1.2	1.2	1.3	1.8	1.0	1.0	1.1	1.8	1.2	1.0	1.1	1.2	1.2	1.1
7	1.1	1.1	1.2	1.3	-	1.1	1.2	1.3	1.8	-	1.1	1.2	1.3	1.2	-
8	1.2	1.4	1.3	-	1.8	1.1	1.3	1.2	-	1.8	1.1	1.3	1.2	-	1.3
9	1.3	1.3	-	1.4	-	1.3	1.1	-	1.7	-	1.3	1.2	-	1.3	-
10	1.2	-	1.3	-	-	1.1	-	1.2	-	-	1.2	-	1.2	-	-
11	1.2	-	-	1.3	1.8	1.1	-	-	1.2	1.4	1.2	-	-	1.2	1.2
12	1.2	-	1.3	-	-	1.1	-	-	1.2	-	1.2	-	-	1.2	-
13	1.2	-	1.3	-	-	1.1	-	-	1.2	-	1.2	-	-	1.2	-
14	-	-	1.3	-	-	-	-	1.1	-	-	-	-	1.2	-	-
15	-	1.3	-	-	2.1	-	1.1	-	-	1.8	-	1.2	-	-	1.2
16	1.4	-	-	1.8	-	1.1	-	-	1.6	-	1.3	-	-	1.4	-
17	-	1.8	-	1.8	-	-	-	1.4	-	1.8	-	-	1.3	-	-
18	1.8	-	-	-	1.8	1.2	-	-	1.7	-	1.4	-	-	1.8	-
19	1.8	-	-	1.8	-	-	-	1.8	-	-	1.4	-	-	1.8	-
20	-	1.8	-	-	2.3	-	1.4	-	1.8	-	-	1.8	-	1.7	-
21	-	1.8	-	-	1.8	1.3	-	-	1.7	-	1.8	-	-	1.8	-
22	1.7	-	-	1.8	-	-	-	1.8	-	-	-	-	1.8	-	-
23	-	-	1.8	-	-	-	-	1.8	-	-	-	-	1.8	-	-
24	-	2.2	-	-	2.1	-	1.7	-	-	1.7	-	1.4	-	-	1.7
25	1.8	-	-	1.7	-	1.2	-	-	1.8	-	1.3	-	-	1.8	-
26	-	-	1.8	-	-	-	-	1.3	-	-	-	-	1.8	-	-
27	-	1.8	-	-	2.1	-	1.3	-	-	1.8	-	1.8	-	-	1.7
28	1.4	-	-	1.7	-	0.8	-	-	1.7	-	1.2	-	-	1.7	-
29	-	-	1.7	-	-	-	-	1.8	-	-	-	-	1.8	-	-
30	-	1.8	-	-	2.1	-	1.4	-	-	1.8	-	1.8	-	-	1.8
31	1.4	-	-	1.8	2.2	1.0	-	-	1.8	1.4	1.3	-	-	1.8	1.8
32	-	-	1.8	1.8	1.8	-	-	1.8	1.8	-	-	-	1.7	2.0	-
33	-	1.8	1.8	-	-	1.1	1.8	-	-	1.8	1.3	1.8	-	-	1.8
34	1.8	-	-	-	2.3	1.1	1.8	-	-	1.8	1.3	1.8	-	-	1.8
35	1.8	-	-	1.8	-	1.3	-	-	2.0	-	1.4	-	-	1.7	-
36	-	-	1.8	-	-	-	-	1.7	-	-	-	-	1.7	-	-
37	-	1.8	-	-	2.0	-	1.8	-	-	1.8	-	1.8	-	-	1.8
38	1.7	-	-	1.7	-	1.2	-	-	1.7	-	1.4	-	-	1.7	-
39	-	-	1.7	-	-	-	-	1.8	-	-	-	-	1.8	-	-
40	-	1.8	-	-	2.4	-	1.4	-	-	2.4	-	1.2	-	-	2.2
41	1.4	-	-	2.0	-	1.0	-	-	2.2	-	1.1	-	-	2.0	-
42	-	-	1.7	-	-	-	-	1.8	-	-	-	-	1.8	-	-
43	-	2.1	-	-	2.4	-	1.8	-	-	2.4	-	1.8	-	-	2.3
44	1.8	-	-	2.2	-	1.3	-	-	2.3	-	1.3	-	-	2.1	-
45	-	-	2.1	-	-	-	-	2.2	-	-	-	-	2.1	-	-
46	-	2.0	-	-	2.8	-	1.8	-	-	2.8	-	1.8	-	-	2.8
47	1.7	-	-	2.2	-	1.4	-	-	2.4	-	1.3	-	-	2.3	-
48	-	-	2.1	-	2.8	-	-	2.2	-	2.8	-	-	2.1	-	2.4
49	-	2.0	-	2.2	-	-	1.8	-	2.2	-	-	1.8	-	2.1	-
50	1.8	-	2.0	-	-	1.3	-	2.1	-	-	1.2	-	2.0	-	-
51	-	1.8	-	-	-	-	1.8	-	-	-	-	1.7	-	-	-
52	1.8	-	-	-	-	1.3	-	-	-	-	1.1	-	-	-	-

Table 14 Concentration of Mg (ug/ml) in the leachates of the Sundance fly ash leached with 0.005 M sulfuric acid

Inc #	Rep 1 Column Number					Rep 2 Column Number					Rep 3 Column Number				
	1	2	3	4	5	1	2	3	4	5	1	2	3	4	5
1	0.0	0.0	0.0	-	-	0.0	0.0	0.0	-	-	0.0	0.0	0.0	-	-
2	0.1	0.0	0.0	0.0	0.0	0.1	0.0	0.0	0.0	0.0	0.1	0.0	0.0	0.0	0.0
3	0.3	0.0	0.0	0.0	0.0	0.3	0.0	0.0	0.0	0.0	0.4	0.0	0.0	0.0	0.0
4	0.4	0.1	0.0	0.0	0.0	0.5	0.1	0.0	0.0	0.0	1.0	0.1	0.0	0.0	0.0
5	0.6	0.1	0.0	0.0	0.0	1.3	0.1	0.0	0.0	0.0	2.1	0.1	0.0	0.0	0.0
6	1.0	0.1	0.0	0.0	0.0	3.3	0.1	0.0	0.0	0.0	3.3	0.2	0.0	0.0	0.0
7	1.5	0.3	0.1	0.0	0.0	4.4	0.2	0.1	0.0	0.0	3.6	0.2	0.1	0.0	0.0
8	2.8	0.5	0.1	0.0	0.0	4.4	0.3	0.2	0.0	0.0	4.3	0.2	0.2	0.0	0.0
9	3.9	0.5	0.1	-	-	5.1	0.5	0.2	-	-	4.5	0.2	0.2	-	-
10	5.5	1.2	-	-	0.0	5.1	0.7	-	-	0.0	4.9	0.2	-	-	0.0
11	5.7	-	-	0.1	-	5.1	-	0.1	-	-	4.8	-	-	0.1	-
12	-	0.1	-	-	-	-	0.1	-	-	-	-	0.1	-	-	-
13	-	0.3	-	-	0.0	-	0.7	-	-	0.0	-	0.3	-	-	0.0
14	5.0	-	0.1	-	-	5.4	-	0.1	-	-	5.1	-	-	0.1	-
15	-	0.2	-	-	-	-	0.1	-	-	-	-	0.2	-	-	-
16	-	0.6	-	-	0.1	-	0.8	-	-	0.0	-	0.4	-	-	0.0
17	7.0	-	-	1.5	-	5.5	-	-	0.1	-	5.3	-	-	0.2	-
18	-	0.2	-	-	-	-	0.3	-	-	-	-	0.5	-	-	-
19	2.5	-	-	-	0.1	5.2	2.5	-	-	0.1	5.0	0.7	-	-	0.1
20	6.0	-	-	0.1	-	5.2	-	-	0.1	-	5.0	-	-	0.1	-
21	-	0.2	-	-	-	-	0.2	-	-	-	-	0.2	-	-	-
22	-	1.8	-	-	0.1	-	2.0	-	-	0.1	-	1.1	-	-	0.1
23	5.1	-	-	0.1	-	4.8	-	-	0.2	-	5.5	-	-	0.1	-
24	-	0.2	-	-	-	-	0.2	-	-	-	-	0.3	-	-	-
25	-	1.1	-	-	0.1	-	1.3	-	-	0.1	-	1.0	-	-	0.1
26	2.7	-	-	0.1	-	2.4	-	-	0.1	-	2.8	-	-	0.1	-
27	-	0.2	-	-	-	-	0.2	-	-	-	-	0.3	-	-	-
28	-	1.5	-	-	0.1	-	1.8	-	-	0.1	-	1.5	-	-	0.1
29	2.5	-	-	0.1	-	2.3	-	-	0.1	-	2.7	-	-	0.1	-
30	-	0.3	-	-	-	-	0.2	-	-	-	-	0.5	-	-	-
31	-	2.1	-	-	0.1	-	2.7	-	-	0.1	-	2.7	-	-	0.1
32	2.5	-	-	0.2	-	2.3	-	-	0.1	-	2.5	-	-	0.1	-
33	-	0.5	-	-	-	-	0.2	-	-	-	-	1.2	-	-	-
34	-	3.3	-	-	0.1	-	3.5	-	-	0.1	-	3.8	-	-	0.2
35	1.3	-	-	0.2	-	2.4	-	-	0.1	-	2.5	-	-	0.1	-
36	-	0.5	-	-	-	-	0.3	-	-	-	-	1.3	-	-	-
37	-	4.5	-	-	0.1	-	4.5	-	-	0.1	-	5.0	-	-	0.1
38	1.3	-	-	0.2	-	1.3	-	-	0.1	-	1.4	-	-	0.1	-
39	-	0.5	-	-	-	-	0.3	-	-	-	-	1.3	-	-	-
40	-	5.4	-	-	0.1	-	5.4	-	-	0.1	-	5.9	-	-	0.1
41	2.5	-	-	0.1	-	2.1	-	-	0.1	-	2.2	-	-	0.1	-
42	-	0.4	-	-	-	-	0.4	-	-	-	-	1.1	-	-	-
43	-	5.5	-	-	0.1	-	5.5	-	-	0.1	-	5.0	-	-	0.1
44	1.0	-	-	0.2	-	1.1	-	-	0.1	-	1.0	-	-	0.1	-
45	-	0.5	-	-	-	-	0.5	-	-	-	-	1.0	-	-	-
46	-	5.5	-	-	0.1	-	5.5	-	-	0.1	-	5.7	-	-	0.2
47	1.0	-	-	0.2	-	1.0	-	-	0.2	-	1.0	-	-	0.2	-
48	-	0.7	-	-	0.1	-	0.6	-	-	0.1	-	1.1	-	-	0.2
49	-	5.1	-	-	0.2	-	5.2	-	-	0.2	-	5.1	-	-	0.2
50	1.0	-	-	-	-	1.0	-	-	-	-	1.0	-	-	1.2	-
51	-	4.7	-	-	-	-	4.8	-	-	-	-	4.8	-	-	-
52	1.1	-	-	-	-	1.1	-	-	-	-	1.0	-	-	-	-

Table 15 Concentration of Fe (ug/ml) in the leachates of the Sundance fly ash leached with 0.005 M sulfuric acid.

Inc. #	Rep. 1					Rep. 2					Rep. 3				
	Column	Number	1	2	3	Column	Number	1	2	3	Column	Number	1	2	3
1	0.1	0.1	0.2	-	-	0.1	0.1	0.1	-	-	0.1	0.1	0.1	-	-
2	0.1	0.1	0.0	0.1	0.0	0.1	0.1	0.0	0.1	0.0	0.1	0.1	0.0	0.1	0.0
3	0.1	0.0	0.1	0.0	0.0	0.1	0.0	0.1	0.0	0.0	0.1	0.0	0.1	0.0	0.0
4	0.0	0.0	0.0	0.0	0.0	0.0	0.0	0.0	0.0	0.0	0.0	0.0	0.0	0.0	0.0
5	0.0	0.0	0.0	0.0	0.1	0.1	0.0	0.0	0.0	0.1	0.0	0.0	0.0	0.0	0.1
6	0.0	0.0	0.0	0.1	0.0	0.0	0.0	0.0	0.1	0.0	0.0	0.0	0.0	0.1	0.0
7	0.0	0.0	0.1	0.0	0.0	0.0	0.0	0.0	0.0	0.0	0.0	0.0	0.1	0.0	0.0
8	0.0	0.1	0.0	0.0	-	0.0	0.0	0.0	0.0	0.0	0.0	0.1	0.0	0.0	-
9	0.0	0.0	0.0	-	-	0.1	0.0	0.0	-	-	0.2	0.0	0.0	-	-
10	0.0	0.0	-	-	0.0	0.5	0.0	-	-	0.0	0.4	0.0	-	-	0.0
11	0.0	-	-	0.0	-	1.3	-	-	0.0	-	0.8	-	-	0.0	-
12	-	-	0.0	-	-	-	-	0.0	-	-	-	-	0.1	-	-
13	-	0.0	-	-	0.0	-	0.0	-	-	0.0	-	0.0	-	-	0.0
14	0.2	-	-	0.0	-	1.9	-	-	0.0	-	0.7	-	-	0.0	-
15	-	-	0.0	-	-	-	-	0.0	-	-	-	-	0.0	-	-
16	-	0.0	-	-	0.0	-	0.0	-	-	0.0	-	0.0	-	-	0.0
17	0.2	-	-	0.0	-	1.4	-	-	0.0	-	0.8	-	-	0.0	-
18	-	-	0.0	-	-	-	-	0.0	-	-	-	-	0.0	-	-
19	-	0.0	-	-	0.0	-	0.0	-	-	0.0	-	0.0	-	-	0.0
20	0.5	-	-	0.0	-	2.5	-	-	0.0	-	1.5	-	-	0.0	-
21	-	-	0.0	-	-	-	-	0.0	-	-	-	-	0.0	-	-
22	-	0.0	-	-	0.0	-	0.0	-	-	0.0	-	0.0	-	-	0.0
23	0.6	-	-	0.0	-	1.5	-	-	0.0	-	1.3	-	-	0.0	-
24	-	-	0.0	-	-	-	-	0.0	-	-	-	-	0.0	-	-
25	0.0	0.0	-	-	0.0	-	0.0	-	-	0.0	-	0.0	-	-	0.0
26	0.8	-	-	0.0	-	1.2	-	-	0.0	-	0.8	-	-	0.0	-
27	-	-	0.0	-	-	-	-	0.0	-	-	-	-	0.0	-	-
28	-	0.0	-	-	0.0	-	0.0	-	-	0.0	-	0.0	-	-	0.0
29	0.4	-	-	0.0	-	1.0	-	-	0.0	-	0.9	-	-	0.0	-
30	-	-	0.0	-	-	-	-	0.0	-	-	-	-	0.0	-	-
31	-	0.0	-	-	0.0	-	0.0	-	-	0.0	-	0.0	-	-	0.0
32	0.6	-	-	0.0	-	0.8	-	-	0.0	-	1.6	-	-	0.0	-
33	-	-	0.0	-	-	-	-	0.0	-	-	-	-	0.0	-	-
34	-	0.0	-	-	0.0	-	0.0	-	-	0.0	-	0.0	-	-	0.0
35	1.4	-	-	0.0	-	1.1	-	-	0.0	-	2.4	-	-	0.0	-
36	-	-	0.0	-	-	-	-	0.0	-	-	-	-	0.0	-	-
37	-	0.0	-	-	0.0	-	0.0	-	-	0.0	-	0.0	-	-	0.0
38	1.7	-	-	0.0	-	1.1	-	-	0.0	-	2.2	-	-	0.0	-
39	-	-	0.0	-	-	-	-	0.0	-	-	-	-	0.0	-	-
40	-	0.0	-	-	0.0	-	0.0	-	-	0.0	-	0.0	-	-	0.0
41	1.7	-	-	0.0	-	1.2	-	-	0.0	-	2.4	-	-	0.0	-
42	-	-	0.0	-	-	-	-	0.0	-	-	-	-	0.0	-	-
43	-	0.0	-	-	0.0	-	0.0	-	-	0.0	-	0.0	-	-	0.0
44	0.9	-	-	0.0	-	0.9	-	-	0.0	-	1.7	-	-	0.0	-
45	-	-	0.0	-	-	-	-	0.0	-	-	-	-	0.0	-	-
46	-	0.0	-	-	0.0	-	0.0	-	-	0.0	-	0.0	-	-	0.0
47	1.4	-	-	0.0	-	1.1	-	-	0.0	-	1.8	-	-	0.0	-
48	-	-	0.0	-	-	-	-	0.0	-	-	-	-	0.0	-	0.0
49	-	0.1	-	-	0.0	-	0.1	-	-	0.0	-	0.1	-	-	0.0
50	1.5	-	-	0.0	-	1.1	-	-	0.0	-	1.9	-	-	0.0	-
51	-	0.2	-	-	-	-	0.2	-	-	-	-	0.2	-	-	-
52	2.1	-	-	-	-	1.3	-	-	-	-	2.0	-	-	-	-

Table 16 Concentration of Mn (ug/ml) in the leachates of the Sundance fly ash leached with 0.005 M sulfuric acid

Inc #	Rep 1					Rep 2					Rep 3						
	Column	Number	1	2	3	4	5	1	2	3	4	5	1	2	3	4	5
1	0.0	0.0	0.0	0.0	0.0	0.0	0.0	0.0	0.0	0.0	0.0	0.0	0.0	0.0	0.0	0.0	0.0
2	0.0	0.0	0.0	0.0	0.0	0.0	0.0	0.0	0.0	0.0	0.0	0.0	0.0	0.0	0.0	0.0	0.0
3	0.0	0.0	0.0	0.0	0.0	0.0	0.0	0.0	0.0	0.0	0.0	0.0	0.0	0.0	0.0	0.0	0.0
4	0.0	0.0	0.0	0.0	0.0	0.0	0.0	0.0	0.0	0.0	0.0	0.0	0.0	0.0	0.0	0.0	0.0
5	0.0	0.0	0.0	0.0	0.0	0.0	0.0	0.0	0.0	0.0	0.0	0.0	0.0	0.0	0.0	0.0	0.0
6	0.0	0.0	0.0	0.0	0.0	0.0	0.0	0.0	0.0	0.0	0.0	0.0	0.0	0.0	0.0	0.0	0.0
7	0.0	0.0	0.0	0.0	0.0	0.0	0.0	0.0	0.0	0.0	0.0	0.0	0.0	0.0	0.0	0.0	0.0
8	0.0	0.0	0.0	0.0	0.0	0.0	0.0	0.0	0.0	0.0	0.0	0.0	0.0	0.0	0.0	0.0	0.0
9	0.0	0.0	0.0	0.0	0.0	0.0	0.0	0.0	0.0	0.0	0.0	0.0	0.0	0.0	0.0	0.0	0.0
10	0.0	0.0	0.0	0.0	0.0	0.0	0.0	0.0	0.0	0.0	0.0	0.0	0.0	0.0	0.0	0.0	0.0
11	0.0	0.0	0.0	0.0	0.0	0.0	0.0	0.0	0.0	0.0	0.0	0.0	0.0	0.0	0.0	0.0	0.0
12	0.0	0.0	0.0	0.0	0.0	0.0	0.0	0.0	0.0	0.0	0.0	0.0	0.0	0.0	0.0	0.0	0.0
13	0.3	0.0	0.0	0.0	0.0	0.0	0.0	0.0	0.0	0.0	0.0	0.0	0.4	0.0	0.0	0.0	0.0
14	0.4	0.0	0.0	0.0	0.0	0.0	0.0	0.0	0.0	0.0	0.0	0.0	0.2	0.0	0.0	0.0	0.0
15	0.4	0.0	0.0	0.0	0.0	0.0	0.0	0.0	0.0	0.0	0.0	0.0	0.4	0.0	0.0	0.0	0.0
16	0.5	0.0	0.0	0.0	0.0	0.0	0.0	0.0	0.0	0.0	0.0	0.0	0.4	0.0	0.0	0.0	0.0
17	0.5	0.0	0.0	0.0	0.0	0.0	0.0	0.0	0.0	0.0	0.0	0.0	0.3	0.0	0.0	0.0	0.0
18	0.4	0.0	0.0	0.0	0.0	0.0	0.0	0.0	0.0	0.0	0.0	0.0	0.2	0.0	0.0	0.0	0.0
19	0.5	0.0	0.0	0.0	0.0	0.0	0.0	0.0	0.0	0.0	0.0	0.0	0.3	0.0	0.0	0.0	0.0
20	0.5	0.0	0.0	0.0	0.0	0.0	0.0	0.0	0.0	0.0	0.0	0.0	0.3	0.0	0.0	0.0	0.0
21	0.4	0.0	0.0	0.0	0.0	0.0	0.0	0.0	0.0	0.0	0.0	0.0	0.2	0.0	0.0	0.0	0.0
22	0.5	0.0	0.0	0.0	0.0	0.0	0.0	0.0	0.0	0.0	0.0	0.0	0.4	0.0	0.0	0.0	0.0
23	0.4	0.0	0.0	0.0	0.0	0.0	0.0	0.0	0.0	0.0	0.0	0.0	0.3	0.0	0.0	0.0	0.0
24	0.4	0.0	0.0	0.0	0.0	0.0	0.0	0.0	0.0	0.0	0.0	0.0	0.4	0.0	0.0	0.0	0.0
25	0.4	0.0	0.0	0.0	0.0	0.0	0.0	0.0	0.0	0.0	0.0	0.0	0.3	0.0	0.0	0.0	0.0
26	0.4	0.0	0.0	0.0	0.0	0.0	0.0	0.0	0.0	0.0	0.0	0.0	0.4	0.0	0.0	0.0	0.0
27	0.4	0.0	0.0	0.0	0.0	0.0	0.0	0.0	0.0	0.0	0.0	0.0	0.4	0.0	0.0	0.0	0.0
28	0.3	0.0	0.0	0.0	0.0	0.0	0.0	0.0	0.0	0.0	0.0	0.0	0.3	0.0	0.0	0.0	0.0
29	0.3	0.0	0.0	0.0	0.0	0.0	0.0	0.0	0.0	0.0	0.0	0.0	0.3	0.0	0.0	0.0	0.0
30	0.3	0.0	0.0	0.0	0.0	0.0	0.0	0.0	0.0	0.0	0.0	0.0	0.3	0.0	0.0	0.0	0.0
31	0.2	0.0	0.0	0.0	0.0	0.0	0.0	0.0	0.0	0.0	0.0	0.0	0.3	0.0	0.0	0.0	0.0
32	0.2	0.0	0.0	0.0	0.0	0.0	0.0	0.0	0.0	0.0	0.0	0.0	0.3	0.0	0.0	0.0	0.0
33	0.2	0.0	0.0	0.0	0.0	0.0	0.0	0.0	0.0	0.0	0.0	0.0	0.3	0.0	0.0	0.0	0.0
34	0.2	0.0	0.0	0.0	0.0	0.0	0.0	0.0	0.0	0.0	0.0	0.0	0.3	0.0	0.0	0.0	0.0
35	0.2	0.0	0.0	0.0	0.0	0.0	0.0	0.0	0.0	0.0	0.0	0.0	0.3	0.0	0.0	0.0	0.0
36	0.2	0.0	0.0	0.0	0.0	0.0	0.0	0.0	0.0	0.0	0.0	0.0	0.3	0.0	0.0	0.0	0.0
37	0.2	0.0	0.0	0.0	0.0	0.0	0.0	0.0	0.0	0.0	0.0	0.0	0.3	0.0	0.0	0.0	0.0
38	0.2	0.0	0.0	0.0	0.0	0.0	0.0	0.0	0.0	0.0	0.0	0.0	0.3	0.0	0.0	0.0	0.0
39	0.2	0.0	0.0	0.0	0.0	0.0	0.0	0.0	0.0	0.0	0.0	0.0	0.3	0.0	0.0	0.0	0.0
40	0.2	0.0	0.0	0.0	0.0	0.0	0.0	0.0	0.0	0.0	0.0	0.0	0.3	0.0	0.0	0.0	0.0
41	0.2	0.0	0.0	0.0	0.0	0.0	0.0	0.0	0.0	0.0	0.0	0.0	0.3	0.0	0.0	0.0	0.0
42	0.2	0.0	0.0	0.0	0.0	0.0	0.0	0.0	0.0	0.0	0.0	0.0	0.3	0.0	0.0	0.0	0.0
43	0.2	0.4	0.0	0.0	0.0	0.0	0.0	0.0	0.0	0.0	0.0	0.0	0.3	0.7	0.0	0.0	0.0
44	0.2	0.0	0.0	0.0	0.0	0.0	0.0	0.0	0.0	0.0	0.0	0.0	0.3	0.0	0.0	0.0	0.0
45	0.2	0.0	0.0	0.0	0.0	0.0	0.0	0.0	0.0	0.0	0.0	0.0	0.3	0.0	0.0	0.0	0.0
46	1.1	0.0	0.0	0.0	0.0	0.0	0.0	0.0	0.0	0.0	0.0	0.0	1.0	0.0	0.0	0.0	0.0
47	0.5	0.0	0.0	0.0	0.0	0.0	0.0	0.0	0.0	0.0	0.0	0.0	0.3	0.0	0.0	0.0	0.0
48	1.2	0.0	0.0	0.0	0.0	0.0	0.0	0.0	0.0	0.0	0.0	0.0	1.0	0.0	0.0	0.0	0.0
49	0.2	0.0	0.0	0.0	0.0	0.0	0.0	0.0	0.0	0.0	0.0	0.0	0.2	0.0	0.0	0.0	0.0
50	1.0	0.0	0.0	0.0	0.0	0.0	0.0	0.0	0.0	0.0	0.0	0.0	0.2	0.0	0.0	0.0	0.0
51	0.3	0.0	0.0	0.0	0.0	0.0	0.0	0.0	0.0	0.0	0.0	0.0	0.3	0.0	0.0	0.0	0.0
52	0.3	0.0	0.0	0.0	0.0	0.0	0.0	0.0	0.0	0.0	0.0	0.0	0.3	0.0	0.0	0.0	0.0

Table 19. Leachate pH values of the Forestburg fly ash leached with 4ASA solution.

Inc #	Rep 1 Column Number					Rep 2 Column Number					Rep 3 Column Number				
	1	2	3	4	5	1	2	3	4	5	1	2	3	4	5
1	11.70	11.80	12.15	-	-	11.50	11.85	12.05	-	-	11.75	12.00	12.05	-	-
2	9.85	11.00	11.80	11.70	11.85	10.25	11.15	11.45	11.30	12.00	10.00	11.00	11.45	11.75	12.10
3	7.30	10.85	10.85	11.05	11.10	8.80	10.85	10.90	11.00	11.25	8.85	10.80	10.70	11.00	11.20
4	5.35	10.10	10.35	11.05	11.10	5.80	10.20	10.35	11.05	10.85	5.75	10.10	10.30	11.10	11.20
5	5.20	9.80	10.40	10.90	10.80	5.05	9.85	10.35	10.80	10.85	5.25	9.90	10.50	10.85	10.85
6	4.85	9.85	10.35	10.35	10.85	4.85	10.05	10.40	10.70	10.85	5.00	9.90	10.40	10.40	10.70
7	4.90	9.75	10.10	10.25	10.80	4.85	9.90	10.15	10.45	10.85	4.90	9.75	10.15	10.30	10.85
8	4.80	9.80	10.05	10.20	10.05	4.85	9.80	10.10	10.40	10.15	4.90	9.75	10.10	10.40	10.15
9	4.75	9.85	10.15	9.85	10.10	4.75	9.80	10.20	9.85	10.10	4.90	9.85	10.25	10.05	10.15
10	4.75	9.80	9.80	10.00	9.85	4.75	9.80	9.75	10.10	10.00	4.75	9.40	9.90	10.05	9.85
11	4.70	9.15	9.85	9.75	9.80	4.80	9.25	9.85	9.85	10.05	4.75	9.10	9.85	9.75	9.85
12	4.85	9.20	9.70	9.85	9.80	4.85	9.85	9.80	9.85	9.90	4.80	9.30	9.80	9.80	9.85
13	4.85	9.85	9.85	9.75	9.90	4.80	7.20	9.70	9.85	10.05	4.80	7.20	9.70	9.70	9.80
14	4.80	9.85	9.80	9.80	9.85	4.85	9.90	9.90	10.00	9.85	4.85	9.20	9.90	9.85	9.85
15	4.85	9.80	9.75	9.80	9.85	4.80	9.85	9.75	9.90	9.80	4.85	9.80	9.75	9.90	9.80
16	4.80	9.40	9.70	9.85	9.85	4.80	9.35	9.85	9.85	9.70	4.85	9.35	9.85	9.70	9.80
17	4.85	9.30	9.80	9.75	9.85	4.80	9.25	9.45	9.80	9.70	4.85	9.25	9.80	9.85	9.70
18	4.80	9.25	9.85	9.70	9.85	4.80	9.15	9.40	9.70	9.80	4.85	9.15	9.45	9.70	9.85
19	4.85	9.15	9.85	9.85	9.80	4.85	9.10	9.40	9.80	9.70	4.85	9.10	9.45	9.70	9.80
20	4.80	9.15	9.85	9.80	9.85	4.80	9.10	9.40	9.85	9.75	4.80	9.05	9.30	9.85	9.80
21	4.80	9.00	9.85	9.80	9.80	4.85	9.15	9.35	9.80	9.80	4.80	9.05	9.25	9.80	9.85
22	4.45	9.00	9.70	9.75	9.80	4.85	9.05	9.35	10.00	9.15	4.80	4.85	9.25	9.80	9.00
23	4.45	9.00	9.85	9.75	9.80	4.85	4.85	9.35	9.05	9.05	4.80	9.05	9.25	9.00	9.25
24	4.80	9.00	9.10	9.25	9.25	4.85	4.85	9.35	9.05	9.10	4.80	4.85	9.25	9.20	9.00
25	4.40	4.85	9.85	9.05	9.80	4.85	9.00	9.85	9.10	9.80	4.40	4.85	9.80	9.05	9.70
26	4.35	4.95	9.90	9.80	9.85	4.45	9.00	9.90	9.75	9.85	4.40	4.85	9.85	9.80	9.85
27	4.45	9.00	9.20	9.85	9.80	4.80	9.05	9.10	9.85	9.80	4.80	9.00	9.80	9.70	9.85
28	4.80	9.10	9.30	9.45	9.80	4.85	9.20	9.80	9.80	9.80	4.80	9.15	9.05	9.80	9.85
29	4.35	9.00	9.80	9.40	9.85	4.85	9.05	7.90	9.30	9.85	4.85	4.85	7.40	9.50	9.70
30	4.30	4.90	7.90	9.85	9.80	4.80	9.00	7.40	9.70	9.80	4.45	4.90	7.20	9.70	9.70
31	4.30	4.90	9.00	9.85	9.80	4.40	9.20	7.20	9.85	9.80	4.40	4.85	9.85	9.85	9.80
32	4.30	4.90	9.25	9.85	9.85	4.85	9.00	7.00	9.50	9.70	4.80	4.85	9.50	9.45	9.85
33	4.40	4.85	9.15	9.45	9.40	4.80	4.85	9.80	9.85	9.45	4.80	4.85	9.30	9.50	9.45
34	4.40	4.90	9.85	9.40	9.45	4.85	4.85	9.40	9.40	9.80	4.80	4.85	9.30	9.45	9.45
35	4.35	4.85	9.75	9.30	-	4.80	9.00	9.15	9.40	-	4.45	4.85	9.80	9.30	-
36	4.35	4.85	9.85	-	-	4.80	4.80	9.25	-	-	4.80	4.75	9.85	-	-
37	4.30	4.90	-	-	-	4.80	4.80	-	-	-	4.35	4.85	-	-	-
38	4.40	-	-	-	-	4.80	-	-	-	-	4.40	-	-	-	-

Table 30. Concentration of Cs (ug/ml) in the leachates of the Forestburg fly ash leached with AASA solution

Inc. #	Rep. 1				Rep. 2				Rep. 3						
	1	2	3	4	1	2	3	4	1	2	3	4			
1	1300	1800	2000	1700	1800	1000	2600	1800	1400	2800	1700	2100	1400	1700	3000
2	780	1000	1100	1400	780	800	1400	800	800	2800	780	1100	800	1400	1400
3	880	880	830	1400	870	660	830	1300	1400	1400	800	810	800	1300	1100
4	280	780	860	1400	400	780	870	1300	1100	1100	420	780	880	880	1100
5	380	780	710	880	310	770	840	810	880	880	310	780	780	770	880
6	280	600	670	710	230	580	780	780	780	800	300	780	800	810	820
7	380	670	670	710	280	700	780	880	880	810	280	870	880	810	820
8	210	530	770	820	170	840	780	840	840	820	210	820	800	800	880
9	200	860	670	820	180	880	810	840	880	880	170	880	770	880	880
10	110	740	870	710	170	870	710	880	880	880	180	840	880	880	880
11	180	740	720	710	180	870	710	880	880	720	170	870	820	840	820
12	180	480	820	620	180	870	880	880	880	880	180	880	880	880	880
13	140	480	820	820	180	880	880	880	880	880	180	880	880	880	880
14	140	380	880	820	180	380	880	880	880	880	180	880	880	880	880
15	110	280	880	820	110	280	880	880	880	880	110	280	880	880	880
16	97	280	880	780	100	280	880	880	880	880	100	280	880	880	880
17	97	280	880	780	100	280	880	880	880	880	100	280	880	880	880
18	110	280	880	880	120	280	880	880	880	880	120	280	880	880	880
19	110	280	880	880	120	280	880	880	880	880	120	280	880	880	880
20	110	280	880	880	120	280	880	880	880	880	120	280	880	880	880
21	100	240	880	880	110	270	880	880	880	880	110	240	880	880	880
22	100	240	880	880	110	270	880	880	880	880	110	240	880	880	880
23	100	180	810	830	110	230	880	870	870	880	110	230	880	880	880
24	84	180	810	830	120	200	880	810	810	880	110	210	880	880	880
25	84	220	810	870	120	200	880	810	810	880	110	210	880	880	880
26	110	180	880	870	110	220	880	870	870	880	110	220	880	880	880
27	110	180	880	870	110	220	880	870	870	880	110	220	880	880	880
28	78	180	880	870	110	180	880	870	870	880	110	180	880	880	880
29	78	170	880	870	88	170	880	870	870	880	87	180	880	880	880
30	92	180	880	870	110	170	880	880	880	880	110	170	880	880	880
31	92	180	880	870	110	180	880	880	880	880	110	170	880	880	880
32	84	170	880	870	80	180	880	880	880	880	88	180	880	880	880
33	84	170	880	870	80	180	880	880	880	880	88	180	880	880	880
34	84	170	880	870	80	180	880	880	880	880	88	180	880	880	880
35	88	150	880	870	88	180	880	880	880	880	88	180	880	880	880
36	88	150	880	870	88	180	880	880	880	880	88	180	880	880	880
37	77	150	880	870	83	180	880	880	880	880	87	180	880	880	880
38	77	150	880	870	83	180	880	880	880	880	87	180	880	880	880

Table 21 Concentration of Ba (ug/mL) in the leachates of the Forestburg fly ash leached with AASA solution

Inc #	Rep 1					Rep 2					Rep 3				
	Column	Number	1	2	3	Column	Number	1	2	3	Column	Number	1	2	3
1	65	170	470			54	200	480			74	180	470		
2	3.8	18	52	320	770	4.8	17	34	320	680	4.0	18	52	280	700
3	4.7	5.0	9.2	52	160	5.1	8.0	0	54	180	5.3	5.8	9.2	50	180
4	4.6	5.2	7.1	8.4	28	4.6	5.5	3.9	10	28	4.6	5.7	7.1	10	28
5	4.6	7.4	8.0	7.7	11	4.2	5.2	3.0	7.7	12	5.5	5.9	6.4	8.2	11
6	5.8	4.8	5.8	7.1	9.4	3.8	4.2	3.2	6.5	9.3	5.7	5.7	6.4	7.4	10
7	4.2	5.2	5.1	5.4	8.8	4.5	5.3	3.5	5.1	8.7	4.6	5.8	6.4	7.7	8.3
8	4.1	5.0	5.2	7.5	7.8	3.8	5.5	5.8	7	7.5	4.7	5.7	5.2	7.7	8.3
9	2.4	5.5	5.2	5.9		4.0	5.2	5.2	5.1		4.4	5.3	5.5	5.8	
10	4.1	5.5	5.0		8.0	4.2	5.1	5.4		7.8	4.3	5.5	5.8		8.0
11	4.0	5.4		5.8		4.1	5.3		5.0		4.4	5.4		5.8	
12	5.9		5.8	5.2	5.0	3.7		5.1		7.7	3.5		5.0		5.1
13		5.0					5.1					5.2			5.1
14	3.3		5.3		5.9	3.8		5.5		7.4	3.8		5.6		7.1
15		4.8		5.3			4.9		7.7			5.2		5.4	
16	3.8		5.1		7.2	3.8		5.9		7.2	3.5		5.4		7.5
17		5.1		5.5			5.2		5.8			4.9		5.7	
18	3.9		5.0		7.3	3.9		5.8		7.4	3.7		5.9		7.3
19		4.8		5.5			5.1		5.8			4.8		5.2	
20	3.7		5.0		7.4	4.0		5.0		7.5	3.8		5.8		5.9
21		4.7		7.0			5.1		5.3			4.5		7.1	
22	3.5		5.0		7.5	4.2		5.2		7.5	3.7		5.8		7.4
23		4.8		7.5			4.9		5.7			4.5		6.4	
24	3.5		5.3		7.5	3.7		5.0		7.5	3.5		5.9		7.5
25		4.7		5.9			4.7		7.0			4.3		5.5	
26	3.5		5.5		7.8	3.8		5.4		7.8	3.2		5.9		7.1
27		4.9		7.1			4.8		5.9			4.7		5.5	
28	3.5		5.1		7.8	3.8		5.2		7.3	3.7		5.9		5.9
29		4.3		5.3			4.4		5.3			4.4		5.1	
30	3.1		5.4		5.4	2.5		5.5		5.8	3.5		5.5		5.5
31		4.2		5.9			4.5		5.0			4.4		5.5	
32	3.3		5.2		5.4	2.5		5.5		5.5	3.8		5.3		5.4
33		4.0		5.1			4.3		5.0			4.2		5.0	
34	3.1		5.3		5.2	3.4		5.5		5.7	3.3		5.2		5.3
35		4.1		5.9			4.3		5.0			4.1		5.0	
36	3.0		5.2			3.7		5.5			3.3		5.3		
37		4.2					4.5					4.1			
38	3.0					3.5					3.5				

Table 22 Concentration of K (ug/ml) in the leachates of the Forestburg fly ash leached with AASA solution

Inc #	Rep 1 Column Number					Rep 2 Column Number					Rep 3 Column Number				
	1	2	3	4	5	1	2	3	4	5	1	2	3	4	5
1	2.8	8.4	2.0	-	-	2.8	7.0	1.9	-	-	3.0	8.2	1.8	-	-
2	1.0	1.8	2.3	9.0	2.8	1.3	1.7	2.2	9.3	2.4	1.0	1.6	2.2	8.3	2.4
3	1.3	0.9	1.0	2.8	7.3	1.8	1.0	1.0	2.8	8.2	1.5	1.0	1.0	2.8	7.4
4	0.8	1.0	1.2	1.1	1.8	1.0	1.1	1.2	1.1	2.3	1.1	1.1	1.3	1.3	2.0
5	1.0	1.2	1.1	1.8	1.0	0.9	1.3	1.2	1.3	1.1	1.0	1.4	1.3	1.4	1.0
6	1.0	1.1	1.5	1.0	1.3	0.8	1.0	1.3	1.0	1.2	1.2	1.4	1.8	1.1	1.4
7	1.0	1.5	1.2	1.8	1.0	1.1	1.4	1.0	1.4	1.0	1.2	1.5	1.2	1.5	1.1
8	1.2	1.1	1.8	1.2	1.1	1.1	1.2	1.4	1.2	1.0	1.3	1.3	1.6	1.3	1.2
9	0.9	1.7	1.4	1.2	-	0.9	1.5	1.2	1.1	-	1.0	1.5	1.4	1.2	-
10	1.2	1.2	1.3	-	1.3	1.2	1.2	1.2	1.1	1.3	1.2	1.3	1.2	-	1.3
11	1.0	1.2	-	1.4	-	1.1	1.1	-	1.3	-	0.8	1.2	-	1.4	-
12	0.8	-	1.3	-	1.4	0.8	-	1.3	1.3	1.4	0.8	-	1.4	-	1.5
13	-	1.2	-	1.3	-	-	1.2	-	1.3	1.3	-	1.3	-	1.4	-
14	0.7	-	1.2	-	1.2	0.9	-	1.4	-	1.3	0.8	-	1.3	-	1.4
15	-	1.1	-	1.2	-	-	1.2	-	1.3	-	-	1.2	-	1.3	-
16	0.9	-	1.5	-	1.2	1.0	-	1.3	-	1.3	1.0	-	1.2	-	1.3
17	-	1.0	-	1.2	-	-	1.2	-	1.2	-	-	1.1	-	1.2	-
18	0.8	-	1.2	-	1.3	1.0	-	1.2	-	1.4	0.8	-	1.2	-	1.2
19	-	1.0	-	1.3	-	-	1.1	-	1.5	-	-	1.0	-	1.2	-
20	0.8	-	1.2	-	1.3	0.9	-	1.4	-	1.4	0.8	-	1.3	-	1.3
21	-	1.1	-	1.2	-	-	1.2	-	1.3	-	-	1.0	-	1.2	-
22	0.8	-	1.3	-	1.5	1.0	-	1.3	-	1.7	0.9	-	1.3	-	1.5
23	-	1.0	-	1.4	-	-	1.1	-	1.5	-	-	1.0	-	1.5	-
24	0.8	-	1.4	-	1.4	0.8	-	1.5	-	1.4	0.8	-	1.5	-	1.3
25	-	1.2	-	1.4	-	-	1.1	-	1.5	-	-	1.1	-	1.3	-
26	0.9	-	1.5	-	1.4	1.0	-	1.4	-	1.5	0.9	-	1.2	-	1.5
27	-	1.0	-	1.3	-	0.8	-	1.3	-	1.3	-	0.8	-	1.3	-
28	0.8	-	1.3	-	1.3	0.8	-	1.1	-	1.2	-	0.8	-	1.3	-
29	-	1.0	-	1.2	-	-	1.1	-	1.2	-	-	1.0	-	1.1	-
30	0.8	-	1.2	-	1.2	1.0	-	1.3	-	1.2	1.0	-	1.3	-	1.2
31	-	1.0	-	1.2	-	-	1.1	-	1.2	-	-	1.0	-	1.3	-
32	0.9	-	1.1	-	1.2	1.0	-	1.3	-	1.3	1.0	-	1.1	-	1.2
33	-	1.0	-	1.2	-	-	1.0	-	1.3	-	-	0.8	-	1.2	-
34	0.8	-	1.1	-	1.3	1.0	-	1.2	-	1.3	0.8	-	1.2	-	1.2
35	-	0.9	-	1.2	-	-	1.1	-	1.3	-	-	1.0	-	1.2	-
36	0.8	-	1.2	-	-	1.0	-	1.2	-	-	0.9	-	1.2	-	-
37	-	0.8	-	-	-	-	1.2	-	-	-	-	0.8	-	-	-
38	0.7	-	-	-	-	0.8	-	-	-	-	0.8	-	-	-	-

Table 23 Concentration of Mg (ug/ml) in the leachates, of the Forstburg fly ash leached with AASA solution

Inc #	Rep 1					Rep 2					Rep 3				
	Column Number	2	3	4	5	Column Number	2	3	4	5	Column Number	2	3	4	5
1	0.2	0.1	0.1	0.0	0.0	0.1	0.1	0.0	-	-	0.2	0.1	0.0	-	-
2	7.1	0.1	0.1	0.0	0.0	4.1	0.1	0.1	0.0	0.0	5.3	0.1	0.1	0.0	0.0
3	18	0.2	0.1	0.1	0.0	18	0.2	0.1	0.1	0.0	18	0.2	0.1	0.1	0.0
4	20	0.4	0.2	0.1	0.1	20	0.2	0.2	0.1	0.1	21	0.4	0.2	0.1	0.1
5	18	0.8	0.2	0.1	0.1	18	0.8	0.2	0.1	0.1	18	0.8	0.2	0.1	0.1
6	18	1.2	0.3	0.2	0.1	13	1.2	0.3	0.1	0.1	17	1.3	0.2	0.2	0.1
7	14	3.0	0.3	0.2	0.1	14	2.9	0.3	0.2	0.1	14	3.7	0.3	0.2	0.1
8	11	8.8	0.3	0.2	0.1	11	8.7	0.3	0.2	0.1	11	8.3	0.3	0.2	0.1
9	11	8.0	0.4	0.2	-	11	10	0.4	0.2	-	11	8.2	0.4	0.2	-
10	10	12	0.8	-	0.2	10	15	0.8	-	0.2	10	12	0.4	-	0.2
11	10	18	-	0.3	-	8.4	17	-	0.2	-	8.4	18	-	0.3	-
12	8.0	-	0.7	-	0.2	8.5	21	1.0	-	0.2	7.7	-	0.8	-	0.2
13	-	20	-	0.3	-	-	-	-	0.3	-	22	-	-	0.3	-
14	7.4	-	1.7	-	0.2	7.8	19	2.3	-	0.2	7.8	18	1.8	-	0.2
15	-	18	-	0.4	-	-	18	-	0.3	-	-	18	-	0.4	-
16	8.7	-	3.8	-	0.3	7.0	18	4.0	-	0.3	7.0	18	2.9	-	0.3
17	-	17	-	0.4	-	-	18	-	0.4	-	-	18	-	0.4	-
18	8.0	-	4.8	-	0.3	8.8	18	8.4	-	0.3	8.1	18	4.8	-	0.3
19	-	18	-	0.4	-	-	18	-	0.5	-	-	18	-	0.4	-
20	8.0	-	2.0	-	0.2	8.8	18	8.8	-	0.3	8.2	18	8.7	-	0.3
21	-	14	-	0.8	-	-	13	-	0.8	-	-	13	-	0.8	-
22	8.8	-	2.8	-	0.4	8.4	13	7.0	-	0.4	8.3	-	8.8	-	0.4
23	-	14	-	0.8	-	-	13	-	0.8	-	-	12	-	0.7	-
24	8.8	-	4.4	-	0.4	8.4	13	8.3	-	0.3	8.0	-	8.3	-	0.3
25	-	11	-	0.8	-	-	12	-	0.7	-	-	11	-	0.8	-
26	8.3	-	7.8	-	0.4	8.2	13	8.3	-	0.4	8.8	-	10	-	0.4
27	-	13	-	1.8	-	-	13	-	1.1	-	-	13	-	1.0	-
28	8.8	-	10	-	0.8	8.8	10	-	-	0.8	8.3	-	12	-	0.8
29	-	10	-	2.2	-	-	10	-	2.4	-	-	10	-	2.1	-
30	4.4	-	13	-	0.8	8.2	10	11	-	0.8	8.1	-	14	-	0.8
31	-	8.0	-	3.1	-	-	9.0	-	3.2	-	-	8.2	-	2.3	-
32	8.0	-	17	-	0.7	8.8	8.8	14	-	0.8	8.8	-	15	-	0.8
33	-	8.8	-	8.8	-	-	8.8	-	4.7	-	-	8.1	-	3.1	-
34	4.8	-	17	-	0.8	8.2	8.8	18	-	0.7	8.1	-	18	-	0.7
35	-	8.8	-	7.8	-	-	9.0	-	8.0	-	-	8.0	-	2.8	-
36	4.8	-	18	-	-	8.7	8.8	18	-	-	8.8	-	18	-	-
37	-	8.7	-	-	-	-	8.1	-	-	-	-	8.1	-	-	-
38	4.8	-	-	-	-	8.8	-	-	-	-	8.3	-	-	-	-

Table 24 Concentration of Pb (ug/ml) in the leachates of the Forestburg fly ash leached with AASA solution

Inc. #	Rep 1					Rep 2					Rep 3				
	Column	Number	2	3	4	5	1	2	3	4	5	1	2	3	4
1	0.1	0.1	0.1	-	-	0.1	0.1	0.1	-	-	0.1	0.1	0.1	-	-
2	0.1	0.1	0.1	0.1	0.1	0.1	0.1	0.1	0.1	0.1	0.1	0.1	0.1	0.1	0.1
3	0.8	0.0	0.0	0.0	0.0	0.2	0.1	0.1	0.0	0.1	0.1	0.1	0.1	0.0	0.1
4	2.3	0.1	0.0	0.0	0.0	2.2	0.1	0.0	0.0	0.0	1.8	0.1	0.0	0.0	0.0
5	4.4	0.0	0.0	0.0	0.0	4.7	0.0	0.0	0.0	0.1	3.8	0.0	0.0	0.0	0.1
6	8.2	0.0	0.0	0.0	0.1	3.8	0.0	0.0	0.1	0.0	8.7	0.1	0.0	0.1	0.1
7	7.2	0.0	0.0	0.1	0.0	8.3	0.0	0.0	0.1	0.0	8.4	0.0	0.0	0.1	0.0
8	7.5	0.0	0.1	0.0	0.1	7.4	0.0	0.1	0.0	0.1	7.8	0.1	0.1	0.0	0.0
9	8.0	0.1	0.0	0.0	-	8.4	0.1	0.0	0.1	-	10	0.1	0.0	0.1	-
10	8.1	0.1	0.0	-	0.1	10	0.0	0.0	-	0.1	10	0.1	0.1	-	0.1
11	10	0.1	-	0.1	-	10	0.1	-	0.1	-	10	0.2	-	0.1	-
12	10	-	0.0	-	0.0	11	-	0.0	-	0.0	11	-	0.1	-	0.1
13	-	0.7	-	0.1	-	-	0.4	-	0.0	-	-	0.8	0.1	0.1	-
14	10	-	0.0	-	0.0	10	-	0.1	-	0.0	11	-	0.1	-	0.0
15	-	1.8	-	0.0	-	-	1.8	-	0.0	-	-	1.9	-	0.0	-
16	10	-	0.0	-	0.0	11	-	0.0	-	0.0	11	-	0.0	-	0.1
17	-	2.8	-	0.0	-	-	2.7	-	0.0	-	-	2.7	-	0.1	-
18	11	-	0.0	-	0.0	11	-	0.0	-	0.0	11	-	0.0	-	0.0
19	-	3.5	-	0.0	-	-	3.8	-	0.0	-	-	4.4	-	0.0	-
20	11	-	0.0	-	0.0	11	-	0.1	-	0.0	11	-	0.1	-	0.0
21	-	5.1	-	0.0	-	-	4.8	-	0.1	-	-	5.2	-	0.0	-
22	12	-	0.0	-	0.0	12	-	0.1	-	0.0	12	-	0.1	-	0.1
23	-	5.9	-	0.0	-	-	5.4	-	0.1	-	-	5.8	-	0.1	-
24	13	-	0.0	-	0.0	13	-	0.1	-	0.0	12	-	0.1	-	0.0
25	-	8.2	-	0.0	-	-	8.1	-	0.0	-	-	8.7	-	0.0	-
26	11	-	0.0	-	0.0	12	-	0.1	-	0.0	11	-	0.2	-	0.0
27	-	5.7	-	0.0	-	-	5.4	-	0.0	-	-	5.7	-	0.0	-
28	11	-	0.1	-	0.1	12	-	0.2	-	0.1	12	-	0.3	-	0.1
29	-	8.2	-	0.1	-	-	5.9	-	0.1	-	-	8.2	-	0.1	-
30	10	-	0.3	-	0.0	12	-	0.3	-	0.0	12	-	0.5	-	0.0
31	-	7.4	-	0.1	-	-	7.4	-	0.1	-	-	7.8	-	0.0	-
32	11	-	1.1	-	0.1	12	-	0.5	-	0.1	12	-	0.7	-	0.1
33	-	7.8	-	0.1	-	-	7.8	-	0.2	-	-	7.8	-	0.1	-
34	11	-	1.4	-	0.1	13	-	0.8	-	0.1	13	-	1.0	-	0.1
35	-	8.3	-	0.2	-	-	8.4	-	0.2	-	-	7.7	-	0.1	-
36	11	-	1.8	-	-	13	-	1.1	-	-	12	-	1.8	-	-
37	-	8.4	-	-	-	-	8.2	-	-	-	-	8.3	-	-	-
38	11	-	-	-	-	12	-	-	-	-	12	-	-	-	-

Table 28. Concentration of Mn (ug/ml) in the leachates of the Forestburg fly ash leached with ASA solution.

Inc. #	Rep. 1					Rep. 2					Rep. 3						
	Column Number	1	2	3	4	Column Number	1	2	3	4	5	Column Number	1	2	3	4	5
1	0.0	0.0	0.0	0.0	0.0	0.0	0.0	0.0	0.0	0.0	0.0	0.0	0.0	0.0	0.0	0.0	0.0
2	0.0	0.0	0.0	0.0	0.0	0.0	0.0	0.0	0.0	0.0	0.0	0.0	0.0	0.0	0.0	0.0	0.0
3	0.3	0.0	0.0	0.0	0.0	0.2	0.0	0.0	0.0	0.0	0.0	0.2	0.0	0.0	0.0	0.0	0.0
4	0.3	0.0	0.0	0.0	0.0	0.4	0.0	0.0	0.0	0.0	0.0	0.4	0.0	0.0	0.0	0.0	0.0
5	0.3	0.0	0.0	0.0	0.0	0.3	0.0	0.0	0.0	0.0	0.0	0.4	0.0	0.0	0.0	0.0	0.0
6	0.3	0.0	0.0	0.0	0.0	0.2	0.0	0.0	0.0	0.0	0.0	0.3	0.0	0.0	0.0	0.0	0.0
7	0.3	0.0	0.0	0.0	0.0	0.3	0.0	0.0	0.0	0.0	0.0	0.3	0.0	0.0	0.0	0.0	0.0
8	0.3	0.0	0.0	0.0	0.0	0.3	0.0	0.0	0.0	0.0	0.0	0.3	0.0	0.0	0.0	0.0	0.0
9	0.2	0.0	0.0	0.0	0.0	0.2	0.0	0.0	0.0	0.0	0.0	0.2	0.0	0.0	0.0	0.0	0.0
10	0.3	0.1	0.0	0.0	0.0	0.2	0.0	0.0	0.0	0.0	0.0	0.3	0.1	0.0	0.0	0.0	0.0
11	0.2	0.1	0.0	0.0	0.0	0.2	0.1	0.0	0.0	0.0	0.0	0.2	0.1	0.0	0.0	0.0	0.0
12	0.2	0.1	0.0	0.0	0.0	0.2	0.1	0.0	0.0	0.0	0.0	0.2	0.1	0.0	0.0	0.0	0.0
13	0.2	0.3	0.0	0.0	0.0	0.2	0.2	0.0	0.0	0.0	0.0	0.2	0.1	0.0	0.0	0.0	0.0
14	0.2	0.4	0.0	0.0	0.0	0.2	0.4	0.0	0.0	0.0	0.0	0.2	0.5	0.0	0.0	0.0	0.0
15	0.2	0.4	0.0	0.0	0.0	0.2	0.4	0.0	0.0	0.0	0.0	0.2	0.5	0.0	0.0	0.0	0.0
16	0.2	0.4	0.0	0.0	0.0	0.2	0.4	0.0	0.0	0.0	0.0	0.2	0.4	0.0	0.0	0.0	0.0
17	0.2	0.4	0.0	0.0	0.0	0.2	0.4	0.0	0.0	0.0	0.0	0.2	0.4	0.0	0.0	0.0	0.0
18	0.2	0.4	0.0	0.0	0.0	0.2	0.4	0.0	0.0	0.0	0.0	0.2	0.4	0.0	0.0	0.0	0.0
19	0.2	0.4	0.0	0.0	0.0	0.2	0.4	0.0	0.0	0.0	0.0	0.2	0.4	0.0	0.0	0.0	0.0
20	0.2	0.5	0.0	0.0	0.0	0.2	0.5	0.0	0.0	0.0	0.0	0.2	0.4	0.0	0.0	0.0	0.0
21	0.2	0.5	0.0	0.0	0.0	0.2	0.5	0.1	0.0	0.0	0.0	0.2	0.4	0.0	0.0	0.0	0.0
22	0.2	0.5	0.0	0.0	0.0	0.2	0.4	0.1	0.0	0.0	0.0	0.2	0.4	0.0	0.0	0.0	0.0
23	0.1	0.4	0.0	0.0	0.0	0.2	0.4	0.1	0.0	0.0	0.0	0.2	0.4	0.1	0.0	0.0	0.0
24	0.1	0.4	0.0	0.0	0.0	0.2	0.4	0.1	0.0	0.0	0.0	0.2	0.4	0.1	0.0	0.0	0.0
25	0.2	0.4	0.0	0.0	0.0	0.2	0.4	0.1	0.0	0.0	0.0	0.2	0.4	0.1	0.0	0.0	0.0
26	0.2	0.5	0.0	0.0	0.0	0.2	0.5	0.1	0.0	0.0	0.0	0.2	0.4	0.1	0.0	0.0	0.0
27	0.2	0.5	0.1	0.0	0.0	0.2	0.5	0.1	0.0	0.0	0.0	0.2	0.4	0.1	0.0	0.0	0.0
28	0.2	0.4	0.1	0.0	0.0	0.2	0.4	0.1	0.0	0.0	0.0	0.2	0.3	0.1	0.0	0.0	0.0
29	0.1	0.4	0.2	0.0	0.0	0.2	0.4	0.2	0.0	0.0	0.0	0.1	0.3	0.2	0.0	0.0	0.0
30	0.1	0.4	0.3	0.0	0.0	0.2	0.4	0.2	0.0	0.0	0.0	0.2	0.3	0.2	0.0	0.0	0.0
31	0.1	0.3	0.3	0.0	0.0	0.2	0.3	0.2	0.0	0.0	0.0	0.2	0.3	0.2	0.0	0.0	0.0
32	0.1	0.3	0.3	0.0	0.0	0.2	0.3	0.2	0.0	0.0	0.0	0.2	0.3	0.2	0.0	0.0	0.0
33	0.1	0.3	0.3	0.0	0.0	0.2	0.3	0.2	0.0	0.0	0.0	0.2	0.3	0.2	0.0	0.0	0.0
34	0.1	0.3	0.3	0.0	0.0	0.2	0.3	0.2	0.0	0.0	0.0	0.2	0.3	0.2	0.0	0.0	0.0
35	0.1	0.3	0.3	0.0	0.0	0.2	0.3	0.3	0.0	0.0	0.0	0.2	0.3	0.5	0.0	0.0	0.0
36	0.1	0.3	0.3	0.0	0.0	0.2	0.3	0.3	0.0	0.0	0.0	0.2	0.3	0.5	0.0	0.0	0.0
37	0.1	0.3	0.3	0.0	0.0	0.2	0.3	0.3	0.0	0.0	0.0	0.2	0.3	0.5	0.0	0.0	0.0
38	0.1	0.3	0.3	0.0	0.0	0.2	0.3	0.3	0.0	0.0	0.0	0.2	0.3	0.5	0.0	0.0	0.0

Table 28. Leachate pH values of the Sundance fly ash leached with AASA solution.

Inc. #	Rep. 1 Column Number					Rep. 2 Column Number					Rep. 3 Column Number				
	1	2	3	4	5	1	2	3	4	5	1	2	3	4	5
1	11.85	12.85	12.80			12.45	12.85	12.55			12.55	12.85	12.55		
2	11.40	12.85	12.80	12.40	12.35	11.35	12.45	12.60	12.35	12.30	11.35	12.40	12.40	12.40	12.40
3	10.85	11.85	12.35	12.25	12.30	10.25	12.30	12.40	12.15	12.30	10.05	12.15	12.25	12.30	12.40
4	8.25	11.00	12.35	12.20	12.35	10.25	11.10	12.25	12.25	12.45	9.35	11.15	12.15	12.35	12.40
5	7.10	10.45	12.15	12.35	12.50	9.50	10.45	12.20	12.35	12.30	7.55	10.50	12.20	12.40	12.30
6	7.10	10.30	11.80	12.35	12.25	9.00	10.50	12.10	12.30	12.30	5.15	10.55	11.30	12.20	12.30
7	7.45	10.35	11.20	12.25	12.30	7.55	10.40	11.25	12.25	12.30	5.55	10.55	11.30	12.30	12.45
8	8.55	10.25	10.80	12.20	12.35	8.90	10.15	10.90	12.30	12.30	5.70	10.30	10.75	12.15	12.30
9	8.30	10.60	10.55	11.55	12.25	8.55	10.05	11.00	11.80	12.20	5.35	10.05	10.50	11.55	12.30
10	8.25	9.85	10.20	11.30	12.20	8.50	9.90	10.05	11.35	12.10	5.40	10.20	10.40	11.05	12.15
11	8.55	9.50	10.10	10.55	12.20	8.15	9.45	9.95	10.70	12.00	5.20	9.50	10.20	10.75	12.15
12	8.50	9.55	9.85	10.50	12.15	8.20	9.25	9.85	10.80	11.85	4.90	10.00	9.50	10.50	11.95
13	8.30	9.15	9.55	9.85	11.80	4.90	8.85	9.70	10.15	11.70	4.90	9.45	9.50	10.10	11.95
14	8.05	8.15	8.80	10.30	11.70	4.80	8.75	9.50	10.35	11.70	4.75	8.45	9.55	10.20	11.80
15	4.50	8.25	8.55	10.30	11.15	4.75	7.35	8.75	10.30	11.20	4.70	8.15	9.50	10.10	11.40
16	4.70	7.25	8.55	9.80	11.60	4.55	8.60	9.60	9.55	10.80	4.55	8.25	9.55	9.55	10.85
17	4.40	8.80	9.60	9.45	11.00	4.45	8.40	9.35	9.70	10.55	4.45	8.55	9.55	9.50	11.00
18	4.80	8.40	9.45	9.45	10.45	4.40	8.85	9.30	9.80	10.05	4.40	8.15	9.55	9.40	10.30
19	4.80	8.10	9.50	9.75	10.25	4.30	8.70	9.30	9.80	10.05	4.30	7.20	9.50	9.55	10.10
20	4.45	8.90	9.30	9.60	10.45	4.25	8.55	9.25	9.70	10.30	4.20	8.90	9.35	9.70	10.35
21	4.50	8.70	9.30	9.85	10.55	4.20	8.50	9.10	9.85	10.25	4.20	8.20	9.50	9.60	10.60
22	4.45	8.60	9.50	10.10	8.90	4.15	8.35	9.15	9.90	9.90	4.10	8.25	9.55	9.55	8.90
23	4.20	8.50	9.50	8.90	8.15	4.70	8.45	9.15	8.80	8.55	4.00	8.00	10.10	8.70	8.55
24	4.20	8.45	8.60	8.95	8.95	4.55	8.35	8.35	8.80	8.95	4.00	8.55	8.50	8.55	8.95
25	4.20	8.35	8.60	9.10	8.95	4.55	8.25	8.50	8.90	9.80	4.05	8.55	8.95	8.75	9.20
26	4.20	8.70	8.75	9.70	9.95	4.80	8.35	8.60	9.50	9.75	3.90	8.75	8.95	9.80	9.95
27	4.20	8.50	9.55	9.75	9.75	4.55	8.20	8.75	9.55	9.50	4.10	8.75	9.55	9.75	9.95
28	4.20	8.70	9.45	9.60	9.55	4.55	8.25	8.60	9.45	9.70	4.10	9.75	9.55	9.45	9.80
29	4.25	8.45	9.30	9.55	10.05	4.50	8.25	8.20	9.45	9.70	4.05	8.60	9.50	9.50	10.00
30	4.10	8.45	9.15	9.70	9.55	4.50	8.10	7.50	9.55	9.55	4.00	8.40	9.35	9.55	9.50
31	4.05	8.50	9.20	9.65	9.50	4.45	8.10	7.50	9.50	9.70	3.80	8.50	9.50	9.55	9.55
32	4.10	8.45	9.10	9.60	9.70	4.60	8.15	7.25	9.50	9.70	3.85	8.35	9.30	9.55	9.60
33	4.20	8.35	9.10	9.60	9.70	4.50	8.10	8.55	9.45	9.35	3.80	8.40	9.30	9.35	9.55
34	4.15	8.35	8.95	9.45	9.40	4.40	8.00	8.75	9.25	9.40	3.95	8.40	9.00	9.35	9.60
35	4.00	8.45	9.05	9.05	9.60	4.45	8.00	8.35	9.05	9.35	3.90	8.25	8.55	9.25	9.50
36	4.00	8.30	8.50	9.05	9.50	4.45	8.05	8.20	9.15	9.20	3.85	8.30	8.60	9.20	9.35
37	3.85	8.30	8.55	9.15	9.45	4.35	8.00	8.15	9.20	9.15	3.70	8.35	8.75	9.25	9.40
38	4.00	8.35	8.55	9.05	8.70	4.35	8.00	8.05	9.05	8.50	3.80	8.30	8.50	9.05	8.70
39	3.85	8.25	8.45	8.35	8.85	4.35	8.00	8.00	8.05	-	3.75	8.15	8.50	9.25	9.55
40	4.00	8.35	8.25	9.40	9.45	4.20	8.00	8.20	-	-	3.50	8.20	8.20	8.00	8.50
41	3.90	8.45	9.05	9.35	9.50	4.15	8.00	-	-	-	3.70	8.30	8.50	9.20	9.40
42	4.05	8.40	8.90	9.20	8.55	4.30	-	-	-	-	3.75	8.20	8.05	9.15	8.80
43	4.05	8.35	8.75	8.85	8.50	-	-	-	-	-	3.70	8.10	7.70	8.75	8.60
44	3.90	8.30	8.50	8.50	-	-	-	-	-	-	3.80	8.10	7.55	8.40	-
45	3.80	8.30	8.40	-	-	-	-	-	-	-	3.85	8.10	7.45	-	-
46	3.85	8.35	-	-	-	-	-	-	-	-	3.85	8.55	-	-	-
47	3.80	-	-	-	-	-	-	-	-	-	3.80	-	-	-	-

Table 33. Concentration of Cs (ug/ml) in the leachates of the Sundance fly ash leached with AASA solution.

Inc #	Rep 1				Rep 2				Rep 3			
	1	2	3	4	1	2	3	4	1	2	3	4
1	1200	8800	2700	3200	2300	2300	2800	2800	2100	2400	2800	2400
2	950	2200	2200	3200	850	1700	2000	2000	770	1000	1000	2000
3	310	1100	2000	2100	700	1700	2000	2000	1500	1500	1500	2000
4	820	700	3200	3100	950	810	2200	2200	610	740	2100	2000
5	800	700	1000	1000	850	720	1000	1000	810	810	1000	1000
6	800	700	1000	1000	850	720	1000	1000	810	810	1000	1000
7	800	700	1000	1000	850	720	1000	1000	810	810	1000	1000
8	800	700	1000	1000	850	720	1000	1000	810	810	1000	1000
9	800	700	1000	1000	850	720	1000	1000	810	810	1000	1000
10	800	700	1000	1000	850	720	1000	1000	810	810	1000	1000
11	800	700	1000	1000	850	720	1000	1000	810	810	1000	1000
12	800	700	1000	1000	850	720	1000	1000	810	810	1000	1000
13	800	700	1000	1000	850	720	1000	1000	810	810	1000	1000
14	370	800	870	800	200	710	740	740	320	700	700	800
15	800	800	800	800	200	400	820	820	220	820	820	800
16	180	800	800	800	100	800	800	800	100	820	800	800
17	170	800	800	800	120	810	800	800	100	820	800	800
18	160	800	800	800	120	800	800	800	100	820	800	800
19	160	800	800	800	120	800	800	800	100	820	800	800
20	160	800	800	800	120	800	800	800	100	820	800	800
21	160	800	800	800	120	800	800	800	100	820	800	800
22	160	800	800	800	120	800	800	800	100	820	800	800
23	110	400	800	800	100	430	870	800	100	800	800	800
24	110	400	800	800	100	430	800	800	100	800	800	800
25	100	400	800	800	120	300	800	800	100	800	800	800
26	100	400	800	800	120	300	800	800	100	800	800	800
27	100	400	800	800	120	300	800	800	100	800	800	800
28	100	400	800	800	120	300	800	800	100	800	800	800
29	100	400	800	800	120	300	800	800	100	800	800	800
30	100	400	800	800	120	300	800	800	100	800	800	800
31	80	400	800	800	91	310	800	800	70	800	800	800
32	80	400	800	800	91	310	800	800	70	800	800	800
33	72	400	800	800	88	280	800	800	77	800	800	800
34	72	400	800	800	88	280	800	800	77	800	800	800
35	72	400	800	800	88	280	800	800	77	800	800	800
36	72	400	800	800	88	280	800	800	77	800	800	800
37	72	400	800	800	88	280	800	800	77	800	800	800
38	72	400	800	800	88	280	800	800	77	800	800	800
39	72	400	800	800	88	280	800	800	77	800	800	800
40	72	400	800	800	88	280	800	800	77	800	800	800
41	72	400	800	800	88	280	800	800	77	800	800	800
42	72	400	800	800	88	280	800	800	77	800	800	800
43	72	400	800	800	88	280	800	800	77	800	800	800
44	72	400	800	800	88	280	800	800	77	800	800	800
45	72	400	800	800	88	280	800	800	77	800	800	800
46	72	400	800	800	88	280	800	800	77	800	800	800
47	72	400	800	800	88	280	800	800	77	800	800	800
48	72	400	800	800	88	280	800	800	77	800	800	800
49	72	400	800	800	88	280	800	800	77	800	800	800
50	72	400	800	800	88	280	800	800	77	800	800	800

Table 30 Concentration of Pb (ug/ml) in the leachates of the Sundance fly ash leached with AASA solution

Inc. #	Rep. 1					Rep. 2					Rep. 3				
	1	2	3	4	5	1	2	3	4	5	1	2	3	4	5
1	30	72	220			28	72	230			28	82	210		
2	3.3	11	35	100	440	8.0	12	38	100	480	3.8	12	58	100	410
3	3.8	4.5	8.4	42	110	4.8	8.8	8.3	40	110	4.3	8.4	8.3	28	100
4	8.8	4.3	8.9	10	28	5.2	8.1	7.8	11	28	4.3	8.8	8.8	10	27
5	3.8	4.3	8.8	7.2	12	8.8	8.8	7.2	8.8	13	8.1	8.4	8.8	8.1	11
6	4.8	4.4	6.2	8.7	8.8	8.2	8.0	7.3	8.1	10	8.4	8.1	8.2	7.8	9.3
7	4.7	4.7	8.3	8.4	8.2	8.2	8.4	7.0	8.2	10	4.7	8.1	8.0	7.4	8.4
8	4.7	4.8	8.8	7.0	7.4	8.8	8.2	8.8	8.0	8.2	4.7	8.8	8.0	7.2	7.8
9	4.8	8.1	8.8	8.3		8.7	8.2	7.3	7.7		4.2	4.8	8.8	8.8	
10	4.7	8.8	8.8		7.8	8.8	8.3	8.7		8.0	4.7	8.8	8.7		8.1
11	4.8	4.8		8.8		8.2	8.7		7.8		4.2	8.8		8.8	
12	4.0		8.0		8.1	4.7		8.4		8.3	3.8		8.7		7.2
13		8.3		8.8			8.7		7.0			4.8		8.4	
14	4.4		8.8		8.3	4.8		8.0		8.4	3.7		8.8		8.8
15		4.8		8.8			8.8		8.8			4.8		8.8	
16	3.2		8.2		7.8	3.8		8.8		8.2	2.8		8.3		7.0
17		3.8		8.7			4.7		8.4			4.3		8.8	
18	2.8		4.7		7.1	3.8		8.2		7.8	2.8		8.0		8.7
19		4.0		8.8			4.4		8.8			4.0		8.8	
20	3.0		4.8		7.2	2.8		4.8		7.0	2.1		8.2		8.8
21		2.8		8.1			4.2		8.8			4.0		8.8	
22	2.7		4.7		8.8	2.8		4.8		7.1	1.8		4.8		8.8
23		3.8		8.8			8.4		8.8			3.8		8.8	
24		2.2		4.4		8.3		7.8		8.3	1.8		8.0		7.0
25		3.7		8.1		8.7		8.8		8.4	1.8		4.1		8.3
26	2.2		4.4		7.3	8.7		7.3		10.0	1.8		8.8		7.8
27		4.4		8.8			8.7		8.2			4.8		8.2	
28	2.3		4.4		7.0	8.8		7.1		8.8	2.0		8.4		7.4
29		4.4		8.8			8.1		7.8			4.3		8.0	
30	2.2		4.8		8.8	8.0		7.2		8.8	1.7		8.0		8.8
31		4.4		8.8			8.0		7.3			4.8		8.8	
32	2.8		4.8		7.8	8.3		8.8		8.2	1.8		8.3		7.3
33		4.8		8.3			8.8		7.8			4.8		8.3	
34	2.4		8.2		7.8	8.2		8.8		8.0	1.4		8.8		7.8
35		4.8		8.3			8.8		7.8			4.7		8.4	
36	2.8		8.8		8.8	8.2		8.7		10.0	1.8		8.7		7.7
37		4.8		8.8			8.8		7.8			4.8		8.7	
38	2.8		8.3		8.1	4.8		7.3		10.0	1.8		8.0		7.8
39		8.8		8.8		4.7		8.7		7.8		4.8		8.8	
40	3.0		8.0		8.8			7.1				1.3		8.8	8.2
41		8.8		8.4									8.1		8.8
42	2.8		8.3		10	4.4						1.4		8.8	8.3
43		8.1		8.7	13								4.3		7.2
44	2.4		8.8	10								1.7		8.8	8.4
45		8.3		8.8									8.7		8.8
46	2.7		8.0									1.3		8.7	
47	3.1											1.4			

Table 31. Concentration of K (ug/ml) in the leachates of the Sundance fly ash leached with AASA solution

Inc #	Rep. 1					Rep. 2					Rep. 3				
	Column Number	1	2	3	4	1	2	3	4	5	1	2	3	4	5
1	0.8	1.8	4.4	-	-	0.8	1.8	4.8	-	-	0.8	1.8	5.8	-	-
2	0.3	0.8	0.8	3.8	7.8	0.8	0.8	0.8	3.8	8.7	0.8	0.8	1.1	3.7	7.1
3	0.8	0.3	0.3	1.0	2.7	0.8	0.4	0.4	1.0	2.9	0.8	0.4	0.4	1.0	2.0
4	0.8	0.4	0.4	0.8	1.0	0.8	0.7	0.8	0.8	1.0	0.7	0.8	0.8	0.8	1.0
5	0.8	0.8	0.4	0.8	0.4	1.0	0.8	0.7	0.7	0.8	0.8	0.8	0.8	0.8	0.4
6	0.8	0.8	0.7	0.4	0.8	1.2	1.1	1.1	0.8	0.4	1.0	0.8	0.8	0.8	0.8
7	0.8	0.8	0.8	0.8	0.8	1.4	1.3	0.9	1.0	0.8	0.8	1.0	0.7	0.8	0.8
8	1.0	0.7	0.8	0.8	0.8	1.5	1.1	1.3	0.8	0.8	1.1	0.8	1.0	0.8	0.8
9	0.8	1.0	0.7	0.8	-	1.1	1.4	1.0	0.8	-	0.8	1.1	0.8	0.8	-
10	1.1	0.8	0.8	-	0.7	1.4	1.1	1.1	-	0.8	1.1	0.8	0.8	-	0.7
11	0.8	0.8	-	0.8	-	1.0	1.0	-	1.2	-	0.8	0.8	-	0.8	-
12	0.8	-	0.8	-	0.8	1.0	-	1.1	-	1.0	0.7	-	0.8	-	0.7
13	-	1.0	-	0.8	-	-	1.1	-	1.0	-	0.8	0.8	-	0.8	-
14	1.0	-	1.0	-	0.8	1.0	-	1.1	-	0.8	0.8	-	0.8	-	0.8
15	-	1.0	-	1.0	-	0.8	-	1.1	-	0.8	0.8	-	0.8	-	0.8
16	0.7	-	0.8	-	0.8	0.8	-	1.0	-	0.8	0.8	-	0.8	-	0.7
17	-	0.7	-	0.8	-	0.8	-	1.0	-	0.8	0.7	-	0.7	-	0.7
18	0.7	-	0.7	-	0.7	0.8	-	0.8	-	0.8	0.7	-	0.7	-	0.7
19	-	0.7	-	0.7	-	0.8	-	0.8	-	0.8	-	-	0.7	-	0.7
20	0.8	-	0.7	-	0.7	0.8	-	0.8	-	0.8	0.8	-	0.7	-	0.8
21	-	0.7	-	0.7	-	0.8	-	0.8	-	0.8	0.7	-	0.7	-	0.8
22	0.8	-	0.7	-	0.8	0.8	-	0.8	-	1.0	0.3	-	0.7	-	0.8
23	-	0.7	-	0.8	-	-	1.2	-	1.1	-	-	0.8	-	0.8	-
24	0.8	-	0.8	-	0.8	1.4	-	1.4	-	1.1	0.4	-	0.8	-	0.8
25	-	0.8	-	0.8	-	1.7	-	1.2	-	-	-	0.8	-	0.8	-
26	0.7	-	0.7	-	0.8	1.8	-	1.3	-	1.4	0.4	-	0.8	-	0.8
27	-	0.7	-	0.8	-	1.3	-	1.4	-	1.4	-	0.8	-	0.8	-
28	0.4	-	0.8	-	0.8	1.2	-	1.4	-	1.8	0.3	-	0.8	-	1.0
29	-	0.8	-	0.8	-	1.4	-	1.4	-	1.4	0.4	-	0.8	-	0.8
30	0.8	-	0.8	-	0.8	1.3	-	1.4	-	1.6	0.4	-	0.8	-	1.0
31	-	1.0	-	0.8	-	1.4	-	1.3	-	1.3	0.4	-	0.8	-	0.8
32	0.8	-	0.8	-	0.8	1.3	-	1.3	-	1.3	0.4	-	0.8	-	0.8
33	-	0.8	-	0.8	-	1.3	-	1.4	-	1.4	0.4	-	0.8	-	0.8
34	0.8	-	0.8	-	0.8	1.3	-	1.8	-	1.3	0.3	-	0.8	-	1.0
35	0.8	-	0.8	-	1.0	-	1.3	-	1.8	-	0.4	-	0.8	-	0.8
36	0.8	-	0.8	-	0.8	1.2	-	1.4	-	1.2	0.4	-	0.8	-	0.8
37	0.8	-	0.8	-	1.0	-	1.3	-	1.2	-	-	0.8	-	0.8	-
38	0.8	-	1.1	-	1.0	1.2	-	1.4	-	1.3	0.3	-	0.8	-	1.0
39	-	1.0	-	1.0	-	-	1.1	-	1.3	-	-	0.8	-	0.8	-
40	0.8	-	1.0	-	1.2	0.8	-	1.2	-	-	0.2	-	0.8	-	1.0
41	-	1.0	-	1.0	-	-	1.2	-	-	-	-	0.8	-	0.8	-
42	0.8	-	1.0	-	1.1	0.8	-	-	-	-	0.2	-	1.0	-	1.0
43	-	1.1	-	1.1	-	-	-	-	-	-	-	0.8	-	1.0	-
44	0.8	-	1.1	-	1.4	-	-	-	-	-	0.3	-	1.0	-	1.2
45	-	1.1	-	1.3	-	-	-	-	-	-	-	0.8	-	1.1	-
46	0.8	-	1.3	-	-	-	-	-	-	-	0.3	-	1.0	-	-
47	0.7	-	-	-	-	-	-	-	-	-	0.3	-	-	-	-

Table 32. Concentration of Mg (ug/mL) in the leachates of the Sundance fly ash leached with AASA solution

Inc. #	Rep 1					Rep 2					Rep 3				
	1	2	3	4	5	1	2	3	4	5	1	2	3	4	5
1	0.1	0.0	0.0	-	-	0.0	0.0	0.0	-	-	0.1	0.0	0.0	-	-
2	0.4	0.0	0.0	0.0	0.0	0.9	0.0	0.0	0.0	0.0	1.3	0.0	0.0	0.0	0.0
3	1.7	0.2	0.0	0.0	0.0	2.1	0.1	0.0	0.0	0.0	2.8	0.1	0.0	0.0	0.0
4	3.7	0.4	0.0	0.0	0.0	3.7	0.2	0.0	0.0	0.0	5.2	0.4	0.0	0.0	0.0
5	4.8	0.8	0.1	0.0	0.0	4.9	0.8	0.1	0.0	0.0	8.4	0.5	0.1	0.0	0.0
6	5.4	1.3	0.2	0.0	0.0	8.4	1.0	0.1	0.0	0.0	8.5	0.7	0.1	0.0	0.0
7	7.0	2.0	0.3	0.0	0.0	7.4	1.5	0.3	0.0	0.0	8.8	0.8	0.3	0.0	0.0
8	7.8	2.6	0.5	0.1	0.0	8.3	2.1	0.5	0.0	0.0	7.8	1.2	0.5	0.1	0.0
9	8.5	3.2	0.7	0.1	-	8.8	2.8	0.7	0.1	-	8.0	1.8	0.7	0.2	-
10	8.1	3.8	1.0	-	0.0	8.7	4.0	1.1	-	0.0	8.4	2.1	0.8	-	0.0
11	10	3.8	-	0.4	-	8.1	4.7	-	0.4	-	7.4	2.8	-	0.4	-
12	8.1	-	1.4	-	0.1	7.5	-	2.0	-	0.1	5.4	-	1.4	-	0.1
13	-	5.4	-	0.8	-	-	5.0	-	0.7	-	-	3.1	-	0.7	-
14	7.5	-	2.0	-	0.2	8.1	-	2.8	-	0.2	8.2	-	1.8	-	0.2
15	-	5.4	-	0.9	-	4.8	5.3	-	0.8	-	4.0	3.7	-	0.9	-
16	5.4	-	2.2	-	0.2	4.8	-	2.8	-	0.4	4.0	-	2.1	-	0.3
17	-	4.8	-	1.0	-	-	5.1	-	1.3	-	4.1	-	1.2	-	-
18	4.5	-	2.7	-	0.3	4.2	-	3.4	-	0.8	4.2	-	2.5	-	0.5
19	-	4.6	-	1.2	-	-	4.8	-	1.4	-	4.7	-	1.4	-	-
20	4.1	-	2.8	-	0.5	3.4	-	3.3	-	0.7	3.4	-	2.8	-	0.5
21	-	4.5	-	1.3	-	-	4.8	-	1.8	-	-	5.1	-	1.0	-
22	3.8	-	3.1	-	0.5	3.0	-	3.7	-	0.9	2.8	-	1.5	-	0.5
23	-	4.3	-	1.7	-	-	5.2	-	2.0	-	-	5.1	-	1.2	-
24	3.0	-	3.5	-	0.6	4.8	-	4.1	-	0.9	2.5	-	1.9	-	0.6
25	-	4.4	-	1.4	-	-	5.0	-	1.8	-	-	5.7	-	1.1	-
26	2.9	-	3.0	-	0.8	4.1	-	3.3	-	1.0	2.2	-	1.7	-	0.7
27	-	4.8	-	1.6	-	-	5.0	-	1.9	-	-	7.3	-	1.5	-
28	3.0	-	3.5	-	0.7	4.1	-	3.8	-	1.3	2.7	-	3.3	-	0.9
29	-	4.8	-	2.1	-	-	4.7	-	2.3	-	-	7.5	-	2.4	-
30	2.4	-	3.9	-	0.8	3.1	-	4.3	-	1.4	2.1	-	4.4	-	1.0
31	-	4.5	-	2.0	-	-	4.4	-	2.4	-	-	7.9	-	2.5	-
32	2.5	-	3.7	-	0.5	3.2	-	4.4	-	1.5	2.0	-	4.7	-	1.1
33	-	4.9	-	2.2	-	-	3.9	-	2.7	-	-	7.8	-	3.0	-
34	2.2	-	4.2	-	0.8	3.0	-	4.7	-	1.8	1.7	-	5.4	-	1.4
35	-	5.1	-	2.4	-	-	3.8	-	3.0	-	-	7.5	-	3.1	-
36	2.2	-	4.4	-	0.9	2.9	-	4.8	-	2.0	1.7	-	5.5	-	1.3
37	-	5.7	-	2.3	-	-	3.9	-	3.1	-	-	7.5	-	3.1	-
38	2.2	-	4.8	-	0.9	2.5	-	5.0	-	2.0	1.5	-	5.2	-	1.3
39	-	7.5	-	2.5	-	-	3.8	-	3.1	-	-	7.4	-	4.1	-
40	1.5	-	5.1	-	1.0	2.1	-	5.2	-	-	-	7.4	-	5.1	-
41	-	7.9	-	2.8	-	-	4.2	-	-	-	-	7.5	-	4.2	-
42	2.2	-	5.4	-	1.2	2.4	-	-	-	-	1.4	-	7.5	-	1.5
43	-	8.2	-	2.1	-	-	-	-	-	-	-	8.0	-	4.9	-
44	1.7	-	7.7	-	1.1	-	-	-	-	-	1.3	-	7.2	-	4.7
45	-	8.1	-	5.5	-	-	-	-	-	-	-	7.1	-	5.7	-
46	1.5	1.2	-	-	-	-	-	-	-	-	1.3	7.5	-	-	-
47	2.5	-	-	-	-	-	-	-	-	-	1.7	-	-	-	-

Table 33. Concentration of Fe (ug/mL) in the leachates of the Sundance fly ash leached with AASA solution.

Inc. #	Rep 1					Rep 2					Rep 3				
	Column 1	Column 2	Column 3	Column 4	Column 5	Column 1	Column 2	Column 3	Column 4	Column 5	Column 1	Column 2	Column 3	Column 4	Column 5
1	0.1	0.1	0.1	-	-	0.1	0.1	0.1	-	-	0.1	0.1	0.1	-	-
2	0.1	0.1	0.1	0.1	0.1	0.1	0.1	0.1	0.1	0.1	0.1	0.1	0.1	0.1	0.1
3	0.1	0.1	0.1	0.1	0.1	0.1	0.1	0.1	0.0	0.1	0.1	0.1	0.1	0.1	0.1
4	0.1	0.1	0.1	0.1	0.0	0.1	0.1	0.1	0.1	0.0	0.1	0.1	0.1	0.1	0.0
5	1.0	0.0	0.0	0.0	0.1	0.1	0.0	0.1	0.0	0.1	0.4	0.0	0.1	0.0	0.1
6	1.0	0.0	0.0	0.1	0.1	0.1	0.1	0.0	0.1	0.1	1.4	0.0	0.0	0.1	0.1
7	0.7	0.0	0.0	0.1	0.0	0.6	0.0	0.0	0.1	0.0	1.8	0.0	0.1	0.1	0.1
8	1.8	0.1	0.1	0.0	0.1	1.8	0.0	0.1	0.0	0.1	1.8	0.0	0.1	0.0	0.1
9	1.8	0.1	0.0	0.1	-	2.8	0.1	0.0	0.1	-	2.8	0.1	0.0	0.1	-
10	1.8	0.0	0.0	-	0.1	3.7	0.0	0.1	-	0.1	2.8	0.0	0.1	-	0.1
11	2.8	0.1	-	0.1	-	8.4	0.1	-	0.1	-	3.8	0.1	-	0.1	-
12	4.3	-	-	-	0.1	8.2	-	-	0.1	0.1	8.1	-	-	0.1	-
13	5.0	0.1	-	0.1	-	8.5	0.1	0.1	0.1	-	4.8	0.1	0.1	0.1	0.0
14	-	-	-	-	0.0	-	-	-	0.1	0.1	-	-	-	-	-
15	-	0.2	-	0.0	-	-	0.8	-	0.0	-	5.4	0.1	0.1	0.0	0.1
16	8.7	-	0.0	-	0.1	8.8	-	0.0	-	0.0	5.4	-	0.1	0.0	0.1
17	-	1.2	-	0.1	-	-	1.8	-	0.1	-	0.1	0.1	0.1	0.1	0.0
18	4.8	-	0.1	-	0.0	4.8	-	0.1	-	0.0	5.4	-	0.0	0.0	0.0
19	-	1.8	-	0.0	-	-	2.8	-	0.0	-	0.7	0.0	0.0	0.0	0.0
20	5.0	-	0.0	-	0.0	3.8	-	0.1	-	0.0	3.8	-	0.0	0.0	0.0
21	-	2.4	-	0.0	-	-	3.7	-	0.0	-	1.7	0.0	0.1	0.1	0.1
22	8.3	-	0.0	-	0.1	3.2	-	0.1	-	0.0	3.3	-	0.1	-	0.1
23	-	3.2	-	0.0	-	-	3.8	-	0.0	-	1.8	0.0	0.0	0.0	0.0
24	4.4	-	0.1	-	0.0	8.2	-	0.1	-	0.0	3.0	-	0.0	0.0	0.0
25	-	3.2	-	0.0	-	-	3.8	-	0.0	-	2.2	0.0	0.0	0.0	0.0
26	3.8	-	0.1	-	0.0	7.4	-	0.1	-	0.0	2.8	-	0.0	0.0	0.0
27	-	2.8	-	0.0	-	-	3.8	-	0.0	-	2.1	0.0	0.0	0.0	0.1
28	3.8	-	0.0	-	0.1	8.4	-	0.1	-	0.1	3.3	-	0.0	0.1	0.1
29	-	2.8	-	0.1	-	-	4.2	-	0.1	-	2.4	0.0	0.1	0.1	0.0
30	4.4	-	0.1	-	0.0	8.4	-	0.4	-	0.0	3.8	-	0.1	0.0	0.0
31	-	3.3	-	0.0	-	-	8.2	-	0.0	-	3.2	0.0	0.0	0.0	0.0
32	8.2	-	0.1	-	0.1	7.8	-	0.7	-	0.1	2.8	-	0.0	0.1	0.1
33	-	2.8	-	0.1	-	-	8.7	-	0.1	-	3.0	0.0	0.1	-	-
34	3.8	-	0.1	-	0.1	7.3	-	1.1	-	0.1	2.3	-	0.1	0.1	0.1
35	-	2.8	-	0.1	-	-	8.0	-	0.1	-	3.8	-	0.1	0.1	0.1
36	4.0	-	0.2	-	0.0	8.8	-	1.4	-	0.0	3.8	-	0.1	0.0	0.0
37	-	3.2	-	0.0	-	-	8.4	-	0.1	-	3.8	-	0.0	0.0	0.0
38	8.1	-	0.2	-	0.1	8.8	-	2.0	-	0.1	2.3	-	0.1	0.1	0.1
39	-	2.8	-	0.1	-	-	8.0	-	0.1	-	8.2	-	0.1	0.1	0.1
40	8.3	-	0.1	-	0.0	8.8	-	1.8	-	-	2.0	-	0.2	0.0	0.0
41	-	2.8	-	0.0	-	-	8.8	-	-	-	8.2	-	0.0	0.0	0.0
42	8.2	-	0.1	-	0.0	8.8	-	-	-	-	2.1	-	0.3	0.0	0.0
43	-	3.3	-	0.0	0.0	-	-	-	-	-	8.7	-	0.0	0.0	0.0
44	8.3	-	0.1	-	0.0	-	-	-	-	-	2.4	-	0.8	0.1	-
45	4.8	-	0.1	-	-	-	-	-	-	-	8.1	-	0.8	-	-
46	4.8	2.8	-	-	-	-	-	-	-	-	2.0	-	8.7	-	-
47	8.0	-	-	-	-	-	-	-	-	-	1.8	-	-	-	-

Table 34 Concentration of Mn (ug/ml) in the leachates of the Sundance fly ash leached with JASA solution

Inj#	Rep 1 Column Number					Rep 2 Column Number					Rep 3 Column Number				
	1	2	3	4	5	1	2	3	4	5	1	2	3	4	5
1	0.0	0.0	0.0	0.0	0.0	0.0	0.0	0.0	0.0	0.0	0.0	0.0	0.0	0.0	0.0
2	0.0	0.0	0.0	0.0	0.0	0.0	0.0	0.0	0.0	0.0	0.0	0.0	0.0	0.0	0.0
3	0.0	0.0	0.0	0.0	0.0	0.0	0.0	0.0	0.0	0.0	0.0	0.0	0.0	0.0	0.0
4	0.0	0.0	0.0	0.0	0.0	0.0	0.0	0.0	0.0	0.0	0.0	0.0	0.0	0.0	0.0
5	0.1	0.0	0.0	0.0	0.0	0.0	0.0	0.0	0.0	0.0	0.0	0.0	0.0	0.0	0.0
6	0.1	0.0	0.0	0.0	0.0	0.0	0.0	0.0	0.0	0.0	0.1	0.0	0.0	0.0	0.0
7	0.1	0.0	0.0	0.0	0.0	0.1	0.0	0.0	0.0	0.0	0.1	0.0	0.0	0.0	0.0
8	0.1	0.0	0.0	0.0	0.0	0.2	0.0	0.0	0.0	0.0	0.1	0.0	0.0	0.0	0.0
9	0.1	0.0	0.0	0.0	0.0	0.2	0.0	0.0	0.0	0.0	0.2	0.0	0.0	0.0	0.0
10	0.2	0.0	0.0	0.0	0.0	0.3	0.0	0.0	0.0	0.0	0.2	0.0	0.0	0.0	0.0
11	0.3	0.0	0.0	0.0	0.0	0.3	0.0	0.0	0.0	0.0	0.2	0.0	0.0	0.0	0.0
12	0.3	0.0	0.0	0.0	0.0	0.3	0.0	0.0	0.0	0.0	0.2	0.0	0.0	0.0	0.0
13	0.3	0.0	0.0	0.0	0.0	0.3	0.0	0.0	0.0	0.0	0.3	0.0	0.0	0.0	0.0
14	0.3	0.1	0.0	0.0	0.0	0.3	0.2	0.0	0.0	0.0	0.3	0.0	0.0	0.0	0.0
15	0.3	0.1	0.0	0.0	0.0	0.3	0.2	0.0	0.0	0.0	0.2	0.0	0.0	0.0	0.0
16	0.2	0.2	0.0	0.0	0.0	0.3	0.2	0.0	0.0	0.0	0.2	0.0	0.0	0.0	0.0
17	0.2	0.2	0.0	0.0	0.0	0.3	0.2	0.0	0.0	0.0	0.2	0.1	0.0	0.0	0.0
18	0.2	0.2	0.0	0.0	0.0	0.2	0.3	0.0	0.0	0.0	0.2	0.1	0.0	0.0	0.0
19	0.2	0.2	0.0	0.0	0.0	0.2	0.3	0.0	0.0	0.0	0.2	0.1	0.0	0.0	0.0
20	0.2	0.2	0.0	0.0	0.0	0.2	0.3	0.0	0.0	0.0	0.2	0.1	0.0	0.0	0.0
21	0.2	0.2	0.0	0.0	0.0	0.3	0.3	0.1	0.0	0.0	0.1	0.1	0.0	0.0	0.0
22	0.2	0.2	0.0	0.0	0.0	0.3	0.3	0.0	0.0	0.0	0.1	0.2	0.0	0.0	0.0
23	0.2	0.2	0.0	0.0	0.0	0.3	0.3	0.0	0.0	0.0	0.1	0.2	0.0	0.0	0.0
24	0.2	0.2	0.0	0.0	0.0	0.3	0.3	0.0	0.0	0.0	0.1	0.2	0.0	0.0	0.0
25	0.2	0.2	0.0	0.0	0.0	0.3	0.3	0.0	0.0	0.0	0.1	0.2	0.0	0.0	0.0
26	0.2	0.2	0.0	0.0	0.0	0.3	0.3	0.0	0.0	0.0	0.1	0.2	0.0	0.0	0.0
27	0.2	0.2	0.0	0.0	0.0	0.3	0.3	0.0	0.0	0.0	0.1	0.2	0.0	0.0	0.0
28	0.2	0.2	0.0	0.0	0.0	0.3	0.3	0.0	0.0	0.0	0.1	0.2	0.0	0.0	0.0
29	0.2	0.2	0.0	0.0	0.0	0.3	0.3	0.0	0.0	0.0	0.1	0.2	0.0	0.0	0.0
30	0.2	0.2	0.0	0.0	0.0	0.2	0.3	0.1	0.0	0.0	0.1	0.3	0.0	0.0	0.0
31	0.2	0.2	0.0	0.0	0.0	0.3	0.3	0.1	0.0	0.0	0.1	0.3	0.0	0.0	0.0
32	0.2	0.2	0.0	0.0	0.0	0.2	0.3	0.0	0.0	0.0	0.1	0.3	0.0	0.0	0.0
33	0.2	0.2	0.0	0.0	0.0	0.2	0.3	0.0	0.0	0.0	0.1	0.3	0.0	0.0	0.0
34	0.2	0.2	0.0	0.0	0.0	0.2	0.2	0.2	0.0	0.0	0.1	0.4	0.1	0.0	0.0
35	0.2	0.2	0.0	0.0	0.0	0.2	0.2	0.2	0.0	0.0	0.1	0.4	0.1	0.0	0.0
36	0.2	0.2	0.0	0.0	0.0	0.2	0.2	0.2	0.0	0.0	0.1	0.4	0.1	0.0	0.0
37	0.2	0.2	0.0	0.0	0.0	0.2	0.2	0.2	0.0	0.0	0.1	0.4	0.1	0.0	0.0
38	0.2	0.2	0.0	0.0	0.0	0.2	0.2	0.2	0.0	0.0	0.1	0.4	0.1	0.0	0.0
39	0.2	0.2	0.0	0.0	0.0	0.2	0.2	0.2	0.0	0.0	0.1	0.4	0.1	0.0	0.0
40	0.2	0.2	0.0	0.0	0.0	0.2	0.2	0.2	0.0	0.0	0.1	0.4	0.1	0.0	0.0
41	0.2	0.2	0.0	0.0	0.0	0.2	0.2	0.2	0.0	0.0	0.1	0.4	0.1	0.0	0.0
42	0.2	0.2	0.0	0.0	0.0	0.2	0.2	0.2	0.0	0.0	0.1	0.4	0.1	0.0	0.0
43	0.2	0.2	0.0	0.0	0.0	0.2	0.2	0.2	0.0	0.0	0.1	0.4	0.1	0.0	0.0
44	0.2	0.2	0.0	0.0	0.0	0.2	0.2	0.2	0.0	0.0	0.1	0.4	0.1	0.0	0.0
45	0.2	0.2	0.0	0.0	0.0	0.2	0.2	0.2	0.0	0.0	0.1	0.4	0.1	0.0	0.0
46	0.1	0.4	0.0	0.0	0.0	0.2	0.2	0.2	0.0	0.0	0.1	0.4	0.1	0.0	0.0
47	0.2	0.2	0.0	0.0	0.0	0.2	0.2	0.2	0.0	0.0	0.1	0.4	0.1	0.0	0.0

Table 37. Chemical composition of the Forestburg fly ash after leaching with 0.005 M sulfuric acid.

Sample	(%)										(ug/g) ^a									
	SIO ₂	Al ₂ O ₃	Fe ₂ O ₃	CaO	MgO	Na ₂ O	K ₂ O	LOI	Ba	Co	Cr	Cu	Mn	Ni	Pb	Sr				
Unleached	56	19	5.9	11	2.4	3.7	1.8	0.2	2400	30	140	30	340	40	70	230				
Column 1																				
Surface	65	17	4.5	3.4	1.5	3.7	2.1	2.0	3200	36	80	20	230	40	80	40				
Middle	61	18	6.4	4.6	1.8	3.7	2.1	1.6	2400	30	130	30	270	40	90	110				
Bottom	59	18	7.6	5.3	1.8	3.5	2.0	2.6	2600	30	130	30	260	40	80	120				
Column 2																				
Surface-Edges	58	18	7.5	6.5	1.9	3.7	1.8	2.2	2400	30	140	40	290	40	80	110				
Surface	56	20	6.3	7.4	2.1	3.7	1.8	1.9	2500	30	140	30	290	40	80	80				
Subsurface	55	21	6.0	8.8	2.1	3.5	1.8	1.5	2200	30	140	40	320	40	80	130				
Middle	53	22	5.8	9.2	2.2	3.7	1.8	1.6	2500	30	140	40	350	40	70	140				
Bottom	58	20	5.8	8.6	2.2	3.5	1.8	1.9	2300	30	130	40	340	40	70	120				
Column 3																				
Surface-Edges	56	21	5.2	8.2	2.1	3.4	1.7	2.4	2000	30	120	40	310	40	70	110				
Surface	54	21	5.7	9.4	2.2	3.8	1.8	1.3	2000	30	120	40	320	40	70	140				
Subsurface	55	21	5.8	9.1	2.2	3.6	1.7	1.4	2200	30	120	40	320	40	70	120				
Middle	56	20	5.8	8.5	2.3	3.5	1.7	2.0	1900	30	120	40	350	40	70	110				
Bottom	54	20	6.1	9.3	2.6	3.7	1.7	2.1	2100	30	120	30	340	40	70	130				
Column 4																				
Surface-Edges	54	19	5.3	11	2.1	3.3	1.7	2.7	2200	30	110	30	320	40	70	230				
Surface	56	20	5.7	10	2.3	3.6	1.8	0.9	2300	30	120	30	350	40	80	160				
Subsurface	56	19	5.9	10	2.4	3.8	1.9	1.0	2500	30	120	30	360	40	80	160				
Middle	55	19	6.0	10	2.4	3.7	1.9	1.4	2300	30	120	30	350	40	70	160				
Bottom	55	19	5.8	10	2.6	3.5	1.9	1.6	2200	30	110	30	350	40	70	160				
Column 5																				
Surface-Edges	53	18	5.3	12	2.2	3.4	1.8	2.7	2300	30	110	30	310	40	70	230				
Surface	56	20	5.6	10	2.2	3.6	1.9	1.1	2800	30	120	30	350	40	80	180				
Subsurface	55	20	5.8	10	2.3	3.7	1.9	1.1	2500	30	120	30	350	40	80	160				
Middle	55	20	5.7	10	2.4	3.7	1.8	1.4	2400	30	110	30	340	40	70	160				
Bottom	55	19	5.9	11	2.4	3.6	1.8	1.4	2000	30	120	30	350	40	70	170				
Base	54	20	5.8	11	2.4	3.6	1.8	1.3	1900	30	120	30	340	40	70	170				

^a Determined by difference.
^b Loss on ignition.

Table 38. Chemical composition of the Forestburg fly ash after leaching with AASA solution.

Sample	(%)										(ug/g)									
	SiO ₂	Al ₂ O ₃	Fe ₂ O ₃	CaO	H ₂ O	Na ₂ O	K ₂ O	LOI	Ba	Co	Cr	Cu	Mn	Ni	Pb	Sr				
Unleached	56	19	5.9	11	2.4	3.7	1.8	0.2	2400	30	140	30	340	40	70	230				
Column 1																				
Surface	59	20	5.2	5.9	2.0	4.0	2.1	1.2	1200	30	100	30	270	40	70	60				
Middle	55	21	6.0	8.1	2.3	3.9	1.9	1.1	1500	30	100	40	320	40	70	110				
Bottom	54	22	6.2	8.3	2.3	4.0	1.9	1.1	1700	30	100	40	330	40	70	110				
Column 2																				
Surface-Edges	55	21	6.0	7.6	2.1	4.1	1.9	2.0	2400	30	110	40	270	40	70	80				
Surface	55	21	6.2	7.8	2.2	4.1	1.9	1.4	2100	30	110	40	300	40	70	90				
Subsurface	55	21	6.3	8.4	2.3	3.8	1.8	0.9	2300	30	110	40	330	40	70	120				
Middle	55	21	6.3	8.4	2.3	3.7	1.8	1.5	2300	30	110	40	330	40	60	120				
Bottom	54	21	6.3	8.7	2.4	3.7	1.8	1.7	2200	30	120	40	340	40	70	120				
Column 3																				
Surface-Edges	54	22	5.7	9.0	2.2	3.8	1.8	1.6	2300	30	110	30	320	40	70	130				
Surface	54	22	5.9	8.8	2.2	3.8	1.8	1.3	2200	30	120	30	330	40	70	140				
Subsurface	54	22	6.1	8.7	2.3	3.7	1.8	1.4	2200	30	110	30	340	40	70	130				
Middle	54	22	5.9	8.4	2.5	3.7	1.8	1.8	2300	30	120	30	370	40	70	120				
Bottom	53	22	6.0	8.7	2.6	3.7	1.8	1.7	2400	30	130	30	390	40	70	140				
Column 4																				
Surface-Edges	55	20	5.4	10	2.2	3.7	1.7	2.0	2600	30	100	30	350	40	70	170				
Surface	55	21	5.7	10	2.3	3.8	1.8	1.0	2400	30	100	30	350	40	70	150				
Subsurface	54	21	5.7	10	2.4	3.8	1.8	1.0	2300	30	110	30	300	40	70	170				
Middle	55	20	5.4	10	2.5	3.7	1.8	1.4	2200	30	110	30	350	40	70	170				
Bottom	54	20	5.6	11	2.5	3.7	1.8	1.4	2300	30	110	30	350	40	70	160				
Column 5																				
Surface-Edges	52	21	5.6	11	2.2	3.7	1.8	2.2	2500	30	100	30	300	40	70	190				
Surface	54	21	5.8	10	2.4	3.8	1.8	1.1	2400	30	100	30	330	40	80	180				
Subsurface	53	21	5.8	11	2.4	3.8	1.7	1.1	2300	30	90	30	340	40	70	170				
Middle	54	20	6.0	11	2.4	3.7	1.7	1.2	2300	30	100	30	340	40	70	170				
Bottom	53	20	5.8	11	2.3	3.7	1.7	1.4	2400	30	90	30	350	40	70	180				
Base	54	20	5.8	11	2.3	3.6	1.7	1.4	2300	30	90	30	340	40	70	180				

* Determined by difference.

** Loss on ignition.

Table 39. Chemical composition of the Sundance fly ash after leaching with 0.005 M sulfuric acid.

Sample	(%)									(ug/g)									
	SiO ₂	Al ₂ O ₃	Fe ₂ O ₃	CaO	MgO	Na ₂ O	K ₂ O	LOI	**	Ba	Co	Cr	Cu	Mn	Ni	Pb	Sr		
Unleached	51	22	4.5	15	1.3	3.7	1.3	0.9		1400	30	100	40	490	40	120	190		
Column 1																			
Surface	68	18	2.9	3.1	0.6	2.7	1.4	3.4		4000	20	40	20	280	30	160	20		
Middle	65	18	4.4	3.6	0.6	2.8	1.3	3.6		3500	30	50	40	290	30	160	30		
Bottom	59	20	6.4	5.1	0.8	3.2	1.3	3.8		2800	30	80	40	330	40	140	30		
Column 2																			
Surface-Edges	55	23	4.9	7.9	0.9	3.6	1.3	3.0		2000	30	80	50	440	40	120	40		
Surface	57	23	5.2	7.2	0.9	3.6	1.4	2.7		2500	30	80	40	420	40	130	30		
Subsurface	53	24	4.6	8.3	1.1	3.6	1.3	2.4		2200	30	70	50	480	40	110	60		
Middle	55	24	4.8	9.1	1.2	3.6	1.3	2.7		1500	30	80	60	490	40	110	60		
Bottom	52	25	4.4	9.0	1.3	3.5	1.3	2.9		1900	40	70	60	510	50	110	50		
Column 3																			
Surface-Edges	52	21	4.4	13	1.1	3.4	1.2	3.3		2600	40	80	40	590	50	120	150		
Surface	52	24	4.4	12	1.3	3.6	1.3	1.6		2600	40	70	40	580	50	120	110		
Subsurface	54	22	4.3	12	1.3	3.6	1.2	1.8		2400	30	70	40	540	50	120	120		
Middle	53	22	4.4	12	1.5	3.5	1.2	1.9		2100	30	80	40	500	50	120	110		
Bottom	51	23	4.4	13	1.4	3.6	1.2	1.8		1600	30	90	40	490	50	120	120		
Column 4																			
Surface-Edges	47	20	3.9	17	1.1	3.3	1.3	6.0		2200	30	80	40	430	40	100	140		
Surface	52	23	4.2	12	1.1	3.6	1.3	2.0		2300	30	80	40	500	40	120	100		
Subsurface	53	23	4.2	12	1.2	3.5	1.3	1.9		2300	30	80	40	500	40	190	100		
Middle	50	24	4.4	13	1.3	3.7	1.3	1.9		2300	30	70	40	500	40	120	110		
Bottom	52	23	4.2	13	1.2	3.5	1.4	1.9		1200	30	80	40	500	40	120	120		
Column 5																			
Surface-Edges	48	21	4.1	16	1.2	3.6	1.3	5.0		2600	30	70	40	460	40	90	150		
Surface	51	23	4.4	13	1.3	3.8	1.3	2.3		2600	30	70	40	490	40	100	100		
Subsurface	51	22	4.3	14	1.3	3.8	1.3	2.2		2300	30	70	40	490	40	110	110		
Middle	51	22	4.4	14	1.4	3.8	1.3	1.8		1600	30	70	40	500	40	100	120		
Bottom	52	21	4.3	14	1.3	3.6	1.2	1.8		1000	30	70	40	480	40	110	120		
Base	51	22	4.2	14	1.3	3.7	1.2	1.9		1000	30	70	40	480	40	100	120		

* Determined by difference.

** Loss on ignition.

Table 40. Chemical composition of the Sundance fly ash after leaching with AASA solution.

Sample	(%)										(ug/g)									
	SiO ₂		Al ₂ O ₃		Fe ₂ O ₃		CaO	MgO	Na ₂ O		K ₂ O	LOI	Ba	Co	Cr	Cu	Mn	Ni	Pb	Sr
Unleached	51	22	4.5	15	1.3	3.7	1.3	0.9	1400	30	100	40	490	40	120	190				
Column 1																				
Surface	56	24	4.3	6.5	0.9	4.1	1.5	1.7	1500	30	70	50	420	40	120	30				
Middle	54	24	4.7	8.7	1.0	3.9	1.3	1.9	1300	40	70	50	500	50	120	50				
Bottom	53	25	4.6	9.0	1.1	3.9	1.3	1.9	2700	30	70	50	500	40	110	60				
Column 2																				
Surface-Edges	56	24	4.2	6.4	0.9	3.9	1.5	2.5	2100	30	70	50	400	40	130	30				
Surface	54	25	4.6	7.2	1.0	4.4	1.5	2.1	2200	30	70	50	420	40	130	30				
Subsurface	51	26	4.9	8.7	1.1	4.0	1.3	2.3	2600	30	80	60	460	40	120	50				
Middle	51	26	4.7	9.0	1.2	3.8	1.3	2.4	2600	30	70	60	480	40	120	50				
Bottom	50	26	4.7	10	1.4	3.9	1.3	2.4	2700	30	80	50	530	50	120	60				
Column 3																				
Surface-Edges	50	26	4.6	10	1.2	3.9	1.3	2.6	3400	30	90	60	480	40	120	80				
Surface	52	25	4.6	10	1.2	3.8	1.3	2.2	3000	30	80	60	500	40	110	100				
Subsurface	53	24	4.4	10	1.3	3.8	1.2	2.1	2800	40	100	50	500	40	120	110				
Middle	50	24	4.2	13	1.3	3.8	1.3	2.0	2500	40	80	40	520	40	120	120				
Bottom	50	24	4.3	13	1.3	3.8	1.2	1.9	2500	40	90	40	510	40	110	130				
Column 4																				
Surface-Edges	46	20	3.9	17	1.1	3.4	1.2	6.9	2900	30	70	40	460	40	110	190				
Surface	49	23	4.2	14	1.2	3.6	1.3	3.4	3100	40	70	40	490	40	120	130				
Subsurface	50	24	4.3	13	1.3	3.8	1.3	1.8	2600	40	70	40	490	40	120	130				
Middle	52	23	4.3	13	1.2	3.7	1.3	1.7	2600	40	70	40	490	40	110	130				
Bottom	49	24	4.3	14	1.2	3.8	1.3	1.7	2300	40	80	40	500	40	110	130				
Column 5																				
Surface-Edges	49	21	4.1	15	1.0	3.4	1.2	5.2	2700	30	60	40	450	40	110	160				
Surface	48	24	4.3	14	1.2	3.8	1.3	2.7	2700	40	60	40	490	40	120	130				
Subsurface	50	24	4.4	13	1.2	3.8	1.3	1.8	2400	30	60	40	490	40	120	120				
Middle	48	25	4.4	14	1.3	3.8	1.3	1.7	2200	30	70	40	480	40	120	130				
Bottom	48	25	4.3	14	1.3	3.8	1.3	1.7	2300	30	80	40	480	40	120	130				
Base	49	24	4.3	14	1.3	3.8	1.3	1.7	2100	30	80	40	480	40	120	130				

* Determined by difference.

** Loss on ignition.

Table 41. Correlation Matrix of the chemical components in the weathered Forestburg ash samples.

AASA Leached

	Al	Ca	Fe	K	Mg	Na	Si	LOI	Ba	Co	Cr	Cu	Mn	Ni	Pb	Sr
Al	1.000	.278	.484	.389	.548	.189	.741	.046	.303	.241	.553	.077	.444	.081	.027	.311
Ca	.278	1.000	.233	.826	.576	.638	.808	.126	.697	.177	.128	.078	.711	.054	.150	.950
Fe	.484	.233	1.000	.394	.540	.115	.626	.092	.356	.160	.363	.763	.296	.789	.322	.116
K	.389	.826	.394	1.000	.686	.752	.772	.347	.885	.569	.547	.049	.746	.144	.399	.796
Mg	.548	.576	.540	.686	1.000	.619	.754	.014	.418	.100	.534	.049	.926	.372	.229	.636
Na	.189	.638	.115	.752	.619	1.000	.473	.075	.464	.344	.366	.250	.761	.009	.470	.748
Si	.741	.808	.626	.772	.754	.473	1.000	.069	.651	.221	.406	.180	.720	.287	.129	.755
LOI	.046	.126	.092	.347	.014	.075	.069	1.000	.518	.493	.459	.061	.024	.002	.096	.022
Ba	.303	.697	.356	.885	.418	.464	.651	.518	1.000	.682	.567	.205	.440	.118	.200	.595
Co	.241	.177	.160	.569	.100	.344	.221	.483	.682	1.000	.590	.060	.137	.122	.320	.122
Cr	.553	.129	.363	.547	.534	.366	.406	.459	.567	.590	1.000	.028	.447	.151	.101	.184
Cu	.077	.078	.763	.049	.049	.250	.180	.061	.205	.060	.028	1.000	.295	.693	.260	.271
Mn	.444	.711	.296	.746	.926	.761	.720	.024	.440	.137	.447	.285	1.000	.162	.179	.817
Ni	.081	.054	.788	.144	.372	.009	.287	.002	.118	.122	.151	.693	.162	1.000	.307	.061
Pb	.027	.150	.322	.399	.229	.470	.125	.096	.200	.320	.101	.260	.179	.307	1.000	.094
Sr	.311	.850	.116	.796	.636	.748	.755	.022	.595	.122	.184	.271	.817	.061	.094	1.000

Sulfuric Acid Leached

	Al	Ca	Fe	K	Mg	Na	Si	LOI	Ba	Co	Cr	Cu	Mn	Ni	Pb	Sr
Al	1.000	.820	.270	.822	.637	.191	.892	.389	.672	.236	.271	.755	.863	.800	.758	.391
Ca	.820	1.000	.170	.886	.875	.390	.845	.224	.739	.164	.209	.621	.900	.893	.774	.768
Fe	.270	.170	1.000	.019	.120	.174	.030	.186	.088	.517	.705	.047	.136	.181	.275	.115
K	.822	.886	.019	1.000	.868	.468	.904	.034	.814	.366	.360	.719	.848	.825	.845	.537
Mg	.637	.875	.120	.868	1.000	.197	.904	.249	.732	.178	.203	.569	.916	.932	.790	.526
Na	.191	.390	.174	.468	.197	1.000	.236	.578	.416	.221	.125	.149	.218	.223	.456	.434
Si	.892	.845	.030	.904	.904	.236	1.000	.301	.774	.341	.431	.730	.921	.881	.745	.676
LOI	.389	.224	.186	.034	.249	.578	.301	1.000	.102	.198	.132	.315	.399	.216	.080	.002
Ba	.672	.739	.088	.814	.732	.416	.774	.102	1.000	.267	.320	.475	.753	.621	.515	.609
Co	.236	.164	.517	.366	.178	.221	.341	.198	.267	1.000	.686	.688	.317	.161	.201	.001
Cr	.271	.209	.705	.360	.203	.125	.431	.132	.320	.686	1.000	.575	.287	.117	.026	.202
Cu	.755	.621	.047	.718	.568	.149	.730	.315	.475	.688	.575	1.000	.736	.553	.665	.282
Mn	.863	.900	.136	.848	.916	.218	.921	.399	.753	.317	.287	.736	1.000	.908	.733	.603
Ni	.800	.893	.181	.825	.932	.223	.881	.216	.621	.161	.117	.553	.908	1.000	.789	.596
Pb	.758	.774	.275	.845	.790	.456	.745	.080	.515	.201	.026	.665	.733	.789	1.000	.369
Sr	.391	.768	.115	.537	.526	.434	.676	.002	.609	.001	.202	.282	.603	.596	.369	1.000

Table 42. Correlation matrix of the chemical components in the weathered Sundance ash samples.

AASA Leached

	Al	Ca	Fe	K	Mg	Na	Si	LOI	Ba	Co	Cr	Cu	Mn	Ni	Pb	Sr
Al	1.000	.679	.825	.239	.141	.722	.080	.698	.016	.264	.130	.725	.007	.196	.257	.732
Ca	.679	1.000	.406	.814	.546	.798	.784	.640	.511	.165	.353	.446	.573	.216	.616	.984
Fe	.825	.406	1.000	.088	.321	.478	.166	.472	.011	.136	.105	.761	.278	.214	.011	.519
K	.239	.814	.088	1.000	.812	.706	.893	.333	.853	.079	.539	.001	.841	.129	.741	.754
Mg	.141	.546	.321	.812	1.000	.350	.867	.034	.625	.011	.688	.070	.871	.162	.446	.458
Na	.722	.798	.478	.706	.350	1.000	.450	.627	.384	.077	.180	.322	.464	.240	.612	.822
Si	.080	.784	.166	.893	.867	.450	1.000	.287	.675	.012	.580	.002	.783	.104	.589	.710
LOI	.698	.640	.472	.333	.034	.627	.287	1.000	.345	.285	.162	.373	.053	.419	.276	.643
Ba	.016	.511	.011	.553	.625	.384	.675	.345	1.000	.430	.471	.153	.405	.360	.426	.509
Co	.264	.165	.136	.079	.011	.077	.012	.285	.430	1.000	.291	.379	.292	.469	.179	.143
Cr	.130	.353	.105	.539	.688	.180	.580	.162	.471	.291	1.000	.054	.641	.271	.214	.337
Cu	.725	.446	.761	.001	.070	.322	.002	.373	.153	.379	.054	1.000	.056	.068	.040	.487
Mn	.007	.573	.278	.841	.871	.464	.783	.053	.405	.292	.641	.056	1.000	.336	.576	.498
Ni	.196	.216	.214	.129	.162	.240	.104	.419	.360	.469	.271	.068	.336	1.000	.246	.257
Pb	.257	.616	.011	.741	.446	.612	.599	.276	.426	.179	.214	.040	.576	.246	1.000	.629
Sr	.732	.984	.519	.754	.458	.822	.710	.643	.509	.143	.337	.487	.498	.257	.629	1.000

Sulfuric Acid Leached

	Al	Ca	Fe	K	Mg	Na	Si	LOI	Ba	Co	Cr	Cu	Mn	Ni	Pb	Sr
Al	1.000	.472	.246	.154	.747	.921	.815	.567	.849	.851	.640	.845	.741	.797	.809	.206
Ca	.472	1.000	.082	.775	.802	.625	.882	.147	.630	.555	.655	.298	.834	.845	.811	.930
Fe	.246	.082	1.000	.043	.014	.385	.199	.016	.311	.449	.601	.277	.019	.143	.103	.181
K	.154	.775	.043	1.000	.717	.322	.593	.278	.422	.366	.464	.106	.627	.616	.463	.855
Mg	.747	.802	.014	.717	1.000	.746	.888	.531	.797	.730	.620	.597	.861	.895	.839	.574
Na	.921	.625	.385	.322	.746	1.000	.803	.489	.876	.841	.829	.710	.786	.861	.825	.386
Si	.815	.882	.199	.593	.888	.803	1.000	.367	.860	.830	.823	.636	.909	.960	.933	.700
LOI	.567	.147	.016	.278	.531	.499	.367	1.000	.319	.423	.164	.296	.465	.414	.190	.114
Ba	.849	.630	.311	.422	.797	.876	.860	.319	1.000	.764	.833	.833	.704	.804	.892	.379
Co	.851	.555	.449	.366	.730	.841	.830	.423	.764	1.000	.720	.792	.842	.880	.772	.402
Cr	.640	.655	.601	.464	.620	.829	.823	.164	.833	.720	1.000	.517	.626	.736	.743	.486
Cu	.845	.298	.277	.106	.597	.710	.626	.296	.833	.792	.517	1.000	.587	.653	.747	.006
Mn	.741	.834	.019	.627	.861	.786	.909	.465	.704	.842	.626	.587	1.000	.975	.830	.758
Ni	.797	.845	.143	.616	.895	.861	.960	.414	.804	.880	.736	.653	.975	1.000	.895	.719
Pb	.809	.811	.103	.463	.839	.825	.933	.190	.892	.773	.743	.747	.830	.895	1.000	.589
Sr	.206	.930	.181	.855	.674	.386	.700	.114	.379	.402	.486	.048	.758	.719	.589	1.000

Table 43. Percent acid ammonium oxalate (AAD) and citrate-bicarbonate-dithionite (CBD) extractable Fe, Al, Si, and Mn in the 0.005 M sulfuric acid leached Forestburg fly ash.

Sample	AAD				CBD			
	Si	Al	Fe	Mn*	Si	Al	Fe	Mn*
Unleached	2.6	1.7	0.91	33	0.07	0.17	0.18	23
Column 1								
Surface	0.08	0.08	0.28	34	0.22	0.02	0.35	28
Middle	0.52	0.60	1.4	30	0.19	0.09	1.1	20
Bottom	1.2	1.0	1.8	38	0.22	0.08	1.6	18
Column 2								
Surface-Edges	1.7	1.8	2.2	52	0.13	0.13	1.6	17
Surface	2.4	2.2	1.6	36	0.08	0.22	0.90	15
Subsurface	2.8	2.5	1.3	33	0.08	0.29	0.48	22
Middle	3.2	2.8	0.96	32	0.08	0.38	0.30	30
Bottom	2.8	2.8	0.92	32	0.07	0.40	0.33	35
Column 3								
Surface-Edges	3.2	3.4	1.2	90	0.10	0.35	0.35	40
Surface	2.6	3.2	0.94	32	0.06	0.30	0.28	28
Subsurface	3.0	3.0	0.98	34	0.11	0.38	0.34	40
Middle	3.2	3.2	1.2	60	0.15	0.50	0.40	55
Bottom	3.0	2.8	1.1	72	0.17	0.42	0.45	140
Column 4								
Surface-Edges	1.6	1.4	0.56	28	0.16	0.22	0.27	40
Surface	2.6	2.2	0.98	44	0.12	0.20	0.28	45
Subsurface	2.6	1.8	0.92	48	0.10	0.22	0.32	48
Middle	2.6	2.2	0.92	42	0.10	0.23	0.32	45
Bottom	2.4	2.2	0.92	50	0.13	0.35	0.33	43
Column 5								
Surface-Edges	3.0	2.4	1.0	52	0.16	0.22	0.28	35
Surface	2.4	2.0	1.0	38	0.13	0.24	0.34	40
Subsurface	2.8	2.8	1.0	40	0.12	0.22	0.32	42
Middle	3.0	2.4	1.0	44	0.11	0.23	0.30	45
Bottom	3.0	2.6	0.80	40	0.10	0.28	0.29	45
Base	2.8	3.0	0.80	38	0.08	0.25	0.27	40

* x10 = %

Table 44. Percent acid ammonium oxalate (AAO) and citrate-bicarbonate-dithionite (CBD) extractable Fe, Al, Si, and Mn in the 0.005 M sulfuric acid leached Sundance fly ash.

Sample	AAO				CBD			
	Si	Al	Fe	Mn*	Si	Al	Fe	Mn*
Unleached	3.2	3.4	0.69	28	0.15	0.09	0.17	28
Column 1								
Surface	0.06	0.06	0.28	40	0.25	0.01	0.40	45
Middle	0.04	0.16	1.0	46	0.25	0.04	1.5	30
Bottom	0.48	1.4	2.1	56	0.22	0.05	2.1	25
Column 2								
Surface-Edges	3.4	3.4	2.2	120	0.24	0.27	1.1	50
Surface	2.4	2.2	1.4	42	0.10	0.22	1.2	40
Subsurface	3.4	2.8	1.1	36	0.07	0.45	0.55	60
Middle	3.2	3.4	1.0	42	0.08	0.50	0.38	70
Bottom	3.6	4.0	0.96	46	0.10	0.55	0.38	82
Column 3								
Surface-Edges	3.6	3.4	0.80	50	0.15	0.14	0.40	180
Surface	3.6	3.0	0.84	58	0.15	0.13	0.45	170
Subsurface	3.6	4.0	0.70	50	0.18	0.24	0.45	100
Middle	3.2	3.2	0.64	46	0.17	0.38	0.50	70
Bottom	3.4	3.0	0.84	36	0.15	0.32	0.55	60
Column 4								
Surface-Edges	3.6	3.2	0.84	32	0.10	0.09	0.39	65
Surface	3.8	3.2	0.76	36	0.11	0.12	0.45	65
Subsurface	3.8	3.2	0.68	36	0.10	0.14	0.48	65
Middle	3.6	3.0	0.62	36	0.10	0.15	0.52	68
Bottom	3.6	3.0	0.76	32	0.09	0.12	0.48	62
Column 5								
Surface-Edges	3.4	3.6	0.86	36	0.10	0.10	0.36	58
Surface	4.0	3.6	0.78	44	0.10	0.12	0.40	62
Subsurface	3.8	3.8	0.88	44	0.15	0.20	0.42	70
Middle	3.6	3.4	0.76	40	0.07	0.13	0.40	62
Bottom	3.2	3.4	0.68	36	0.10	0.18	0.40	62
Base	3.4	3.4	0.80	34	0.10	0.14	0.40	60

* x10⁻⁴ %

Table 45. Percent acid ammonium oxalate (AAO) and citrate-bicarbonate-dithionite (CBD) extractable Fe, Al, Si, and Mn in the AASA leached Forestburg fly ash.

Sample	AAO				CBD			
	Si	Al	Fe	Mn*	Si	Al	Fe	Mn*
Unleached	2.6	1.7	0.91	33	0.07	0.17	0.18	23
Column 1								
Surface	0.72	0.76	0.80	48	0.14	0.10	0.38	30
Middle	2.2	1.8	1.2	40	0.11	0.20	0.52	28
Bottom	2.8	2.2	1.2	40	0.11	0.20	0.52	28
Column 2								
Surface-Edges	2.6	2.2	1.4	52	0.16	0.29	0.69	40
Surface	2.4	2.4	1.5	38	0.10	0.30	0.58	30
Subsurface	2.4	2.4	1.4	46	0.10	0.35	0.52	40
Middle	2.8	2.4	1.3	48	0.10	0.38	0.50	52
Bottom	2.8	2.4	1.2	48	0.10	0.40	0.45	58
Column 3								
Surface-Edges	3.0	2.2	0.92	38	0.12	0.40	0.42	38
Surface	2.8	2.4	0.92	36	0.08	0.32	0.39	30
Subsurface	2.8	2.6	0.96	46	0.10	0.32	0.38	50
Middle	3.6	2.2	0.96	62	0.10	0.40	0.40	75
Bottom	3.4	2.4	0.96	60	0.10	0.42	0.42	80
Column 4								
Surface-Edges	2.6	2.2	0.92	46	0.12	0.40	0.32	62
Surface	2.6	2.4	0.96	46	0.12	0.28	0.36	60
Subsurface	2.4	2.0	0.92	48	0.09	0.25	0.30	52
Middle	2.4	2.2	0.96	46	0.11	0.30	0.32	45
Bottom	2.6	2.0	0.84	44	0.09	0.30	0.30	42
Column 5								
Surface-Edges	2.6	2.0	1.1	32	0.10	0.25	0.28	40
Surface	2.6	2.4	1.2	36	0.09	0.30	0.22	45
Subsurface	2.8	2.2	1.0	38	0.09	0.32	0.30	45
Middle	2.8	2.6	0.96	42	0.06	0.35	0.31	45
Bottom	2.8	2.0	1.2	46	0.09	0.32	0.28	42
Base	2.8	2.4	1.2	44	0.09	0.30	0.28	40

* x10 = %

Table 46. Percent acid ammonium oxalate (AAO) and citrate-bicarbonate-dithionite (CBD) extractable Fe, Al, Si, and Mn in the AASA leached Sundance fly ash.

Sample	AAO					CBD				
	Si	Al	Fe	Mn*	Mn*	Si	Al	Fe	Mn*	Mn*
Unleached	3.2	3.4	0.69	28	28	0.15	0.09	0.17	28	28
Column 1										
Surface	2.4	2.8	1.6	54	54	0.12	0.16	0.75	48	48
Middle	3.6	3.2	1.8	44	44	0.09	0.28	0.58	60	60
Bottom	4.0	3.0	1.5	44	44	0.10	0.30	0.55	62	62
Column 2										
Surface-Edges	2.2	2.4	1.2	84	84	0.15	0.16	0.64	75	75
Surface	3.0	2.8	1.4	56	56	0.08	0.20	0.80	45	45
Subsurface	3.8	2.8	1.5	52	52	0.10	0.32	0.75	55	55
Middle	4.6	3.0	1.0	56	56	0.14	0.40	0.68	70	70
Bottom	4.0	3.2	0.94	62	62	0.12	0.38	0.58	92	92
Column 3										
Surface-Edges	3.6	4.0	1.4	34	34	0.12	0.52	0.72	62	62
Surface	3.6	3.4	1.2	38	38	0.14	0.55	0.66	72	72
Subsurface	3.4	3.4	1.2	46	46	0.12	0.35	0.52	100	100
Middle	3.6	2.6	1.0	40	40	0.10	0.22	0.49	70	70
Bottom	3.2	2.6	0.92	38	38	0.08	0.20	0.48	70	70
Column 4										
Surface-Edges	4.0	3.0	0.72	38	38	0.14	0.32	0.46	88	88
Surface	4.0	3.4	0.76	38	38	0.12	0.25	0.50	75	75
Subsurface	3.8	2.8	0.92	36	36	0.14	0.30	0.46	65	65
Middle	3.6	3.2	0.84	36	36	0.10	0.20	0.45	60	60
Bottom	3.6	3.0	0.76	34	34	0.11	0.22	0.42	58	58
Column 5										
Surface-Edges	3.6	3.2	1.0	40	40	0.09	0.20	0.52	62	62
Surface	4.4	3.2	1.1	42	42	0.10	0.22	0.55	70	70
Subsurface	4.2	3.4	1.0	40	40	0.07	0.18	0.52	60	60
Middle	3.8	3.2	0.84	38	38	0.14	0.20	0.51	62	62
Bottom	3.6	3.2	0.80	36	36	0.13	0.15	0.46	58	58
Base	3.8	3.6	0.76	34	34	0.09	0.12	0.40	55	55

-4
x10 %